Current Challenges and Routes Forward for Non-aqueous Lithium-Air Batteries

Tao Liu,*[,1,2] J. Padmanabhan Vivek,[3] Evan Wenbo Zhao,[2] Jiang Lei,[1] Nuria Garcia-Araez,[3] Clare P. Grey*[,2]

1. Shanghai Key Laboratory of Chemical Assessment and Sustainability, Department of Chemistry, Tongji University, Shanghai 200092, P. R. China.
2. Chemistry Department, Lensfield Road, University of Cambridge, Cambridge, UK CB2 1EW
3. Chemistry Department, University of Southampton, Highfield Campus, Southampton, UK SO17 1BJ

* corresponding authors: tliu@tongji.edu.cn; cpg27@cam.ac.uk

Abstract

Non-aqueous lithium-air batteries have garnered considerable research interests over the past decade due to its extremely high theoretical energy densities and potentially low cost. Great advances have been achieved in both the mechanistic understanding of cell reactions and in the development of effective strategies to help realize a practical energy storage device. By drawing attention to reports published mainly within the past 8 years, this review demonstrates an updated mechanistic picture of the lithium peroxide based cell reaction, and highlights key remaining challenges due to the parasitic processes occurring at the reaction product-electrolyte, product-cathode, electrolyte-cathode and electrolyte-anode interfaces. We introduce the fundamental principles and critically evaluate the effectiveness of the important strategies that have been proposed to mitigate issues of the battery, which include the use of solid catalysts, redox mediators, solvating additives for oxygen reaction intermediates and gas separation membranes, *etc*. Recently established cell chemistries based on the superoxide, hydroxide and oxide phases are also summarized and discussed.

1. Introduction

Currently more than 80% of the global energy demand is supplied by fossil fuels.[1-3] This worldwide use of fossil energy leads to massive release of carbon dioxide and other greenhouse gases that cause issues of global climate change. The petroleum that is consumed in automobile applications represents around one third of the global primary energy sources and results in a third of greenhouse gases released. There is no doubt that electrification of our current transportation systems from renewable energy sources (such as solar, wind energies) will significantly improve our environment and energy security. This transition from fossil fueled vehicles to hybrid electric vehicles (HEV) and electric vehicles (EV) has already begun. Driven by government policies in many countries as well as technological development in private sectors, rapid growth rates (around 50% per year) in HEV/EV sales are recorded over the past few years. In 2018, the global EV sales reached 2 million where more than half (62.5%) of the cars are sold in China alone.

The core issue facing complete electrification of transportation is the development of a good battery, that is, a long-lived, safe, affordable battery with sufficient power and energy densities to cover most driving range scenarios for a day. Current EVs are predominantly based on lithium ion batteries (LIB) and active R&D efforts are still being devoted to further optimizing the LIB chemistry. Around 5 years ago, one opinion evolved in the battery community that LIBs may not be the energy storage technology that can realize mass EV adoption, because scientists estimate that the scope for energy density improvement in LIBs is at most another 30%. Therefore, the LIB – unless it is large and thus extremely costly – is unlikely to allow a driving range of 500 miles/charge to be achieved, this range being offered by a single refill of a petrol tank.[4] This idea certainly drives more fundamental research activities to the so-called beyond Li-ion battery chemistries (such as Si, S and O_2-based Li redox chemistries). Nevertheless, in 2017 Tesla Model 3 successfully demonstrated a driving range of more than 300 miles based on current LIB technologies, and a new Tesla model to be released soon is claimed to achieve even 400 miles/charge; these improvements in driving ranges are mainly obtained by loading more batteries on board (478 kg for battery packs of 80.5 kWh accounting for 30% of vehicle weight in Model 3). While Tesla's performance highlights the importance and necessity of re-engineering car manufacturing in developing EVs, their strategy, however, increases the cost and reduces the effective loading capacity of the car. In the long term, much energy-denser batteries that can significantly reduce battery cost, weight and afford long driving ranges is the research direction forward.

One of the high-energy candidates considered for EV applications is metal-air batteries.[5-8] Metal-air batteries have garnered considerable research interests over the past decade. In 2009, only 25 papers were published on the subject, this number continuing to rise, reaching over 800 in 2018. Most papers describe lithium-air, sodium-air, potassium-air, zinc-air and aluminum-air batteries, which can involve one, two or four electrons stored per O_2 molecule due to the versatility of the O_2 redox chemistry. Since O_2 from the air acts as the active material storing

electric charge, in principle, the battery should have a denser energy, lower cost, potentially less toxicity and better recyclability, as compared to LIBs that use transition metal oxides as the positive electrode. Among them, the lithium-air battery possesses the highest theoretical energy density and is most intensely studied; this is the focus of this review.

There are two types of lithium-air batteries, one based on aqueous electrolytes and the other using non-aqueous electrolytes.[9-12] The non-aqueous lithium-air batteries will have varied theoretical specific energies (defined as Wh/kg of the redox active material), depending on the type of lithium-oxygen product formed during discharge. For instance, the formation of Li_2O_2 ($2Li+O_2 \leftrightarrow Li_2O_2$), Li_2O ($4Li+O_2 \leftrightarrow 2Li_2O$), LiOH ($4Li+2H_2O+O_2 \leftrightarrow 4LiOH$) lead to theoretical capacities of 1165, 1787 and 1117 mAh/g, respectively; hence the corresponding specific energies, assuming a voltage of around 3 V for them, would be 3495, 5361, 3350 Wh/kg, clearly several times higher than those of typical LIBs (500-800 Wh/kg). On the other hand, the aqueous lithium-air cell (*e.g.*, at alkaline conditions) is described by the following reaction: $4Li+6H_2O+O_2 \leftrightarrow 4LiOH \bullet H_2O$, the forward reaction characterizing discharge and the backward one for charge.[13, 14] During discharge, the generated LiOH is dissolved in the electrolyte until reaching its saturation solubility; $LiOH \bullet H_2O$ then precipitates and deposits on the positive electrode. Since $LiOH \bullet H_2O$ rather than LiOH (as in the non-aqueous system) is the product, the specific energy of the aqueous system is much lower, around 2170 Wh/kg. As a result, much less research is done on the aqueous system compared to the aprotic one. Most contents of this review will be dedicated to discussing non-aqueous lithium-air batteries.

Although we do not attempt to give a full history of development for lithium-air batteries, it is important to acknowledge important early work. Originally proposed in the 1970s as a potential power source for electric vehicles,[15-21] non-aqueous lithium-air batteries started to regain research interests since late 1990s. Jiang and Abraham in 1996 accidently identified the Li_2O_2-based Li-O_2 electrochemistry when they attempted to intercalate Li^+ into graphite via a gel polymer electrolyte in the presence of some air leaks.[22, 23] Later on, more researchers studied the discharge reaction of lithium-air batteries using various electrolytes.[24-26] In 2006, Bruce and coworkers showed that Li_2O_2 can be decomposed on recharging, an important first step in producing a reversible Li-O_2 battery.[27]

Since Bruce *et al*'s work, and also driven by the advances of materials science and the increased need for renewable energies, research on lithium-air batteries has increased substantially. It is also worth noting that many early studies should be interpreted with caution, because many of the cell electrochemistries reported were mainly based on parasitic reactions (*e.g.*, where a carbonate electrolyte is used, and the major product on charge is CO_2). A major reason for this mistake is that the non-aqueous Li-O_2 electrochemistry is prone to undergo unwanted degradation side reactions. The situation is further complicated by the multiple interfaces and phases (solid vs. liquid) at which the chemical transformations occur. As a result, simple coulometry and non-quantitative diffraction/microscopy characterization are insufficient to fully evaluate the battery chemistry. Instead, a wide range of *in situ* quantitative gas, chemical titration,

spectroscopy techniques are usually required to assess the true reversibility and unravel the mechanisms of the Li-O_2 electrochemistry.

It is now well-recognized by the community that the development of a practical non-aqueous lithium-air battery faces many technical challenges. The cell suffers from poor rate capability, which results in a low practical specific energy. The voltage hysteresis during cycling is large, giving rise to low energy efficiencies. These high overpotentials in turn cause significant electrode and electrolyte decomposition and consequently, the cell life is quite limited. The use of a lithium metal anode involves safety concerns. In addition, other components in air (such as CO_2, H_2O) can interfere with the Li-O_2 electrochemistry and cause further parasitic reactions. As such, most lab-basedlithium-air battery research is simplified and uses pure O_2 rather than air. In this context, it is more accurate to use the term Li-O_2 rather than Li-air batteries.

To put the requirements for lithium air batteries into context, the calculations by Gallagher and coworkers of the figures of merit achievable by Li-air batteries at a *system level* for electric vehicle applications (**Fig. 1a)** are worth considering.[28] Using the data originally reported in Gallagher and co-workers' article, we compiled **Figure 1b** to show the energy densities, specific energy and cost per usable energy, as a function of the electrode areal capacity for a Li-air battery at a system level, where the areal capacity is defined as the capacity normalized by the geometric electrode area. The figure shows that very high energy densities (>380 Wh/l), specific energies (>330 Wh/kg) and very low costs per usable energy (<105 $/kWh) can be achieved with Li-air cells with high areal electrode capacities (>10 mAh cm^{-2}). For comparison, when these estimates are performed with Li-ion battery materials such as graphite and NMC111 at a system level, these authors obtained energy densities (ca. 360 Wh/L), specific energies (ca. 180 Wh/kg) and costs per unit density (ca. 200 $/kWh) that are inferior to the values projected in **Figure 1b** for Li-air batteries. Two points should be stressed however: first, Gallagher and coworkers have pointed out that advanced Li metal anode batteries paired with a high performance layered NMC metal oxide could provide a more competitive performance, but these novel battery chemistries need to overcome a number of fundamental challenges to reach commercialization, as it is the case for metal-air batteries. Second, the energy densities for traditional Li-ion batteries have continued to improve and costs have dropped noticeably since this paper was published largely due to incremental improvements, changes in cathode chemistries and massive increases in production. Nonetheless, the calculations by Gallagher and coworkers illustrate target requirements in terms of areal electrode capacity, rate capability, electrolyte loading, excess of anode capacity and cycle life required for building competitive Li-air batteries for electric vehicles. Recent improvements in Li-air batteries are critically analyzed in view of these challenging target requirements in Section 4 of this review article.

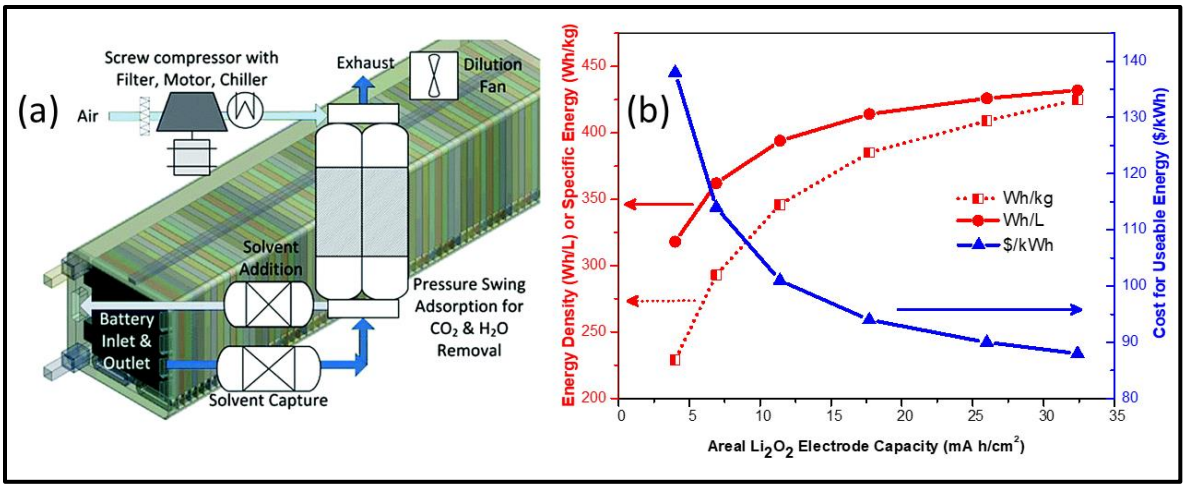

Fig. 1 Figures of merit of Li-air batteries at a system level. (a): Illustration of required components for an open Li-O_2 system. (b): Plot of the energy density, specific energy and cost per usable energy as a function of the areal Li_2O_2 electrode capacity, as obtained from the data reported by Gallagher and coworkers.[28] Values of areal Li_2O_2 electrode capacities (called "loadings" in the original article) relate to the content of Li_2O_2 per geometrical unit area of the electrode. The calculations were made considering that the wet, discharged electrode contained 60% Li_2O_2, 8% carbon, 2% binder, 5% open porosity and 25% of liquid electrolyte (volume percentages). The values shown are for an open Li-air system, but similar results are obtained with a closed Li-O_2 system. Figure 1(a) reprinted with permission from ref 28. Copyright 2014 The Royal Society of Chemistry.

At the fundamental level, great effort has been made to unravel the principles underpinning the irreversibility of lithium-air batteries. Nevertheless, many fundamental questions remain unresolved. For instance, the reactive interfaces of a lithium-oxygen battery during discharge and charge are still under debate: whether are they at the product-electrolyte interface or the product-electrode interface and what are the influential factors determining the operation of different reaction mechanisms? The answer to this question is crucial to guide the design of efficient electrocatalysts for the oxygen reduction and evolution reactions in lithium-air batteries. The true species/processes responsible for the side reactions at the cathode also merit further research; previously, the superoxide and Li_2O_{2-x} species were considered to be the main cause. However, recent studies suggest that singlet oxygen might be playing a more detrimental role. This demands the development of suitable singlet oxygen quenchers, electrolytes and mediators that are stable against singlet oxygen. Furthermore, trace amounts of water, carbon dioxide, and nitrogen are probably inevitable in practical lithium-air cells, their impact on the anode and cathode chemistry and stability needs more attention.

In this article, we review literature published until June 2019, focusing on the fundamental aspects of the key scientific and technical challenges in developing a successful and technologically relevant lithium-air battery. In Section 2, we first discuss the current understanding of the discharge and charge reaction mechanisms – the fundamentals of a basic Li-O_2 reaction based on Li_2O_2 formation and decomposition. We will show that great advances in improving the cell chemistry have been achieved through fundamental studies. Next in Section 3,

we highlight the outstanding key challenges, which relate to parasitic reactions occurring at the electrode/electrolyte interfaces. In Section 4, we introduce some novel and useful materials and strategies to address the key challenges and discuss improvements in chemistries beyond those used in Gallagher's original model. In Section 5, we discuss some recent reported new types of Li-O_2 electrochemistry, based on LiO_2, Li_2O and LiOH, which really highlight the tremendous opportunities for research to understand and modulate the versatile O_2 electrochemistry. Finally, in Section 6, we present our own, subjective perspectives and future research directions.

2. Fundamentals of Non-aqueous Lithium-Oxygen Electrochemistry

A basic non-aqueous lithium air battery consists of a lithium metal anode, a non-aqueous electrolyte (including organic solvent and lithium-containing salt) soaked in a separator and a porous carbon-based cathode (**Fig. 2**).[5] The carbon cathode is not the active material for energy storage, but simply a porous framework to host the active materials.[6] Carbon is a commonly chosen cathode host due to its light wei

ght, low cost, good electrical conductivity and relatively high chemical stability. On discharging, dioxygen molecules from the air react with lithium ions and electrons at the cathode surface (**Fig. 2a**). As a result, a solid reaction product, typically lithium peroxide (Li_2O_2), is formed and deposits within the porous carbon framework. Upon charging, Li_2O_2 is decomposed and O_2 is released back to the atmosphere (**Fig. 2b**).[7]

The characteristic electrochemical profile of a cell using a carbon-based cathode is shown in **Figure 2c**. Based on the standard Gibbs free energy change of reaction (1), the equilibrium voltage is calculated to be 2.96 V versus Li^+/Li.[29] The discharge profile shows a relatively flat plateau followed by an abrupt polarization region, also known as the 'sudden death', marking the end of the discharge process. The charging process exhibits a much larger overpotential (typically ~1 V) than the discharge (~0.2 V): a sloping region in the beginning, then a flatter charge plateau and finally a high voltage tail can usually be identified.[8]

$$2Li_{(s)} + O_{2(g)} \leftrightarrow Li_2O_{2(s)},\ E°=2.96\ V \qquad (1)$$

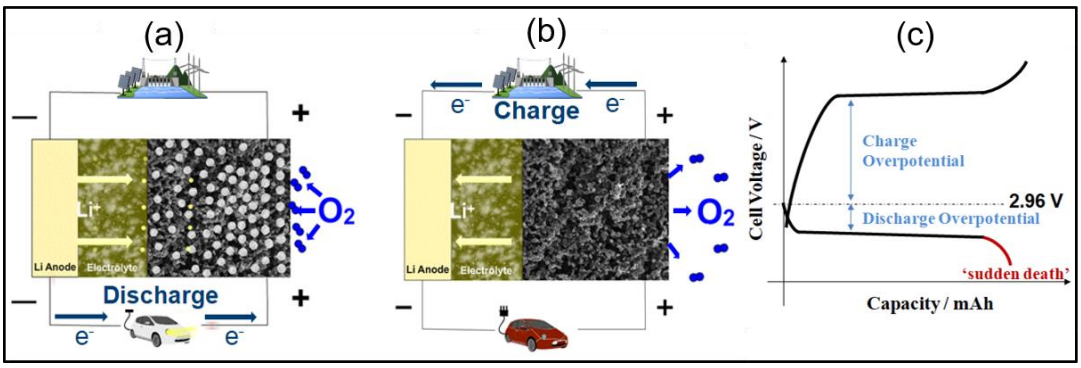

Fig. 2 Schematic illustration of the discharge (a) and charge (b) processes of a non-aqueous Li-O_2 battery and its typical electrochemical profile (c). The potential of the O_2/Li_2O_2 vs. Li^+ (2.96 V) is marked.

2.1 Discharge Reaction Mechanisms

2.1.1 Surface Mechanism versus Solution-Mediated Process

Because of its close link to the practical energy density of Li-O_2 batteries, the discharge reaction has been extensively studied. Through studies using a wide range of experimental techniques, it is suggested that the discharge reaction at the cathode can proceed either *via* a surface mechanism or a solution mediated pathway.[30-35] These different scenarios are summarized in reactions (2-6), where 'ads' and 'sol' subscripts refer to species that adsorb on the surface and that exist in solution, respectively.

In the *surface mechanism* (reactions (2-3)), lithium superoxide (LiO_2) forms *via* one-electron O_2 reduction, where the electron transfer and association with a Li^+ cation occur at the electrode surface. The surface bound $LiO_{2(ads)}$ then undergoes another one-electron electrochemical reduction to form $Li_2O_{2(ads)}$. In the *solution-mediated mechanism* (reactions (4-6)), the formation of $LiO_{2(sol)}$ occur *via* two steps: first one-electron electrochemical reduction of O_2 to form lithium superoxide at the surface, which then diffuses into solution (reaction (4)); the $LiO_{2(sol)}$ species is dissolved in the electrolyte (in equilibrium) with its Li^+ and O_2^- ions solvated by the solvent (reaction (5)). The $LiO_{2(sol)}$ generated in solution can undergo a disproportionation reaction to produce $Li_2O_{2(sol)}$ and $O_{2(g)}$ (reaction (6)). Due to a low solubility in organic electrolyte, Li_2O_2 quickly precipitates out of the solution (reaction (6)), nucleating and growing as Li_2O_2 crystallite. A strong evidence for the solution-mediated Li_2O_2 precipitation is the observation of Li_2O_2 particles forming on the electrically insulating glass fiber separators.[36]

$$O_{2(g)} + e^- + Li^+_{(sol)} \rightarrow LiO_{2(ads)} \quad (2)$$
$$LiO_{2(ads)} + e^- + Li^+_{(sol)} \rightarrow Li_2O_{2(ads)} \quad (3)$$
or
$$O_{2(g)} + e^- + Li^+_{(sol)} \rightarrow LiO_{2(sol)} \quad (4)$$
$$LiO_{2(sol)} \leftrightarrow O_2^-{}_{(sol)} + Li^+_{(sol)} \quad (5)$$
$$2LiO_{2(sol)} \rightarrow Li_2O_{2(sol)} + O_{2(g)} \quad (6)$$

A key distinction between these two scenarios is whether significant amounts of reduced oxygen species (superoxide and peroxide) are transported from the surface into the electrolyte solution to promote large Li_2O_2 crystal formation (not necessarily on the current collectors). Next, we introduce existing evidence that supports the proposed elementary steps (reactions (2-6)) and discuss factors dictating the discharge mechanism.

2.1.2 Evidence for the Superoxide Intermediate

The existence of a superoxide reaction intermediate either at the surface or in solution has been verified by electrochemical analysis,[33, 34] Raman spectroscopy,[30, 37-39] chemical analysis,[40]

ultraviolet-visible(UV-vis) spectroscopy,[38, 41] rotating ring disc electrode (RRDE),[42-45] electron spin resonance (ESR) spectroscopy[46] and fluorescence spectroscopy.[47] While surface-enhanced Raman spectroscopy techniques can be used to probe superoxide species at the electrode surface region,[30, 37, 39] the other techniques are useful to quantify the superoxide species dissolved in the electrolyte.[38, 41-47]

Hardwick and coworkers studied the oxygen reduction reaction (ORR) in acetonitrile (ACN) and dimethyl sulfoxide (DMSO)-based electrolytes on glass carbon (GC) electrodes using shell isolated nanoparticle enhanced Raman spectroscopy (SHINERS).[39] The electric field enhancement (**Fig. 3a**) between the SiO_2-coated gold nanoparticles allowed the detection of reaction species on non-metallic electrode surfaces, whilst removing any potential surface catalytic effect due to gold. Superoxide species ($\upsilon_{O\text{-}O}^{-}$) with Raman shifts at 1125 and 1128 cm^{-1} were detected in ACN and DMSO electrolytes respectively, which are ascribed to $LiO_{2(ads)}$. While SHINERS enables the detection of reaction products close to the electrode surface (red areas in **Figure 3a**, note that the SHIN particles are *ca.* 55 nm), surface-enhanced Raman spectroscopy (SERS) is most sensitive to species directly adsorbed on the electrode surface. SERS was used by Bruce and coworkers to detect the reaction intermediates in the reduction of O_2 on roughened gold electrodes (**Fig. 3b**).[30] In DMSO, the superoxide peak (1117 cm^{-1}) was ascribed to superoxide anions, O_2^- (since the same peak position was obtained in solutions with TBA^+ cations substituting the Li^+ cations), while in ACN, the superoxide peak was at higher frequencies (1128 cm^{-1}), consistent with the stronger O-O bond expected in $LiO_{2(ads)}$, due to the lower occupancy of $2\pi^*$ antibonding orbital of LiO_2 compared to O_2^-. These results demonstrate that the main reaction intermediates change with the solvation strength of the solvents: solvents that strongly solvate lithium cations (*e.g.* DMSO), favor the formation of soluble superoxide anions, $O_2^-{}_{(sol)}$ (or, strictly speaking, superoxide anions coordinated with highly solvated lithium cations), while poorly solvating solvents favor the formation of poorly-soluble, surface bonded lithium superoxide intermediates, $LiO_{2(ads)}$.

Dissolved superoxide species in highly solvating electrolytes (e.g., DMSO) can also be analyzed by other techniques. In a typical RRDE experiment,[42-45] the disc electrode is swept negatively (*e.g.*, from 3.0 to 2.0 V), whereas the ring electrode is held at a potential high enough to electrochemically oxidize the soluble oxygen intermediates (*e.g.*, typically set to 3.0-4.0 V). The generation of soluble superoxide species is thus manifested as an oxidation current at the ring electrode, whose magnitude is proportional to the corresponding cathodic peak at the disc electrode. *In-situ* UV-vis absorption spectroscopy provides another means to study the behavior of soluble superoxide species, the superoxide species showing a characteristic absorption band at 252 nm due to the $1\pi_u \rightarrow 1\pi_g$ transition.[38, 41] Based on the absorption coefficient,[48] the signal of superoxide can be quantified and correlated with the electrochemistry, the intensity being observed in these experiments being close to that expected for a one-electron oxygen reduction reaction.

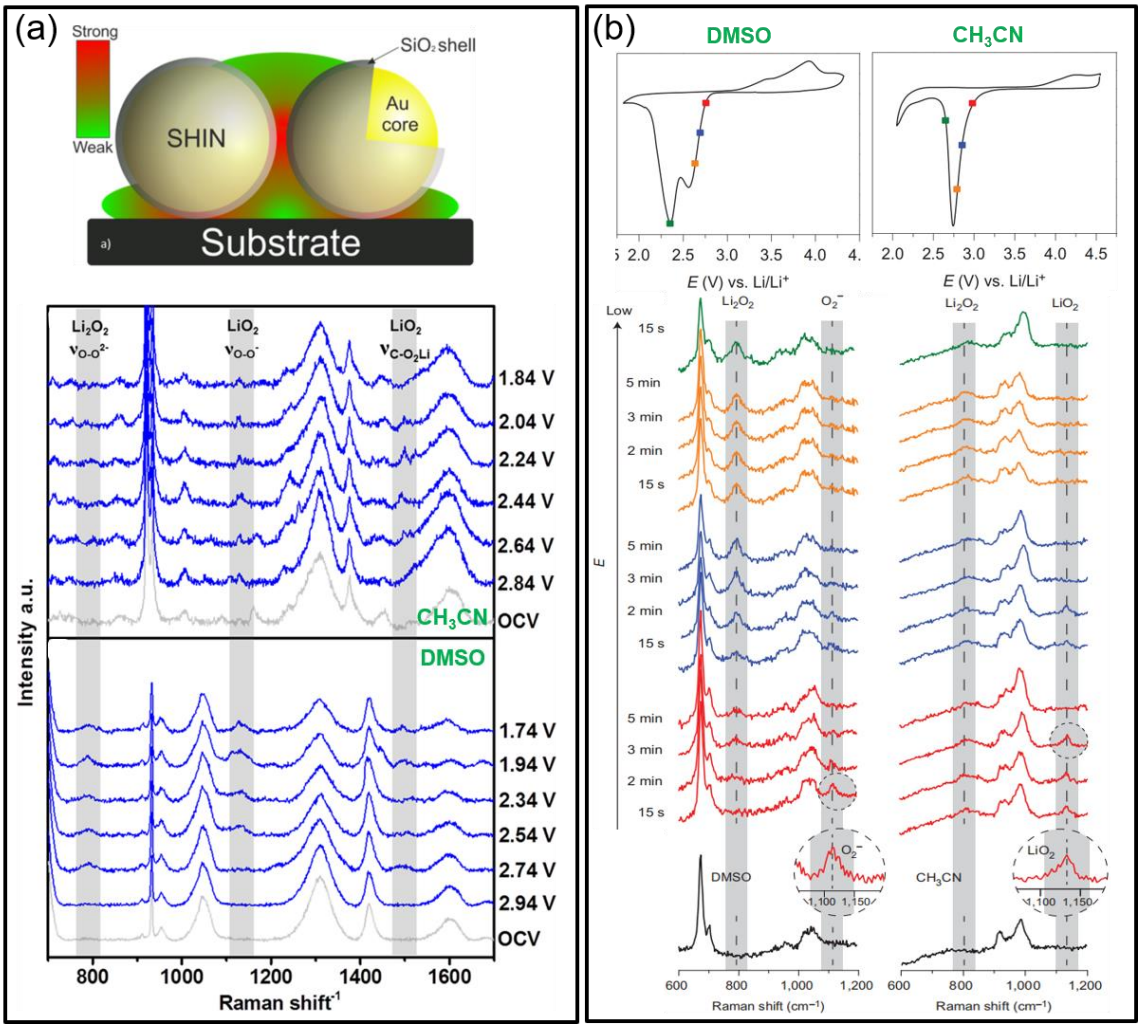

Fig. 3 *In situ* SHINERS (a) and SERS (b) characterization of reduced oxygen species in acetonitrile and dimethyl sulfoxide-based $LiClO_4$ electrolytes. The SHINERS technique (a) uses nanoparticles (~55 nm) composed of an Au core and SiO_2 shell (<4 nm) to enhance Raman sensitivity specifically to regions between particles, as indicated by the red-colored areas (some enhancement also occurs between particles and the substrate); multiple Raman spectra are acquired while the electrode potential is being swept negatively from open circuit voltages; as a result, peroxide and superoxide are observed.[39] The SERS technique (b) here uses roughened gold electrode to enhance Raman sensitivity, which is maximal at the electrode surface-electrolyte interface; the Raman spectra are acquired at different times at the specified potentials (as indicated).[30] Note that the appearance of the band associated with $LiO_{2(ads)}$ at ~1125 cm^{-1} in DMSO in (a) is probably a result of low reductive potentials, compared to the case in (b) where at higher potentials $O_2^-{}_{(sol)}$ (1117 cm^{-1}) species form. Reprinted with permission from ref 30 and 39. Copyright 2014 Nature Publishing Group and 2016 ACS.

2.1.3 LiO_2 Formation, Li_2O_2 Precipitation, Growth and Termination

To investigate whether the formation of lithium superoxide is a surface process (reaction (2)) or a solution-based process (reactions (4-5)), cyclic voltammetry measurements were performed by McCloskey,[35] Bruce[30, 37] and coworkers on the O_2/O_2^- redox couple in ACN and DMSO electrolytes (**Fig. 4a**). When TBA^+ (tetrabutyl ammonium) is the cation, it is well established that

O_2 undergoes a reversible one-electron redox reaction to form O_2^- as a highly solvated species.[33, 34, 49, 50] In the presence of a Li^+ salt, the reduction of O_2 takes place at higher potentials, indicating that the redox potential of the O_2/LiO_2 couple is higher than the O_2/O_2^- couple. This reflects the thermodynamics of the process: the association energy of Li^+-O_2^- is larger than TBA^+-O_2^-, this being controlled by the coordination of the corresponding cation by solvent molecules. A more negative $\Delta G°$ of the electrochemical reaction implies a higher $E°$.

The difference in redox potentials of the O_2/O_2^{2-} and O_2/Li_2O_2 couples has been used to obtain an estimate of the solubility product constant of Li_2O_2:[51]

$$Li_2O_{2(s)} \leftrightarrow 2Li^+_{(sol)} + O_2^{2-}{}_{(sol)} \quad K_{Li_2O_2} = \frac{a^2_{Li^+}\, a_{O_2^{2-}}}{a_{Li_2O_2}} \quad (7)$$

where a_i is the activity of species i, and since Li_2O_2 is a solid, $a_{Li_2O_2} = 1$. Strictly speaking, $K_{Li_2O_2}$ is the dissociation constant of Li_2O_2 into Li^+ and O_2^{2-}, but if ion pairing effects are considered minor, $K_{Li_2O_2}$ is also equal to the solubility product. A value of $K_{Li_2O_2} \approx 10^{-51}$ in pyrrolidinium-based ionic liquids(IL) was estimated,[51] which was later corroborated by computational studies.[52] Following a similar approach, the difference in redox potential of the O_2/O_2^- and O_2/LiO_2 couples can be used to estimate the LiO_2 dissociation equilibrium constant:

$$LiO_{2(s)} \leftrightarrow Li^+_{(sol)} + O_2^-{}_{(sol)} \quad K_{LiO_2} = \frac{a_{Li^+}\, a_{O_2^-}}{a_{LiO_2}} \quad (8)$$

The LiO_2 dissociation constant provides a measure of the coordination strength of Li^+ cations with O_2^- anions. In ACN the onset potential of ORR is 0.25 V higher in the presence of LiTFSI than TBATFSI (**Fig. 4a(i)**). This value of potential difference of 0.25 V corresponds to a LiO_2 dissociation constant of K_{LiO_2} =exp(-FΔE/RT)≈6x10^{-5}. This low value suggests that LiO_2 precipitation occurs early in the discharge of Li-O_2 cells in ACN, which agrees with the suggestion that the ORR in ACN proceeds *via* the formation of a LiO_2 surface-bond intermediate. This leads to a high rate of surface passivation, which results in a much decreased ORR current (**Fig. 4a(i)**).[35] In the DMSO electrolyte (**Fig. 4a(ii)**), on the other hand, the redox peaks show little intensity change and potential shift with increasing Li^+ concentrations. Using a shift in the ORR onset potential of *ca*. 60 mV upon Li^+ addition, a dissociation constant of K_{LiO_2}= exp(-FΔE/RT) ≈ 0.1 is obtained. This calculation demonstrates that the energy associated to Li^+ ion pairing with O_2^- is much smaller in DMSO than in ACN. This is consistent with the stronger solvation of Li^+ by DMSO than by ACN.[30]

Shao-horn and coworkers[53] performed electron microscopy measurements to follow the nucleation and growth process of Li_2O_2 in a dimethoxyethane (DME)-based electrolyte. They observed that during discharge Li_2O_2 first existed as platelet and continued to grow anisotropically into a toroidal morphology (**Fig. 4b**), the toroids later being typically taken as a characteristic feature of a liquid-phase mediated process. To understand how fresh Li_2O_2 is

added to the existing toroidal crystal, McCloskey *et al.*,[35] Lu *et al.*[54] studied Li_2O_2 precipitation mechanism using differential electrochemical mass spectrometry (DEMS) and time of flight secondary ion mass spectrometry (ToF-SIMS) aided with isotopic labeling. For example, Lu et al.[54] discharged a cell sequentially under $^{16}O_2$ and then $^{18}O_2$ in a tetraglyme electrolyte. Subsequent SEM and ToF-SIMS measurements of the discharged electrode confirmed that the toroidal Li_2O_2 products have a $Li_2{}^{16}O_2$ core and $Li_2{}^{18}O_2$ shell, as indicated by the depth-analysis of $^{18}O^-$ ToF-SIMS signals (**Fig. 4c**), strongly supporting the formation of fresh Li_2O_2 on the existing product particles at the Li_2O_2-electrolyte interface (**Fig. 4e**). Nevertheless, it should be noted that a toroidal Li_2O_2 morphology does not always necessitate a solution-mediated discharge mechanism. At very high overpotentials (>6 V) toroidal morphologies of Li_2O_2 has also been observed in an all-solid-state Li-O_2 battery;[55] no liquid electrolyte was present in these batteries, suggesting a different mass/charge transport mechanism in this case.

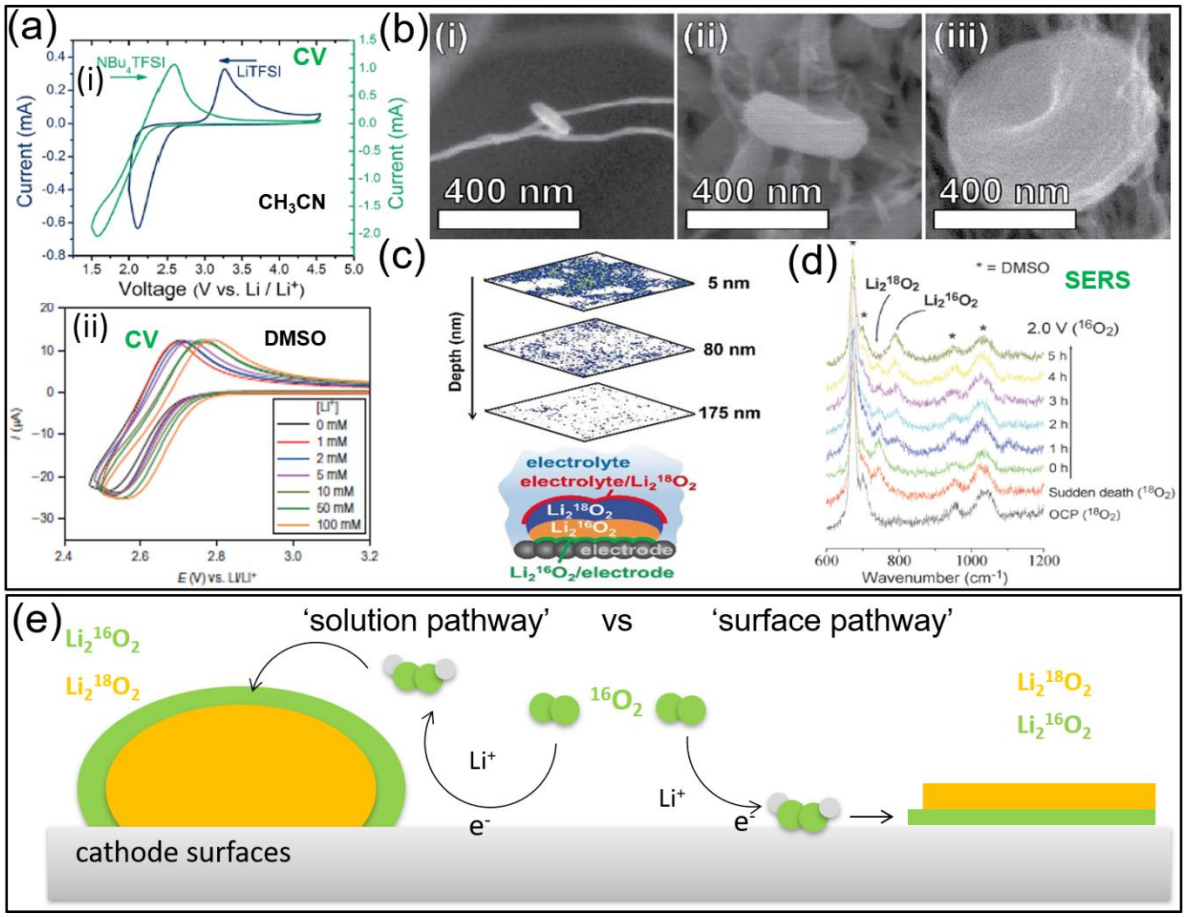

Fig. 4 Investigating the processes of LiO_2 formation, Li_2O_2 precipitation, growth and termination. (a): Cyclic voltammograms of the O_2/O_2^- couple in CH_3CN (i) and DMSO (ii) electrolytes as a function of Li^+ concentration; the effect of replacing the TBATFSI (0.5 M) solute by LiTFSI (1 M) in CH_3CN results in a positive shift of 0.25 V in the O_2 reduction potential, whereas in DMSO replacement of $TBAClO_4$ salt by $LiClO_4$ (total cation concentration is always 0.1 M) leads to positive voltage shift by only 60 mV.[30, 35] Reprinted with permission from ref 30 and 35. Copyright 2014 Nature Publishing Group and 2012 ACS. (b): SEM images show the progressive growth of Li_2O_2 particles from small nuclei with deeper discharge.[53] Reprinted with permission from ref 53. Copyright 2013 ACS.

(c): three selected layers from a 3D image of $^{18}O^-$ signals using ToF-SIMS depth scan of the discharged electrodes and a reproduced structure of a toroidal Li_2O_2 particle showing a shell region of $Li_2{}^{18}O_2$ and a core region of $Li_2{}^{16}O_2$.[54] Reprinted with permission from ref 54. Copyright 2019 Wiley-VCH Verlag GmbH & Co. KGaA, Weinheim. (d): *in situ* surface enhanced Raman spectra acquired at open circuit potential (OCP) and at the end of passivation under $^{18}O_2$ (red) followed by measurements performed at various times of further discharging under $^{16}O_2$ at 2.0 V versus Li^+/Li.[56] Reprinted with permission from ref 56. Copyright 2016 Wiley-VCH Verlag GmbH & Co. KGaA, Weinheim. (e): schematic illustration of Li_2O_2 precipitation and growth process via a solution-mediated pathway or a surface mechanism.

Subsequently, using *in situ* surface enhanced Raman spectroscopy (SERS), Peng and coworkers[56] studied the Li_2O_2 growth process occurring *via* the surface mechanism, where high discharge currents were applied and Li_2O_2 films formed. A cell was first fully discharged in $^{18}O_2$ to form a surface film of $Li_2{}^{18}O_2$ on a gold electrode. Then the cell was forced to discharge further in $^{16}O_2$ using a large overpotential at 2 V. As a result, the $Li_2{}^{18}O_2$ Raman signal was gradually replaced by $Li_2{}^{16}O_2$ (**Fig. 4d**). Since SERS is only sensitive to interfacial species close to the gold electrode surface, this replacement suggests fresh $Li_2{}^{16}O_2$ formation occurs at the buried interface between $Li_2{}^{18}O_2$ and the gold electrode,[56] as schematically depicted in **Figure 4e**. In this case, clearly O_2 and Li^+ can, perhaps in the presence of some defects, be transported through the previously deposited Li_2O_2 film, and reach the underlying gold surfaces.[56]

The phenomenon of 'sudden death' that marks the end of a cell discharge is important due to its close connection to the obtainable energy density. This rapid electrochemical polarization can stem from rising impedance at the anode and at the cathode. Many groups have shown that as Li-O_2 cells (using ether electrolytes) continue to discharge, more byproducts including LiOH, Li_2CO_3, Li_2O etc., accumulate at the Li anode surfaces due to electrolyte decomposition.[57-59] Formation of this SEI can help reduce further electrolyte decomposition, but a poor quality SEI layer (with low lithium ion conductivity) can also significantly increase the charge transfer impedance at the anode. At the cathode, it is thought that the discharge terminates when all active surfaces have been passivated by a thick layer of Li_2O_2 (a wide band gap insulator)[60, 61] and consequently the tunneling current through Li_2O_2 can no longer support electrochemical current.[62-65] Several groups have probed the charge transfer through Li_2O_2 using reversible redox couples and in situ electrochemical impedance spectroscopy, observing that the rate constants of the reversible redox couples exponentially decreased with thickening Li_2O_2 films;[62, 63, 65] The EIS measurements also revealed that the impedance associated with electronic transport through Li_2O_2 deposited at the cathode increases abruptly and considerably at the 'sudden death' on discharging,[66] whereas the impedance linked to the anode SEI increases only slightly, indicating that the rapid termination of discharge is predominantly limited by an electronic charge transport through Li_2O_2 layers covering the cathode surface.

2.1.4 Factors Governing the Solution-mediated Mechanism

From the above discussion, it is clear that promoting the solution-mediated mechanism on discharging is beneficial as it can postpone the 'sudden death'. In fact, large toroidal Li_2O_2

crystals up to tens of micron meters in diameter has been reported via a solution-phase reaction pathway (**Fig. 5a**);[67] this results in both higher specific and volumetric energy densities, because the geometric pore volume can be more efficiently taken up, thereby increasing the active/non-active material ratio. Whether the surface or solution-mediated mechanism dominates in a cell discharge is dependent on a wide range of factors, including the donor number (DN) or acceptor number (AN) of solvents,[30, 31, 34, 68, 69] association strength of salt anion with Li^+,[32, 70, 71] presence of larger cation additives that can stabilize O_2^-,[72, 73] H_2O/weak acid additives that solubilize Li_2O_2,[31, 74-76] the use of redox mediators,[41, 77-81] the reduction potential/rate,[36, 44, 82] the temperature and pressure of the cell,[83-85] and/or a combination of these factors.

The most critical factor is linked to the ability of the electrolyte to promote the formation of soluble LiO_2 in the form of $Li^+_{(sol)}$ and $O_2^-{}_{(sol)}$ or $LiO_{2(sol)}$ (**Fig. 5a**). Bruce[30] and Aetukuri[31] and coworkers found that both solvents with high DN (*e.g.*, DMSO, which better solvates Li^+), and additives with high AN (*e.g.*, H_2O, which better stabilizes O_2^-), can promote LiO_2 dissolution and thus the formation of large toroidal Li_2O_2 *via* a solution-mediated mechanism (**Fig. 5b**). They predicted that solvents with both high DN and AN are essential to realize a high capacity Li-O_2 batteries.[31] Unfortunately, high DN solvents such as DMSO,[31, 86-89] dimethylformamide (DMF),[90] N-methyl pyrrolidone (NMP)[91] are known to be less electrochemically stable than low DN solvents such as ACN[89] and ethers.[91] Khetan and coworkers, using thermodynamic analysis,[92] further showed that the chemical stability of a solvent against nucleophilic attack by superoxide and peroxide species is anticorrelated with the solvent ability to promote a solution-mediated mechanism **(Fig. 5c**). Therefore, alternative strategies to improve energy densities without compromising cell rechargeability are needed.

Many groups subsequently reported that LiO_2 dissolution can also be promoted by a judicious choice of lithium salt anion (**Fig. 5d**),[32, 70, 71] *e.g.*, NO_3^-, even in a low DN solvent, DME: the association strength of NO_3^- with Li^+ is stronger than $TFSI^-$, thereby stabilizing Li^+ in solution. The cell capacity using a $LiNO_3$ electrolyte is increased by 5 times compared to the case of LiTFSI. In addition to the salt anion, having larger alkali cations (*e.g.*, K^+) as electrolyte additives can also increase the discharge capacity by promoting a solution pathway;[72, 73] this is because according to the Hard and Soft Acid and Base Theory (HSAB), K^+ as a softer (more polarizable) cation binds less strongly with a soft O_2^- anion than the harder Li^+ cation, thus promoting the formation of a stabilized O_2^- .

Therefore, by optimizing the electrolyte salt, the constraint of identifying an electrolyte solvent that can both solubilize LiO_2 well and have good chemical stability can be relaxed, potentially providing a pathway to find an optimized electrolyte system that can afford both good rechargeability and high energy density. Another promising strategy to decouple various stringent requirements for an ideal electrolyte is the use of redox mediators that can chemically reduce O_2 and effectively drive the reaction zone of Li_2O_2 precipitation away from surface;[41, 77-81] this concept is discussed in detail in Section 4.2.

Beside the factors discussed above, electrochemical cycling parameters[36, 44, 82] and cell operation temperatures[83, 85] and O_2 pressures[84] can also affect the discharge reaction mechanism and capacity. Lower current rates, lower discharge overpotentials, higher cell temperatures and pressures all tend to promote larger Li_2O_2 formation and usually higher discharge capacities (where higher temperatures being an exception in fact lead to lower capacities). It is worth noting that increasing the solubility of LiO_2 or Li_2O_2 in electrolyte is not always a positive strategy for a Li-O_2 battery, because it may also incur serious shuttling of reduced oxygen species towards the separator and Li metal anode.[83] As a result, the Li_2O_2 deposited far away from the cathode becomes difficult to be decomposed on recharge and the anode may also be degraded due to reactions with reduced oxygen species shuttling from the cathode. Optimizing the performance of Li-O_2 batteries requires a holistic approach considering all cell components.

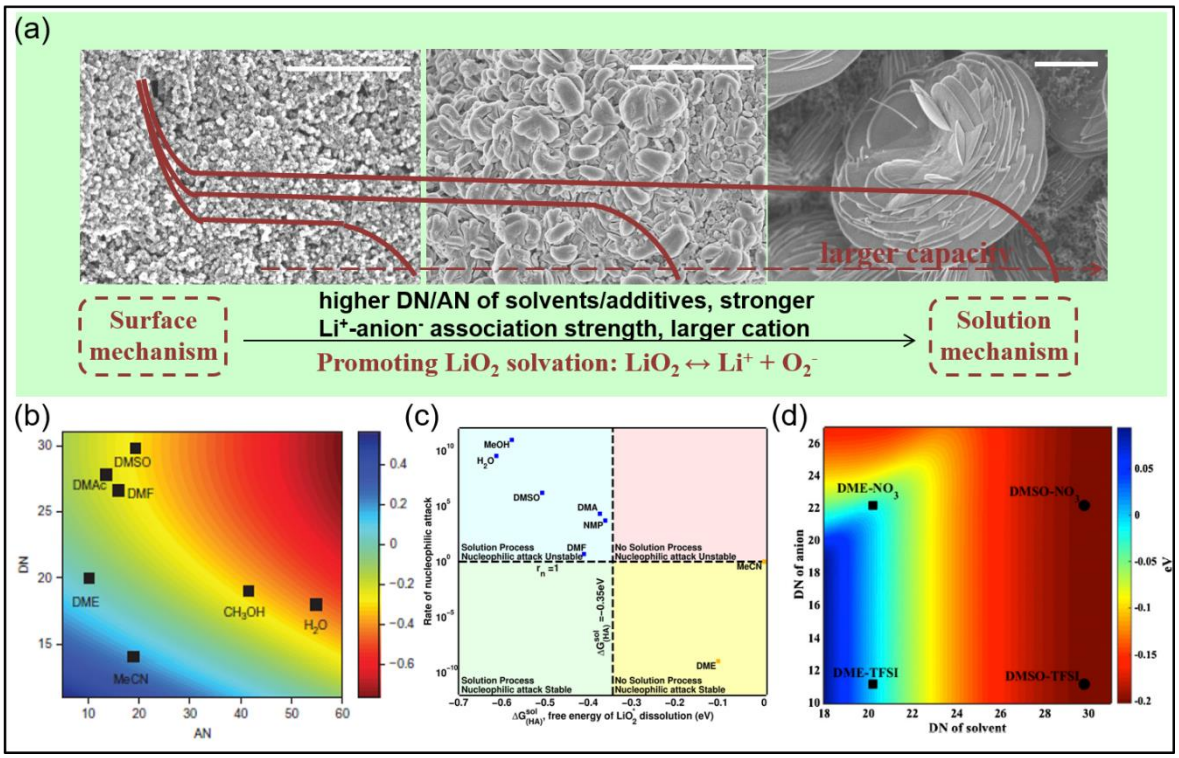

Fig. 5 Influence of electrolyte properties on the discharge reaction mechanism via a surface or a solution mediated pathway. (a): Physicochemical properties of the solvent and salt (such as donor/acceptor numbers (DN/AN), Li^+ cation-anion association strength) that can help promote a solution-mediated discharge process, which typically leads to larger discharge capacities and Li_2O_2 crystal sizes (up to tens of microns, all scale bars are 5 μm).[67] Reprinted with permission from ref 67. Copyright 2018 ACS. (b): The free energy of dissolution of LiO_2 into Li^+ and O_2^- in various solvents as a function of Gutman acceptor and donor numbers; dimethyl sulfoxide (DMSO), dimethyl formamide (DMF) and dimethyl acetamide (DMAc) have high DNs and thus can stabilize Li^+, whereas solvents (water and methanol) that have high ANs can stabilize O_2^-.[31] Reprinted with permission from ref 31. Copyright 2015 Nature Publishing Group. (c): Solvent stability against proton/hydrogen abstraction via nucleophilic attack and solvent ability to facilitate the solution mediated discharge; the susceptibility of solvents to parasitic processes is evaluated as the rate of nucleophilic attack normalized against that of acetonitrile, and their solvation capabilities are evaluated in terms of ΔG^{sol}, free energy of LiO_2 dissolution; solvents that promotes LiO_2 dissolution

can lead to higher discharge capacity, but they are susceptible to nucleophilic attack by O_2^- and suffer from limited cycle life.[92] Reprinted with permission from ref 92. Copyright 2015 ACS. (d): Contour plot showing the free energy of Li^+ solvation for electrolytes with varying DN of the solvent and salt anion, in kcal/mol; the free energy is normalized with respect to that of DME and 1 M LiTFSI. The electrolyte is a 50:50 mixture of LiTFSI and a salt consisting of Li^+ and the labelled salt anion in the solvent; red regions correspond to those can trigger solution-mediated discharge, whereas those in blue regions cannot.[32] Reprinted with permission from ref 32. Copyright 2015 National Academy of Sciences.

2.2 Charge Reaction Mechanisms

2.2.1 Solid Solution Decomposition and Liquid Phase Mediation

The mechanisms by which the charge processes occur are more varied than those seen on discharge and there is less consensus in the literature. The very different electrochemical profile and the much higher overpotentials needed for recharge compared to discharge (**Fig. 2c**) suggest that charge occurs *via* a different reaction mechanism rather than simply being a mirror process of the discharge reaction.

Earlier studies, using electrochemistry methods and *in situ* Raman spectroscopy, revealed that a high overpotential is required for the oxidation of Li_2O_2 and that no LiO_2 intermediate was observed by Raman in an ACN-based electrolyte on charging.[33, 34, 37] Consequently, it was proposed that the oxidation of Li_2O_2 is *via* a direct two electron electrochemical reaction (reaction (9)).

$$Li_2O_{2(s)} \rightarrow O_{2(g)} + 2e^- + 2Li^+_{(sol)} \quad (9)$$

Later studies suggested that the charging process can involve a mixed solid-solution decomposition and liquid phase-mediated process, depending on the solvating properties of the electrolyte, as summarized in reactions (10-13).[36, 45, 93-98] Reactions (10-11) are solid-state steps and (12-13) involve the formation of species dissolved in solution. Overall, there are still two electrons per Li_2O_2 decomposed on charging.

$$Li_2O_{2(s)} \rightarrow Li_{2-x}O_{2(s)} + xe^- + xLi^+_{(sol)} \quad (10)$$
$$Li_{2-x}O_{2(s)} \rightarrow O_{2(g)} + (2-x)e^- + (2-x)Li^+_{(sol)} \quad (11)$$
Or
$$Li_{2-x}O_{2\,(s)} \rightarrow LiO_{2(sol)} + (1-x)Li^+_{(sol)} + (1-x)e^- \quad (12)$$
$$2LiO_{2(sol)} \rightarrow Li_2O_{2(s)} + O_{2(g)} \quad (13)$$

Wagemaker and coworkers[93] investigated the charging process in a TEGDME-based (DN=16.6) electrolyte using an *operando* XRD method and observed two distinct stages in the electrochemical profile (**Fig. 6a**): an initial sloping region (3.0-3.4 V) and then gradual polarization to a flat plateau (at 3.8 V). Interestingly, the (100) and (101) diffraction peak areas of Li_2O_2 are essentially constant in the sloping region (**Fig. 6b,c**) but the Li site-occupancy

continues to decrease (**Fig. 6d**), which suggests that this sloping stage is associated with decomposition of Li_2O_2 crystal surfaces or amorphous Li_2O_2. When smaller particles (high Li_2O_2 surface areas) and more amorphous Li_2O_2 phases are formed using higher discharge rates (**Fig. 6e**)[36], a longer sloping region is observed on the following recharge. Of note, this low voltage sloping region cannot be attributed to decomposition of LiO_2 species, due to the observed two electrons per evolved O_2 in the corresponding DEMS experiments.[99] At the second stage, continuous weakening of the diffraction peak intensities and decreases in Li occupancy are observed (**Fig. 6c,d**), which supports a solid-solution reaction route and this stage is ascribed to the delithiation of bulk crystalline Li_2O_2 *via* a Li-deficient intermediate, $Li_{2-x}O_2$ (reactions (10-11)). Wagemaker *et al.* postulated that the Li_2O_2 particles continue to decompose preferentially at the surface and disappear layer by layer (schematically illustrated in **Fig. 6a**).[93] Shao-Horn and coworkers' PITT (Potentiostatic Intermittent Titration Technique) result[96] obtained in a DME-based (DN=20) electrolyte further supports this solid-solution view: the observed current in response to potentiostatic steps in the plateau region shows a peak, which is indicative of nucleation and growth of reactive sites (*e.g.*, Li vacancies) in a solid-solution reaction.

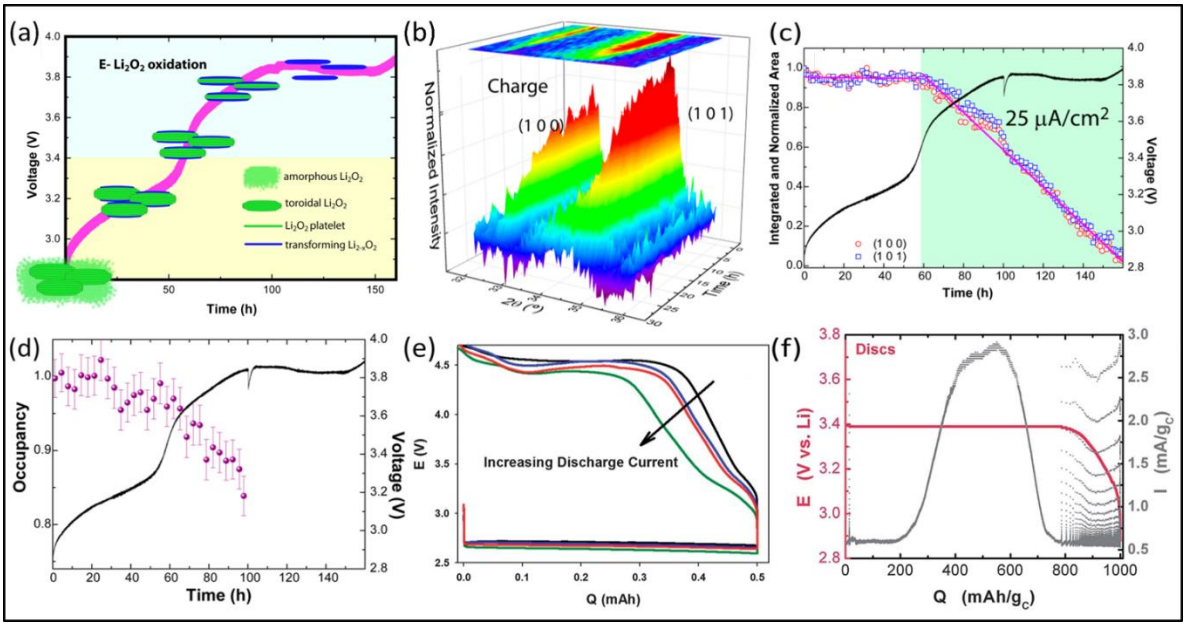

Fig. 6 Investigation of the electrochemical decomposition of toroidal Li_2O_2 crystals in a TEGDME-based electrolyte by *operando* X-ray diffraction and electrochemical methods. (a): Schematic illustration showing that the charging process undergoes first amorphous Li_2O_2 decomposition, and then anisotropic delithiation of bulk Li_2O_2 crystals. (b): three dimensional charge plots of the Li_2O_2 XRD patterns in the 2θ region of 32-36° recorded *in operando* during charging. (c): Integrated and normalized areas under the (100) and (101) peaks as a function of charging time; the pink line indicates the linear fit of the points within the shaded or unshaded areas. (d): Evolution of average lithium occupancy as a function of charging time.[93] (e): Electrochemical charge profiles of Li-O_2 cells (at a constant charging rate) following prior discharges with increasing discharge currents.[36] (f): PITT (which probes the minimum potential needed to drive an electrochemical reaction) charging of a pre-discharged cell in a TEGDME-based electrolyte.[98] (a-d) Reprinted with permission from ref 93. Copyright 2014 ACS and (e) from ref 36. Copyright 2013 The Royal Society of Chemistry. (f) From ref 98. Copyright 2013 The Royal Society of Chemistry.

Lu and coworkers[45] recently investigated in detail the correlation between the donicity of solvents and the charging mechanism. Unlike the solid-solution charging mechanism that dominates in low donicity solvents (such as TEGDME and DME discussed in **Fig. 6**), high donicity solvents such as DMSO (DN=30) and Me-Im (1-methylimidazole, DN=47) can lead to charging reactions mediated *via* the liquid phase (**Fig. 7a**). By the use of rotating ring disc electrode (RRDE) during charging, for the first time, the oxidation of LiO_2 intermediate at the ring electrode was unambiguously observed in a DMSO electrolyte, but no LiO_2 was seen in TEGDME (**Fig. 7b,c**). Similar previous attempts to observe in DMSO was unsuccessful;[44] this was probably due to the low concentration of solvated LiO_2 generated by a planar GC disc electrode: Lu *et al.* used a high surface-area particulate carbon disc electrode. Furthermore, the presence of surface LiO_2 species during charging in a high donicity solvent (*e.g.*, Me-Im) was also detected by X-ray absorption near edge structure (XANES) spectroscopy (**Fig. 7d,e**). Both the RRDE and XANES results thus strongly support the formation of LiO_2 reaction intermediate, as solid surface species and dissolved solution species, on charging. Considering that the ring current due to LiO_2 oxidation only starts to emerge beyond 3.7 V, Lu and coworkers proposed that in high-donicity solvents the first step on charging is the same as in low-donicity solvents, namely, it occurs *via* the solid-state reaction (10). The Li-deficient $Li_{2-x}O_2$ can be further delithiated to generate LiO_2 that dissolves and disproportionates to form Li_2O_2 in high donicity electrolytes, namely, *via* reactions (12-13). This redistribution of Li_2O_2 on charging was also observed by electron microscopy by the same authors.

Although high donicity solvents can promote an additional liquid-phase mass transport pathway on charging, the overpotential in Me-Im is only reduced by 0.2 V compared to diglyme (**Fig. 7f**), and a large overpotential 0.7 V remains. It thus suggests that reaction (10) is the dominant step determining the charging overpotential. Strategies to facilitate the first delithiation step of Li_2O_2 need further investigation. In addition, even though the charging voltage is slightly lower, more CO_2 evolution due to Me-Im decomposition occurs than in TEGDME,[45] consistent with many earlier conclusions that polar solvents are more susceptible to nucleophilic attack.[86-92] Therefore, under the mechanism described above, high-donicity solvents are probably not good choices to realize highly rechargeable nonaqueous Li-O_2 batteries.

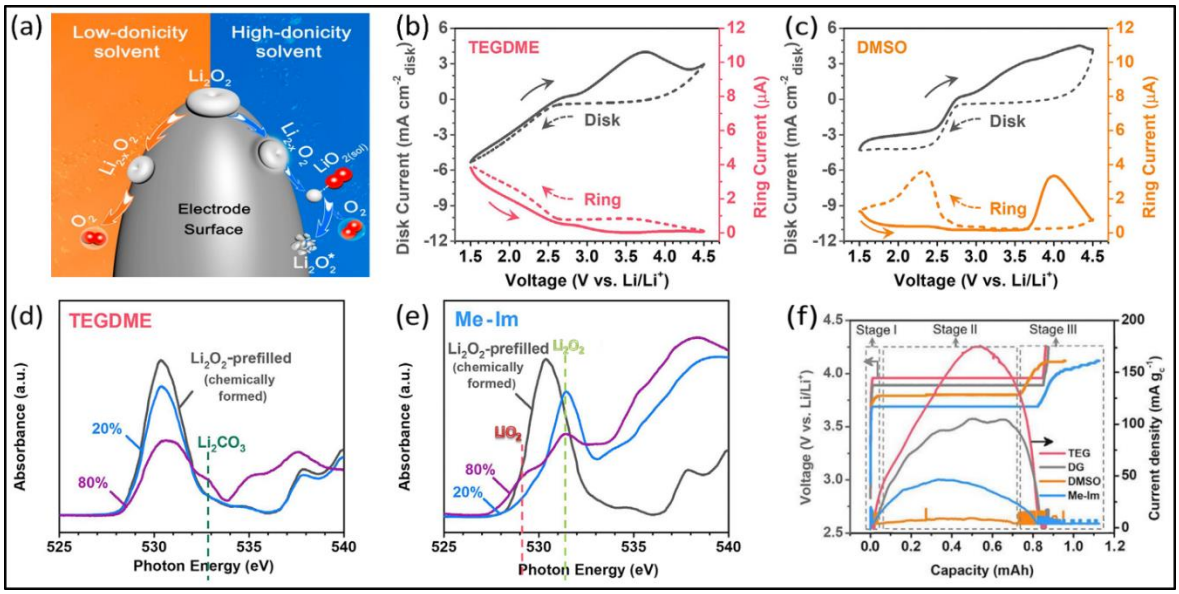

Fig. 7 Solvent dependent oxidation mechanism of Li_2O_2 in Li-O_2 batteries (a). Thin-film RRDE measurements probing the existence of any $LiO_{2(sol)}$ reaction intermediate species during Li_2O_2 formation and decomposition in 0.2 M LiTFSI TEGDME (b) and DMSO (c) electrolytes; the solid and broken lines correspond to the currents recorded in positive- and negative-direction scans, respectively. O K-edge XANES total-electron yield spectra of various charging stages for Li_2O_2-prefilled electrodes in LiTFSI/TEGDME (d) and LiTFSI/Me-Im (e) electrolytes. (f): Electrochemical profiles and current responses during PITT charging of Li_2O_2-prefilled electrodes in four model solvents, namely, tetraglyme (TEG), diglyme (DG), DMSO and Me-Im.[45] Reprinted with permission from ref 45. Copyright 2018 Elsevier.

It is worth noting that some solvents (*e.g.*, hexamethylphosphoramide[100]) and additives (Phenol[76] and water[74, 75]) can significantly increase the solubility of Li_2O_2 in the electrolyte, thereby enabling a solution-phase mediated mass transport route on charging. Effectively, the charging reaction becomes a three-step process: dissolution of solid Li_2O_2 in electrolyte, diffusion of solvated peroxide species to the surface, and decomposition of solvated peroxide at the electrode surface. This electrolyte-mediated mechanism is further discussed in Section 4.3.

2.2.2 Reaction Interfaces and Charge Transport Pathways

As can be seen from the above discussion (**Figs. 6 and 7**), many researchers have pictured, at least at low rates and overpotentials, the solid-solution decomposition and the solvent-mediated steps on charging as starting from Li_2O_2 surfaces,[35, 45, 53, 93, 95, 96, 98] that is, initiating at the Li_2O_2-electrolyte interface. This view is broadly consistent with many electron microscopic observations,[55, 101] isotope-assisted DEMS/OEMS and time of flight secondary ion mass spectrometry (ToF-SIMS) results,[35, 54] and observations in other alkali-metal oxygen batteries.[102-104] **Figure 8a(i-vi)** shows the progressive disappearance of Li_2O_2 particles with increasing depths of charge.[101] These toroidal particles gradually decrease in diameter with larger gaps being simultaneously developed between individual platelets; an intimate solid-solid contact between Li_2O_2 and the carbon electrode surface appears to be always maintained. At some point (**Fig.**

8a(iv)), individual platelets of Li_2O_2 crystals can be identified and they continue to shrink in diameter **(v)**, until complete removal **(vi)**. The constant contact between Li_2O_2 and carbon electrode suggests that O_2 evolution at the Li_2O_2-carbon interface is unlikely; otherwise, physical detachment will probably occur. If O_2 evolution occurs at the Li_2O_2-electrolyte interface, electronic and ionic charge transport through Li_2O_2 must occur on charging, even if Li_2O_2 is a known wide bandgap insulator; feasible charge transport through Li_2O_2 crystals is further supported by an *in situ* SEM study of an all solid-state Li-O_2 battery where liquid phase mediation can be ruled out.[55] Indeed, many theoretical studies identified that Li^+ vacancies and hole polarons are the charge carriers in Li_2O_2.[60, 61, 105-109] In the presence of defects, *e.g.*, generation of Li^+ vacancies in $Li_{2-x}O_2$ (a Li-deficient intermediate), the ionic and electronic conductivities of Li_2O_2 can be increased by orders of magnitude,[60, 61, 106, 110, 111] especially at the surfaces.[112, 113]

The potential charge transport mechanisms during the decomposition of a Li_2O_2 crystal are schematically illustrated in **Figure 8c**. When the reaction occurs at the Li_2O_2-electrolyte interface (**Fig. 8c(i-ii)**), charge transport can be either dominated by Li^+ vacancy diffusion or polaron hopping, or a mixture of both. Charge transport is likely to be predominantly confined to the surface, because of the higher conductivity due to a higher concentration of defects and its proximity to sites where O_2 is released. During charging, the constant solid contact between Li_2O_2 and the electrode surface indicates a strong interaction between them, especially in the presence of high overpotentials; The formation of this chemical bond at the interface has been confirmed by several studies.[54, 114, 115] On one hand, the coupling strength of the electrode surface with Li_2O_2 can be used to mediate the interfacial delithiation of Li_2O_2, but on the other hand, it also requires the substrate material to be quite resistant to Li_2O_2 oxidation.

Finally, it should be stressed that the reaction interface on charging is highly dependent on the charge rate and voltages, i.e., high rates/overpotentials tend to cause O_2 evolution at the Li_2O_2-electrode interface,[56] detaching the remaining Li_2O_2 from the electrode (**Fig. 8b,c(iii)**). This disintegration has been reported in both liquid electrolyte[116] and all-solid-state Li-O_2 setups (**Fig. 8b**).[117] This high dependence of the reaction interface on the charging rate and voltages is in part connected to the intrinsically low conductivity of Li_2O_2 for both electrons and Li^+.[56, 60, 105-109, 118] As discussed above, charging reactions occurring at the Li_2O_2-electrolyte interface necessitate continuous transport of Li^+ and/or hole polarons through Li_2O_2 (**Fig. 8c**). At low rates, Li_2O_2 decomposition at the Li_2O_2/electrolyte interface may be sustained by Li^+ and hole polaron diffusion through Li_2O_2 bulk/surfaces. However, once the transport rate cannot keep up with the current, the reaction interface can switch to the Li_2O_2/electrode interface. The latter is often observed in CV tests, where voltage sweeps induce high charging rates and as a result, the charge reaction primarily takes place at the Li_2O_2/electrode interface, thus leading to detachment of Li_2O_2 from the electrode.[119-121] Therefore, to determine where the reaction interface is, one should consider the solvating properties of the electrolyte (**Fig. 7**), the charging current, overpotentials, and more generally factors that can affect the kinetics of charge transport through

Li_2O_2 (e.g., temperature). Of note, other charging mechanisms, such as the use of redox mediators and phase transfer catalysts can also alter the reaction interface; this is discussed in detail in Sections 4.2 and 4.3.

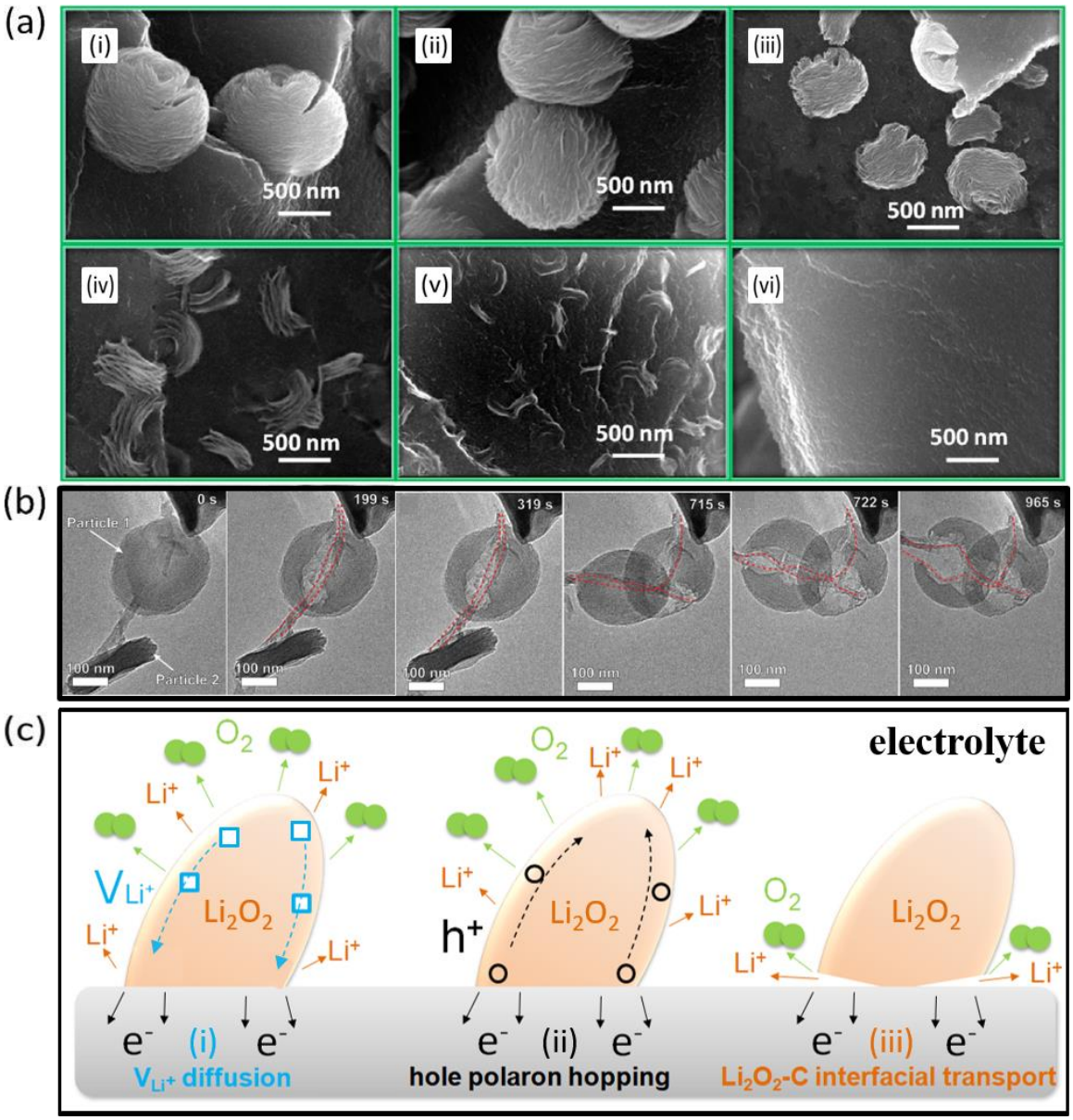

Fig. 8 Electron microscopic investigation of Li_2O_2 oxidation on charging. (a): Morphological evolution of Li_2O_2 decomposition with progressively deeper charge in a TEGDME-based electrolyte (i-vi).[101] Reprinted with permission from ref 101. Copyright 2013 ACS. (b): *in situ* TEM measurements on the decomposition of toroidal Li_2O_2 particles deposited on a carbon nanotube (CNT) electrode (highlighted by red broken lines), where a high bias voltage of 10 V against a Si anode is applied to drive the reaction.[117] Reprinted with permission from ref 117. Copyright 2013 ACS. (c): Schematic representation of three mechanistic scenarios for Li_2O_2 decomposition on charging; in the first two cases (i-ii), the reaction occurs at the Li_2O_2-electrolyte interface, where charge transfer in Li_2O_2 is mediated by diffusion of Li^+ vacancies (i) and hole polaron hopping (ii); in the third case, the reaction occurs at the Li_2O_2-electrode interface.

2.2.3 The Origins of High Charging Overpotentials

Unlike the discharge process, the charging is typically characterized by a much larger average overpotential even at low currents: the voltage profile progressively increases with deeper states of charge, from just over 3.0 V to 4.5 V, distinct plateaus being observed in many cases (**Fig. 6 and Fig. 9a**).[36, 66, 96-99] This high charging overpotential can cause considerable parasitic reactions among Li_2O_2, the cathode material and organic electrolytes, posing a significant challenge for achieving a highly rechargeable and energy efficient Li-O_2 battery.[91, 99, 122-126] Despite of its importance, the origins of the high overpotential, however, remain somewhat elusive.

Since Li_2O_2 is a wide band-gap insulator,[60, 61] many researchers ascribe this high charging overpotential to its low electrical and ionic conductivities. A number of theoretical and experimental studies show that the electrical conductivity is in the range of 10^{-9} to 10^{-12} S/cm and the Li^+ ionic conductivity is of the order of 10^{-10} S/cm at room temperature.[56, 60, 105-109, 118] These values are considerably lower than those of active materials for high-rate Li-ion battery. Nonetheless, many researchers argue that delithiation of Li_2O_2, especially at its surfaces, is quite facile[111, 112, 118] and that when in the presence of defects, the electronic and ionic conductivities of Li_2O_2 can be increased by orders of magnitude.[105, 110-113] *In situ* impedance measurements during charge following a full discharge reveal that the polarization resistance actually *decreased* from several kΩ (due to the 'sudden death' on discharging) to around 500 Ω at the beginning of charge (**Fig. 9**),[66] suggesting that low conductivities of Li_2O_2 is not an major reason for the observed high charging voltage, at least under low charging currents. CV and DEMS measurements show that the onset voltage for an oxidation current in CVs (**Fig. 4a**) is quite close (<0.2 V) to its equilibrium value,[35] where O_2 evolution is indeed detected,[99] implying a low reaction kinetic barrier and a small ohmic loss.

Another viewpoint relates the continuously rising overpotential with charging capacity to the gradual detachment of Li_2O_2 from the cathode,[127, 128] where the decomposition reaction is considered to occur preferentially at the cathode-Li_2O_2 interface (**Fig. 8c(iii)**). This mode of charging mechanism, as discussed previously, is typically observed at high charging currents or high overpotentials.[56, 116, 117] If this were indeed the case, an increase of the charge resistance by at least an order of magnitude would be expected; but experimentally the resistance upon charging does not increase,[66] so physical detachment cannot explain the high overpotentials seen at low current conditions.

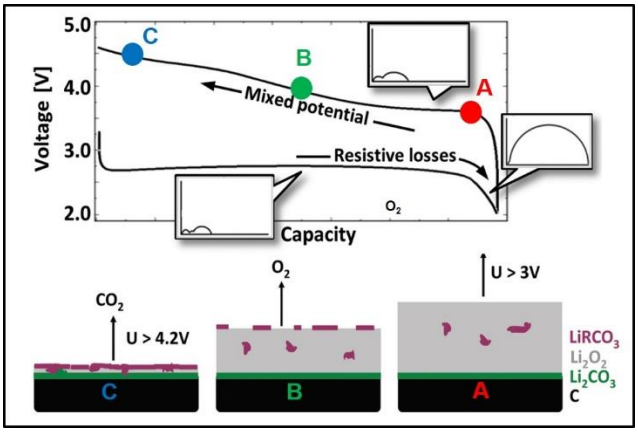

Fig. 9 Electrochemical impedance measurements of Li_2O_2 formation and decomposition processes at various stages of charge, A-C. Substantial increase in polarization resistance occurs towards the end of the discharge, whereas at the beginning of the charging, this polarization resistance decreases compared to that at the end of the prior discharge.[66, 99] Reprinted with permission from ref 66 and 99. Copyright 2015 ACS and 2012 ACS.

McCloskey, Shao-Horn and coworkers proposed that the rising overpotential with a deeper charge is primarily caused by parasitic reactions.[66, 99, 123, 129] It has been shown by many groups that on charging considerable parasitic reactions occur involving Li_2O_2, the carbon electrode and the organic electrolyte.[91, 99, 122-124, 126] As a result, layers of Li_2CO_3 (and other insulating by-products) accumulate at the Li_2O_2-cathode and Li_2O_2-electrolyte interfaces with deeper states of charging and over repeated cycles (**Fig. 9**).[91, 99, 122-124, 126] The interfacial Li_2CO_3 likely plays a decisive role in determining the sluggish oxidation kinetics. It is established that Li_2O_2 decomposition can readily occur at just over 3 V, whereas Li_2CO_3 can only be decomposed at beyond 4 V.[66, 99, 129] McCloskey *et al.*[66, 99, 129] thus proposed that the gradual rising charging profile is a reflection of mixed potentials due to the low oxidizing potential of Li_2O_2 and the high decomposition potential of Li_2CO_3, its actual value being critically dependent on the Li_2O_2/Li_2CO_3 ratio at the interfaces, and thus depth of charge (**Fig. 9**).[66] Their hypothesis is consistent with the experimental observation that the average charging voltage increases when more Li_2CO_3 is present at the Li_2O_2-electrlyte interface: as the voltage rises on charging, O_2 evolution due to Li_2O_2 progressively reduces while CO_2 evolution due to Li_2CO_3 decomposition continues to increase beyond 4 V.[99, 123, 124, 126, 129] Subsequent modeling shows that just two monolayers of Li_2CO_3 on top of Li_2O_2 can reduce the transport current by two orders of magnitude, reiterating the critical challenge due to the interfacial Li_2CO_3 formation.[99]

In summary, at lower rates, the observed high overpotentials are likely to be a combined result from both byproducts accumulation at the reaction interfaces and the insulating nature of all deposits (Li_2O_2, Li_2CO_3 and so on). At high rates, physical detachment of Li_2O_2 from the electrode and loss of electrical contact may become the dominant reason. In addition to the aforementioned factors, clogging of porous carbon electrode[130] by byproducts and degradation of

Li metal anode[131] due to an unstable solid-electrolyte interface (SEI) are other plausible reasons for the increasing polarization.

Although further investigations are required to fully unravel the origins of high charging voltages, existing evidence highlights the necessity of enabling faster charge/mass transport kinetics and minimizing parasitic byproduct formation and accumulation during charge. Soluble redox mediators that can chemically decompose Li_2O_2 have been considered as a promising strategy to achieve these goals.[127] Facile charge (electron/hole) transfer pathways in electrolytes are realized by shuttling of reduced/oxidized mediator molecules between the electrode surface and Li_2O_2, the latter being decomposed by the oxidized state of the mediator. This approach will be discussed in detail in Section 4.2.

2.2.4 Parameters Characterizing the Reaction Reversibility

The reversibility and performance metrics have been intensively discussed since the early days of lithium-air battery research.[91, 126, 132, 133] It was gradually realized that coulometry alone is insufficient to evaluate the true reversibility of a Li-O_2 battery. Therefore, it is of paramount importance to use multiple quantification methods to investigate the discharge-charge cycles.[132] McCloskey[35, 91, 99, 132], Bruce[134] and their coworkers designed a series of *in situ* and *ex situ* characterization methods, namely mass spectrometry (differential electrochemical mass spectrometry, DEMS [27, 122] and online electrochemical mass spectrometry, OEMS[135, 136]) and chemical titration,[126, 137] to quantify the O_2 consumption/evolution and Li_2O_2 formation/decomposition at different stages of cycling. Parasitic reaction products, such as Li_2CO_3 and Li carboxylates *etc*., can also be quantified by FTIR, NMR, mass spectrometry and UV-vis methods.[132, 134, 138]

Since gaseous O_2 is converted to a solid on discharging and is expected to be released back to the atmosphere on charging, the ratio of O_2 evolution/consumption or O_2 recovery efficiency (OER/ORR) of a single electrochemical cycle is the most critical parameter to assess the battery reversibility.[91, 132] This parameter can be obtained by DEMS/OEMS measurements. **Figure 10(a-c)** shows the quantification of O_2 and Li_2O_2 at different states of discharge and charge using DEMS and titration. When O_2 is reduced on discharging, DEMS data show that the oxygen reduction reaction closely follows the expected 2 electrons per O_2 stoichiometry, although Li_2O_2 titration suggests that not all the reduced O_2 ends up as Li_2O_2. During Li_2O_2 decomposition on charging, titration shows that the Li_2O_2 is quantitatively removed as expected from stoichiometry, with small deviations only toward the end of charge. What is more significant on charging, however, is that the actual released O_2 is much less than the expected value from the decomposed Li_2O_2; this discrepancy was later associated with the fact that part of the O_2 evolved is released in the form of singlet O_2, which is consumed in degradation reactions.[139, 140] Overall, O_2 evolution amounts to only ~75% of O_2 consumption (OER/ORR=0.75).[132] The lost oxygen is

primarily converted to parasitic reaction products, such as CO_2, Li_2CO_3, LiOH, $LiRCO_3$ *etc*., by corroding the carbon electrode and decomposing the organic electrolyte (**Fig. 10a**). To achieve a highly reversible Li-O_2 battery, these parasitic reactions must be considerably suppressed.

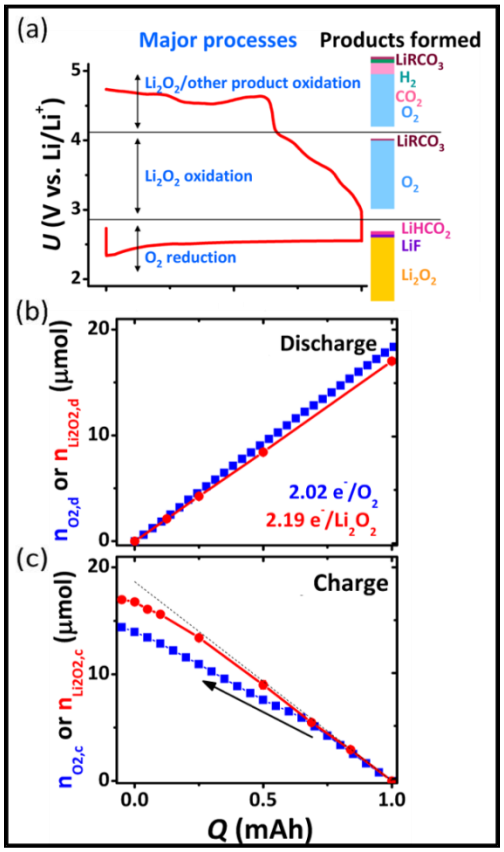

Fig. 10 A combination of quantitative gas and chemical analysis techniques (such as DEMS, titration, NMR etc.) are needed to quantify the amount of Li_2O_2 and parasitic reaction species formed and decomposed, and the associated O_2 consumption/evolution at the different states of discharge and charge (a). On discharging, the electrochemical O_2 reduction reaction closely follows the $2e^-/O_2$ molar ratio (b), although not all the electrochemical reduced O_2 ends up as Li_2O_2, resulting a slight deviation of the titrated Li_2O_2 from that of e^-/O_2. On charging (c), Li_2O_2 removal closely follows the $2e^-/Li_2O_2$ trend line until the end of charge, although the detected O_2 evolution considerably deviates from the ideal $2e^-/O_2$ molar ratio.[132] Reprinted with permission from ref 132. Copyright 2013 ACS.

3. Key Remaining Challenges: Parasitic Processes

In the early years of research, there were many daunting challenges facing lithium-air batteries,[5-8] such as low rate capability, low practical capacity, large voltage hysteresis, Li metal anode dendrite formation, and very poor rechargeability due to parasitic reactions. Over the past 8 years, significant progress has been made to address some of these challenges. For example, we now understand that the practical cell capacity can be improved by wisely choosing the salt/solvent/additives for an electrolyte,[30-32] the rate can be increased by the use of mediators,[67, 81] overpotentials and carbon/electrolyte corrosion can be reduced by using catalysts/redox

mediators.[115, 127, 141, 142] As a result, the rechargeability of a lithium-air battery has significantly improved over the past few years.

Nevertheless, many critical challenges still remain concerning the stability of electrodes and electrolytes due to parasitic processes. Reactive oxygen species formed during discharge and charge can seriously degrade the cathode material and the organic electrolyte; the situation is even worse in the presence of high overpotentials. Further reduction of these unwanted side reactions is required to realize practical applications of the battery. In addition, most current lab-scale lithium-air batteries still use pure O_2 as the atmosphere. Gas separation and purification technologies have been proposed[28] to resolve the air contamination issue to both O_2 cathode and Li anode. These air treatment and handling accessories, however, will significantly compromise the specific energy of lithium-air batteries. Simpler and lighter components, such as a single gas separation membrane, currently cannot remove to a low enough level all the unwanted air contaminants (*i.e.*, H_2O, CO_2 and N_2) that can react the lithium metal and the various products and intermediates found in Li_2O_2 chemistries. This is related to the similarities of gas kinetic diameters and molecular chemical properties as compared to O_2, making it very difficult to achieve both high permeance and selectivity of O_2 in a single stage separation.[143-147] Hence a practical lithium-air battery may eventually have to tolerate hundreds ppm of CO_2, H_2O, and N_2, if it were to be used in electric vehicles, a commonly proposed application. In this section, we review the original causes of parasitic reactions occurring to the organic electrolyte, the carbonaceous electrode and the lithium anode, and discuss the effects of other air components (N_2, CO_2, H_2O) on the electrochemistry at both the O_2 cathode and Li anode.

3.1 (Electro-)chemical Instability of Electrolytes

An ideal electrolyte for lithium-air batteries should satisfy the following requirements:[8, 91, 122, 148-152](1) low volatility and nonflammability; (2) high O_2 solubility and diffusivity; (3) formation of a stable solid electrolyte interface layer with the Li metal anode; (4) outstanding chemical and electrochemical stability in the presence of reactive oxygen species. Among them, electrolyte stability in the presence of electrode reactions is the most basic and critical requirement; this is the focus of discussion in this section, particularly on the stability issues involving the O_2 electrochemistry. The compatibility of Li metal anode and electrolytes will be discussed in Section 3.3. As we will see, to satisfy even just the stability requirement of electrolytes presents a substantial scientific challenge, primarily because many of the desired physicochemical properties of an electrolyte are inversely correlated with each other.

3.1.1 Mechanisms of Electrolyte Decomposition by Reactive Oxygen Species

A nonaqueous electrolyte for a lithium-air battery typically consists of a lithium salt and an organic solvent.[91] At the end of Section 2, we mentioned that there is significant electrolyte decomposition at the cathode during battery cycling.[40, 91, 99, 122-126, 139, 153] These parasitic

reactions are caused by a number of reactive oxygen species, including superoxides (O_2^-, LiO_2, HO_2),[40, 154] peroxides (Li_2O_2, $Li_{2-x}O_2$)[93, 94, 101, 125, 155, 156] and singlet oxygen ($^1O_2$).[139, 153]

Since the 1970s, many insightful studies have been performed on the reactivity of these oxygen species, particularly superoxide, towards organic solvents.[50, 157-161] Their reactivity derives from the fact that they are strong nucleophiles (superoxide and peroxide), strong bases (superoxide and peroxide), good one-electron transfer agent (superoxide), and radicals (superoxide). Because of its high nucleophilicity, O_2^- has the tendency to attack the positively charged components of any organic species in the absence of protons.[90, 91, 122, 134, 157] When acidic groups are present in a solvent molecule, proton abstraction from the solvent by O_2^- due to its basicity may play a significant part in the reaction characteristic.[87, 90, 150] Autoxidation by O_2^- and O_2 has also been proposed to be a general mechanism that degrades electrolytes.[162-165] On the other hand, parasitic processes due to the radical nature of superoxide are much less discussed in literature; but it may become more relevant in the presence of redox mediators, where irreversible reaction of superoxide with redox mediator radicals may occur.[166] **Figure 11** summarizes some common side-reaction mechanisms of the reactive oxygen species with organic solvents, namely, nucleophilic attack, acid-base reaction, proton-mediated degradation, and autoxidation.[167] Some of these reactions can also involve the peroxide species, which are nucleophilic and basic as well. Another pivotal factor that must be mentioned is the coordination of solvents with Li^+, which being a strong Lewis acid can further polarize solvents, facilitating degradation processes *via* nucleophilic attack and proton abstraction.[88, 168-170]

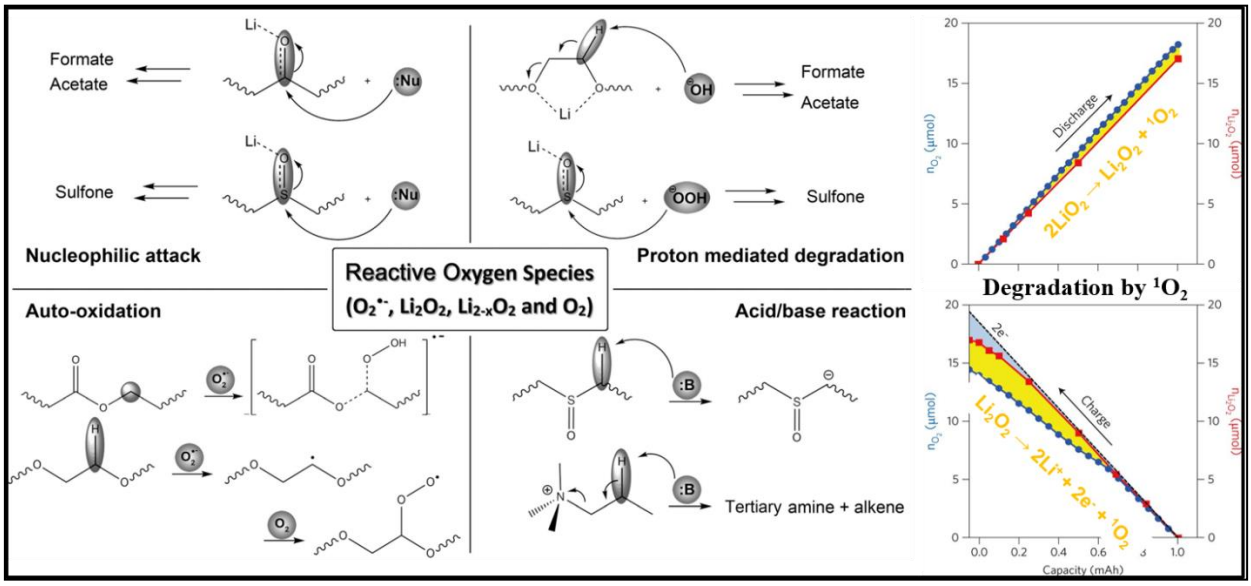

Fig. 11 Schematic illustration of various decomposition mechanisms of organic electrolytes by reactive oxygen species (O_2^-, Li_2O_2, $Li_{2-x}O_2$, O_2, $^1O_2$) in a Li-O_2 battery, such as nucleophilic attack, proton mediated decomposition, autoxidation, acid/base reactions, degradation induced by singlet oxygen.[167, 171] Reprinted with permission from ref 167 and 171. Copyright 2016 Wiley-VCH Verlag GmbH & Co. KGaA, Weinheim and 2017 Nature Publishing Group.

Given the above information and experimental observations, considerable effort has been made to find an ideal electrolyte solvent, which is optimized with respect to the electrolyte's properties against nucleophilic attack, hydrogen/proton abstraction, and on promoting electrochemical stability. Unfortunately, even with large-scale solvent screening methods, this search for an optimal organic electrolyte has largely proven fruitless thus far.[91, 163, 165, 172-177] For instance, through screening a large number of solvents, a few groups[175, 177] have identified descriptors that can characterize the stability of a solvent in the lithium air battery context (**Fig. 12**): bond dissociation energy (relating to H-abstraction), deprotonation free energy/pK_a (relating to acid-base reaction), nucleophilic substitution free energy (relating to nucleophilic attack) and HOMO level (electrochemical stability against oxidation). As can be seen in **Figure 12**, the scope for a promising electrolyte is quite constrained.[91, 175, 177] High chemical stability to nucleophilic attack and H abstraction dictate a solvent with low electron affinity, whereas high electrochemical stability requires a solvent with high ionization potential. These two requirements, unfortunately, are inversely correlated. To alleviate this issue, one needs to find alternative strategies to decouple these requirements for an optimal electrolyte. For instance, the use of redox mediators that significantly reduce the overpotentials is an effective strategy to achieve a more stable electrolyte against reactive oxygen species; this is because the smaller electrochemical window (due to lower overpotentials) permits the use of electrolytes with low electron affinity, thereby less prone to nucleophilic attack or H abstraction by superoxide species. The strategy of redox mediators is discussed in detail in Section 4.2.

Recently, the important role of singlet oxygen ($^1O_2$) in electrolyte decomposition of metal-oxygen batteries has been unraveled.[139, 140, 153, 178, 179] There is a rich literature on the reactivity of $^1O_2$ with organic materials, where peroxide, hydroperoxide species and hydroxyl radicals can be generated by $^1O_2$ reactivity and cause further transformation of organic molecules.[180] By using $^1O_2$ trapping molecules such as 2,2,6,6-tetramethyl-4-piperidone[139] and 9,10-dimethylanthracene (DMAn)[153], several groups found that $^1O_2$ was formed on both discharge and charge. Two major processes have been suggested for $^1O_2$ generation:[139, 153] 1) chemical disproportionation of superoxide species (LiO_2 or HO_2) to form peroxide on either discharge or charge; 2) electrochemical LiO_2 or Li_2O_2 decomposition occurring at charging voltages higher than 3.26-3.43 V (estimates for the thermodynamic $^1O_2$ generation voltage=equilibrium potential of O_2/LiO_2 + energy difference between $^1O_2$ and $^3O_2$).[153] Electrolyte decomposition products due to $^1O_2$, such as Li_2CO_3 and Li formate, are detected in a DME-based electrolyte, similar to those incurred by reduced oxygen species;[153] this may be connected to the fact that reactive oxygen species (*e.g.*, peroxides) can be generated via reactions of $^1O_2$ with organic solvents.[180] Further quantitative analysis suggests that $^1O_2$ accounts for a major fraction of the side reaction product formed during cycling of aprotic lithium-oxygen batteries.[153] These results nicely explain the large discrepancy observed between quantities of evolved O_2 actually detected and that expected from the decomposition Li_2O_2 on charging (**Fig. 11**),[171] which amounts to ~20% of O_2 loss per cycle. If reactions of $^1O_2$ are indeed the dominant underlying issue hampering reversibility, the current strategies centered around superoxide/peroxide reactivities to minimizing parasitic

reactions must be adjusted. New strategies that can either prevent formation of singlet O_2 or quench its reactivity with the electrolyte are urgently needed; this is discussed in Section 4.3.3.

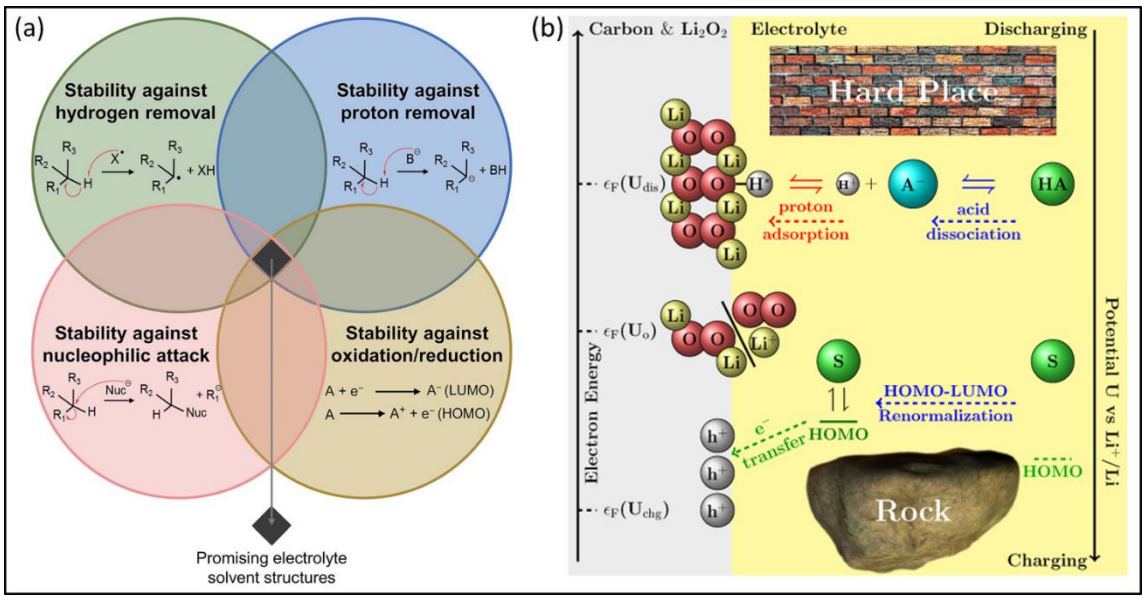

Fig. 12 Criteria for assessing the electrochemical and chemical stability of an organic electrolyte in a Li-O_2 battery, including bond dissociation energies, acidity (deprotonation free energies), nucleophilic substitution free energy, and electrochemical stability. These parameters are used to evaluate the susceptibility of molecules to hydrogen abstraction, deprotonation, nucleophilic substitution and redox reactions. Some of these required properties (e.g., nucleophilic substitution free energy and electrochemical stability) for an ideal organic solvent are inversely correlated, leading to a significant challenge in identifying an optimal electrolyte.[175, 177] Reprinted with permission from ref 175 and 177. Copyright 2014 ACS and 2017 The Royal Society of Chemistry.

3.1.2 Progress in Solvent Discovery

A wide range of organic solvents with different functional groups and structures has been explored experimentally and theoretically as electrolytes for lithium-air batteries. These mainly include carbonates,[134, 181, 182] sulfoxides,[86-89] sulfones,[183-185] polyethers,[164, 169, 186-191] nitriles,[91] amides[90, 100, 149, 192-194] and room temperature ionic liquids.[150, 195-202] As discussed earlier, all these electrolytes suffer from parasitic reactions due to reactive oxygen species, but to a different extent. Unlike in most other electrolytes where Li_2O_2 is the main discharge product, carbonate-based electrolytes mainly lead to byproduct formation (such as Li_2CO_3 and carboxylates) due to the nucleophilic attack of superoxide.[134, 181, 182] Later on, another polar solvent, DMSO, had been considered as a promising electrolyte, encouraged by a few earlier reports.[203, 204] But the subsequent investigations suggest that it is also prone to nucleophilic attack and H abstraction by superoxide,[86-89, 205] and that the OER/ORR ratio is actually lower than those using less polar electrolytes.[45, 91, 132, 206, 207] Ethers such as glymes are less polar and generally suffer less from side reactions, although H abstraction by superoxide and peroxide species still occur.[164, 169, 186-191]

More interesting but yet less understood properties have been reported on using nitriles, ionic liquids and amides as solvents for lithium air batteries. In one systematic study, an acetonitrile electrolyte exhibits the highest reversibility of all other 8 solvents, with OER/ORR of 88% (**Fig. 13a**).[91] On discharging, the e^-/O_2 ratio equates to 2.01. On charging, O_2 evolution nicely follows the expected trend line until the end of charging, where CH_3CN decomposition starts to occur above 5 V versus Li^+/Li. This result suggests that little parasitic reaction due to reactive oxygen species (Li_2O_2, $Li_{2-x}O_2$, $^1O_2$ etc.) occurred during 90% of the recharge, that is, acetonitrile exhibits both high electrochemical stability and chemical stability against nucleophilic attack and H abstraction (clearly an outlier from the theoretical considerations). The origin of these observations is thus worthy of further investigation. Of note, although CH_3CN is not stable in contact with the lithium anode, protection of the lithium anode with a solid electrolyte coating could overcome that issue.

Many room-temperature ionic liquids, such as imidazolium-, pyrrolidinium-, and piperidinium-based ionic liquids, have been explored as solvents for lithium air batteries. Not all the ionic liquids exhibit suitable chemical stability in lithium oxygen cells, but pyrrolidinium-based ILs have been reported to be stable against superoxide attack.[150, 198, 200, 208-211] It is interesting to note that, under some conditions, the onset charging voltage is just over 3 V and the majority of charging capacity finishes below 3.5 V (**Fig. 13b**).[150, 199, 212] Online mass spectrometry measurements confirm that the charging process is close to $2e^-/O_2$.[150] This ability to decompose Li_2O_2 at well below 3.5 V, much lower than in other common organic solvents, is useful and intriguing. Is this lowered kinetic barrier linked to a better solvation of O_2^- by the soft ionic liquid cation, so that the sluggish 1st step delithiation of Li_2O_2 to $Li_{2-x}O_2$ (or LiO_2) becomes easier? Or does the ionic liquid better dissolve parasitic reaction products (e.g., Li_2CO_3) and the discharge product (Li_2O_2) by solvating CO_3^{2-} and O_2^{2-}, so that the mixed charging potential issue is alleviated; or is a more facile mass transport route for peroxide via the liquid phase enabled by the ionic liquid, which essentially acts as a phase transfer catalyst promoting an electrolyte-mediated charging process? While the reactivity of IL cations with superoxide can be improved via molecular engineering, the significance of understanding the above questions may have a broad impact on how to improve the Li-O_2 electrochemistry. It could help further understand the origin of high charging voltages and develop new mechanisms to improve the energy efficiency. In general, a low cycling voltage hysteresis is always desirable, as it relaxes the other constraints on satisfying the challenging chemical stability requirement in a lithium-air battery.

Another group of solvents that have been intensely studied are amides. Bruce and coworkers investigated common amide solvents, including N,N-dimethyl formamide (DMF), N,N-dimethyl acetamide (DMA) and N-methyl-2-pyrrolidone (NMP).[90] Due to high polarity and acidity of amides, considerable parasitic reactions due to nucleophilic attack and acid-base reactions were observed, and the battery's capacity faded by more than 50% in 10 cycles, even when lithium iron phosphate was used as the counter electrode.[90] Later on, however, Walker, Addison and coworkers reported that by using DMA and N-methylacetamide (NMA) as the electrolyte solvent,

the cell showed no discharge capacity decay after 80 cycles, at 1 mAh/cm^2 per cycle. O_2 evolution over extended cycles was confirmed and OER/ORR ratio was estimated to be ~85% (based on pressure measurements).[90, 149, 194] More recently, Peng and coworkers reported the use of hexamethylphosphoramide (HMPA) as the electrolyte solvent.[100] An outstanding cycling stability, that is, no discharge capacity decay (~1 mAh/cm^2 per cycle) up to 180 cycles, was demonstrated. Furthermore, more than 95% of oxygen was recovered on charging (OER/ORR>95%) over the first 100 cycles, suggesting that only very minimal side reactions occur during discharge and charge. The authors ascribed the excellent performance to the increased solubility of Li_2O_2, LiOH and Li_2CO_3 in HMPA that helps reduce the charging overpotential and postpone the complete electrode passivation caused by side reactions. The work by Peng and coworkers indicates that solvents with higher Li_2O_2 solubility can potentially provide a facile solution-phase charging mechanism and significantly lower the charging voltage, consistent with the role of a phase transfer catalyst proposed in literature.[75, 76, 104] Therefore, influential factors that promote Li_2O_2 dissolution in electrolytes and the mechanism of the solvated peroxide decomposition on the electrode surface are worth exploring further.

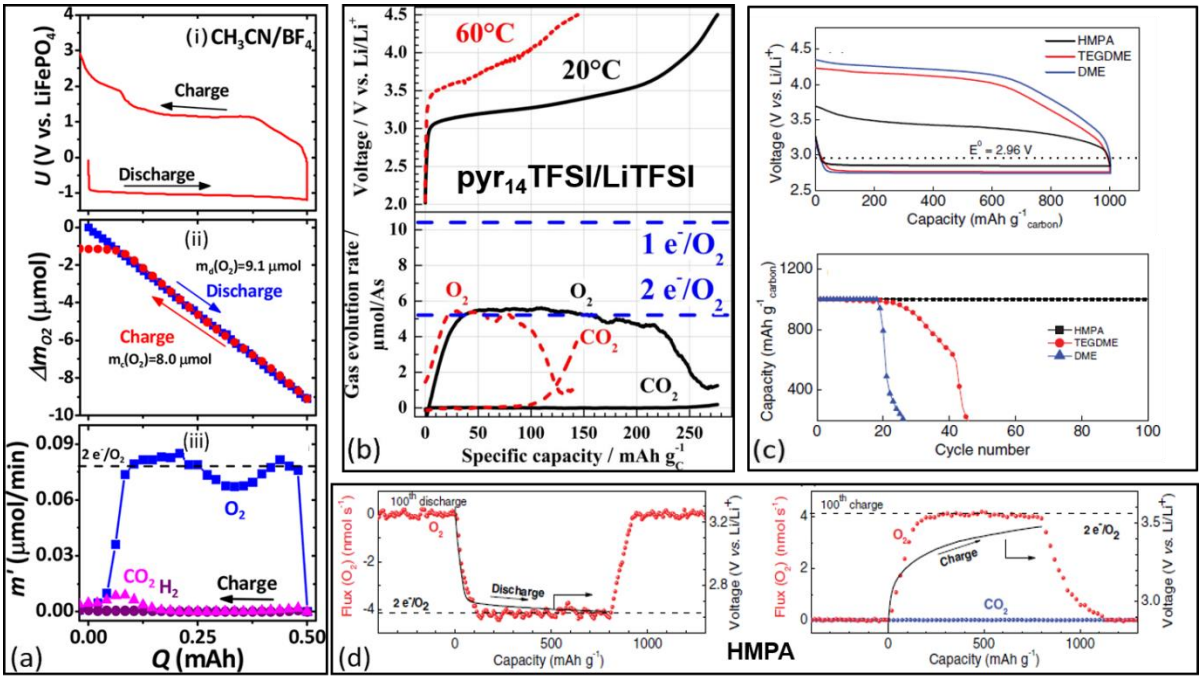

Fig. 13 A few selected electrolyte systems that exhibit interesting properties for Li-O_2 batteries. (a): Galvanostatic discharge-charge (i) for a cell using 1 M $LiBF_4/CH_3CN$ electrolyte (note: $LiFePO_4$ is the counter electrode); the cell was discharged under O_2 and charged under Ar, the corresponding O_2 consumption and evolution were quantified (ii-iii).[91] (b): OEMS analysis of the first charge of a Li-O_2 cell using a LiTFSI/Pyr_{14}TFSI ionic liquid electrolyte at 20 and 60°C; O_2 evolution from Li_2O_2 decomposition occurs at as low as 3.0 V in this electrolyte system.[150] (c): Galvanostatic cycling of Li-O_2 cells using hexaphosphoroamide (HMPA), tetraglyme (TEGDME) and monoglyme (DME) based electrolytes, where HMPA shows a superior performance with much lower charging overpotential and better rechargeability than the other two cases; the corresponding DEMS analysis on O_2 consumption and evolution is presented in (d), where at the 100th cycle the OER/ORR ratio is still close to 100%.[100] (a) Reprinted with

permission from ref 91. Copyright 2012 ACS and (b) from ref 150. Copyright 2014 Electrochemical Society. (c-d) From ref 100. Copyright 2017 Wiley-VCH Verlag GmbH & Co. KGaA, Weinheim.

3.2 Parasitic Reactions at the Carbon Cathode

3.2.1 Carbon Corrosion at the Carbon-Electrolyte and Li_2O_2-Carbon Interface

Carbon is the most extensively explored host material for Li_2O_2, due to its light weight, low cost, high electrical conductivity, processability into various structures and forms, relative stability *etc*. The chemical stability of carbon cathode against the reactive oxygen species has a profound impact on the reversibility of the battery. Many fundamental studies have been performed to elucidate the corrosion mechanism of carbon cathode, especially in the presence of high overpotentials.[99, 123, 124, 126, 213-215] It is now realized that charging overpotentials,[99, 126] types of electrolyte,[91, 126] the carbon surface defect and functionalization[126, 215] can all affect carbon degradation in a Li-O_2 battery.

McCloskey and coworkers[99] first raised the issue that in the presence of the discharge product, Li_2O_2, and a highly oxidizing environment, carbonaceous cathode may undergo oxidation reaction to form Li_2CO_3, *via* reactions (14-15).

$$Li_2O_2 + C + ½\ O_2 \rightarrow Li_2CO_3 \qquad (14)$$

, where ΔG^o is equal to -542.4 kJ/mol at 300 K.

$$2Li_2O_2 + C \rightarrow Li_2O + Li_2CO_3 \qquad (15)$$

, where ΔG^o is equal to -533.6 kJ/mol at 300 K.

As suggested by the ΔG^o of these reactions, the formation of Li_2CO_3 by reacting Li_2O_2 with carbon cathode is thermodynamically highly favorable. It implies that there should be significant Li_2CO_3 formation at the Li_2O_2-carbon interface at the end of discharge. Nonetheless, only very little Li_2CO_3 byproduct was detected on discharging,[132] for example, in ether-based electrolytes. To further investigate this source of Li_2CO_3, Xu and coworkers[213] performed solid state ^{13}C nuclear magnetic resonance measurements on a ^{13}C-enriched (99%) carbon cathode after discharge, which was then compared to that detected on natural abundance carbon cathode. If the formed Li_2CO_3 was indeed due to a direct reaction with the ^{13}C cathode, the ^{13}C NMR signal of Li_2CO_3 would be higher by around two orders of magnitude than that of a natural abundance sample. However, this was not observed to be the case. In addition, the Li_2CO_3 species was easily rinsed off by solvents.[213] Therefore, on discharging the observed Li_2CO_3 is likely to be due to electrolyte decomposition rather than direct carbon corrosion.[91, 126, 132, 213] Although thermodynamics permits the Li_2O_2-carbon reaction (reactions (14-15)), the kinetics of the Li_2O_2-carbon reactions is slow.

At the carbon-electrolyte interface, carbon corrosion can also be induced by other reactive oxygen species, such as superoxide (O_2^-, LiO_2,) and singlet oxygen (discussed in Section 3.1.1); this process is dependent on the type, crystallinity and surface functionality of the carbon cathode.[215-219] Bruce, Shao-horn and coworkers[126, 215, 218] found that carbon cathodes (graphitic carbon or reduced graphene oxides) with high density of oxygenated groups (C=O, C-O, C-OH, COOH *etc*.) exhibit limited stability against the lithium-oxygen electrochemistry: superoxide species formed during discharge can oxidize carbon at the defect site to form Li_2CO_3.[215] Kang, Itkis and coworkers[216, 217] further pointed out that the crystallinity of the carbon cathode also has an impact on its chemical stability: more ordered carbon structures are preferred for a stoichiometric Li_2O_2 reaction.

Charging is a completely different case. McCloskey, Bruce and coworkers[99, 126] made cells using ^{13}C-labeled carbon electrode but naturally abundant ether-based electrolytes, and monitored the CO_2 evolution on charging using DEMS. They observed that $^{12}CO_2$ evolved at all charging voltages, but significant $^{13}CO_2$ only started to evolve beyond 3.8 V (**Fig. 14a**); this observation suggests that electrolyte decomposition occurs at all charging voltages (due to reactions[45, 91, 125, 139, 178] with Li_2O_2, $Li_{2-x}O_2$, LiO_2 and $^1O_2$), whereas direct carbon corrosion happens only at higher charging overpotentials, CO_2 being evolved due to electrochemical $Li_2{}^{13}CO_3$ decomposition.[99, 129] Furthermore, they also observed that ^{18}O-labeled $Li_2{}^{18}O_2$ formed in the prior discharge led to scrambled $^{12}C^{16,18}O_2$ evolution on charging (**Fig. 14a**),[99] which indicates that the oxygen in CO_2 comes from both Li_2O_2 and the electrolyte. McCloskey and coworkers[99] thus proposed that as the charge proceeded, parasitic reactions occurred at both the Li_2O_2-electrolyte and Li_2O_2-carbon interfaces, with Li_2CO_3 being accumulated over repeated cycles. The proposed locations of the interfacial Li_2CO_3 were confirmed later by X-ray absorption near edge structure spectroscopy (total electron yield, TEY mode)[123] and ^{13}C-^{13}C 2D homonuclear correlation NMR spectroscopy (**Fig. 14b**).[214] The NMR cross peaks (**Fig. 14b**) between ^{13}C resonances of Li_2CO_3 and the carbon electrode (indicated by the arrows) suggest that they are in direct contact (within a few angstroms).[214] These interfacial passivating Li_2CO_3 films cause significant polarization on charging,[66, 99, 123, 129, 214] which induces further parasitic reactions. Hence, to avoid serious carbon corrosion and minimize the formation of interfacial Li_2CO_3, it was suggested that the charging voltage in a carbon-based Li-O_2 battery should be kept below 3.5 V (**Fig. 14c**).[126]

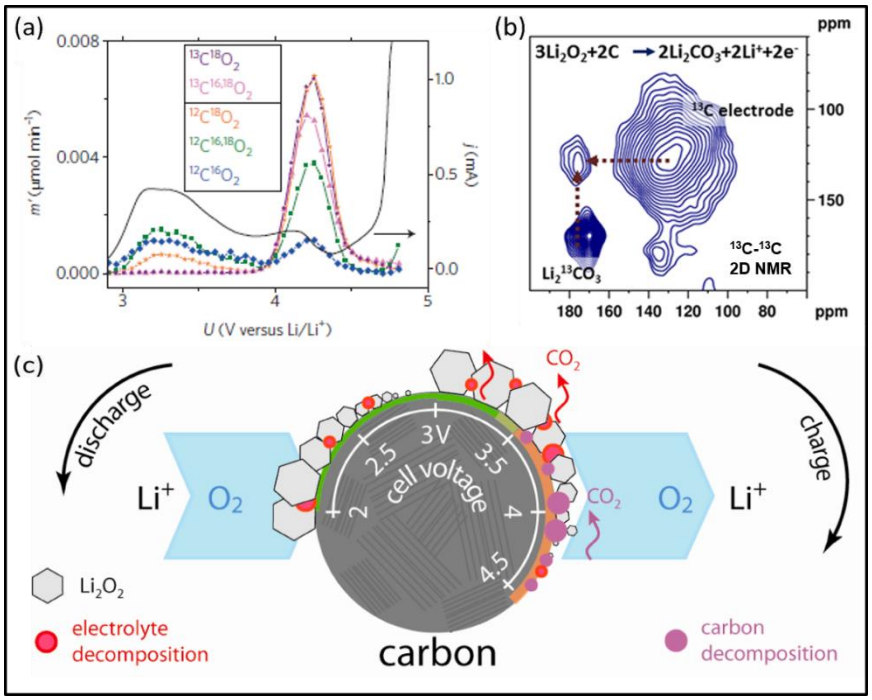

Fig. 14 Challenges associated with the carbon electrode in Li-O_2 batteries. (a): Linear sweep voltammogram and concomitant CO_2 evolution from a Li-O_2 cell discharged under $^{18}O_2$, using a ^{13}C cathode and natural abundance electrolyte (1 M LiTFSI/DME); $^{13}CO_2$ is evolved at potentials >3.8 V, and is linked to parasitic reactions occurring at the Li_2O_2/^{13}Carbon interface.[99] (b): ^{13}C-^{13}C 2D homonuclear NMR correlation experiment of a ^{13}C carbon enriched cathode on its 5th discharge to 2 V, the method probing spatial proximity between ^{13}C sites; a homonuclear correlation (a cross peak, indicated by the arrows) was detected between Li_2CO_3 resonance at 168 ppm and the carbon electrode signal at 130 ppm, indicating that at least some of the Li_2CO_3 forms directly (within a few angstroms) on the carbon surface.[214] (c): Schematic illustration showing that on discharging to 2 V and on charging below 3.5 V, CO_2 evolution primarily originates from electrolyte decomposition, whereas above 3.5 V on charging, carbon corrosion also leads to CO_2 evolution.[126] (a) Reprinted with permission from ref 99. Copyright 2012 ACS and (b) from ref 214. Copyright 2013 ACS. (c) From ref 126. Copyright 2013 ACS.

3.2.2 Influence of N_2, CO_2 and H_2O on the Non-aqueous O_2 Electrochemistry

Apart from carbon corrosion, the other constituents of the air can also incur undesirable processes at the cathode. In this section, we discuss in sequence the N_2, CO_2 and H_2O effects on the non-aqueous O_2 electrochemistry in lithium-air batteries.

N_2 gas composes 78% of the air. Fortunately it does not seem to affect the oxygen reduction reaction in Li-O_2 batteries. In some studies, Li-O_2 batteries have been cycled in ambient air,[220-222] but few studies have reported involvement of nitrogen in the oxygen electrochemistry within the typical electrochemical testing window (2-4.5 V), *i.e.*, N_2 seems inactive to any reactions with the reduced oxygen species and it does not undergo any redox reaction itself. Indeed, to electrochemically reduce N_2 and generate Li_3N, one needs to reach to very low potentials,[223] the equilibrium voltage is calculated to be around 0.46 V versus Li^+/Li (formation free energy for

Li_3N, $\Delta G°$=-129~-135 kJ/mol).[224, 225] The absence of any N_2 interference with O_2 electrochemistry is encouraging, because it avoids increased complexity of cathode reaction and the necessity of complete separation of O_2 and N_2 from the air.

CO_2, by contrast, can react readily with reduced oxygen species (superoxide and peroxide) in a nonaqueous Li-O_2 battery.[129, 226-233] First, CO_2 can react with Li_2O_2 to form Li_2CO_3 *via* reaction (16).[129, 227, 230]

$$Li_2O_2 + CO_2 \rightarrow Li_2CO_3 + ½\ O_2,\ \Delta G°\text{=-166.6 kJ/mol} \qquad (16)$$

This reaction has a few consequences: 1) parasitic reactions with aprotic polar electrolyte solvent can be induced by intermediates of this reaction, *e.g.*, peroxydicarbonate (**Fig. 15a**): significant oxidation of DME and DMSO solvents (to methyl methoxyacetate and $DMSO_2$) was detected when exposing Li_2O_2 to CO_2 in these solvents;[232] 2) the conversion of Li_2O_2 to Li_2CO_3 causes further polarization on recharging the battery, the high overpotentials in turn accelerating the battery degradation.[129, 227, 230] The decomposition of Li_2CO_3 typically involves irreversible reactions (**Fig. 15b**).

Secondly, O_2^-, as a strong nucleophile and a good charge transfer agent, [112, 157] can react with CO_2 to form a series of peroxycarbonate species, namely, CO_4^-, CO_4^{2-}, $C_2O_6^{2-}$ (**Fig. 15a**).[226, 227, 230, 231] Some of these species have indeed been confirmed by Qiao and coworkers[231] using *in situ* Raman spectroscopy in a Li-free $TBAClO_4$/DMSO electrolyte (**Fig. 15c(i-iii)**). When increasing the CO_2/O_2 molar ratio in the cell atmosphere, the dominant electrochemistry switches from O_2/O_2^- to O_2-$CO_2/C_2O_6^{2-}$ (**Fig. 15c(i-iii)**).[231] At O_2/CO_2 of 4/1 (**Fig. 15c(iii)**), $C_2O_6^{2-}$, CO_4^{2-}, and O_2^- appear in sequence on reduction following reactions (17), (18) and (4).[231] Of note, no carbonate formation (~1095 cm^{-1}) occurs in the Li-free electrolyte (**Fig. 15c(ii)**). In the presence of Li^+, however, Li_2CO_3 forms as the dominant discharge product (**Fig. 15c(iv-vi)**). Clearly, the soft TBA^+ cation can more effectively stabilize the soft peroxydicarbonate anion than the harder Li^+, hence avoiding further conversion of $C_2O_6^{2-}$ to CO_3^{2-}. Overall, the discharge reaction has been proposed to occur *via* reaction (19),[227, 230] whereby 1.33 electrons are consumed per gas molecule; this has been confirmed by *operando* electrochemical pressure measurements.[230]

$$O_2 + CO_2 + 2e^- \leftrightarrow CO_4^{2-},\ E° = 2.89\ \text{V} \qquad (17)$$

$$O_2 + 2CO_2 + 2e^- \leftrightarrow C_2O_6^{2-},\ E° = 3.27\ \text{V} \qquad (18)$$

$$O_2 + 2CO_2 + 4e^- + 4Li^+ \leftrightarrow 2Li_2CO_3,\ E° = 3.82\ \text{V} \qquad (19)$$

On charging, many groups[129, 227-231, 233, 234] have reported that the discharge product Li_2CO_3 is removed at voltages typically higher than 4 V (**Fig. 15c(iv)**); however, this should not be taken as the evidence for a reversible reaction. In fact, the change in pressure deviates significantly from the predicted 1.33 e^-/gas molecule (**Fig. 15b**)[230] and no O_2 evolution was observed,[129, 229-231] resulting in a continuously dropping cell pressure over many cycles (**Fig. 15b**). The missing

oxygen may remain in the cell, either as a component of passivating solid byproducts at the cathode or soluble species in the residual electrolyte (*e.g.*, cumulative $DMSO_2$ formation seen over cycles in **Fig. 15c(vi)**[231]). Freunberger and coworkers[179] recently reported that the electrochemical decomposition of Li_2CO_3 involves stoichiometric generation of singlet oxygen (as in the reversal of reaction (19)), and that the absence of O_2 evolution on charging can be attributed to the parasitic reactions of $^1O_2$ with cell components. These authors[179] further showed that with singlet oxygen quencher additives in the electrolyte, a small fraction of the formed $^1O_2$ can be released as $^3O_2$; this observation suggests that electrochemical Li_2CO_3 decomposition in aprotic media involves O-O reformation and that with a suitable singlet oxygen quencher, the reversibility of reaction (19) could be improved.

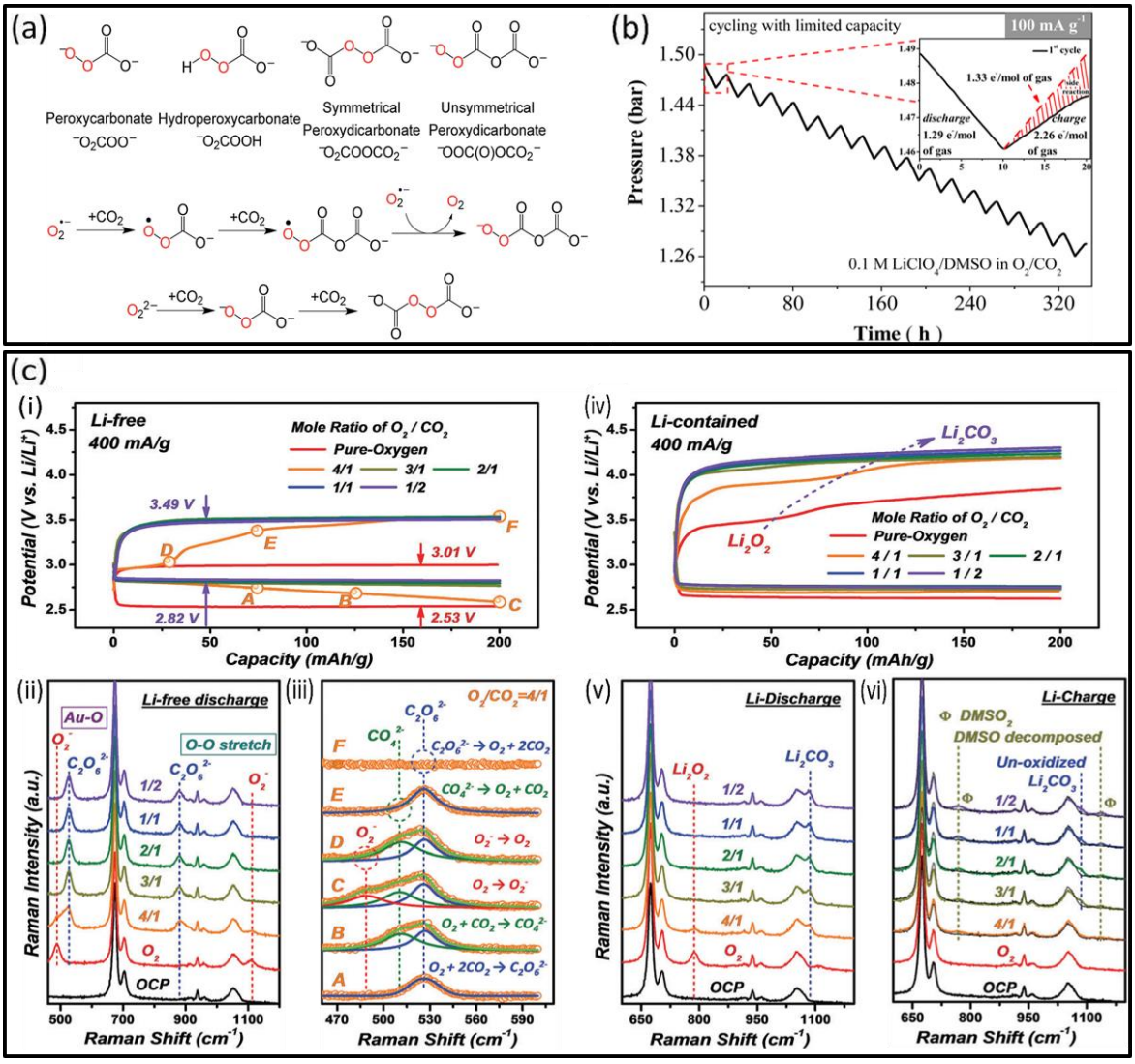

Fig. 15 The impact of CO_2 on the O_2 electrochemistry in non-aqueous media. (a): Possible reaction intermediates involved in the reaction between CO_2 and reduced O_2 species (O_2^-, O_2^{2-}).[232] (b): Operando pressure measurements during cycling of a Li-O_2/CO_2 cell (O_2:CO_2=7:3) in a $LiClO_4$/DMSO electrolyte; the discharge process (pressure drop) shows an e^-/gas ratio of 1.3 (close to the expected 1.33 value), but the charge process exhibits an e^-/gas ratio of

2.26 indicating an irreversible electrochemistry in the Li-O_2/CO_2 cell.[230] (c): *in situ* surface enhanced Raman (roughened gold electrode surfaces) investigation on the O_2/CO_2 electrochemical reaction mechanism in the absence (i-iii) and presence (iv-vi) of Li^+; in the absence of Li^+, the electrochemistry can be modulated from O_2/O_2^- to O_2-CO_2/$C_2O_6^{2-}$ by increasing the CO_2/O_2 molar ratio in the cell atmosphere; in the presence of Li^+, the cell electrochemistry is dominated by Li_2CO_3 formation and decomposition, the latter involves DMSO electrolyte oxidation to $DMSO_2$.[231] (a) Reprinted with permission from ref 232. Copyright 2017 The Royal Society of Chemistry and (b) from ref 230. Copyright 2017 ACS. (c) From ref 231. Copyright 2018 The Royal Society of Chemistry.

In summary, contamination of CO_2 in Li-O_2 batteries can cause significant degradation of the electrolyte during its reactions with reduced oxygen species to form Li_2CO_3; Li_2CO_3 cannot be oxidized reversibly *via* reaction (19), and its removal is actually associated with the degradation of the electrode/electrolyte, likely due to the generation of $^1O_2$ on charging. Besides, it significantly raises the charging overpotential, imposing stringent requirements on the cell components (cathode and electrolyte) to achieve a reversible Li_2O_2 chemistry. At the current stage, Li_2CO_3 formation should therefore be avoided in a Li-O_2 battery.

Inspired by the potential stabilization of $C_2O_6^{2-}$ by the softer TBA^+ ion (vs. Li^+), Qiao and coworkers[231] explored the effect of a complexed $Li^+(DMSO)_3$ in concentrated LiTFSI/DMSO electrolyte to stabilize $C_2O_6^{2-}$, where the coordinating DMSO molecules effectively screen the charge of Li^+, thereby decreasing the interactions of Li^+ with $C_2O_6^{2-}$. As a result, they found that the dominant charging reaction gradually changes from solid-state Li_2CO_3 decomposition at 4.2 V to decomposition of soluble $Li_2C_2O_6$ species at 3.5 V (**Fig. 16a**), *via* reaction (18). This reaction is further confirmed by chemical titration of $Li_2C_2O_6$ and DEMS measurements during cycling (**Fig. 16b,c**). Little electrolyte decomposition product $DMSO_2$ was detected and the cell rechargeability was improved considerably.[231] The generally fatal issues associated with high charging overpotentials and electrolyte decomposition due to Li_2CO_3 formation and decomposition seem to be circumvented altogether, even at high concentrations of CO_2 (CO_2:O_2=1). Although further efforts are required to improve the solubility of $Li_2C_2O_6$ (thus energy densities) and minimize its shuttling to the Li anode, this work exemplifies how a judicious design of electrolytes can modulate the reaction mechanism of CO_2 contaminated Li-O_2 batteries.

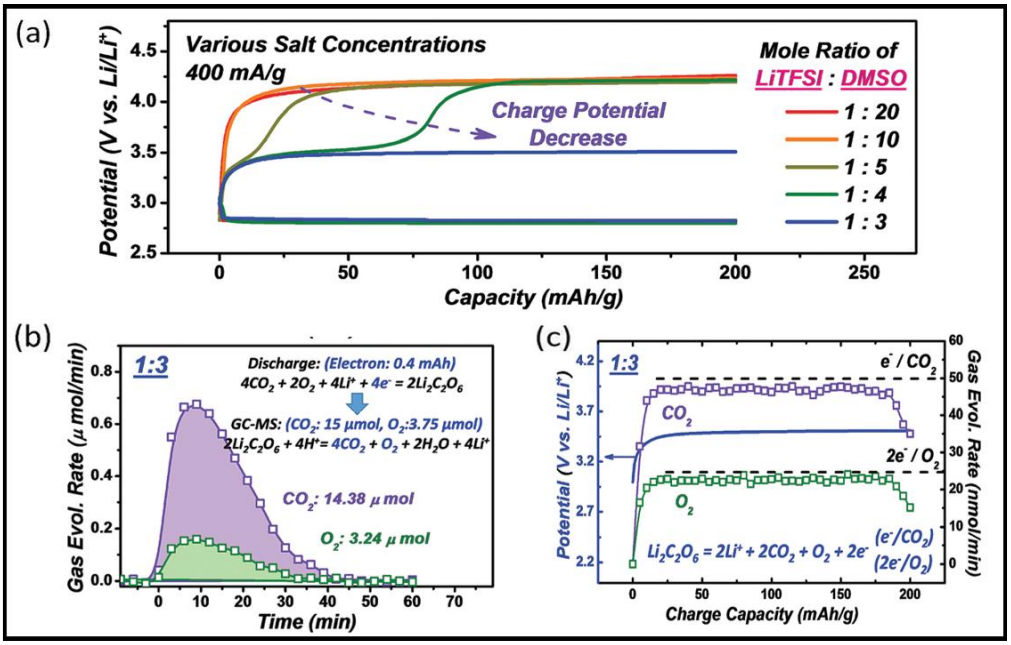

Fig. 16 Modulating the reaction mechanism of CO_2 contaminated Li-O_2 battery by tuning the solvation condition of Li^+ in the DMSO electrolyte. (a): By increasing the LiTFSI/DMSO molar ratio from 1:20 to 1:3, the cell electrochemistry changes from Li_2CO_3 formation to $Li_2C_2O_6$ formation, the latter is characterized by a much low charging voltage than that of Li_2CO_3. Chemical titration of $Li_2C_2O_6$ (b) and DEMS measurements (c) confirm the reversibility of the $Li_2C_2O_6$ formation and decomposition reactions.[231] Reprinted with permission from ref 231. Copyright 2018 The Royal Society of Chemistry.

It is worth mentioning that the possibility of a Li-CO_2 battery based on pure CO_2 electrochemistry has also been investigated. Contradicting observations were reported by various groups. McCloskey[129], Grimaud[230] and coworkers showed that almost no current in the CV and no capacity in galvanostatic discharging experiments were detected in the electrochemical reduction of CO_2 in DME/DMSO-based lithium or sodium electrolytes using various carbon-based electrodes (Super P, XC-72 and gas diffusion layer). These authors[129, 230] thus concluded that CO_2 is not electrochemically active within the typical testing window of 2.0-4.5 V versus Li^+/Li. By contrast, Zhou and coworkers[235, 236] provided a wealth of evidence supporting the electroreduction of CO_2 using a DMSO-based electrolyte on Ketjen carbon and on porous gold electrodes. By using a porous gold electrode, they showed that in addition to Li_2CO_3 formation, amorphous carbon deposits also simultaneously form on discharge, the process being proposed as reaction (20). Furthermore, they discovered that the metal catalyst can play a critical role in improving the reversibility of the cell reaction:[235, 236] when carbon or gold electrodes were used, only Li_2CO_3 was removed on charge, whereas with a ruthenium catalyst concomitant removal of Li_2CO_3 and C on charging was achieved at a lower potential of 3.6-3.8 V. Quantitative gas analysis is required to further verify the battery reversibility, because the continuing polarization (>3.6 V) due to the solid-state Li_2CO_3 decomposition on charging may incur unwanted side reactions.[179] Nevertheless, the mechanism whereby a solid catalyst can simultaneously decompose two solid products is fundamentally intriguing and warrants further studies.

$4Li^+ + 3CO_2 + 4e^- \leftrightarrow 2Li_2CO_3 + C$ (20)

, where $E°$ is equal to 2.8 V, versus Li^+/Li.

H_2O Finally, we discuss the impact of water on the non-aqueous O_2 electrochemistry. For the operation of Li-O_2 cells open to the air, in which O_2 is taken from air, the tolerance of the battery to the presence of water is critical, since water removal would require an additional water trap that would increase the weight and volume of the battery system considerably, thus making it less competitive compared to other types of batteries. Water can also be present as a contaminant in Li-O_2 cells from leaks in imperfect cells or from residual water present in the oxygen supply tubing/electrolyte/cell components. Early studies by Gasteiger and coworkers[74, 75] showed that hundreds to thousands ppm levels of water, present either as electrolyte additive or in leaky cells, produced a marked *increase* in the capacity of Li-O_2 cells. Surprisingly, water did not change the nature of the discharge product, which remained Li_2O_2.[31, 74, 75, 237-239] Interestingly, Li_2O_2 is also the main discharge product in water-in-salt Li-O_2 batteries, which contain no organic solvent and thus have no issues of solvent decomposition during cycling.[240] The reaction of water with Li_2O_2 to form LiOH is thermodynamically favorable:[241, 242]

$2Li_2O_2 + 2H_2O \rightarrow 4LiOH + O_2$, $\Delta G°$=-152 kJ/mol (21)

Nevertheless, the fact that, for some of the reported water-containing Li-O_2 cells (at or lower than thousands of ppm H_2O), Li_2O_2 is not converted into LiOH in the presence of water suggests the above reaction (21) is kinetically slow. If LiOH precipitates and forms a surface coating on Li_2O_2, then for the reaction to proceed and convert the Li_2O_2 core of the particles to LiOH, it would require proton transport from water through the LiOH layer to the Li_2O_2 core, coupled to O_2 evolution from the Li_2O_2 core. At higher water concentrations, however, the LiOH passivation effect may be attenuated by a much increased LiOH solubility, where evident conversion of Li_2O_2 to LiOH may be observed. Xia and coworkers[243] investigated the effect of moisture in O_2 (15% relative humidity) on the battery chemistry using a Ketjen black cathode and a LiTFSI/TEGDME electrolyte. As a result, LiOH and Li_2O_2 coexist as the discharge product. The carbon-based cathode does not decompose LiOH effectively, leading to large polarization on recharging.[243] These studies show that the sluggish kinetics of Li_2O_2 conversion to LiOH can only alleviate, but does not radically mitigate the LiOH-induced rechargeability issue for Li-O_2 cells exposed to moisture in air. From a scientific point of view, many of the water-induced effects such as higher capacities and suppressed degradation reactions are fundamentally intriguing. The detailed mechanism of water effect on the O_2 electrochemistry in organic media will be discussed in Section 4.3.1.

3.3 Lithium Metal Anode Instability

Lithium metal is a promising anode material due to its exceptionally high specific capacity, 3860

mAh g^{-1} (where this number is calculated based on the mass of lithium, *i.e.*, the battery in the charged state).[7, 244] Its use is implicit in the high energy density quoted for lithium-air batteries.[7, 33] In contrast to the extensive investigation of the cathode (electro)chemistry, in-depth studies of lithium metal anode in non-aqueous lithium air battery are relatively scarce. In many fundamental studies that focus on the cathode, $LiFePO_4$ (LFP) is used as a replacement to Li metal anode to avoid complication induced by the anode degradation.[90, 127, 245] Nonetheless, to realize the high specific energy of lithium-air batteries, challenges associated with Li metal anode warrant future endeavors.

3.3.1 Planar, Mossy versus Dendritic Li Deposition and Low Coulombic Efficiency

One of the biggest challenges associated with Li metal anode is the adverse morphological change during repeated stripping and plating. In particular, mossy (compact porous microstructures on the Li metal surface) and, at higher current densities, dendritic growth (spiny projections grow outward from the Li metal surface) (**Fig. 17a**), rather than smooth plating on the Li metal surface, occurs.[246] Dendrite formation can potentially result in electrical shorting of the battery, if the dendrites penetrate the separator and reach the oxygen electrode, thus causing severe safety concerns. In addition, formation of mossy structures results in poor Coulombic efficiency: this is due to the loss of capacity involved in the formation of a new SEI on the increasing lithium surface area, and also due to formation of electrically isolated lithium metal structures that are, thus, electrochemically inactive.[247-249]

The formation of Li dendrites is associated to depletion of Li^+ ions in the vicinity of the Li metal surface in Li plating experiments. When the Li^+ salt concentration drops to zero at the Li metal-electrolyte interface (which happens at a time known as the Sand's time),[250] the scarcity of Li^+ ions supply promotes the deposition onto surface protrusions (tip growth mode), over the growth of mossy deposits that grow from their roots (**Fig. 17a**).[247] A clear demonstration of the correlation between Li^+-ion depletion at the Li metal surface and Li dendrite growth was achieved via *in-situ* Magnetic Resonance Imaging (MRI).[251] Because of the sensitivity of ^7Li NMR shift to the local chemical environment and morphology,[251] the changes of both Li salt concentration profile and the growth of different types of Li microstructure can be tracked (**Fig. 17b(i)**), and indeed a clear transition from mossy to dendritic growth was observed during the *in situ* MRI experiments.[252, 253] This growth occurs from the tip of the dendrites towards the positively charged electrode, as later verified by Bai *et al*. using optical measurements.[246] As shown in **Fig. 17c(i)**, in a capillary cell, the growth of Li mossy and later dendritic microstructures was visualized, and the abrupt voltage increase (**Fig. 17c(ii)**) can be correlated to the onset of dendritic growth.[246] The MRI study shows that at high charge rates, there is a strong correlation between the onset of dendrite growth and the local depletion of the electrolyte at the surface of Li metal anode (**Fig. 17b(ii)**). Unfortunately, the formation of dead Li and mossy structures slows down the transport of Li^+ ions due to the increased tortuosity of the Li^+ ion pathway and, as a result, also accelerates the formation of Li dendrites.[254]

The low Coulombic efficiency of lithium plating/stripping is the other major challenge involved in the development of any batteries using a lithium metal anode. The requirement of >1000 cycles of charge and discharge for electric vehicle applications[28] requires a Coulombic efficiency of 99.98% in order to conserve >80% of the initial lithium material after the 1000 cycles.[add 261] Therefore, improving the Coulombic efficiency of lithium metal electrodes is a key requirement. Significant improvements in electrolyte formulations have achieved high values of Coulombic efficiency of lithium electrodes approaching 99%.[248, 255-261] Studies with LiPON thin-film cells in which all of the Li originates from the cathode demonstrated hundreds of cycles, thus implying high Li Coulombic efficiency above 99.9%.[262, 263] The significant progress achieved on Li metal anode development gives reasons for optimism, although much further work is still required. The requirements for commercial Li metal anodes have been recently summarized in excellent review articles,[263, 264] demonstrating that further work is needed in fundamental studies using thinner Li foils (e.g., <30 μm) and lean electrolyte, which are required to produce results representative of commercial conditions.

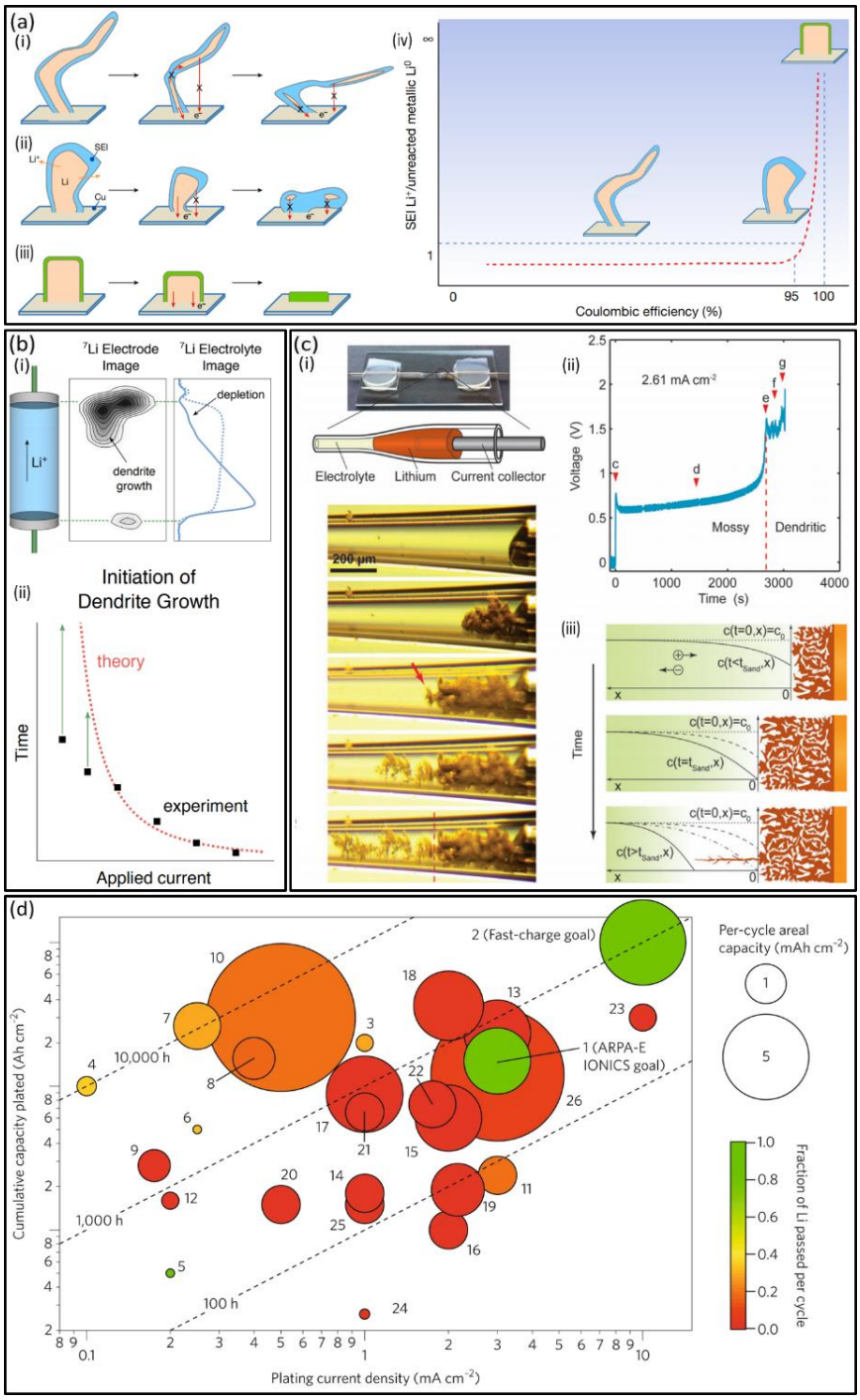

Fig. 17 Inactive Li formation mechanisms, origins and current state of reversible Li metal development. (a) schemes (i-iii) for various inactive Li plating mechanisms and a general correlation (iv) between morphologies of plated Li with the Coulombic efficiency and the ratio of SEI Li^+ versus unreactive metallic Li^0.[247] Whisker Li morphology (i) is more likely to lead to electronic disconnects and more Li^0 trapped in SEI; granular (ii) Li morphology tends to maintain good electronic contact and only small amounts of Li are trapped; an ideal Li deposit (iii) should have a columnar microstructure with large granular size. Reprinted with permission from ref 247. Copyright 2019 Nature Publishing Group. (b) Electrolyte depletion and dendrite growth revealed by MRI and optical measurements: (i) ^7Li chemical shift image of the metal (left) and the ^7Li electrolyte concentration profile (right); (ii) Plot of the theoretical

Sand's time and the initiation time of dendrite growth measured experimentally from ^{7}Li NMR spectra.[252] Reprinted with permission from ref 252. Copyright 2015 ACS. (c) Illustration of the capillary cell (i) and *in situ* snapshots of the growth of lithium microstructures during the electrodeposition;; The corresponding voltage profile of the cell in (i) is shown in (ii) where the red dash line separates the different morphologies before and after the Sand's time.; (iii) schematic illustrations of the growth mechanism of mossy and dendritic microstructures based on the electromigration-limited model.[246] Reprinted with permission from ref 246. Copyright 2016 The Royal Society of Chemistry. (d) Status of efforts in the literature on the cycling of Li metal.[263] Four parameters are included in this analysis: cumulative areal capacity plated, per-cycle areal capacity (represented by the size of each point), plating current density, and the fraction of the initial lithium metal present that is plated per cycle (indicated by the color). Points 1 and 2 are goals, 3-6 are for LiPON thin-film cells, 7-9 are PEO-based solid polymer electrolytes, 10-12 are solid inorganic separators, 13 and 14 are custom nanostructures and 15-26 are liquid electrolytes. Reprinted with permission from ref 263. Copyright 2018 Nature Publishing Group.

3.3.2 The Effects of O_2, CO_2 and H_2O on Li Metal Instability

Extensive research endeavors to investigate the reversibility of Li metal anode in the context of Li-ion batteries have been described in recent review articles and references therein.[265, 266] In the lithium-air battery systems, while lessons can be learnt from Li-ion rechargeable batteries, Li anode stability needs to be reassessed under different gaseous environments, solvents, salts and electrolyte additives. Next, we review the (electro)chemical reactions among Li metal, different air constituents, typical solvents used in lithium-air batteries. The resulting SEI and its effect on the anode stability will be discussed.

O_2 is a key component in lithium-air battery systems. The effects of O_2 crossover to the Li metal anode on the anode stability remain a topic under debate. Some researchers[267] reported that O_2 causes continual electrolyte (e.g., DMSO and TEGDME) decomposition over repeated cycles at the Li anode surface (**Fig. 18a-c**),[58] resulting in formation of less stable SEI layers, and a much worse electrochemistry. Other groups,[57, 268] however, propose that O_2 can stabilize the SEI. Zhou and coworkers[57] demonstrated a beneficial effect of O_2 using a TEGDME-based electrolyte. SEM **(Fig. 18e-h)** shows that during charge, the O_2-rich electrolyte allows uniform Li deposition generating a columnar structure with a higher Coulombic efficiency, compared to a filamentary structure without O_2. *In-situ* Raman experiments (**Fig. 18i-l**) revealed relatively constant signals of Li_2O, Li_2O_2 and LiOH layers on the Li surface that seems to stabilize Li, whereas in the absence of O_2, the electrolyte decomposition products Li_2SO_3 and CH_3OLi, together with Li_2O and LiOH, continually accumulate through the first two discharge/charge cycles. Zhou and coworkers[57] further pointed out that a high O_2 concentration (*e.g.*, direct O_2 exposure and diffusion of O_2 through macroporous Cu mesh) is required to form a stable SEI and prevent further reaction between Li and the electrolyte; this may help explain the opposite opinions, because in the former study[58] O_2 supply can be limited by diffusion through the microporous cathode. Nonetheless, clarifying the influence of O_2 crossover on Li metal stability requires further investigation.

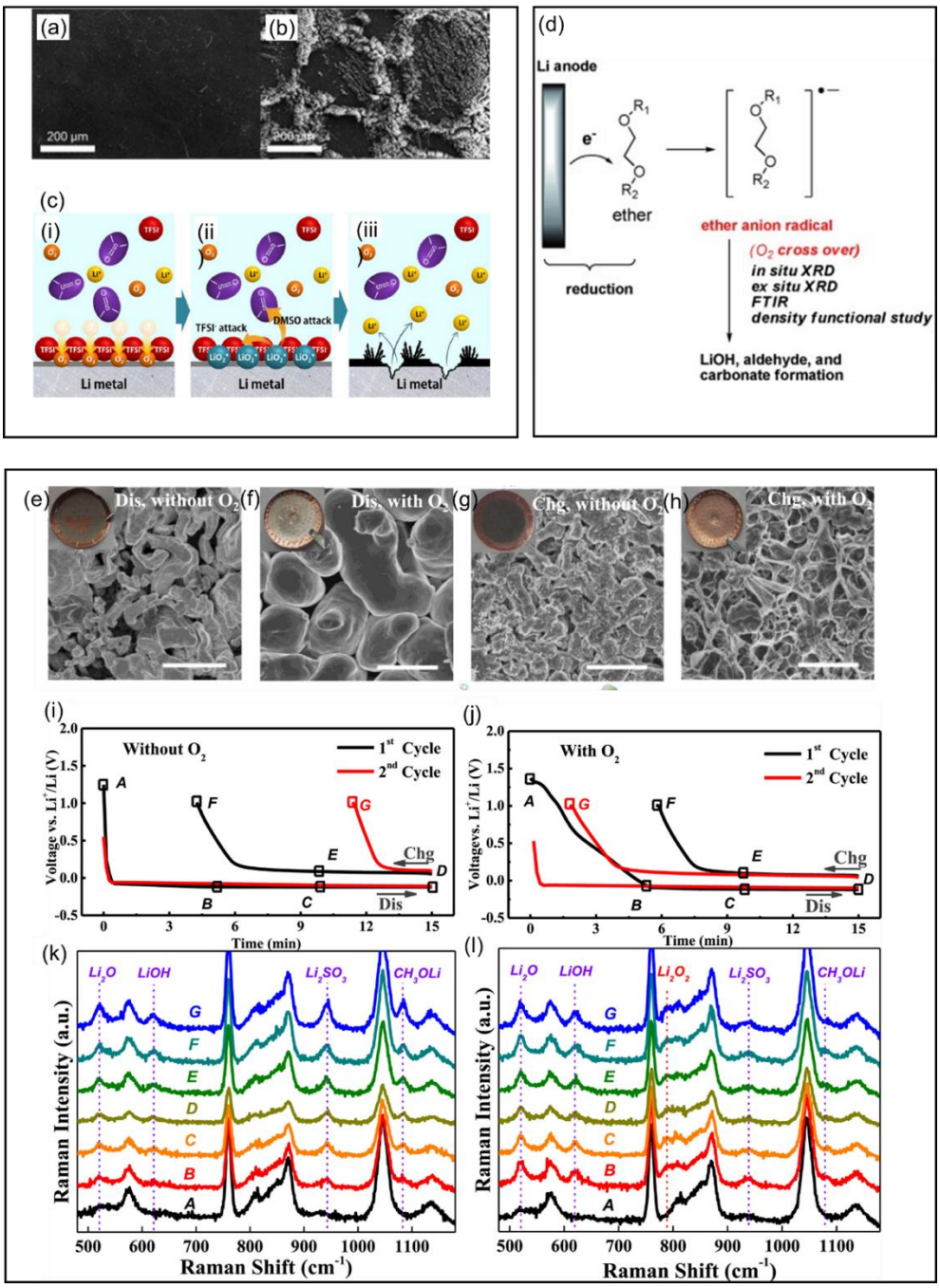

Fig. 18 Effect of O_2 crossover on the morphology and composition of the anode surface. SEM images of Li metal foil immersed in (a) 1.15 M LiTFSI-DMSO and (b) 1.15 M LiTFSI-DMSO-O_2 solution for 30 days. (c) Proposed degradation mechanism of Li metal surface in 1.15 M LiTFSI-DMSO-O_2 solution. Step i: adsorption of $TFSI^-$ anions and oxygen molecules on the Li metal surface; step ii: formation of LiO_2 and nucleophilic attack on surrounding DMSO solvent and $TFSI^-$ anions; step iii: precipitation of decomposed compounds of mossy structures and continuous Li^+ dissolution via oxidative reactions.[126] (d) Illustration of Li anode reduction in ether-based electrolyte when O_2 crossover occurs.[58] SEM images of the plated Li metal foil in TEGDME/$LiCF_3SO_3$ without (e) and with O_2 (f), and the stripped Li metal foil without (g) and with (h) O_2. *In situ* Raman spectra and voltage profiles of Li plating/stripping without (i, k) and with (j, l) O_2.[57] (a–c) Reprinted with permission from ref 126. Copyright

2014 Elsevier and (d) from ref 58. Copyright 2013 Wiley-VCH Verlag GmbH & Co. KGaA, Weinheim. (e-l) From ref 57. Copyright 2018 Elsevier.

CO_2 constitutes 0.04% of dry air, which is much less than N_2 and Ar, however, CO_2 is known to be generally more active than N_2 and Ar, and it can undergo chemical reactions with Li (some involving O_2), *e.g.*, $2Li + 1/2O_2 + CO_2 \rightarrow Li_2CO_3$. In the 1990s, Osaka and coworkers demonstrated that Li metal electrodes showed a prolonged cycling life in a CO_2 saturated $LiClO_4$/propylene carbonate electrolyte, and the formation of Li_2CO_3 in the subsurface layer was found to suppress dendritic deposition.[269, 270] The authors concluded: "To improve cycle life, carbon dioxide must be present when lithium is initially electrodeposited onto the nickel substrate". An example recently demonstrates that a pre-coated Li_2CO_3/C layer can indeed protect the lithium metal anode; when this anode is used together with a molybdenum disulfide cathode and an ionic liquid/DMSO electrolytes, the resulting Li-O_2 cell could be operated in an air-like atmosphere.[220] The Li_2CO_3/C protective layer was pre-synthesized electrochemically in pure CO_2 atmosphere, following the net reaction $4Li(s) + 3CO_2(g) \rightarrow 2Li_2CO_3 + C(s)$. As shown in **Fig. 19a**, after ten discharge-charge cycles, a dense network of rod-shape structures was formed on the surface. The composition of the surface is Li_2CO_3/C, confirmed by Raman (**Fig. 19b**), XPS (**Fig. 19c**) and electron energy loss spectroscopy. The authors argued based on DFT calculations that migration of N_2 and O_2 through the Li_2CO_3/C layer has a high energy barrier (1.2 – 3.2 eV) while diffusion of lithium should be facile. This study did not report in-depth studies aimed at understanding the protecting role of Li_2CO_3. It will be interesting to study the morphology and composition of the Li metal buried beneath the Li_2CO_3/C layer, to see whether there is any evidence of gas and electrolyte penetration and associated SEI formation.

The combined effect of N_2, O_2, and CO_2 on Li metal anodes has been investigated in few studies. Momma *et al*. studied the SEI layers formed on Li metal by XPS (in $LiPF_6$/ethylene carbonate (EC)-diethyl carbonate (DEC) electrolyte) when cells were assembled in different atmospheres, *i.e.* dry air versus dry argon.[271] They found that the topmost surface of Li metal deposited in dry air and dry argon were similar, whereas the underlying SEI layers (revealed after Ar^+ milling) contained concentrated Li_3N, Li_2CO_3 and LiOH in the former case. The cell assembled in dry air exhibited a better cycling performance, *i.e.* higher Coulombic efficiency than the one in dry Ar, especially in the presence of ionic liquid. These studies underscore the need for fundamental understandings of the interaction between O_2, CO_2, N_2 and Li metal anode surface in different electrolytes/salts, and the role of associated SEI layers in protecting the metal anode.

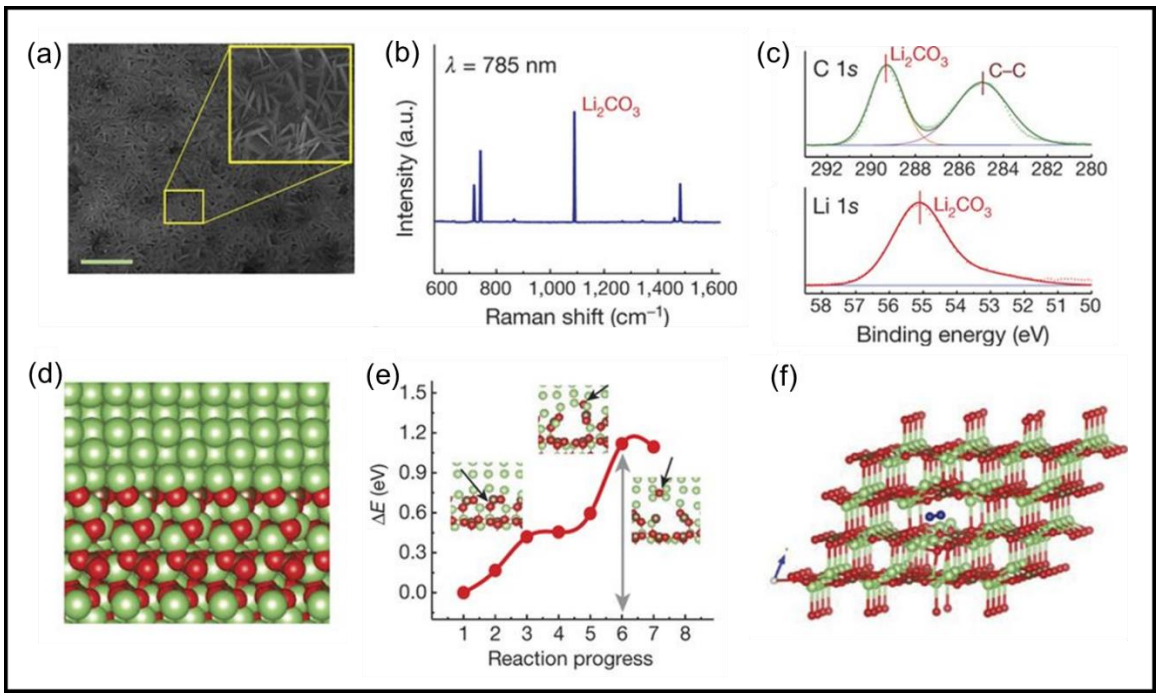

Fig. 19 Li_2CO_3/C coated Li metal anode and its characterizations. (a) SEM image of the rod-shape Li_2CO_3/C layer (scale bar, 1 μm). (b) Raman spectrum of the protected anode. (c) XPS spectra of the protected anode surface in the Li 1s and C 1s regions. (d) DFT-derived interface between (001) Li_2CO_3 and (100) Li with carbon termination. Green sphere: Li, red sphere: O, brown sphere: C. (e) DFT-derived energy profile that shows the breaking of the C-O bond of Li_2CO_3 at the interface, and the migration of oxygen to the bulk lithium (black arrows highlight oxygen). (f) DFT-derived adsorption of O_2 in a Li_2CO_3 channel. The adsorption is endothermic, with an energy of 3.1 eV.[220] Reprinted with permission from ref 220. Copyright 2018 Nature Publishing Group.

H_2O is present in air to varying degrees. It readily reacts with Li metal to form LiOH. Zaghib and coworkers studied the effect of moisture contamination on Li metal anodes in Li-O_2 cells.[272] Using the setup shown in **figure 20a**, the authors observed different extents of increases in discharge capacity and weight gains from the 1st to the 6th cell, following the order of O_2 flow through the cells (**Fig. 20b**). The additional capacity was explained by the following electrochemical reactions at the cathode:

$$2H_2O + Li_2O_2 + 2Li^+ + 2e^- \rightarrow 4LiOH \qquad (22)$$

The excessive weight gain of cell 2nd to 6th was attributed to the following chemical reaction as moisture penetrates through the battery systems:

$$2H_2O + 2Li \rightarrow 2LiOH + H_2 \qquad (23)$$

The morphology revealed by SEM and composition by XRD agree with the formation of LiOH, supporting the proposed reaction (23). In a separate study, the formation of LiOH on Li metal anode was also recorded when cycling a Li-O_2 battery in ambient air.[273] How the presence of

water affects the composition and morphology of the SEI in different combinations of electrolytes/salts will be invaluable information to the lithium-air battery community.

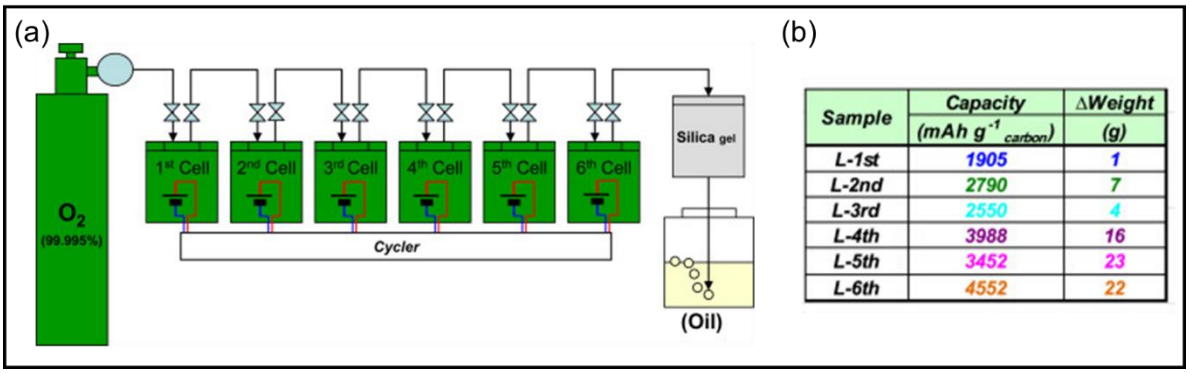

Sample	Capacity (mAh g^{-1}_{carbon})	ΔWeight (g)
L-1st	1905	1
L-2nd	2790	7
L-3rd	2550	4
L-4th	3988	16
L-5th	3452	23
L-6th	4552	22

Fig. 20 Effect of moisture contamination on Li metal anode. (a) Schematic diagram of O_2 flow and cell connections. The 1st to the 6th cells were connected in series by a single gas line of O_2, while the cells were independently controlled by cyclers. (b) A table shows the discharge capacities and weight gains of the six cells in (a).[272] Reprinted with permission from ref 272. Copyright 2014 Elsevier.

4. Potential Solutions

From the discussion in Sections 2 and 3, we can see that the technological challenges of non-aqueous Li-O_2 batteries are closely linked to relevant scientific hurdles, a critical one being the parasitic reactions occurring at the interfaces, namely, the Li anode-electrolyte, Li_2O_2-cathode (current collector), cathode-electrolyte and Li_2O_2-electrolyte interfaces. The situation is aggravated in the presence of large overpotentials on charging, because carbon cathode corrosion, electrochemical electrolyte decomposition, $^1O_2$ generation are all sensitive to the high charging voltages. The first major issue to tackle is thus to decrease the charging overpotential, preferably well below 3.5 V. As such, a range of strategies have been developed, including the use of solid catalysts,[115, 141, 203, 204, 207, 274-276] redox mediators,[127, 277, 278] photo-assisted charging,[279-283] phase-transfer catalysts[75, 76, 239] and so on. Furthermore, $^1O_2$ trapping/quenching molecules[139, 153, 284] as electrolyte additives, protective thin films[285-289] on the Li anode and gas-separation membranes[290-293] have also been used to reduce damages due to singlet oxygen, to enable a more reversible Li plating and stripping, and to minimize unwanted air contamination, respectively. These strategies will be reviewed in the following sections.

4.1 Electrocatalysis in Non-aqueous Li-O_2 Batteries

The use of solid electrocatalysts for Li-O_2 batteries is an intensely studied subject. Numerous studies report that with catalysts, *e.g.*, metal/metal oxides, lower charging voltages and much improved battery rechargeability are often observed compared to the case without catalysts. Nevertheless, many reports also stress that the apparent improved rechargeability by coulometry does not reflect the true reversibility of Li-O_2 electrochemistry.[91, 132, 181, 205-207, 274, 294-296] In fact,

similar or even worse O_2 recovery efficiency (OER/ORR) occurs with these catalysts,[132, 181, 274, 294, 295] compared to a carbon cathode. This seemingly improved rechargeability can be connected to at least three other factors in addition to the desirable effect on Li_2O_2 decomposition: 1) insulating byproducts (Li_2CO_3, LiOH, carboxylates) can be removed by catalysts at a lower voltage so that they do not accumulate and rapidly passivate the cathode;[99, 141, 181] 2) organic electrolyte decomposition is promoted in the presence of catalysts, so that the repeated cycling is in fact primarily at expense of electrolyte;[181, 242, 274, 295] 3) some electrolytes tend to more effectively dissolve the common byproducts (Li_2CO_3, LiOH) or form very soluble decomposition products, thus postponing cell failure.[87, 88, 100, 297] Therefore, efficient catalysts and stable electrolytes should be considered collectively when seeking to develop a truly reversible Li-O_2 battery.

Due to the lack of quantitative analysis, it is very difficult to judge in the many reported studies whether the improved battery performance is genuinely a result of electrocatalytic effects on the O_2 electrochemistry. Herein, we thus focus on reviewing studies that have quantified the O_2 consumption and evolution during battery cycling. We acknowledge the many reviews[219, 298, 299] existing already on the subject, which provide a more exhaustive list of electrocatalysts studied for Li-O_2 batteries.

4.1.1 A Real Need for Electrocatalysis on Charging?

The overpotential on charging is typically observed to be several times (> 1 V) larger than that of discharge (0.2 V). Hence, there is a greater need to further improve the kinetics during charge. To investigate whether there is a true role of electrocatalysis, McCloskey and coworkers[181] studied the charging process of Li-O_2 batteries using XC72 carbon, Au-XC72 and MnO_2-XC72 based cathodes (**Fig. 21a**). The authors observed overlapping charging voltage profiles starting from the equilibrium voltage of ~3.0 V, where O_2 begins to evolve in the corresponding DEMS tests;[181] this observation thus indicates there is hardly any kinetic barrier for the onset of Li_2O_2 decomposition for all three cathode materials. Furthermore, analysis of cathodic and anodic Tafel plots of Li-O_2 electrochemistry on a flat glassy carbon electrode (**Fig. 21b**) leads to an exchange current density of 1 mA/cm^2, consistent with a fast reaction.[112] McCloskey, Luntz and coworkers thus argued that there is no need for electrocatalysis in the Li-O_2 electrochemistry.[112, 170, 181] In addition, in conventional catalysis, reaction intermediates are sufficiently mobile so that reactants and products can access and escape from the active site, the site thereby being regenerated. By contrast, the catalyst particles are covered by solid Li_2O_2 products in lithium-oxygen batteries, and thus catalyst surfaces would be quickly deactivated for further reaction.[181] Clearly, the conventional catalysis concept is not applicable.

Nevertheless, many other groups[207, 276, 295, 300, 301] indeed observed that cells using solid catalysts exhibit different onset charge voltages, the overpotentials throughout the whole charge capacity being decreased compared to that observed using just a carbon-based cathode (**Fig. 21c**); these observations thus support the existence of catalytic effects on charging (that is, through the use

of a catalyst, the overpotential of a battery reaction is reduced). The next question is how does a solid catalyst facilitate Li_2O_2 decomposition? Several hypotheses have been put forward to account for the solid-solid effect involved in Li_2O_2-catalyst interactions. Nazar and coworkers[300] proposed that solid catalysts (*e.g.*, Co_3O_4) promote mass transport of Li_xO_2 species on electrode surfaces by reducing their binding energies with the surface, which in turn facilitates both further oxidation and reduction of Li_xO_2. Shao-horn and coworkers suggest that solid-state Li_2O_2 oxidation is mediated by chemical conversion of Li_2O_2 to a lithium metal oxide at the Li_2O_2-metal catalyst interface, where Li_2O_2-catalyst interaction at the interface clearly matters.[114] Others have suggested an electrolyte-mediated charging process,[96, 197, 302] which is later confirmed to be dependent on the donicity of electrolyte solvents.[45] To provide more clear-cut evidence that there is solid-state promotion of Li_2O_2 decomposition by solid catalysts, Lu and coworker[115] studied the electrochemical behavior of all solid-state Li-O_2 batteries using Vulcan Carbon (**Fig. 21d**) and Ru-Vulcan Carbon electrodes (**Fig. 21e**). Compared to the case using carbon electrode, the authors observed more O_2 evolution at a lower overpotential using Ru catalysts;[115] this result thus verifies that some solid catalysts can indeed reduce the kinetic barrier for Li_2O_2 oxidation and increase O_2 recovery efficiency. The authors[115] then propose that solid catalysts operate by stabilizing reaction intermediates such as $Li_{2-x}O_2$ *via* formation of surface-$Li_{2-x}O_2$ species, which then facilitates delithiation of the bound $Li_{2-x}O_2$ species (**Fig. 21f**). This delithiation occurs *via* Li^+ vacancy transport through the Li_2O_2 particle bulk or surfaces and triggers O_2 evolution from the particle surface (**Fig. 21f**). This mechanistic picture proposed by Lu *et al.*[115] for the all solid-state battery is consistent with the general understanding on solid-state Li_2O_2 decomposition on carbon electrodes (discussed in Section 2.2.1) and is supported by the observation that O_2 evolution typically occurs at the Li_2O_2-electrolyte interface (as discussed in Section 2.2.2). As a result, by modulating the interaction between the catalyst surface and reaction intermediates, the charging voltages can be reduced, providing a guideline for catalyst design.

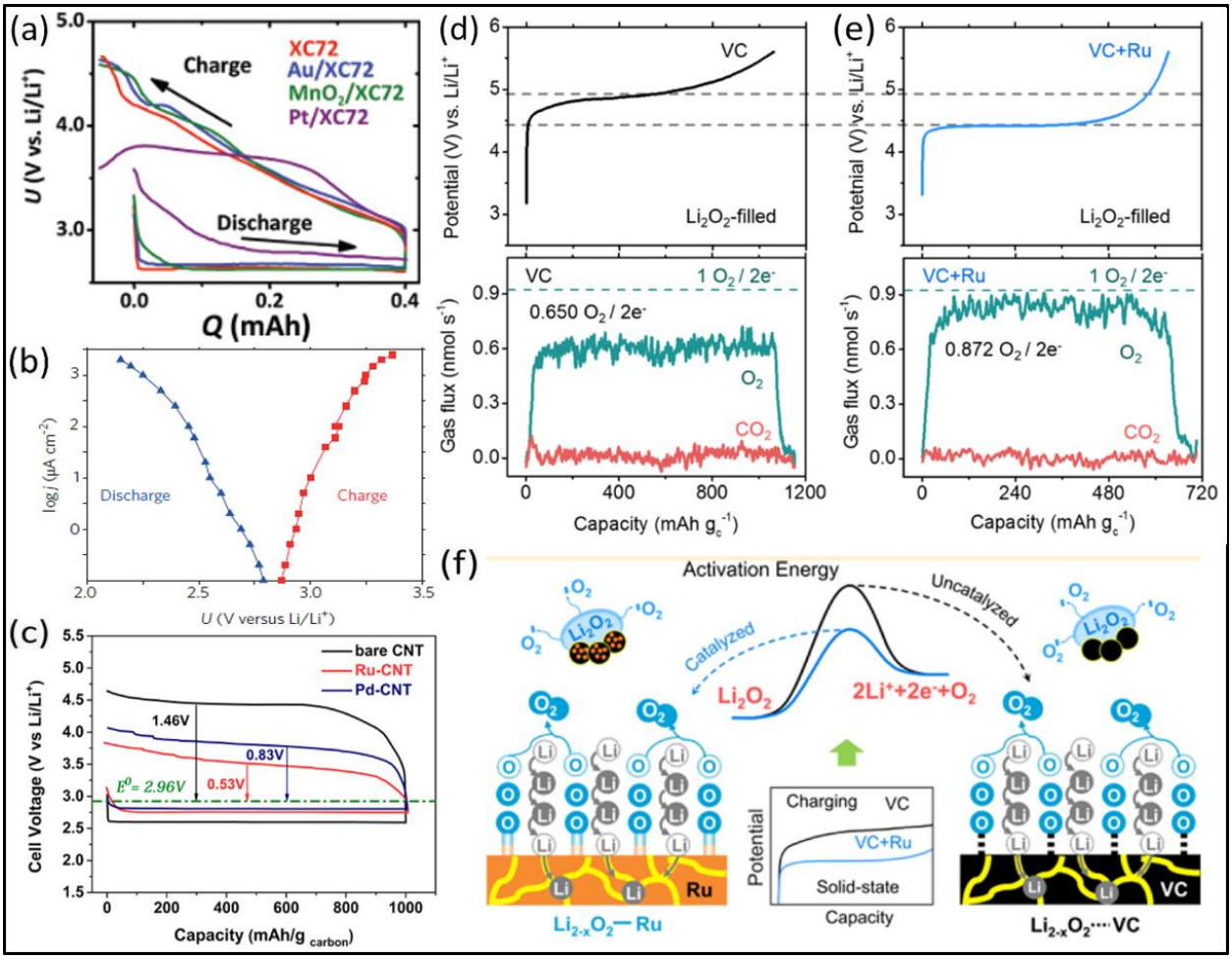

Fig. 21 The role of solid catalysts in charging a nonaqueous Li-O_2 battery. (a): Electrochemical profiles of Li-O_2 cells employing a DME-based electrolyte and various metal/metal oxide catalysts.[181] Reprinted with permission from ref 181. Copyright 2011 ACS. (b): Cathodic (discharge) and anodic (charge after a short discharge) Tafel plots for Li-O_2 electrochemistry at a flat, nonporous glassy carbon working electrode in a well-defined bulk electrolysis cell (1 M LiTFSI/DME as the electrolyte).[170] Reprinted with permission from ref 170. Copyright 2016 Nature Publishing Group. (c): Electrochemical profiles during discharge/charge of Li-O_2 cells using CNT, Ru/CNT and Pd/CNT as the cathode (0.1 M LiTFSI/TEGDME as the electrolyte), showing an evident reduction in charging overpotentials when a metal catalyst is present.[295] Reprinted with permission from ref 295. Copyright 2015 ACS. (d-e): Electrochemical charging profile and the corresponding gas evolution of Li-O_2 cells using a solid electrolyte and pre-loaded Li_2O_2 cathodes without (d) and with (e) a Ru catalyst. (f): Schematic illustration of the roles of solid catalysts in reducing the charging overpotential for Li_2O_2 oxidation.[115] (d-f) Reprinted with permission from ref 115. Copyright 2016 ACS.

4.1.2 Noble Metals, Transition Metal Carbides and Oxides

Among noble metals, nanoporous gold (NPG[204]) and ruthenium-based[141, 295, 303-306] catalysts have been reported to show the best electrochemical performance. For example, a Li-O_2 cell using NPG electrode and DMSO-based electrolyte shows an onset charging voltage from 3.0 V and O_2 recovery efficiency higher than 98% for 100 cycles.[204] The stability of DMSO for Li_2O_2 electrochemistry, however, was later questioned.[87, 88, 132, 205] It is now known that solvents with

higher DN (high polarity) are more prone to nucleophilic attack and electrochemical decomposition,[31, 32, 91, 175, 307] compared to low DN solvents (low polarity). Higher O_2 recovery ratios are typically obtained using the same catalyst with low donicity solvents (*e.g.*, TEGDME) than high donicity solvents (*e.g.*, DMSO).[91, 207] Nevertheless, a subsequent study using Ru catalysts and DMSO-based electrolytes provided further evidence that Li-O_2 batteries using a DMSO electrolyte can achieve high O_2 recovery ratios.[141]

The reversibility of cells using ruthenium catalysts seems to be dependent on the electrolyte in use.[141, 274, 294, 295] In ether-based electrolytes, ruthenium cathodes exhibit an O_2 recovery of only ~64%,[274, 295] similar to that using a carbon electrode, although the Ru-catalyzed cell is still highly rechargeable for many cycles (probably due to some parasitic processes, discussed in the beginning of Section 4.1).[274, 294] In a more polar DMSO-based electrolyte, however, Ru was reported to effectively catalyze O_2 reduction and evolution reactions, with 92% of O_2 recovered on charging.[141] Other noble metals such as Pt and Pd have been consistently reported to cause significant electrolyte decomposition in ether-based electrolytes.[181, 274, 295]

Transition metal carbides have been considered as a promising class of cathode materials due to the high electrical conductivity and high oxidation resistance.[203, 207] Bruce and co-workers reported that cells using a TiC cathode and a $LiClO_4$/DMSO electrolyte can be cycled with ~99% O_2 recovery for 100 cycles.[203] Nazar *et al*.[207] later pointed out that Li-O_2 electrochemistry is very sensitive to the TiC surface condition – a surface TiO_2 film as thin as 3 nm can completely shut down interfacial electron transfer, whereas pristine TiC surfaces with a sub-nanometer TiO_2/TiOC passivation film can effective catalyze Li_2O_2 decomposition. Given the need to passivate the TiC surface by a thin oxide layer in the Li-O_2 cell environment, Nazar and co-workers[276] further exploited titanium oxide phases with high electrical conductivity for Li-O_2 battery applications. The authors[276] found that cells using Ti_4O_7-based cathodes exhibit an ultralow onset voltage from 3.0 V and e^-/O_2 ratio of 2.42 on charging.

Although many solid catalysts enable a very low onset charging voltage at 3.0 V (such as Ru,[141] NPG,[204] Ti_4O_7,[276] $TiCrO_x$[275]), a common issue is that cells all gradually polarize toward 4.0 V or higher with deeper states of charging, which is usually connected to parasitic products accumulating at the reaction interfaces.[66, 99, 123, 129] Above 3.5 V, additional carbon corrosion and electrochemical/chemical electrolyte decomposition occurs to a greater extent,[66, 99, 123, 129, 214] becoming a grave issue for the battery reversibility. Again, minimizing parasitic reactions occurring at the interfaces and constantly keeping the charging voltage below 3.5 V is required to improve the reversibility of catalyzed Li-O_2 batteries.

A desirable solid catalyst should satisfy at least the following criteria: (1) the catalyst needs to be stable against the oxidizing environment (reactive oxygen species and high overpotentials especially on charging) in a lithium-oxygen battery; (2) the catalyst should not promote significant electrolyte decomposition within the battery discharge-charge window (where 2.5-3.5 V is typically the operating window to aim for in order to minimize degradation reactions); (3) a

high binding energy between OER reaction intermediates (*e.g.*, $Li_{2-x}O_2$) and the catalyst surface is preferred, as this property is linked to critical steps of Li_2O_2 delithiation on recharging; (4) it is also desirable that the catalyst can readily decompose LiOH and Li_2CO_3, because the continued formation of these typical byproducts (if formed) will rapidly clog the porous cathode and cause early cell failure.

4.2 Redox Mediators: Enabling Facile Solution-Phase Charge Transfer

4.2.1 Fundamental Principles

Redox mediators (RM) are electrochemically active species that are used to facilitate electrochemical reactions. The operational mechanism of RMs in Li-O_2 batteries is illustrated in **Figure 22a**. During discharge, RMs transfer electrons from the electrode to an O_2 molecule forming Li_2O_2, and during charge, RMs transfer electrons from Li_2O_2 to the electrode, evolving O_2. In the following, the oxidized and reduced forms of the RM will be termed RM^{OX} and RM^{RED}, respectively. These reactions involve the following steps:

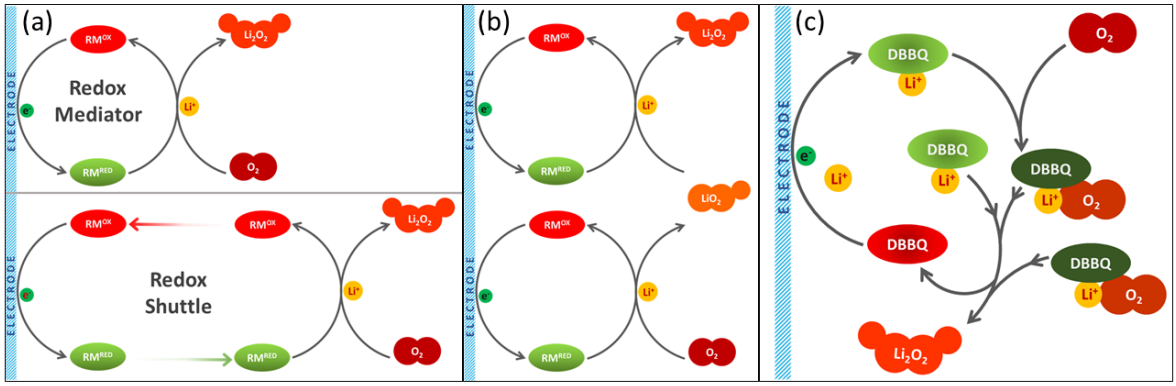

Fig. 22 Proposed reaction mechanisms in mediated Li-O_2 batteries. (a): Differences in the mode of operation of RMs and redox shuttles, where RMs are homogeneous catalysts that enhance the rate of reactions which is largely confined to regions near the electrode surfaces within microns, and RSs are charge carriers that receive or donate electrons and then transport that charge over long distances (typically, hundreds of microns or more). The sketch shows discharge reactions; charge reactions would be the reverse ones. (b): Simplified reaction mechanism of mediated Li-O_2 cell discharge involving formation of superoxide species (LiO_2) as reaction intermediate. (c): Proposed reaction mechanism of mediated Li-O_2 cell discharge involving the formation of a complex between the redox mediator (DBBQ) and superoxide that bypasses the formation of superoxide as reaction intermediate. In all these sketches, the reduced forms of the mediators are shown in green, the oxidized in red. The light green color in (c) represents a reduced DBBQ associated with a Li^+ cation, and the dark green color represent a reduced DBBQ associated with O_2 and Li^+.

<u>Discharge:</u>

$$RM^{OX}{}_{solution} \rightarrow RM^{OX}{}_{electrode\ surface} \qquad (24)$$

eq. 24: mass transport of RM^{OX} from solution to the electrode surface.

$$\mathrm{RM^{OX}}_{electrode\ surface} + e^- \rightarrow \mathrm{RM^{RED}}_{electrode\ surface} \quad (25)$$

eq. 25: electron transfer to RM^{OX} to form RM^{RED} at the electrode surface.

$$\mathrm{RM^{RED}}_{electrode\ surface} \rightarrow \mathrm{RM^{RED}}_{solution} \quad (26)$$

eq. 26: mass transport of RM^{RED} from the electrode surface to the solution.

$$2\mathrm{RM^{RED}}_{solution} + O_2 + 2Li^+ \rightarrow 2\mathrm{RM^{OX}}_{solution} + Li_2O_2 \quad (27)$$

eq. 27: electron transfer from RM^{RED} to O_2 forming Li_2O_2 suspended in solution.

Charge:

$$\mathrm{RM^{RED}}_{solution} \rightarrow \mathrm{RM^{RED}}_{electrode\ surface} \quad (28)$$

eq. 28: mass transport of RM^{RED} from solution to the electrode surface.

$$\mathrm{RM^{RED}}_{electrode\ surface} \rightarrow \mathrm{RM^{OX}}_{electrode\ surface} + e^- \quad (29)$$

eq. 29: electron transfer from RM^{RED} to form RM^{OX} at the electrode surface.

$$\mathrm{RM^{OX}}_{electrode\ surface} \rightarrow \mathrm{RM^{OX}}_{solution} \quad (30)$$

eq. 30: mass transport of RM^{OX} from the electrode surface to the solution.

$$2\mathrm{RM^{OX}}_{solution} + Li_2O_2 \rightarrow 2\mathrm{RM^{RED}}_{solution} + O_2 + 2Li^+ \quad (31)$$

eq. 31: electron transfer from Li_2O_2 to RM^{OX} evolving O_2.

The reduction and oxidation of RMs (reactions (25) and (29)) involve, in some cases, lithium cations, and the reactions of RMs with O_2 and Li_2O_2 (reactions (27) and (31)) are not elementary reactions.

The reaction steps shown above illustrate that RMs do not change the net ORR or OER reactions, but they alter the reaction pathway in such a way that the kinetics of the reaction are improved. RMs act as electron/hole "carriers" and facilitate Li-O_2 cell reactions by shuttling electrons between O_2 or Li_2O_2 and the electrode. Thus, RMs not only alter the reaction mechanism, but they also enlarge the region where reactions can take place. This is key to the development of high-capacity Li-O_2 batteries, for the following two reasons: 1) RMs tend to circumvent rapid electrode passivation due to the surface mechanism during discharge, and lead to larger discharge capacities *via* solution-mediated processes; 2) RMs can help realize a facile charge transfer pathway *via* the electrolyte, so that the high charging overpotentials incurred by the insulating nature of Li_2O_2 can be circumvented. An alternative mechanism pathway involving the dissolution of solid Li_2O_2 forming soluble Li_2O_2, which could then diffuse to the electrode

surface and get oxidized, is unlikely to proceed at significant rates due to the poor solubility of Li_2O_2 in most electrolytes.[51, 52] The mediated reaction of Li_2O_2 oxidation *via* RMs thus appears very promising.

The reactions of RMs with O_2 and Li_2O_2 (reactions (27) and (31)) involve a net transfer of two electrons; thus they require at least two, one-electron transfer reactions (reactions (32) and (33)). **Figure 22b** illustrates a suggested simplified reaction mechanism involving the formation of superoxide species LiO_2 as reaction intermediates [41]:

$$Li^+ + \mathrm{RM}^{\mathrm{RED}} + O_2 \leftrightarrow LiO_2 + \mathrm{RM}^{\mathrm{OX}} \quad (32)$$

$$Li^+ + \mathrm{RM}^{\mathrm{RED}} + LiO_2 \leftrightarrow Li_2O_2 + \mathrm{RM}^{\mathrm{OX}} \quad (33)$$

Due to the reactivity of superoxide species, the development of mediators that can quickly reduce superoxide to peroxide on discharge (reaction (33)) would be highly advantageous.[41] However, the actual reaction mechanism might be much more complex than the simplified reaction mechanism with reactions (32-33), and it may involve interaction between the different species or the formation of different reaction intermediates. Indeed, Bruce and coworkers[81] ascribed the excellent catalytic activity of the DBBQ (2,5-di-tert-butyl-1,4-benzoquinone) RM to the formation of a DBBQ-superoxide reaction intermediate (reactions (34-37)) that bypassed the formation of superoxide (**Fig. 22c**).

$$DBBQ + e^- + Li^+ \rightarrow LiDBBQ \quad (34)$$

$$LiDBBQ + O_2 \rightarrow LiDBBQO_2 \quad (35)$$

$$2LiDBBQO_2 \rightarrow Li_2O_2 + O_2 + 2DBBQ \quad (36)$$

$$LiDBBQO_2 + LiDBBQ \rightarrow Li_2O_2 + 2DBBQ \quad (37)$$

Unfortunately, the direct detection of the proposed $LiDBBQO_2$ reaction intermediate is difficult, but it was found that the discharge potentials of mediated Li-O_2 cells containing DBBQ was significantly higher than those without DBBQ, which supports the hypothesis that an alternative reaction pathway, involving intermediate species more stable than LiO_2, is promoted by DBBQ.[308] Similar conclusions were reached in the study of coenzyme Q10,[309] vitamin K_2[310] and anthraquinone[311] RMs. Furthermore, in the case of anthraquinone, additional support for the formation of alternative reaction intermediate was obtained from the characterization of the complex formed with anthraquinone and lithium superoxide by UV-vis, NMR and computational studies.[311] *In situ* FTIR measurements of Li-O_2 cells containing DBBQ also supported the formation of a reduced DBBQ – O_2 complex.[312]

It should be noted that electrochemical measurements alone cannot be used to determine whether a mechanism occurs *via* reactions (32-33) or reactions (34-37), i.e., whether the reaction occurs *via* a reduced RM-O_2 complex. Since, in most cases, mediators exhibit fast electron transfer kinetics, the electrode potential will depend on the surface concentrations of the oxidized and

reduced forms of the mediator *via* the Nernst equation.[313] Thus, the consumption of the reduced form of the mediator via reactions (32-33) will produce an increase in electrode potential; and the higher the reaction rate, the higher the associated increase in electrode potential. Thus, an increase in discharge potential of cells incorporating discharge RMs upon addition of O_2 could also be explained *via* the mechanism involving reactions (25,32-33).

In conclusion, the identification of the reaction mechanism and detection of reaction intermediates is not possible based on electrochemical data alone. Additional analytical techniques are required. The possibility of altering the reaction mechanism by exploiting the interaction of RMs with O_2 or O_2-reduced species, to form reaction intermediates more stable and less prone to induced degradation reactions than superoxide is, without a doubt, a promising approach worth exploring further.

4.2.2 Selection Criteria for Redox Mediators

RMs should fulfil a number of requirements in order to effectively promote Li-O_2 cell reactions. First of all, RMs should exhibit a high catalytic activity towards the Li-O_2 cells reactions, as well as high chemical stability against degradation reactions. Experimental data suggest that those two requirements can be achieved simultaneously.[197, 314, 315] But further work is still required to identify the fundamental descriptors leading to high mediation activity and chemical stability of RMs.

The mass transport rate of RMs (that is their diffusion coefficients) can also be an important factor. Fast diffusion enables the RM to access more regions of the cathode promoting a more homogeneous reaction. Ideally, RMs should also exhibit a high solubility. The kinetics of mediated reactions is, in principle, proportional to the mediator concentration, thus high RM concentrations can increase the cell rate performance. Therefore, the concentration and diffusion coefficient of RMs should be as high as possible. Specifically, for discharge, the product of the diffusion coefficient and concentration of the discharge RM should be higher than that of O_2,[316] since in this way, the electrochemical reactions at the cathode are those of the RM, and the reduction of O_2 to Li_2O_2 via RMs only happens further away from the electrode surface, thus preventing Li_2O_2 deposition on the cathode (**Fig. 23a**).[316] Similarly, for charge, the product of the diffusion coefficient and concentration of the charge RM should be high enough in order to be able to sustain the charging current; the maximum current associated with the mediated O_2 evolution reaction, j^{ss}, has been calculated with a simple model and validated with experimental data, see **Figure 23b**.[317] In addition, RMs should also be stable in contact with the lithium anode. If that is not the case, lithium protective membranes need to be incorporated, and the mediator should not react in contact with the membrane. Most of the fundamental work on redox mediators for Li-O_2 batteries has been done using solid lithium ion conductors (e.g. the glass-ceramic membrane from Ohara-GmbH) to prevent the reaction of the redox mediators with the Li metal anode, but future work should address the development of suitable membranes compatible with both Li and redox mediators. In the next section, we present a further discussion

of the two most important selection criteria (redox potential and chemical stability) that should be considered for the successful mediation of Li-O_2 cell reactions.

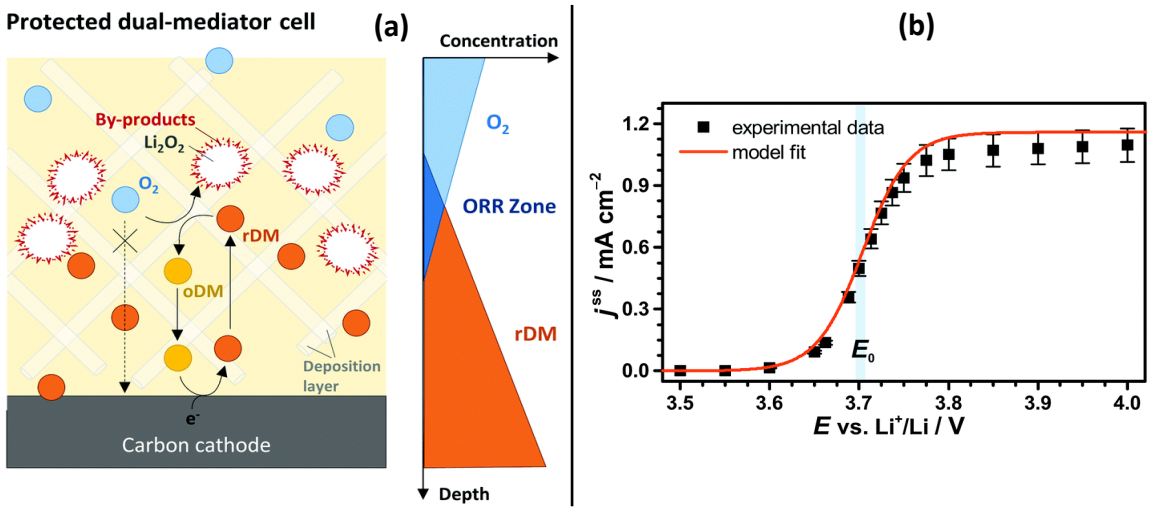

Fig. 23 Mass transport effects on mediation of Li-O_2 reactions. (a): Schematics of the working principle of the protected dual-mediator Li–O_2 battery, where the cathode surface is protected from passivation and corrosion by deposition of discharge products (Li_2O_2) or degradation by reaction with Li–O_2 reaction intermediates by means of a dynamic O_2 shield made of reduced discharge redox mediator. oDM and rDM correspond to the discharge mediator in its oxidized and reduced forms, respectively.[316] (b): Comparison of calculation and experimental results of the limiting current density (j^{ss}) that can be held by a charge redox mediator whose reaction with Li_2O_2 is limited by mass transport. Experiments were performed in a cell with a glassy carbon working electrode, a LFP counter electrode and Li reference electrode, containing 100 mM TEMPO redox mediator in 1M LiTFSI/diglyme, with a distance between the working and counter electrodes of 200 µm.[317] Reprinted with permission from ref 316 and 317. Copyright 2018 The Royal Society of Chemistry and 2015 The Royal Society of Chemistry.

1. Redox Potentials

In general, the selection of redox mediations usually starts by considering the redox potential. Ideally, both redox potentials will be close to $E^o(O_2/Li_2O_2)$=2.96 V vs. Li^+/Li, while still keeping high mediation activity. Very low redox potentials (*e.g.* <2.4 V vs. Li^+/Li) are unsuitable, because then the unmediated discharge reaction would compete with the mediated one, the former resulting in the passivation of the electrode and, thus, low capacities. A high discharge RM potential is also advantageous because then the formation of LiO_2 intermediates, which can induce degradation reactions, would be minimal. A low charge RM potential is advantageous because it prevents degradation reactions induced by application of high potentials (electrochemical electrolyte degradation, carbon corrosion, *etc*.), and also, because it improves the energy efficiency of the battery.

More work is required in order to elucidate the effect of the RM potential on the kinetics of mediated Li-O_2 cell reactions, with standardized testing conditions and involving systematic studies comparing different RMs under the same conditions. Studies of different RMs are often

performed under different conditions of electrolyte composition, cathode material, current density, *etc.*, thus hampering a quantitative comparison of RM activities.

Tables 1-3 summarizes key properties reported in studies of discharge, charge, bifunctional and dual RMs for Li-O_2 batteries. In the following, we will discuss some recent studies in which a comparison of several RMs has been performed under the same conditions.

The discharge mediation activity of a few quinone compounds has been compared,[81, 310] and DBBQ was found to produce the highest increase in current (in cyclic voltammograms) or capacity (in galvanostatic discharge), followed in mediator activity by vitamin K2. Since other quinones with similar redox potentials did not produce such dramatic effect on the Li-O_2 cell discharge reaction, it can be concluded that the RM potential is not the only determining factor in the enhancement of the rate of the ORR. Since DBBQ and vitamin K2 are both sterically hindered benzoquinones, it can be tentatively proposed that the enhanced stability of the reduced quinone, facilitated by the bulky substituent groups in DBBQ and vitamin K2, might promote a higher stability of the reduced quinone-oxygen complex,[81, 310] thus facilitating the oxygen reduction *via* reactions of type (34-37). Coenzyme Q10 is another sterically hindered quinone that showed great improvements of discharge capacity of Li-O_2 cells with Super P electrodes and tetraglyme electrolytes[309]; surprisingly, with gas diffusion electrodes and DME electrolytes, the mediation action of co-enzyme Q10 was only minor.[310] In another study, an anthraquinone, which has a lower redox potential than DBBQ (see **Table 1**) was found to lead to higher or lower capacities in Li-O_2 than DBBQ, depending on the cathode material used.[311]

Bruce and coworkers have compared the activity of a number of charge RMs by quantifying the kinetics of Li_2O_2 oxidation by RMs with scanning electrochemical microscopy experiments.[318] The oxidized form of RM was generated at a microelectrode that acted as the tip of the scanning electrochemical microscope. When the tip approached a Li_2O_2 pellet, an increase in the rate of oxidation of the RM was observed, the so-called positive feedback effect, as the reduced form of the RM is regenerated upon reaction of the oxidized form of the RM with the Li_2O_2 substrate (**Fig. 24a**). The analysis of the current detected at the microelectrode as a function of the distance of approach to the Li_2O_2 substrate has been used to quantify the apparent rate constant of the reaction of the RM with Li_2O_2, k_{app}. The results are shown in **Figure 24b**, for different RMs, as a function of the standard potential of the RM. It is observed that the highest values of rate constant are obtained with nitroxy radical compounds (AZO, MAZO and TEMPO: pink data points). These values are comparable to those reported for the mediation of Li^+ insertion/extraction from $LiFePO_4$.[319] Moderate values of rate constant are obtained with thiazine compounds (MPT, PPT and BPPT: green data points), while the other compounds studied, amines (TMPD, DPAB and TDPA: purple data points) and other-class compounds (DMPZ, TTF and FC: black data points) show much lower rate constants. There is not a clear correlation of the magnitude of the rate constant with the redox potential of the mediator; this indicates that the rate determining step of the reaction is not an electron transfer process, and it appears that the

kinetics of Li_2O_2 oxidation are more affected by the type of chemical functionality of the RM than by its redox potential.[318]

Differences in the rate of Li_2O_2 oxidation by different RMs have also been evaluated by means of rotating disc electrode experiments in which the change in the diffusion-limiting current of RMs with and without Li_2O_2 particles suspended in solution was measured (**Fig. 24c**).[320] The results of the increase in the limiting current upon addition of Li_2O_2 in solution are shown as a function of the standard redox potential of the RMs in **Figure 24d**. To facilitate comparison with the results by Bruce and coworkers[318] (**Fig. 24b**), the mediators that are common to both studies have been circled, and only the first electron-transfer process of the mediator has been considered. It is seen that the differences in mediation activity in **Figure 24d** agree well with the differences in the apparent rate constant of Li_2O_2 obtained in scanning electrochemical microscopy experiments shown in **Figure 24b**. This corroborates that the mediation activity is not a simple function of the mediator redox potential, as discussed by Bruce and coworkers.[318]

Table 1. Discharge mediators

Mediator	[c]	Redox potential	Discharge voltage	Discharge capacity		Current density	C_m/C	Electrodes (cathode/anode)	Electrolyte	Ref.
				Without mediator (C)	With mediator (C_m)					
	mM	V vs. Li/Li^+	V vs. Li/Li^+			$mAcm^{-2}$				
Tris(2,4,6-trichlorophenyl) methyl radical (TTM)	1	2.6	~2.65^P-2^T	~3.5 mAh cm^{-2} (~3500 mAh g^{-1})$^{\#}$	~7.5 mAh cm^{-2} (7500 mAh g^{-1})$^{\#}$	0.1	2.1	Super P/Li	1 M LiOTf / TGDME	321
Ethyl viologen (EtV)	2	2.4	~2.45^P-2.1^T	~2 µAh cm^{-2}	~4.7 µAh cm^{-2}	0.02	2.4	GC/Li	0.1 M LiTFSI / $Py_{14}TFSI$	41
2,5-di-tert-butyl-1,4-benzoquinone (DBBQ)	10	2.6	~2.7^P-2.4^T	~11 mAh m_{BET}^{-2}	~440 mAh m_{BET}^{-2}	0.1	40	GDL/LFP	1 M LiTFSI / TGDME	81
2,5-di-tert-butyl-1,4-benzoquinone (DBBQ)	10		~2.65^P -2.25^T	~1.5 mAh cm^{-2}	~4.5 mAh cm^{-2}	0.1	3	Super P/LFP	0.25 M LiTFSI / DME	67
2,5-di-tert-butyl-1,4-benzoquinone (DBBQ)	10		~2.6^P -2.25^T	~1 mAh cm^{-2}	~4 mAh cm^{-2}	0.1	4	RGO/LFP	0.25 M LiTFSI / DME	67
2,5-di-tert-butyl-1,4-benzoquinone (DBBQ)	10	~2.6	~2.65^P -2^T	2.3 mAh cm^{-2} (3300 mAh g^{-1})$^{\#}$	4.5 mAh cm^{-2} (6400 mAh g^{-1})$^{\#}$	0.07	1.9	Ketjen Black/Li	1 M LiTFSI / TEGDME	311
Anthraquinone (AQ)	2	~2.35^*	~2.58^P -2.1^T	~7.5 mAh m_{BET}^{-2}	~340 mAh m_{BET}^{-2}	0.1	45	GDL/$Li_{(LIPON\ coated)}$	0.1 M $LiClO_4$ / MeCN	308
Anthraquinone (AQ)	10	~2.35	~2.65^P -2^T	2.3 mAh cm^{-2} (3300 mAh g^{-1})$^{\#}$	7.7 mAh cm^{-2} (11000 mAh g^{-1})$^{\#}$	0.07	3.3	Ketjen Black/Li	1 M LiTFSI / TEGDME	311
Naphthoquinone (NQ)	10	~2.6	~2.6^P -2^T	2.3 mAh cm^{-2} (3300 mAh g^{-1})$^{\#}$	3.1 mAh cm^{-2} (4400 mAh g^{-1})$^{\#}$	0.07	1.3	Ketjen Black/Li	1 M LiTFSI / TEGDME	311

Ubiquinone (CoQ_{10})	10	2.63	~2.65^{P} -2.0^{T}	15.7 mAh m_{BET}^{-2}	570 mAh m_{BET}^{-2}	0.1	37	Super P/Li	1 M LiTFSI / TEGDME	309
Polyoxometalate (POM) $TBA_4SiW_{12}O_{40}$	50	2.65	~2.7^{P} -2.5^{T}	~0.2 mAh cm^{-2}	~0.6 mAh cm^{-2}	0.03	3	GDL/LFP	1 M LiTFSI / DMSO	314
Vitamin K2	10	2.54	~2.67^{P} -2.4^{T}	~0.14 mAh cm^{-2}	~3.7 mAh cm^{-2}	0.09	26	GDL/LFP	1 M LiTFSI / DME	310

Superscript P indicates that a voltage plateau was observed around this potential and the superscript T indicates the voltage at which the discharge curve terminates.

If the capacity or current density provided in the article were in mAh g^{-1}, the corresponding capacity normalized to area was estimated from the mass loading.

* For surface-immobilized redox mediator (estimated from CV).

Unless otherwise specified, the normalized areas correspond to geometrical area.

Table 2. Charge mediators

Mediator	**[c]**	**Redox potential**	**Discharge capacity**	**Charge capacity**	**Current density**	**Charging voltage**	**OER/ORR (O_2 ratio)**	**Electrodes (cathode/anode)**	**Electrolyte**	**Ref.**
	mM	V			$mAcm^{-2}$	V				
Tetrathiafulvalene (TTF)	10	~3.5	300^{L} mAh g^{-1}	300 mAh g^{-1}	0.078	3.4^{P}	~1 (reaction of mediator with Li_2O_2)	Au(nanoporous) /LFP	1 M $LiClO_4$ / DMSO	127
TTF	50	3.38, 3.69	~2.4^{L} mAh cm^{-2} (1500^{L} mAh g^{-1})$^{\#}$	~2.4^{L} mAh cm^{-2} (1500^{L} mAh g^{-1})$^{\#}$	0.15	3.2-4.7^{T}		Super C65/Li	1 M LiTFSI / TEGDME	322
TTF	10	3.75, 3.95	0.2^{L} mAh cm^{-2}	0.2^{L} mAh cm^{-2}	0.1	3.4-3.7^{P}		Ketjen Black/LFP	0.5 M $LiClO_4$ / DMSO	323
TTF	50	3.38	~0.8^{L} mAh cm^{-2} (1000^{L} mAh g^{-1})$^{\#}$	~0.6 mAh cm^{-2} (~800 mAh g^{-1})$^{\#}$	~0.16	3.6^{P}-4.5^{T}	0.33	CNT/Li	1 M LiTFSI / DME	324

TTF	30	~3.35	1 mAh cm^{-2} (1000^{L} mAh g^{-1})$^{\#}$	1 mAh cm^{-2} (1000 mAh g^{-1})$^{\#}$	0.2	~3.4^{P}		RGO/Li	0.5M LiTFSI / TEGDME	325
TEMPO (2,2,6,6-tetramethyl-1-piperidinyloxy)	10	3.74	~7600 mAh g^{-1}	~7500 mAh g^{-1}	0.1	~3.25-4.25^{T}	0.77 (assuming ideal ORR)	Ketjen Black/Li	0.1 M LiTFSI / DME	278
TEMPO	10	3.73	2.1 mAh cm^{-2} (~3500 mAh g^{-1})$^{\#}$	2.1 mAh cm^{-2} (~3500 mAh g^{-1})$^{\#}$	0.1	3.2-4.2^{T}		Ketjen Black/LFP	1M LiTFSI / DME	317
4-methoxy-TEMPO (4-methoxy-2,2,6,6-tetramethyl-1-piperidinyloxy)	10	3.76	2.2 mAh cm^{-2} (~3500 mAh g^{-1})$^{\#}$	1.9 mAh cm^{-2} (~3200 mAh g^{-1})$^{\#}$	0.1	3.2-4.2^{T}		Ketjen Black/LFP	1M LiTFSI / DME	317
1-methoxy-AZADO (1-methyl-2-azaadamantane-*N*-oxyl)	10	3.6	2.9 mAh cm^{-2} (~4900 mAh g^{-1})$^{\#}$	2.8 mAh cm^{-2} (~4700 mAh g^{-1})$^{\#}$	0.1	3.2-4.2^{T}		Ketjen Black/LFP	1M LiTFSI / DME	317
TMAO (1,1,3,3,-tetramethyl-2,3-dihydro-2-azaphenalene-2-yloxyl)	10	3.89	2.5 mAh cm^{-2} (~4200 mAh g^{-1})$^{\#}$	2.4 mAh cm^{-2} (~3500 mAh g^{-1})$^{\#}$	0.1	3.2-4.2^{T}		Ketjen Black/LFP	1M LiTFSI / DME	317
10-methylphenothiazine (MPT)	50	~3.8	0.4^{L} mAh cm^{-2} (1000^{L} mAh g^{-1})$^{\#}$	0.4^{L} mAh cm^{-2} (1000^{L} mAh g^{-1})$^{\#}$	0.12	~3.5^{P}-3.7^{P}		Ketjen Black/LFP	1M LiOTf/ TEGDME	326
10-methylphenothiazine (MPT)	100	3.67	533^{L} mAh g^{-1} load	533^{L} mAh g^{-1}	0.1	3.2-3.6^{P}-4.2^{T}		Super P/LFP	1M LiOTf/ TEGDME	327
10-methylphenothiazine (MPT)	100	~3.8	21.4^{L} mAh cm^{-2} (1000^{L} mAh g^{-1})$^{\#}$	21.4^{L} mAhcm^{-2} (1000^{L} mAh g^{-1})$^{\#}$	3.2	3.6^{P}		Super P/LFP	1M LiOTf/ TEGDME	328

Iodide	50	~	Li_2O_2-prefilled cathode	0.39 mAh cm^{-2} (1000 mAh g^{-1})#	~0.05	~3.8^P-4.2^T	0.92 (estimated from yield)	VC/Li	0.5 M LiTFSI / DME	197
Iodide	50	~	1000^L mAh g^{-1}	1000^L mAh g^{-1}	(2000 mA g^{-1})	~3.25^P		CNT/Li	1M LiTFSI/ TEGDME	277
Bromide	10	3.48	0.2^L mAh cm^{-2} (500^L mAh g^{-1})#	0.2 mAh cm^{-2} (~500 mAh g^{-1})#	0.2	~3.1-4.2^T	0.86	Ketjen Black/Li	1 M LiTFSI / DME	315
Cobalt bis(terpyridine)	50	3.41	0.8 mAh cm^{-2} (1000^L mAh g^{-1})#	0.8 mAh cm^{-2} (1000^L mAh g^{-1})#	0.16[1]	3.3^P-4.5^T	0.23	CNT/Li	1 M LiTFSI / DME	324
Heme (biomolecular)	2.3	~3.4	~2800 mAh g^{-1} load	~2800 mAh g^{-1}	(100 mA g^{-1})	~3.05-4.25^T		CNT/Li	1 M $LiClO_4$ / TGDME	329
TDPA (tris[4-(diethylamino)phenyl]amine)	3.6	~	~4.1 mAh cm^{-2} (~8200 mAh g^{-1})#	~4.1 mAh cm^{-2} (~8200 mAh g^{-1})#	0.1	~3.2-3.75^T	0.74	Ketjen Black/Li	0.5 M LiTFSI/ TEGDME	206

Superscript L indicates that the capacity vas limited to the corresponding value rather than limiting the potential.

Superscript P indicates that a voltage plateau was observed around this potential and the superscript T indicates the voltage at which the discharge curve terminates.

If the capacity or current density provided in the article were in mAh g^{-1}, the corresponding capacity normalized to area was estimated from the mass loading.

Unless otherwise specified, the normalized areas correspond to geometrical area.

Table 3. Bifunctional and dual redox mediators.

Mediator	[c]	Redox potential	Discharge capacity	Charge capacity	Current density	Voltage Discharge / Charge	Electrodes	Electrolyte	Ref.
	mM	V			mA cm^{-2}	V			
Iron phthalocyanine (FePC)	2	2.5, 3.65	1.8 mAh cm^{-2} (1800 mAh g^{-1})#	1.7 mAh cm^{-2} (1750 mAh g^{-1})#	0.1	~ 2.6-2.0 / 3.1-4.4^{T}	C-Fiber /Li	0.1M LiTFSI /TEGDME	78
2-phenyl-4,4,5,5-tetramethylimidazoline-1-oxyl-3-oxide (PTIO)	50	2.3, 3.8	1.5 mAh cm^{-2} (6900 mAh g^{-1})#	1.5 mAh cm^{-2} (6900 mAh g^{-1})#	0.1	~ 2.75^{P} / 3.5-4.2^{T}	CNT/Li	1M LiTFSI /DMSO	330
cobalt-based polyoxometalate (Co-POM)	0.33	~2.6	~1.82 mAh cm^{-2} (4050 mAh g^{-1})#	~1.85 mAh cm^{-2} (4100 mA g^{-1})#	~0.05	~2.7 / 3.2-4.5^{P}	CNT/Li	1M LiTFSI /TEGDME	331
2,5-di-tert- butyl-p-benzoquinone (DTBBQ / tris{4-[2-(2-methoxyethoxy)ethoxy]phenyl}amine (TMPPA)	10/10	2.63, 3.63	1.5 mAh cm^{-2}	1.5 mAh cm^{-2}	0.5	~ 2.7^{P} / 3.75^{P}, 3.9^{P}	C-Felt/Li (redox flow battery)	1M LiTFSI /TEGDME	332
DBBQ / TEMPO	25/25	2.58, 3.74	2 mAh cm^{-2}	2 mAh cm^{-2}	1	~2.7^{P} / 3.7^{P}	GDL/LFP	0.3 M $LiClO_4$ /DME	333
Ethyl viologen / LiI	10/10	2.65, 3.1/3.7	1.5 mAh cm^{-2}	1.5 mAh cm^{-2}	0.05	2.75^{P} / 3.5-3.75^{P}-4^{T}	C-Felt/Li (redox flow battery)	1M LiTFSI /TEGDME	334

If the capacity or current density provided in the article were in mAh g^{-1}, the corresponding capacity normalized to area was estimated from the mass loading.

Superscript P indicates that a voltage plateau was observed around this potential and the superscript T indicates the voltage at which the discharge curve terminates.

Unless otherwise specified, the normalized areas correspond to geometrical area.

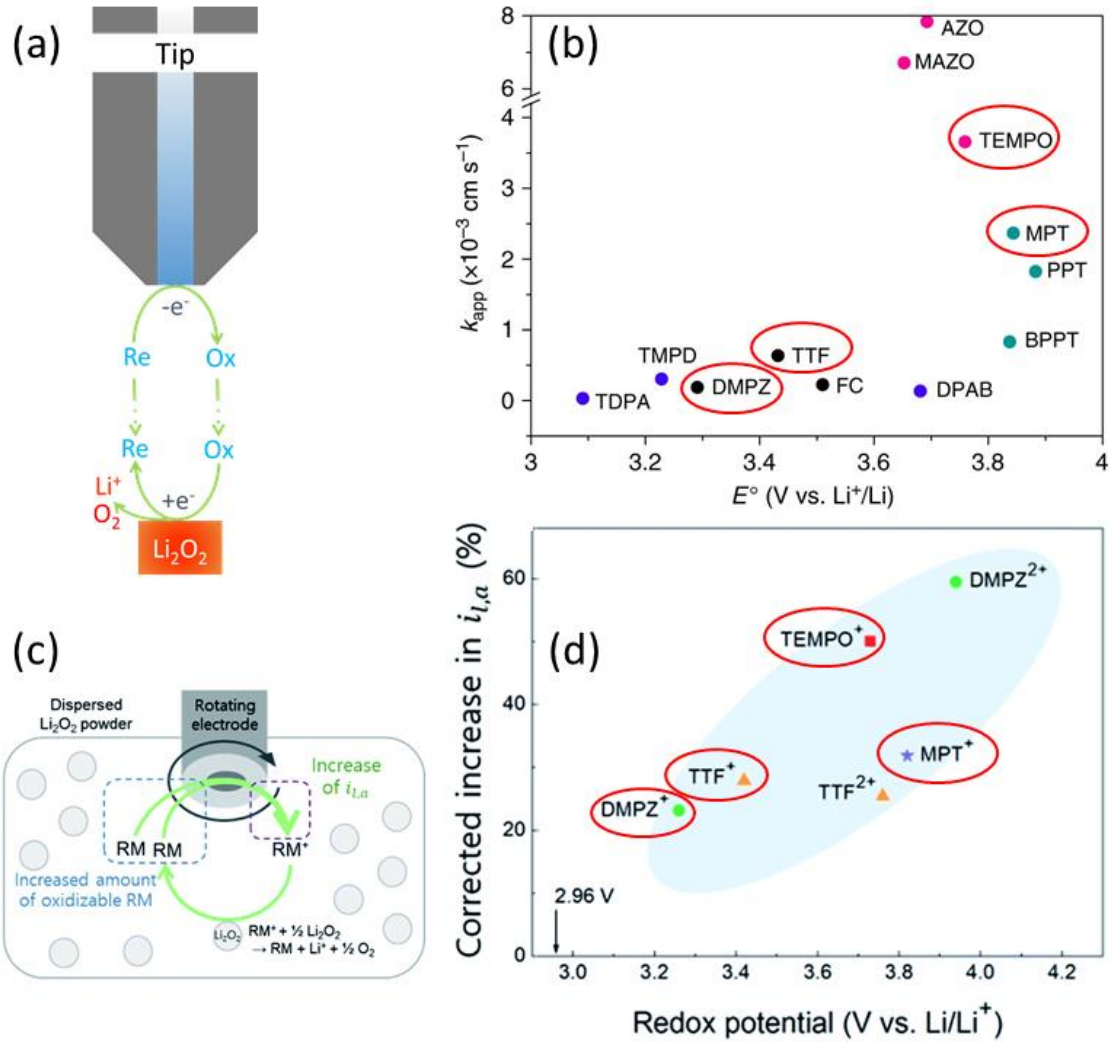

Fig. 24 Systematic studies of mediator activities in Li-O_2 reactions. (a): Analysis of the reaction rate of Li_2O_2 oxidation by RMs using scanning electrochemical microscopy. (b): Plot of the apparent rate constant, k_{app}, of the reaction of RMs with Li_2O_2 against the redox potential of the RM, E^o. Amines, nitroxy and thiazine compounds are marked in blue, pink and green.[318] (c): Schematic displaying the increase in the diffusion-limiting current of RMs in rotating disc experiments (RDE) in the presence of Li_2O_2 suspended in solution, as a result of the reaction of the oxidized RMs with Li_2O_2. (d): Plot of the increase in the diffusion-limiting current, $i_{l,a}$, vs. the redox potential of the RMs in RDE experiments.[320] (b) Reprinted with permission from ref 318. Copyright 2018 Macmillan Publishers Limited and (c-d) from ref 320. Copyright 2019 The Royal Society of Chemistry.

While scanning electrochemistry microscopy and rotating disc experiments are very powerful approaches to compare the rate of Li_2O_2 oxidation by different RMs,[318, 320] these techniques only provide information about the rate of regeneration of the oxidized RM upon reaction with Li_2O_2. Unfortunately, the detection and quantification of the O_2 evolved in these experiments is very challenging; therefore, additional techniques are needed in order to validate the trends obtained, since the complexity of Li-O_2 reactions and proneness to degradation have shown in the past that interpretation of electrochemical data without the support of gas analysis can lead to incorrect conclusions.[134, 335] The evolution of O_2 from the reaction of RM with Li_2O_2 powder has been monitored with an oxygen sensor,[336] which shows that a solution containing a mixture of $I_2 + I_3^-$ (equilibrium potential: 3.60 V vs. Li^+/Li)

exhibited the fastest rate of O_2 evolution, followed by a mixture of $TEMPO^+$ + TEMPO (equilibrium potential; 3.74 V vs. Li^+/Li) while Fc^+ + Fc mixtures (equilibrium potentials: 3.28-3.36 V vs. Li^+/Li) had very low reaction rate and I_3^- + I^- mixtures did not produced any detectable O_2. Interestingly, addition of a proton donor (BuOH) significantly increased the O_2 evolution rate by the I_3^- mediator (in the I_3^- + I^- mixture). As discussed in Section 4.3 proton donor additives enable the formation of a more soluble intermediate (LiOOH) in Li-O_2 cell reactions, which can explain the enhanced kinetics (since higher solubilities afford a higher concentration, which then promotes a higher reaction rate). While much more work is necessary to elucidate the mechanism of these reactions and the fundamental descriptors affecting reactivity, all these studies show that the redox potential of the mediator is not the only factor determining the activity towards O_2 evolution from Li_2O_2.

2. Chemical Stability

Degradation of RMs in Li-O_2 batteries would be even more detrimental than the degradation of the electrolyte, since mediators are present in a much lower concentration than the solvent and their role in Li-O_2 cell reactions is critical. However, one advantage of RMs is that they facilitate electron transfer reactions that can deactivate the reactivity of degradation triggers (such as superoxide anion and singlet oxygen).

For example, Sawyer and coworkers showed that reduced methyl viologen (MV^+) reacts with superoxide (O_2^-) *via* radical-radical coupling producing various degradation products:[166]

$$MV^{\cdot+} + O_2^{\cdot-} \rightarrow [MV - O_2] \rightarrow degradation\ products \qquad (38)$$

However, an analogous viologen, ethyl viologen (EtV^{2+}), has been shown to be a suitable discharge mediator for Li-O_2 batteries.[41] By undergoing fast electron transfer reactions, in Li^+ containing electrolytes, ethyl viologen promotes the reduction of oxygen to lithium superoxide:[41]

$$EtV^+ + O_2 + Li^+ \rightarrow EtV^{2+} + LiO_2 \qquad (39)$$

and also the reduction of lithium superoxide to lithium peroxide:

$$EtV^+ + LiO_2 + Li^+ \rightarrow EtV^{2+} + Li_2O_2 \qquad (40)$$

The absence of degradation of ethyl viologen in Li^+ containing electrolytes was explained by the fact that the electron transfer reaction from EtV^+ to LiO_2, forming Li_2O_2 (reaction (40)), was much faster than degradation reactions such as radical-radical coupling (reaction(38)).[41]

In the search for efficient RMs for Li-O_2 batteries, the characterization of the reaction of RMs with LiO_2 can be used to evaluate the absence of degradation of the RM, but also, a quantitative evaluation of the reaction rate can be used to rank the mediator activity of different RMs. But LiO_2 is not the only degradation trigger present in Li-O_2 cells. A recent

study has shown that some RMs (5,10-dimethyl phenazine and tetrathiafuvalene) that are resistant against the attack by superoxide, degrade in the presence of singlet oxygen.[337] Although there are methods to decrease the presence of singlet oxygen using quenchers,[153] and the generation of superoxide using RMs[41, 81] in Li-O_2 cells, the long term stability of the battery would require the RM to be reasonably stable in contact with these two potential degradation triggers. Therefore, testing the stability against superoxide and singlet oxygen would be an important part of the protocol for screening new RMs, and the test should be performed for all the oxidation states of the mediator relevant for the operation of the battery. In addition to experiments, *ab-initio* calculations can be very helpful for the rational screening of sufficiently stable RMs, which can provide an estimation of the redox potential and also of the chemical stability of the RMs in different oxidation states.[338]

In the search for more stable RMs, polyoxometalates have been recently proposed as a new type of RMs for Li-O_2 cells.[314, 331] Polyoxometalates are metal-oxygen clusters with multiple oxidation states exhibiting high stability in oxidizing environments. Although substantial improvements in the polyoxometalates mediation activity in Li-O_2 cells are required, they promise improved resistance against degradation reactions, compared to organic RMs, which warrants further investigation.

4.2.3 Progress in RMs Development

Many promising RMs have been proposed for Li-O_2 batteries applications (**Tables 1-3**). As discussed above, different RMs have been tested under different conditions, and therefore, ranking in terms of RM activity is currently not possible and the use of analytical techniques to quantify the oxygen recovery efficiency (OER/ORR) during cell reactions is essential in order to evaluate the true mediation activity.

To put the requirements of RM activity into context, we return to the calculations by Gallagher and coworkers (**Fig. 1**) performed at a system level to take into account the requirements for electric vehicle applications. It was demonstrated that high values of areal electrode capacities (normalized by the geometric electrode area) are required to reach competitive values of specific energy, energy density and cost per usable energy that would make Li-air batteries superior to the current state-of-the-art Li-ion batteries. To fulfill the requirements for electric vehicle applications, cells should also be able to deliver 90% of the capacity at C/5 (where C/5 corresponds to a current of 2 mA cm^{-2} for a capacity of 10 mAh cm^{-2}). The authors also mentioned a target of >1000 cycles of cycle life.[28] This requires an oxygen recovery efficiency (OER/ORR) and Coulombic efficiency >99.9% per cycle.

While the cell parameters considered by Gallagher and coworkers were very optimistic at the time of the publication, recent studies of Li-O_2 cells incorporating RMs have achieved comparable performance. Bruce and coworkers reported that addition of DBBQ to Li-O_2 cells produced areal capacities (normalized to the geometric area of the electrode) of *ca.* 11 mAh cm^{-2} at an areal current density of 0.2 mA cm^{-2} (**Fig. 25a**).[81] Grey and coworkers later reported that the synergistic combination of DBBQ and water produced Li-O_2 cells capacities of up to 18 mA h cm^{-2} at 0.1 mA cm^{-2} (**Fig. 25b**).[67] Interestingly, in that latter study, reduced

graphene oxide electrodes with very low carbon content (of *ca.* 0.2 mg_c cm^{-2}) were employed; normalization of capacities by the mass of carbon would produce an impressive (but potentially misleading) value of *ca.* 180000 mAh/g_c, *i.e.*, both high specific and areal capacities were obtained; these capacity values also remind us that caution should be taken when evaluating the energy density of a lithium-air battery only based on specific capacities normalized by the carbon mass.[133] Low carbon content in the electrodes is essential to achieve high figures of merit of energy density, specific energy and cost per usable energy, since carbon adds to the volume, weight and cost of the battery. The carbon content considered in the calculations by Gallagher and coworkers[28] was 9% in mass of the dry, discharged electrode. The carbon content in the work by Grey and coworkers[67] corresponded to only 1% in mass of the dried, discharge electrode; the remaining 99% was Li_2O_2 (as confirmed by NMR and quantification of the O_2 consumed by mass spectrometry). The next challenge is to significantly improve the reversibility of these systems, i.e., high oxygen recovery efficiencies and Coulombic efficiencies.

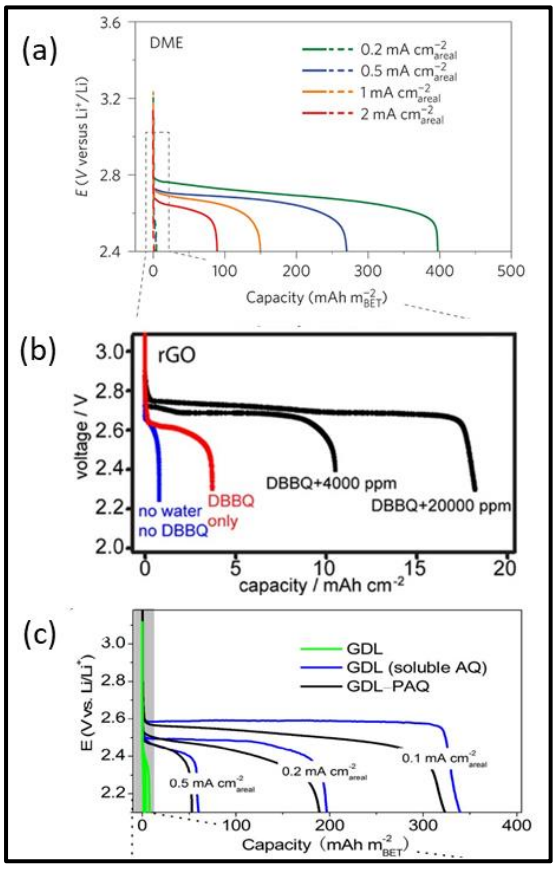

Fig. 25 Selected examples of high-capacity, mediated Li-O_2 batteries. (a): Discharge curves of Li-O_2 cells with a gas diffusion electrode discharged in 1M LiTFSI in DME with 10mM DBBQ (solid lines) and without DBBQ (dashed lines) at various areal current densities from 0.1 $mAcm^{-2}$ to 2$mAcm^{-2}$.[81] (b): Discharge curves of Li-O_2 cells made of reduced graphene oxide electrodes either with neat 0.25 M LiTFSI/DME electrolyte, with only DBBQ added (10 mM), or with both DBBQ and H_2O added to the neat electrolyte (as labeled in the figures).[67] (c) Discharge curves of Li–O_2 batteries with (green) pristine, (blue) soluble anthraquinone (AQ)-, and (black) polyanthraquinone (PAQ)-catalyzed GDL cathodes in 0.1 M $LiClO_4$ MeCN at various current densities.[308] (a) Reprinted with permission from ref 81. Copyright 2016 Macmillan Publishers Limited and (b) from ref 67. Copyright 2018 ACS. (c) From ref 308. Copyright 2018 ACS.

Other RMs have also produced high values of areal discharge capacity at reasonably high areal current densities (see **Tables 1-3**). It is also worth mentioning that immobilization of the anthraquinone (AQ) RM forming a thin conductive polymer film of polyanthraquinone produced the same areal capacities as with the freely diffusing anthraquinone (**Fig. 25c**).[308] This is a highly promising approach since it overcomes the problem of RM shuttling to the anode, which would degrade the RM, decrease the battery capacity and hamper rechargeability.

While major improvements have been made in the discharge reaction of Li-O_2 cells *via* the incorporation of RMs, efficient recharging is still one of the most important bottlenecks in Li-O_2 cell development. A key figure of merit is the production, during charge, of the same amount of O_2 that has been consumed during discharge. This is quantified by the oxygen recovery efficiency (OER/ORR), which is defined as the ratio of the amounts of O_2 evolved and consumed in Li-O_2 cell cycling (see Section 2.2.4). As shown in **Table 2**, oxygen recovery efficiencies approaching 100% OER/ORR have not been found yet, but some promising values have been reported.

High oxygen recovery efficiencies of 98% to 61% OER/ORR have been reported for LiBr-containing Li-O_2 cells, which vary with the applied current (**Fig. 26**).[315] Although the experiments were performed by limiting the discharge capacity to 500 mAh/g (corresponding to only 0.2 mAh/cm^2), the results are certainly encouraging, as typical O_2 recovery ratios are lower than 75% in non-mediated Li-O_2 cells.[35, 91, 99, 132] A very high oxygen recovery efficiency of 92% OER/ORR has been reported for charging Li_2O_2-prefilled electrodes in LiI-containing solutions.[197] A 78% OER/ORR has been reported for a LiI-containing Li-O_2 cell containing a flexible Li-ion conducting membrane to protect the lithium anode, as estimated from *operando* pressure measurements.[339] With the aid of redox mediators, the electrochemical decomposition of Li_2O_2 is switched to chemical Li_2O_2 decomposition, Li_2O_2 reacting with the oxidized form of the mediators. Lu and coworkers[315] have proposed that accounts for the increase in oxygen recovery, as it minimizes the formation of reactive oxygen species during direct electrochemical recharging. It is interesting to further verify which reactive oxygen species are avoided and by how much, and in particular, whether the generation of singlet oxygen is circumvented with the use of LiBr/LiI. Recent studies[337] indicate that organic redox mediators, such as tetrathiafuvalene and dimethylphenazene, are prone to degradation when exposed to singlet oxygen. Whether these inorganic mediators are more resistant to singlet oxygen attack is another interesting question.

Taken together, the promotion of O_2 evolution from Li_2O_2 by both LiI and LiBr deserves further investigation. Of note, LiI also has the potential to promote LiOH formation *via* a nominal four-electron ORR in the presence of proton donor molecules (*e.g.*, H_2O); this will be discussed in Section 5.2.

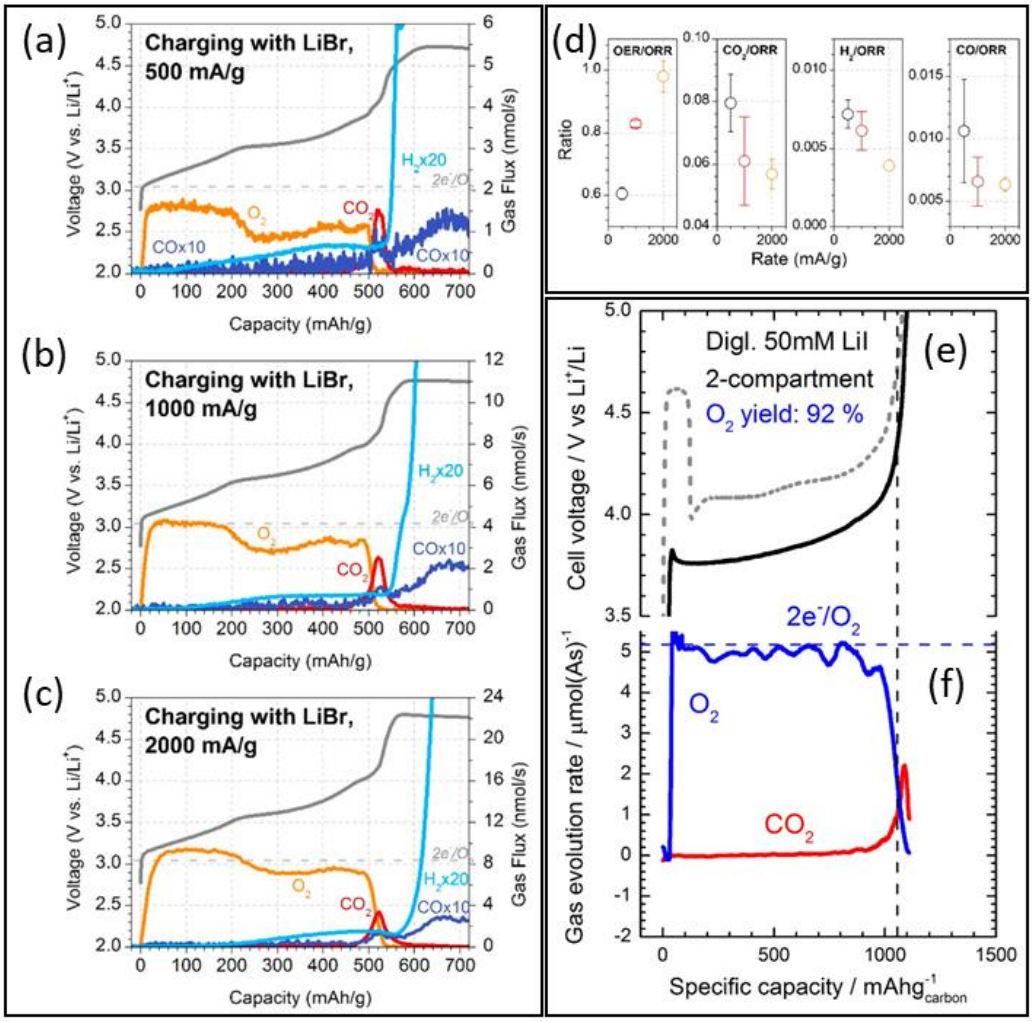

Fig. 26 Examples of mediated Li-O_2 cells with high oxygen recovery efficiency. Voltage and gas evolution profiles during charging with 10 mM LiBr at (a) 500, (b) 1000, and (c) 2000 mA/g after discharge to 500 mAh/g at 1000 mA/g. (d) A plot showing the statistics based on at least three replications (right pantel).[315] (e) galvanostatic charge of *pre-filled* Li_2O_2/VC electrodes and (f) current normalized gas evolution rates for CO_2 and O_2 using 0.5 M LiTFSI + 50 mM LiI (RM) in diglyme in a 2-compartment cell. Electrode loading 0.39 $mg_{carbon}cm^{-2}$ (1:1 Li_2O_2:carbon ratio (90% Li_2O_2 purity), *i.e.*, 0.35 $mgcm^{-2}$ of pure Li_2O_2). The cell was galvanostatically charged at 120 mAg_{carbon}^{-1} (corresponding to 82.8 µA). The voltage profile in a 2-compartment cell without LiI is superimposed for comparison (dotted gray line). The dotted black line indicates the specific capacity of 1051 $mAhg_{carbon}^{-1}$ for the expected reaction $Li_2O_2 \rightarrow 2Li^+ + O_2 + 2e^-$, whereas the blue dotted line indicates the expected oxygen evolution rate corresponding to $2e^-/O_2$.[197] (a–d) Reprinted with permission from ref 315. Copyright 2016 ACS and (e-f) from ref 197. Copyright 2014 Electrochemical Society.

Nitroxide compounds (such as TEMPO) are another highly promising family of RMs. An efficiency of 87% OER/ORR has been reported *via* pressure/DEMS measurements for TEMPO-containing Li-O_2 cells, containing a Li anode protected with a solid electrolyte.[340] An efficiency of 70% OER/ORR has been reported for triphenylamines (such as TDPA) from the total amount of O_2 evolved during charging;[206] these mediators have a very low redox potential (3.1 V vs. Li^+/Li for TDPA), but high activity for the oxidation of Li_2O_2 to O_2.[206] TTF was the first reported charge mediator for Li-O_2 batteries,[127] and the reaction of oxidized TTF, TTF^+, with Li_2O_2 was reported to produce a ratio of 2.01 electrons per O_2 evolved,

which can potentially translate in remarkable efficiencies of >99% OER/ORR. Addition of Cl^- in the electrolyte improves the mediation activity of TTF via the formation of an organic electronic conductor deposited on the cathode surface (TTF^+-Cl^-).[325]

In conclusion, impressive improvements in performance have been achieved in recent years *via* the incorporation of RMs, and a good number of promising RMs has been identified (**Tables 1-3**). Major improvements are still required to reach the targets for commercialization, and the current main bottlenecks in performance are the poor OER/ORR recovery efficiency, insufficient stability against degradation, and lack of fundamental understanding of the key properties leading to high mediation activity.

4.3 Functional Additives

This section presents an in-depth discussion of the mechanism of phase-transfer catalysis (by water and alcohols) and singlet oxygen quenchers. (The use of electrolyte additives as RMs ~~and~~ to promote the solution-based mechanism of discharge has already been discussed in Sections 4.2 and 2.1, respectively). We believe that in order to reach the requirements for commercial applications, Li-O_2 batteries will need to exploit the synergistic combination of several functional additives, and that the combination of RMs, phase-transfer catalysts and singlet oxygen quenchers is particularly promising. The use of fluorinated electrolyte additives in Li-O_2 batteries is also discussed, since this approach has received considerable attention in recent years.

4.3.1 Water

The effect of water on the electrochemistry of Li-O_2 cells has been briefly discussed in Section 3.2.2. Drastic improvements in capacity have been reported upon water addition.[31, 74, 75, 238, 239, 341, 342] The observed increase in capacity has been ascribed to an increase in solubility of Li-O_2 cell reaction intermediates due to two possible effects: i) solvation effects, and ii) proton-transfer reactions. The following discussion demonstrates that, although solvation effects are definitively present and contribute to the increase in capacity, the dominant factor is the occurrence of proton-transfer reactions that enable a new reaction pathway involving a LiOOH intermediate, which overrides the "usual" reaction mechanism involving LiO_2 or O_2^- intermediate formation.

The mechanistic understanding of the water-induced capacity enhancement is discussed below in light of older and recent studies of the electrochemistry of oxygen in aprotic media.

1. <u>Solvation effects</u>

Marked variations of the solvation energy of superoxide in different media were demonstrated in early work by Sawyer and coworkers: the change of the standard potential of the O_2/O_2^- couple, as measured with cyclic voltammetry experiments, showed that the solvation of superoxide by water was much stronger than in other solvents.[343]

Such a strong superoxide-water interaction can be ascribed to the very high acceptor number of water, which readily accepts electron density from the superoxide, acting as a donor or

Lewis base. But water also has a very high donor number.[344] Abraham and coworkers[34] showed that lithium superoxide is stabilized in high-donor-number solvents, and Bruce and workers[30] demonstrated that Li-O_2 cells with high-donor-number solvents discharge via a mechanism in which the high solubility of the lithium superoxide intermediate product enables the formation of large Li_2O_2 deposits away from the electrode surface: the solution-based mechanism described in Section 2.1, thus producing a marked capacity enhancement. Having a very high donor number, the incorporation of water as an additive or co-solvent produces a similar effect on the solubility of LiO_2. On the other hand, using a quantitative model of Li-O_2 cell reactions, Luntz and co-workers[31] explained the observed enhanced capacities of Li-O_2 cells with added water by the strong interaction of water with superoxide due to the high acceptor number of water. Combining experiments and a computational analysis, Shao-Horn and coworkers studied the effects of donor number and acceptor number of water to the observed increase in lithium superoxide solubility.[69] All these studies agree that water addition is expected to increase the solubility of the LiO_2 intermediate product. While that effect is expected to produce enhanced capacities, other effects might also be at play, or even dominate, in practical Li-O_2 cells.

2. Proton transfer reactions

Sawyer and coworkers demonstrated that, in aprotic media (*e.g.* dimethylformamide), protonation of superoxide by water is thermodynamically unfavorable; this is due to the very low pK_a of water (low Bronsted acidity, $pK_a \approx 33$):[345]

$$H_2O + O_2^- \leftrightarrow HO_2 + OH^- \qquad (41)$$

, where K_{eq} is equal to 10^{-21}, and ΔG^o is equal to +119.7 kJ/mol.

However, it was found that this reaction is followed by the rapid disproportionation of protonated superoxide forming HO_2^- (which is the base of H_2O_2), and the net reaction is thermodynamically favorable:[345]

$$H_2O + 2O_2^- \leftrightarrow HO_2^- + O_2 + OH^- \qquad (42)$$

, where K_{eq} is equal to 10^5, and ΔG^o is equal to -28.5 kJ/mol.

Thus, in the presence of water, the oxygen reduction reaction may proceed via an alternative reaction pathway involving the formation of an HO_2^- intermediate, which is expected to have reasonably high solubility and diffusion coefficient in aprotic solvents. This would explain the fact that higher capacities are obtained in Li-O_2 electrolytes containing water, since the solubility of the HO_2^- intermediate will be higher than the solubility of the superoxide intermediate formed in the reaction in the absence of water. Once the saturation concentration of HO_2^- is reached, it will precipitate in the form or Li_2O_2. The following mechanism can be proposed for Li-O_2 discharge reactions in the presence of water:

$$O_2 + e^- \leftrightarrow O_2^- \qquad (43a)$$

$$H_2O + 2O_2^- \leftrightarrow HO_2^- + O_2 + OH^- \quad (43b)$$

$$HO_2^- + 2Li^+ + OH^- \leftrightarrow Li_2O_2 + H_2O \quad (43c)$$

$$\overline{O_2 + 2e^- + 2Li^+ \leftrightarrow Li_2O_2}$$

The mechanism above shows that water acts as a catalyst that promotes an alternative reaction mechanism with faster kinetics, where the water is not consumed in the reaction. A variation of the above reaction mechanism can be proposed considering that anions are paired with lithium cations:

$$O_2 + e^- + Li^+ \leftrightarrow LiO_2 \quad (44a)$$

$$H_2O + LiO_2 \leftrightarrow LiOOH + O_2 + LiOH \quad (44b)$$

$$LiOOH + LiOH \leftrightarrow Li_2O_2 + H_2O \quad (44c)$$

$$\overline{O_2 + 2e^- + 2Li^+ \leftrightarrow Li_2O_2}$$

where LiOOH could be a soluble species (HO_2^- and Li^+ ion pair) or a solid intermediate product. Note that the thermodynamics and kinetics of these reactions are expected to change as the solvent is changed (due to solvation effects) and also as a result of the interaction of the anions with lithium ions.

In the first studies of the effect of water addition to Li-O_2 cells, Gasteiger and co-workers proposed that proton transfer effects could lead to a partial chemical "solubilization" of solid Li_2O_2, but they also pointed out that full protonation of Li_2O_2 to form H_2O_2 was thermodynamically unfavorable:[75]

$$Li_2O_2 + 2H_2O \leftrightarrow H_2O_2 + 2LiOH; \Delta G^o = +41\ kJ\ mol^{-1} \quad (45)$$

Thus, the formation of a LiOOH or HO_2^- intermediate would bring together these observations: water acts as a proton donor, but it favors the formation of LiOOH or HO_2^-, not H_2O_2, since the HO_2^- is not basic enough to be protonated by water. The formation of LiOOH in the discharge of water-containing Li-O_2 cells was first proposed by Wang and coworkers to explain the different reactivity of Li-O_2 cells upon addition of water (**Fig. 27a**).[346] In addition, recent work has reported the presence of a Raman signal ascribable to hydroperoxide species (HO_2^- or LiOOH) on wet, discharged cathodes from water-containing Li-O_2 cells (**Fig. 27b**).[239] Interestingly, the HO_2^- or LiOOH Raman signal was found to appear at the beginning of discharge, prior to the formation of Li_2O_2 or LiO_2, and formation of LiO_2 was not observed at high enough water concentrations. These findings support the hypothesis that proton-transfer reactions leading to the formation of LiOOH or HO_2^- intermediates constitute an alternative pathway in Li-O_2 reactions, which overrides the LiO_2 intermediate pathway for high enough water concentrations. The suppression of degradation reactions in water-containing Li-O_2 cells was, indeed, ascribed to bypassing LiO_2 formation, and Raman spectra of the dried electrodes (**Fig. 27c**) shows negligible formation of side reaction products at high water content (**Fig. 27c**).[239] The delay in Li_2O_2 deposition in the presence of water in

the electrolyte has also been observed in *in situ* surface-enhanced Raman spectroscopy measurements.[347]

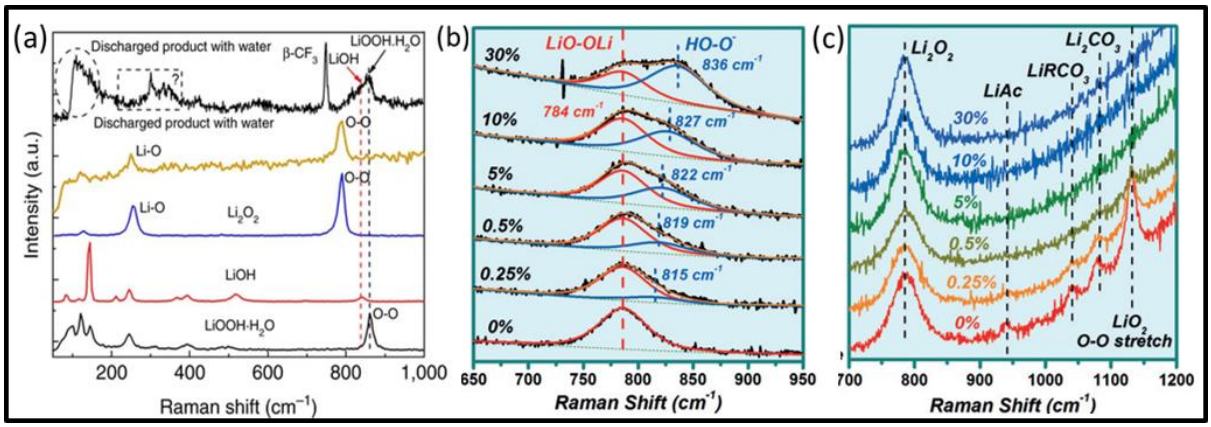

Fig. 27 Evidence of formation of LiOOH or HO_2^- intermediates in Li-O_2 cells. (a): Raman spectra of Li_2O_2, LiOH, LiOOH·H_2O and that of the discharge product collected from the cathode of a Li-O_2 cell without water or containing 9.1 vol.% H_2O in the electrolyte.[346] (b): Raman spectra and analysis on the discharged cathodes with differing water content in electrolytes (1 M LiTFSI/TEGDME); the spectra were collected with the wet, discharged cathodes. (c): Spectra of dry cathodes collected from the discharged electrodes (similar to (b)), but after washing and vacuum drying to clean off the residual electrolyte.[239] (a) Reprinted with permission from ref 346. Copyright 2017 Macmillan Publishers Limited and (b-c) from ref 239. Copyright 2017 Wiley-VCH Verlag GmbH & Co. KGaA, Weinheim.

In conclusion, the mechanism of the increased discharge capacity observed upon addition of water in electrolytes is mainly due to proton transfer reactions that, coupled to electron transfer reactions, produce the formation of a soluble LiOOH or HO_2^- reaction intermediate and, as a result, the growth of Li_2O_2 takes in solution, rather than on the electrode surface, thus resulting in the growth of large Li_2O_2 deposits. The formation of LiOOH or HO_2^- reaction intermediate is supported by thermodynamic considerations and the direct detection of the species by Raman spectroscopy. Therefore, water acts as a proton-donor phase-transfer catalyst that favors the formation of soluble reaction intermediates *via* proton transfer reactions. Since the net reaction is the reduction of O_2 to Li_2O_2, water is not consumed in the reaction, but the effect on the electrochemistry of Li-O_2 cells can be dramatic. Interestingly, Nazar and coworkers have also shown that trace amount of water, incorporated in the cell as hydration water impurities in the electrolyte salt, can also produce a dramatic effect in the electrochemistry of Na-O_2 cells (increased discharge capacity and decreased charge overpotential).[104]

4.3.2 Alcohols

The discussion above (Section 4.3.1) has shown that, despite the very high pK_a of water in organic media (that is, very low Bronsted acidity), water acts as a proton-donor catalysts in Li-O_2 cell discharge reactions by inducing the protonation of superoxide to form LiOOH or HO_2^- reaction intermediates, which are soluble, and thus favor a solution-based discharge reaction that leads to Li_2O_2 formation in solution, resulting in high discharge capacities.

The pK_a of water in dimethylformamide is, $pK_a \approx 33$.[345] The pK_a of alcohols is similar or lower than that of water: For example, in dimethylformamide, the pK_a's of phenol and of 3,5-di-tertbutylcatechol are $pK_a \approx 20$. This is because of the stabilization of the PhO^- anion by resonance (electron delocalization in the benzene ring); for linear alcohols like 1-butanol the pK_a is the same as water: $pK_a \approx 33$.[345] Therefore, these pK_a values show that alcohols can be stronger Bronsted acids than water.

In view of these considerations, it is not surprising that the addition of an alcohol as electrolyte additive in Li-O_2 batteries can produce an even more dramatic effect than water addition.[76] Indeed, phenol was found to produce a very high value of discharge capacity of 9 mAh/cm^2, which was attributed to a phase-transfer catalysis effect, in line with the discussion above about proton-transfer induced reactions. It was also demonstrated that the increase in discharge capacity was not due to side reactions, since the reaction stoichiometry was found to be of two electrons consumed per O_2 (as obtained from *in-situ* mass spectrometry measurements), and Li_2O_2 was identified as the main discharge produce with FTIR and XRD measurements.[76]

2,6-Di-Tert-Butyl-Hydroxytoluene (BHT) was also found to increase the discharge capacity of Li-O_2 cells,[348] which could also be ascribed to the proton-donor phase-transfer catalysis effect. A mediation of BHT of the oxygen reduction reaction, as suggested in the original article,[348] is unlikely, since BHT is already in the reduced form, thus if it was reductive enough to mediate the reduction of O_2, the BHT present in solution would directly react with O_2 as the O_2 was incorporated in the cell, forming Li_2O_2 even before the discharge of the cell started.

The proton-donor phase-transfer catalysis of alcohols and water is a promising venue to increase the discharge capacity of Li-O_2 cells because their Bronsted acidity is high enough to promote the formation of LiOOH or HO_2^- soluble reaction intermediates, but it is low enough to preserve the Li_2O_2 as the final discharge product. By contrast, introduction of stronger Bronsted acids, such as $HClO_4$, was found to lead to various proton-triggered degradation reactions, and hence, should be avoided.[75]

4.3.3 Singlet Oxygen Quenchers

Singlet oxygen has been identified as an important trigger of degradation reactions in Li-O_2 cells.[139, 153] Singlet oxygen formation during the charge of Li-O_2 cells was first identified using a spin trap (4-oxo-TEMP, see structure in **Figure 28**) that reacts with singlet oxygen forming an stable radical (4-oxo-TEMPO), which was detected by *operando* EPR spectroscopy.[139] In a later work by Freunberger and coworkers, the specific emission of singlet oxygen at 1270 nm (involved in the decay of singlet oxygen to triplet oxygen) was detected in *operando* measurements of Li-O_2 cells, and in addition, *operando* fluorescence measurements using a chemical trap (dimethyl anthracene, DMA) that reacts irreversibly with singlet oxygen also demonstrated the formation of singlet oxygen during charge of Li-O_2 cells.[153]

Interestingly, it has been shown that the damaging effects of singlet oxygen can be removed *via* the incorporation of a chemical trap or a physical quencher to deactivate singlet oxygen; this was shown to decrease the amount of side products formed during discharge and increase the amount of oxygen evolved during charge.[153] While the first physical quencher of singlet oxygen (DABCO) used in Li-O_2 cells limited the operation voltage to *ca.* ≤ 3.5 V vs. Li^+/Li, due to instability of the quencher at higher voltages, a very efficient new quencher has been recently proposed (DABCOnium, which is the cation obtained by alkylation of the amine group of DABCO, see structure in **Figure 28**) that increases the upper voltage limit to *ca.* 4.2 V vs. Li^+/Li.[284] While the rechargeability of the Li-O_2 cells with the DABCOnium quencher was poor, due to the intrinsic slow kinetics of Li_2O_2 oxidation, the incorporation of RMs to facilitate electron transfer reactions can enable further improvements in performance. For that purpose, the selection of suitable RMs is critical, since some organic RMs degrade in the presence of singlet oxygen.[337] The selection of the redox potential of the mediator is also critical, since singlet oxygen can be generated by the reaction of superoxide anions with the oxidized RM. This occurs when the difference in redox potentials of RM^{RED}/RM^{OX} and O_2^-/O_2 is higher than the energy difference between singlet and triplet oxygen, the latter being ~1 eV. For example, Bard and coworkers demonstrated that this is the case for electrochemically generated ferrocenium cations and superoxide anions:[349]

$$O_2^- + Fc^+ \rightarrow {}^1O_2 + Fc \quad (46)$$

Other reactions generating singlet oxygen include the oxidation of Li_2O_2 at potentials higher than 3.45-3.55 V vs. Li^+/Li[139]:

$$Li_2O_2 \rightarrow {}^1O_2 + 2Li^+ + 2e^- \quad (47)$$

the chemical disproportionation of superoxide during discharge or charge:[153]

$$2LiO_2 \rightarrow Li_2O_2 + {}^1O_2 \quad (48)$$

$$2HO_2 \rightarrow H_2O_2 + {}^1O_2 \quad (49)$$

where HO_2 could be formed due to water contamination, and the oxidation of Li_2CO_3 (a typical degradation product in Li-O_2 cells):[179]

$$2Li_2CO_3 \rightarrow {}^1O_2 + 2CO_2 + 4Li^+ + 4e^- \quad (50)$$

In summary, the following strategies can be proposed to avoid or minimize singlet oxygen formation: 1) introduction of singlet oxygen quenchers, 2) operation of the battery at potentials below 3.45-3.55 V vs. Li^+/Li, thus preventing singlet oxygen generation via reaction (47), 3) tuning the electrolyte properties so that the potential of LiO_2 formation, $E^0(^3O_2/LiO_2)$ is close to the thermodynamic potential of O_2 reduction to Li_2O_2, $E^0(^3O_2/Li_2O_2)$ = 2.96 V vs. Li^+/Li, thus making generation of singlet oxygen via reaction (48) thermodynamically unfavorable, 4) controlling the cell impurity levels to prevent formation of HO_2, thus preventing singlet oxygen generation *via* reaction (49), 5) minimizing degradation reactions leading to Li_2CO_3 formation, thus preventing singlet oxygen generation via reaction (50), 6) selection of charge RMs with redox potential close to $E^0(^3O_2/Li_2O_2)$ =

2.96 V vs. Li^+/Li, thus enabling the operation of the battery at low charging potential, and preventing singlet oxygen generation via reactions like (46) and (47).

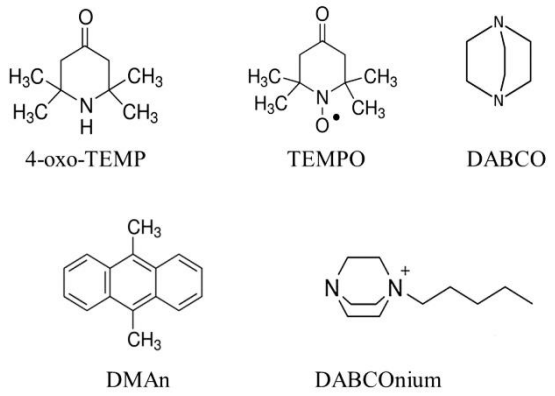

Fig. 28 Structures of 4-oxo-TEMP, TEMPO, DABCO, DMAn and DABCOnium molecules.

4.3.4 Fluorinated Additives

Fluorinated compounds have been used as O_2 carriers in artificial blood substitutes, due to their extremely high O_2 solubility, acting in a similar way as hemoglobin-based formulations.[350-352] The high solubility of gases (such as O_2) in fluorinated liquids is attributed to the weak intermolecular interactions in these fluids.[353] Inspired by their role as very efficient O_2 carriers in blood substitute formulations and breathing liquids, due to their outstanding O_2 solubility and low toxicity, several fluorinated compounds were added to Li-O_2 cells as electrolyte additives or cathode coatings in the early stages of development of Li-O_2 batteries.[354-358] Significant improvements in capacity were reported, which were tentatively attributed to the increased O_2 solubility achieved by the fluorocompound. Unfortunately, those early studies were done in organic carbonate electrolytes (PC and others), which are now known to be unsuitable for Li-O_2 batteries due to poor stability against superoxides. Later work has used more suitable electrolytes, such as tetraglyme,[359-365] DME,[366] DMSO,[151] and significant improvements in capacity were again reported. To increase the miscibility of fluorinated compounds with the other co-solvent, the use of a perfluorinated lithium salt surfactant has been reported (lithium perfluorooctane sulfonate: LiPFOS, see structure in **Figure 29a**), which enabled an impressive solubility of >60 wt.% of BrC_6F_{13} in tetraglyme. Fluorine-functionalized ionic liquids are another interesting option with very high O_2 solubility.[367] Since increasing the content of the fluorinated additive in the electrolyte has been shown to increase the O_2 solubility,[151, 359, 368] the improved O_2 supply to the electrode surface has often been claimed to be the reason for the improved discharge performance. However, much further work is required to elucidate the origin of the capacity improvements, which, in some cases, is due to degradation reactions.

Ab-initio calculations predicted that fluorinated ethers are susceptible to degradation by superoxide attack.[163] Fluorination of the α-carbon of the ether (for instance CH_3-O-$CHFCF_3$ or CH_3-O-CF_2CH_3) leads to low activation energy of nucleophilic attack by superoxide. In contrast, β-fluorinated ethers (e.g. CH_3-O-CH_2CHF_2 or CH_3-O-CH_2CF_3) are expected to be

much more stable. These predictions have been confirmed by experimental work,[359, 366] as discussed below.

Yazami and coworkers used electrochemical and analytical techniques to demonstrate the degradation of an α-fluorinated ether (1-methoxyheptafluoropropane: 1-PFC, see structure in **Figure 29a**) in Li-O_2 cells.[366] Cyclic voltammetry experiments at a glassy carbon electrode (**Fig. 29b**) showed that addition of 1-PFC increased the current due to reduction of O_2 to O_2^-, but decreased the current due to oxidation of O_2^- to O_2 in the reverse scan, evidencing the consumption of O_2^- via irreversible degradation reactions with the 1-PFC additive. The degradation of 1-PFC was also supported by the finding that the increase in capacity upon addition of 1-PFC to Li-O_2 cells decreases at higher discharge current. If the only effect of 1-PFC was to increase the O_2 supply to the electrode surface, the opposite behavior would be expected: increasing the discharge current would make the effect of 1-PFC higher, due to the higher effect of the limited rate of O_2 supply. Furthermore, degradation of 1-PFC in Li-O_2 cells (most likely, upon reaction with O_2^-) was also demonstrated by ^{1}H-NMR and XPS measurements of the discharged electrolytes and cathodes, respectively.

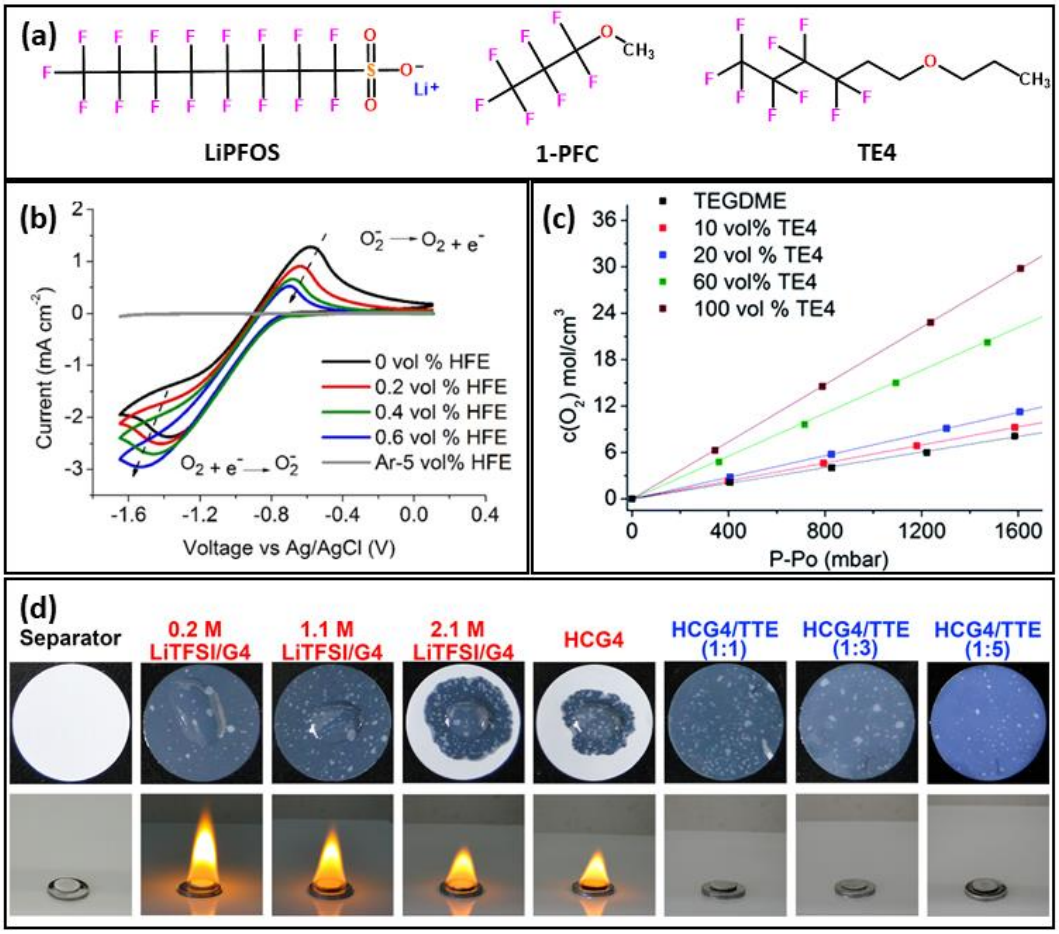

Fig. 29 (a) Structure of some selected fluorinated compounds. (b) IR-corrected CVs of a glassy carbon in 0.15 M $TBAPF_6$ in DME saturated with either Ar or O_2 with various concentrations of 1-PFC additive (noted in the legend as HFE: hydrofluoroether), scan rate: 100 mV/s.[366] (c) O_2 concentration for various TE4 additive concentrations in TEGDME as a function of O_2 pressure.[359] (d) Photographs of the wetting behaviors (top) and flammability tests (bottom) of glass fiber separators pre-soaked in different electrolytes. The electrolytes in red

fonts indicate conventional TEDGME electrolytes and the ones on blue font indicate fluorinated blends. G4: tetraglyme(TEGDME); HCG4: highly concentrated tetraglyme electrolyte (3.4 M LiTFSI/TEGDME); TTE: 1,1,2,2-tetrafluoroethyl 2,2,3,3-tetrafluoropropyl ether (TTE).[361] (b) Reprinted with permission from ref 366. Copyright 2016 Electrochemical Society and (c) from ref 359 Copyright 2015 The Royal Society of Chemistry. (d) From ref 361. Copyright 2018 ACS.

In contrast, the same group showed that a γ-fluorinated ether (1,1,1,2,2,3,3,4,4-nonafluoro-6-propoxyhexane: TE4, see **Figure 29a**) was stable against degradation in Li-O_2 cells.[359] The improvement of the discharge capacity and discharge voltage of Li-O_2 cells upon TE4 addition was more pronounced at high discharge current, were the O_2 supply is more critical, in agreement with the hypothesis that the beneficial effect of TE4 is due to the increase in O_2 solubility. Direct measurement of the increase of O_2 solubility in the electrolyte upon TE4 addition were reported, as obtained by monitoring changes in pressure in O_2 uptake experiments (see **Figure 29c**). The absence of degradation of TE4 during discharge of Li-O_2 cells was confirmed by ^{1}H and ^{19}F-NMR of the discharged electrolytes and FTIR and XPS measurements of the discharged cathodes.

Another interesting advantage of fluorinated additives is their flame retardant behavior.[361] **Figure 29d** (bottom) illustrates the ignition tests of glass fiber separators pre-soaked in different electrolytes, which demonstrate that the separators do not ignite in any of the electrolytes containing fluorinated additives. **Figure 29d** (top) illustrates the improved wettability facilitated by the addition of fluorinated additives: a drop placed on top a pre-soaked glass fiber separator fully wets the separator with electrolytes containing fluorinated additives, whereas the drop does not wet (small contact angle) in the conventional electrolytes containing LiTFSI in tetraglyme.

In summary, fluorinated additives exhibit some highly beneficial properties that can potentially lead to major improvements in Li-O_2 batteries, such as their very high O_2 solubility, good wettability and flame retardant properties. From a broader perspective, the role of mass transport limitations in Li-O_2 batteries needs to be investigated further. Mass transport limitations in ionic-liquid based Li-O_2 batteries were evidenced by the fact that drastic improvements in capacity could be achieved by either stirring or flowing an electrolyte saturated with O_2 through the cell.[369, 370] Due to the high viscosity of ionic liquids, mass transport limitations were shown to be important even at low current densities of around 0.1 mA cm^{-2}. For less viscous electrolytes, combination of experiments and simulations concluded that mass transport limitations could be an issue for current densities in the range of 1-10 mA cm^{-2}.[62] Those current density values are relevant for commercial applications in, for example, electric vehicles,[28] thus improving mass transport should be addressed in further studies of Li-O_2 batteries. Of note, in mediated Li-O_2 cells, the transport of the RM from the cathode/electrolyte to the O_2/electrolyte interface will substitute the transport of O_2, thus in that case the transport rate of the RM will be the most critical. In conclusion, further studies assessing mass transport limitations (from all species involved in the reactions: lithium ions, RMs, dissolved O_2, superoxide, *etc*.) are required for the development of batteries able to fulfil the power requirements for commercial applications.

4.4 Protection Strategies for Li Metal in Lithium-Air Batteries

In the previous discussion of Section 4, we focused on approaches addressing the challenges associated with the O_2 electrochemistry. In this section, we present strategies that can mitigate the problems at the reaction interface of Li metal anodes and the electrolyte. We summarize the protection strategies into on two categories: 1) solid-electrolyte interface (SEI) formed on Li metal anode surface by reacting Li metal with additives, electrolytes, salts and air constituents; 2) inorganic/organic protective layers used as separators or coatings on Li metal anode. Literature examples are selected with emphasis on the interplay between the protection method and effect of air constituents.

4.4.1 Solid Electrolyte Interface

The SEI is a protective surface layer, with low electronic conductivity but that enables lithium ion transport. It is formed on reaction of Li metal with organic electrolytes, and consists of a complex mixture of inorganic and organic components.[371-374] It can be formed by reactions among electrolyte, salt, additives and Li metal during chemical pre-treatment or during electrochemical cycling. A stable SEI enables a prolonged stripping/plating cycles of a Li metal anode at high Coulombic efficiencies. In principle, any effective electrolyte system that has been reported to sustain a reversible Li stripping/plating process and is compatible with the oxygen redox chemistry at the cathode is worth considering as a candidate for the lithium-air battery system. Many functional additives have been proposed to facilitate the formation of a stable SEI, including dissolved O_2 and CO_2 species,[57, 220, 268, 375-377] trace H_2O contamination,[378] lithium nitrate,[268, 379] boric acid,[380] germanium,[381] polyphosphoric acid,[382] 1,4-dioxacyclohexane,[383] Super P® carbon,[384] tetraethyl orthosilicate,[385] Indium and cesium iodide.[386-388] Some of them[57, 268, 377-379, 388] have been reported to be beneficial to processes at both electrodes, their effects on the Li anode being discussed below.

Lithium nitrate is an electrolyte additive widely used in lithium sulfur batteries.[389, 390] It is thought that $LiNO_3$ reacts with Li to form a protective layer (likely to be Li_2O due to the reduction of $LiNO_3$ by Li),[149] which prevents further reactions of Li with polysulfide intermediates shuttling from the cathode. Li_2O being an active component in a stable SEI layer has been confirmed by cryo-TEM and Raman spectroscopy.[57, 391] Addison and coworkers found that the salt $LiNO_3$ is also effective in generating a stabilized SEI in lithium-air battery systems, where an amide-based electrolyte would otherwise be incompatible with a Li anode.[149, 379] The authors[149, 379] further added that O_2 also plays a beneficial role in stabilizing Li metal anodes, which is consistent with the observation by Edström,[268] Zhou[57] and Wang[377] and coworkers (Section 3.3.2). Although the causes of Li_2O formation in SEI layers may vary case to case, these studies suggest that its presence is beneficial to a stable SEI.

Water at ppm levels is usually an inevitable contamination in a battery system. It can serve as a solvating additive to improve the ORR at the cathode, as discussed in Sections 2.1.1 and 4.3.1. At trace quantities, it can also benefit the anode. Zhang and coworkers[378] found that when 25~50 ppm water is used together with a $LiPF_6$ salt in the electrolyte, a more reversible

Li deposition/dissolution reaction can be promoted. Instead of forming a mossy structure, Li anodes with 50 ppm water exhibit a columnar morphology for the deposited lithium (**Fig. 30a**). Detailed analysis revealed that HF is generated via the reaction of $LiPF_6$ and H_2O, the generated HF being subsequently reduced during the initial Li deposition and forming a LiF-rich SEI layer. LiF as a critical component in SEI for reversible Li deposition has been previously demonstrated by many groups;[374, 392-397] the fluorinated SEI is proposed to enable much faster Li^+ diffusion at the Li anode-electrolyte interface, and guide an ordered columnar Li deposition.

The use of redox mediators is an important strategy to improve the cell reversibility (Section 4.2). One common issue facing their successful implementation concerns their incompatibility with the Li anode. For example, the oxidized form of an iodide mediator, i.e., I_3^-, tends to shuttle over to the Li anode and becomes chemical reduced thereby corroding the Li anode. Zhou and coworkers[388] demonstrated that by using InI_3 additives, the lithium anode can be protected against I_3^- attack (**Fig. 30b**); the In^{3+} becomes electrochemical reduced at the Li anode on charging, forming a protective indium layer on Li, which was also found to suppress lithium dendrite formation. While the In layer is likely reduced further to form a lithium indium alloy, redox shuttling is most likely prevented by the formation a stable SEI.

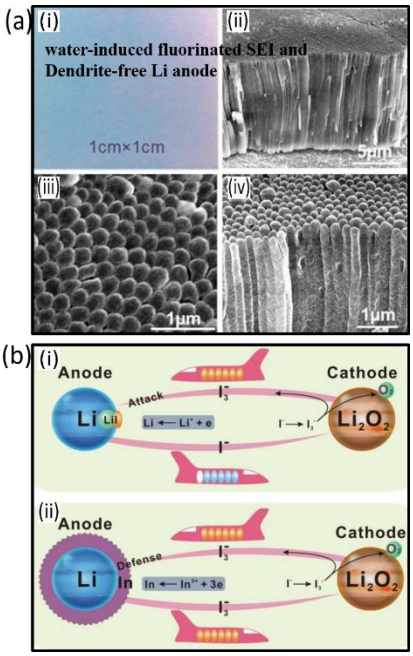

Fig. 30 (a) Optical (i) and SEM images (ii-iv) revealing water (50 ppm H_2O in $LiPF_6$/PC electrolytes) induced fluorinated SEI formation and uniform Li metal deposition.[378] (b) Scheme illustrating that (i) I_3^- shuttle reaction with Li metal in the case of LiI mediated battery chemistry and that (ii) protection of Li against I_3^- shuttle reaction by an In layer in the case of InI_3 mediated cell reaction.[388] (a) From ref 378. Copyright 2015 Elsevier. (b) From ref 388. Copyright 2016 The Royal Society of Chemistry.

When a single electrolyte system is used in the lithium-air battery, finding an optimal electrolyte to satisfy the requirements from both anode and cathode is challenging, especially in the complex (electro-)chemical environment of lithium-air batteries. However, once a dual compartment cell structure is employed, more strategies in the general Li metal research can

be transferred to lithium-air batteries, because the anolyte and catholyte are separated by a solid electrolyte membrane so that they can be optimized independently.

4.4.2 Inorganic/Organic Protective Membranes

Inorganic, organic and hybrid membranes have been used in lithium-air batteries to prevent the reactions occuring between the air electrode consituents and the Li anode. While the membrane can be used as a separator between the cathode and anode, *i.e*. a protected anode design;[286, 287, 289, 384, 398-402] it can also be applied at the interface of the cathode and ambient air, *i.e*. a protected cathode design.[290-293, 403-406] In the protected anode design, a membrane should have high Li^+ ionic conductivity. Proton transport and reaction with water and CO_2 should also be minimised. In the protected cathode design, a membrane should have high O_2 permeability, high rejection rate of H_2O, CO_2, and high immiscibility with organic electrolytes to suppress electrolyte evaporation.

The first example of using inorganic solid state electrolytes to protect Li metal anode was demonstrated by Visco and coworkers in 2007.[285] They developed an aqueous/organic hybrid Li-O_2 system, where the two compartments in the battery were separated by a NASICON-type ($Li_3M_2(PO_4)_3$) solid state electrolyte with high Li^+ conductivity, thus protecting the Li metal anode from reaction with the aqueous electrolyte contained in the oxygen electrode compartment. The authors reported a stable discharge up to 14 hours. Following the dual-compartments design, a number of studies reported improved stability and energy efficiency by optimizing the activity of oxygen reduction catalyst,[407, 408] using protective layers for solid state electrolyte against water and Li corrosion,[409, 410] better electrolyte,[411-413] and adjusting operational temperatures.[407] The concept of dual-compartments was later adapted to non-aqueous lithium-oxygen batteries; in this approach two different electrolytes are used at the oxygen and lithium electrode compartments, thus enabling a higher flexibility that allows separate optimization of electrolytes, salts, redox mediators, *etc.* for the cathode and anode.[288, 409-411, 414] For example, the cell can be separated by an Ohara glass, $Li_{1+x+y}Al_xTi_{2-x}Si_yP_{3-y}O_{12}$.[288] **Figure 31a** shows an example of a dual-compartment Li-O_2, where the cathode compartment contains LiTFSI /TEGDME with a redox mediator dimethylphenazine (DMPZ), while in the anode compartment contains fluoroethylene carbonate (FEC) and the salt LiTFSI which is known to form a stable SEI on Li metal anode.[415] The SEM image revealed the smooth surface morphology on the cycled Li metal anode. Due to the isolation from TEGDME/DMPZ that would otherwise react to form an unstable SEI, the Li metal anode shows much improved cycling stability in the FEC electrolyte (**Fig. 31a(ii)**). Many other protection methods can be potentially applied in the dual-compartment configuration, including the solvent-in-salt (A new class of solvent‐in‐salt electrolyte for high-energy rechargeable metallic lithium batteries),[416] self-healing electrostatic shield,[386] 3D current collectors (Accommodating lithium into 3D current collectors with a submicron skeleton towards long-life lithium metal anodes),[417] additives (Dendrite-free Li deposition using trace-amounts of water as an electrolyte additive),[378] and nanoengineering methods.[418, 419].

Recently, there has been growing interests in applying polymer membranes to protect Li metal anode, because of the flexibility in materials design and the potentially low cost.[286, 289,

[384, 402] This field builds on the extensive work on polymer electrolytes for lithium-ion batteries.[420] A representative example is the application of poreless polyurethane (PU) membrane (**Fig. 31b(i)**).[289] As shown in **Figure 31b(ii)**, the PU membrane is composed of two domains: hard and soft domains. Because of the poreless structure, the Gurley time (the time required for 100 cm^3 of air to pass through a separator under air pressure of 0.862 kgf cm^{-2}) was out of the detection range in an air permeability test (**Fig. 31b(iii)**), suggesting that the PU membrane is air-impermeable. The PU membrane also has excellent electrolyte wettability and Li ion conductivity (**Fig. 31b(iv)**), and therefore affords an improved cycling lifetime of the Li metal anode. Compared to the Li metal anode protected by porous polyethylene (PE) separator in which particulate LiOH was detected by XRD and SEM, only Li metal signals were detected after 100 cycles when the anode is protected by the PU separator.

While the PU separator successfully prevents the crossover of H_2O and O_2, Li dendrite still grows, possibly due to the low mechanical strength. This is a problem common to many polymer membranes, which can be improved by inorganic additives. For example, aluminum oxide (Al_2O_3) nanoparticles have been added into a lithiated Nafion membrane to form a composite protective layer.[421] As schematically illustrated in **Figure 31c(i,ii)** pulverization of the protective layer during Li plating/stripping experiments occurs without the Al_2O_3 nanoparticles (Nafion layer: NL), whereas the protective layer remains intact when Al_2O_3 nanoparticles (Nafion-based composite layer: NCL) are included. This composite layer has also been shown to suppress dendrite growth. A symmetric Li cell protected by the composite layer shows an improved cycling lifetime compared to the unprotected or Nafion-only protected cells (**Fig. 31c(iii)**). Furthermore, the authors stress that the chemical stability of the membrane must be tested in the presence of reactive oxygen species in lithium-oxygen batteries: the stability of the Nafion-based composite membranes were compared to that of a polyvinylidene fluoride (PVdF)-based composite membrane (composite protective layer: CPL). As measured by online electrochemical mass spectrometry (OEMS),[286, 287] irreversible O_2 reduction and CO_2 evolution were observed in the latter case (**Fig. 31c(iv,vi)**), likely due to the decomposition of PVdF, whereas the O_2 reduction and evolution are more reversible when Nafion-based membrane is used (**Fig. 31c(v,vi)**). This result is in agreement to an earlier work that reported the instability of PVdF against the O_2^- radical.[40] In contrast, the NCL affords a more reversible O_2 reduction and evolution.

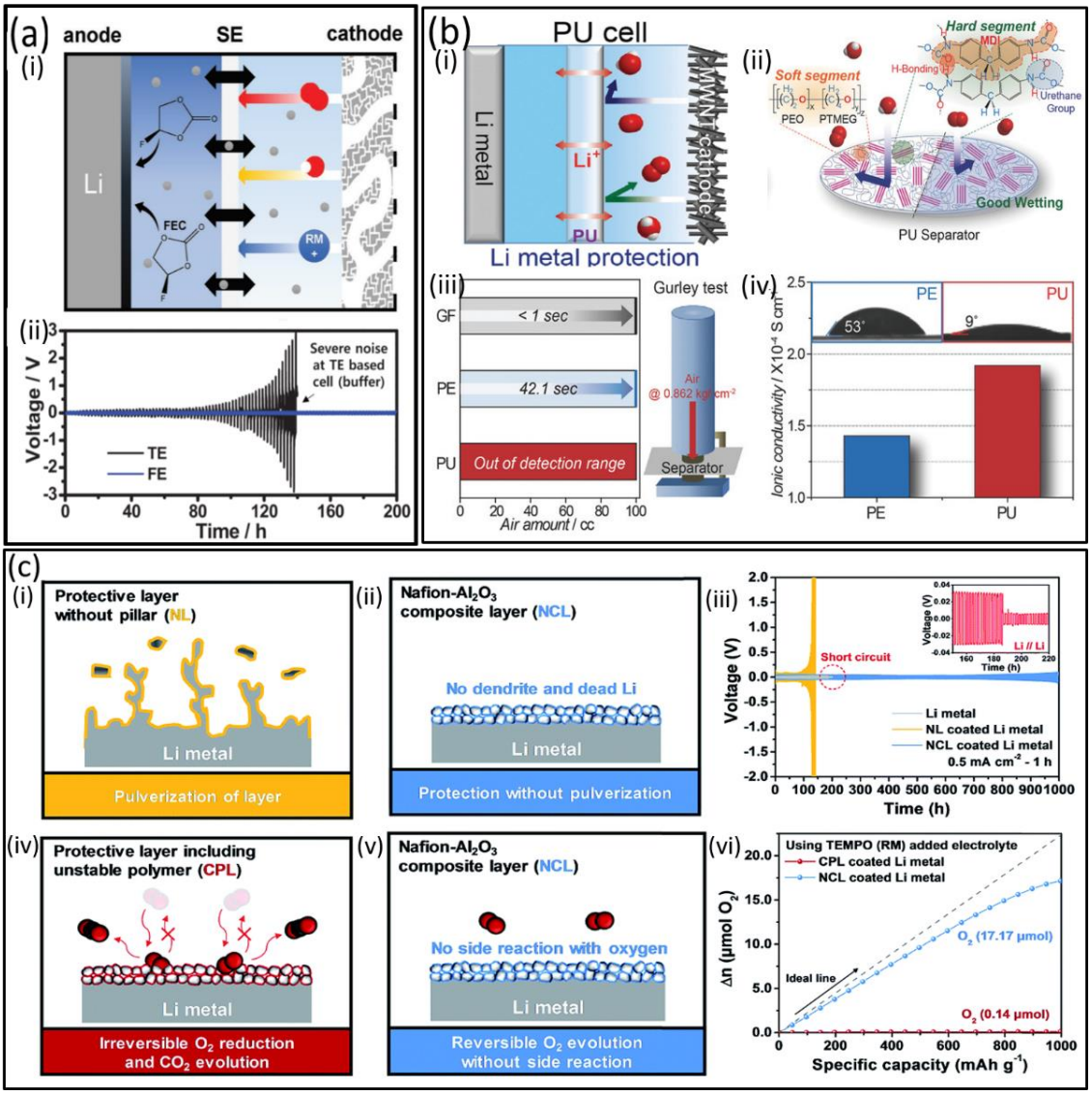

Fig. 31 Inorganic/organic membranes to protect Li anodes. (a) The bicompartmental cell configuration with dual organic electrolytes for optimized stability of Li-O_2 batteries. (i) Schematic illustration of the cell showing the two compartments, separated by a Li^+ ion conducting solid electrolyte, with the Li anode compartment containing Li SEI protective additives such as fluoroethylene carbonate (FEC), and the oxygen electrode compartment containing redox mediators (RM). (ii) The voltage profiles of Li/TEGDME/Li and Li/FEC/Li symmetrical cells during repeated plating/stripping at 1 mA/cm^2. The cell voltage is below 50 mV in FEC (labelled at FE in the figure legend) while the cell voltage increases to 3V in TEGDME (labelled as TE in the figure legend).[288] Reprinted with permission from ref 288. Copyright 2017 Wiley-VCH Verlag GmbH & Co. KGaA, Weinheim. (b) A supported poreless polyurethane (PU) separator used to protect Li metal anode (i) Schematic illustration of the rejection of O_2 and H_2O by the poreless PU separator. In a cell, the PU membrane was placed between the Li metal anode and the glass fiber. The salt/electrolyte are $LiClO_4$/TEGDME. (ii) Molecular structure of the PU separator, containing hard and soft domains. The hard domain consists of 4,4-diphenylmethane diisocyanate (MDI), providing the mechanical rigidity through the π-π interactions and the hydrogen bonding between the end urethane groups. The soft domain consists of poly(ethylene oxide) and polytetramethylene glycol (PTMEG), providing the softness and wettability. (iii) The air permeability test results showing the Gurley time for glass fiber (GF), polyethylene (PE) and PU. (iv) The electrolyte (TEGDME) contact angle (top) to PE and PU, 5s after the electrolyte drop; the Li ion conductivities of the PE and PU separators (bottom).[289] Reprinted with permission from ref 289. Copyright 2016 Wiley-VCH Verlag GmbH & Co. KGaA, Weinheim. (c) Schematic illustration of the pulverization of the Nafion-based membrane without (i)

and with (ii) Al_2O_3 nanoparticles. (iii) Voltage profiles of Li symmetric cells without protection, with Nafion-only (NL) and Nafion-Al_2O_3 composite layer (NCL) during plating/stripping reactions at 0.5 mA/cm^2 for 1000 hours. Schematic illustration of the O_2^- radical attack to the PVdF-based protective layer (CPL) (iv) and the Nafion-based protective layer (NCL) (v). (vi) The OEMS signal of O_2 evolved at different specific capacities from the cells with CPL and NCL protection. The dotted line shows the theoretical $2e^-/O_2$ relationship.[421] Reprinted with permission from ref 421. Copyright 2019 The Royal Society of Chemistry.

In the protected cathode design, an oxygen selective membrane (OSM) was placed at the interface of cathode and ambient air. The OSM should allow the fast transport of O_2 while rejecting or trapping other air constituents, such as H_2O and CO_2. Since the molecular size of H_2O is smaller than O_2, simply tuning the porosity of the membrane will not achieve a selective transport of O_2. A non-polar membrane with a high solubility and diffusivity of the non-polar molecule O_2 should achieve the high selectivity of O_2 over the polar molecule H_2O. For example, low-density polyethylene was applied to dehydrate ambient air and greatly prolonged the cycling lifetime of the lithium-air battery.[221] Silicone oil loaded into a porous metallic Ni substrate also achieved a good O_2/H_2O separation.[422] Compared to O_2/H_2O separation, separation of O_2 from CO_2 is more challenging since both molecules are non-polar. While considerable research has been performed to separate CO_2 from the air (for CO_2 sequestration, for example), literature reporting O_2/CO_2 separation in Li-air batteries is scarce. In one example, a composite membrane made of a polydopamine-coated metal organic framework CAU-1-NH_2 dispersed in a polymethylmethacrylate (PMMA) was attached to the cathode and the battery showed an improved cycling life in ambient air.[291] The functional group -NH_2 in CAU-1-NH_2, -OH in the polydopamine and -C=O in PMMA were demonstrated to trap CO_2 and afford a high selectivity of O_2 over CO_2. In another work, perfluoropolyether-based membrane was demonstrated to dehydrate ambient air and suppress DMSO evaporation effectively. Interestingly, the allowed permeation of CO_2 through the membrane stabilizes the Li metal anode by forming a protective layer of Li_2CO_3. On the cathode, however, Li_2CO_3 that could be potentially formed from the reaction of discharge product Li_2O_2 and CO_2 (reaction 14) was not detected. Therefore, the permeation of CO_2 without H_2O appears to improve Li metal anode stability without compromising the cathode stability by the irreversible formation of Li_2CO_3.

In summary, Li-metal protection strategies have been demonstrated in lithium-air battery systems, including the protected anode design by forming stable SEI using electrolyte additives or inorganic/organic protective membranes, and the protected cathode design by applying oxygen selective membranes. Significant progress has been made in prolonging battery cycling lifetime. With further demand for more practical and scaled up lithium-air batteries, more stringent requirements will be placed on the materials involved in the proposed strategies. At the anode side, many protective solid-state layers are reactive to Li metal causing side reactions and reduction in Coulombic efficiencies; buffer layers between solid state electrolyte and Li metal can greatly circumvent the problem, but they also increase system cost/complexity and reduce energy density. Meanwhile, even with protective solid state layers, lithium dendrites still form in some cases; a more complete picture of the origins of this dendritic growth needs to be obtained to come up with effective strategies to resolve this. At the cathode side, the chemical stability of gas selective membranes against reactive

oxygen species may be an issue, which should not be overlooked. Finally, other air constituents (CO_2, H_2O) might have impact on the material properties and interfacial processes (such as the stability of SEI, solid state electrolyte etc.) involved in these proposed strategies. Further fundamental studies are required in this direction to aid any rational materials design.

5. Alternative Battery Chemistries

While tremendous efforts are being devoted to developing strategies that mitigate the issues of a Li_2O_2-based non-aqueous Li-O_2 battery, many researchers also exploited alternative chemistries. For instance, one-electron superoxide based metal-oxygen batteries were found to exhibit much smaller voltage hysteresis than the peroxide chemistry.[104, 423-431] A nickel-based cathode together with a $LiNO_3$-KNO_3 inorganic electrolyte at 150°C has been reported to promote Li_2O formation and decomposition in a Li-O_2 battery.[135] The synergistic effects of water additives and catalysts can be used to modulate the battery chemistry as a nominal four-electron oxygen electrochemistry *via* LiOH formation and decomposition.[130, 297, 432] These novel strategies shed new light on how to tackle the long-standing issues of high overpotentials, organic electrolyte decomposition, battery chemistry sensitive to H_2O and CO_2 contamination and so on, further deepening and widening the mechanistic understanding of metal-oxygen electrochemistries. In this section, we discuss the fundamental characteristics and implications of these battery electrochemistries.

5.1 MO_2 or M_2O as the Potential Discharge Products?

It has been long established that the cation size (or softness) can significantly impact on the O_2 redox processes in non-aqueous media. According to the Hard Soft Base and Acid Theory, larger cations, such as Na^+, K^+, TBA^+, tend to afford the one-electron O_2/O_2^- redox reaction, whereas smaller Li^+ induces Li_2O_2 formation;[33, 34, 195] the oxygen CVs measured with the former larger cations show narrower redox peak separations, while with Li^+ CVs show wider separations and irreversibility.[33, 34, 104, 195, 429] These phenomena are rooted in the thermodynamic properties of superoxide, peroxide and oxide species for these alkali metals, as summarized in **Table 4**.[426]

The one-electron KO_2 formation reaction has a standard potential of 2.48 V vs. K^+/K, higher than that of two-electron K_2O_2 formation (2.20 V vs. K^+/K). Therefore, in a K-O_2 battery, electrochemical KO_2 formation is both thermodynamically and kinetically favored.[426] In Na-O_2 batteries, the standard potential of the NaO_2 formation reaction is slightly lower than Na_2O_2 formation by 60 mV, Na_2O_2 thus being thermodynamically preferred.[423] Nonetheless, in practice NaO_2 is still observed to form preferentially during experiments; this preference can be attributed to a higher kinetic barrier associated with the two-electron charge transfer for Na_2O_2 formation.[423] In the case of Li-O_2 batteries, LiO_2 is thermodynamically unstable at standard conditions and thus does not form as a stable discharge product. Once it is transiently generated upon electro-reduction, LiO_2 chemically disproportionate to form Li_2O_2, which is then electrochemically decomposed at anodic potentials.[33, 35, 37] The high

irreversibility typically observed in CVs for a Li-O_2 battery is in part a reflection of the asymmetric operating mechanisms for Li_2O_2 formation (an electrochemical then chemical steps) and decomposition (electrochemical processes), in contrast to the symmetric processes for KO_2, NaO_2 formation and decomposition (both are one-electron electrochemical processes). The formation of Li_2O_2 is both thermodynamically and kinetically favored over Li_2O formation, because the former has a higher equilibrium voltage and the O-O bond does not need to be cleaved. However, at above 150°C, formation of Li_2O becomes the thermodynamically more favorable reaction over Li_2O_2 and with the right catalyst, Li_2O can be formed electrochemically during cell discharge; this is discussed further in Section 5.1.2.

Table 4. Thermodynamics of possible discharge reaction products in K-O_2, Na-O_2 and Li-O_2 batteries and corresponding specific capacity as well as energy density.

Product	Reaction	Δ_rS (J/(mol·K))	Δ_rH (kJ/mol)	Δ_rG (kJ/mol)	z	E° (V)	Specific Capacity (mAh/g)	Energy Density (Wh/kg)
KO_2	$K + O_2 \rightarrow KO_2$	116.7	-284.9	-239.4	1	2.48	377.0	934.9
K_2O_2	$2\,K + O_2 \rightarrow K_2O_2$	102.1	-494.1	-425.1	2	2.20	486.4	1070.2
K_2O	$2\,K + {}^1/_2\,O_2 \rightarrow K_2O$	94.1	-363.2	-322.2	2	1.67	569.1	950.3
NaO_2	$Na + O_2 \rightarrow NaO_2$	-140.6	-260.7	-218.8	1	2.27	488.2	1108.2
Na_2O_2	$2\,Na + O_2 \rightarrow Na_2O_2$	-212.9	-513.2	-449.7	2	2.33	689.0	1605.4
Na_2O	$2\,Na + {}^1/_2\,O_2 \rightarrow Na_2O$	-130.1	-415.1	-376.3	2	1.95	867.4	1691.4
Li_2O_2	$2\,Li + O_2 \rightarrow Li_2O_2$	-206.9	-632.5	-570.8	2	2.96	1168.3	3458.3
Li_2O	$2\,Li + {}^1/_2\,O_2 \rightarrow Li_2O$	-123.2	-597.9	-561.2	2	2.91	1793.9	5220.2

Note: Δ_rS, Δ_rH and Δ_rG are the standard entropy, enthalpy and Gibbs energy of the reaction, z is the number of electrons involved, E^0 is the standard voltage of the associated metal-O_2 battery. (Data used for calculating Na-O_2 and Li-O_2 batteries are from the article by Ji *et al.*[433]) Reprinted with permission from refs 421 and 428. Copyright 2013, 2017 ACS.

In light of the aforementioned properties of alkali metal oxides, NaO_2 and KO_2 as the discharge products in Na-O_2 and K-O_2 batteries, respectively, have been demonstrated under galvanostatic cycling conditions.[423, 426] By contrast, LiO_2 as a stable final discharge product in non-aqueous Li-O_2 batteries was not observed until Amine and coworkers' work.[431] They suggested that Ir metal catalysts on a reduced graphene oxide electrode can stabilize LiO_2 due to the lattice match between LiO_2 and Ir_3Li, allowing them to realize a LiO_2-based Li-O_2 battery.[431] Although doubts were raised by McCloskey and coworkers[434, 435] on the existence of LiO_2 as the final discharge product, another group[436] later on also reported LiO_2 formation on a Pd/rGO catalyst, supporting the concept of LiO_2-based Li-O_2 batteries. It is clear from **Table 4** that the theoretical energy densities of NaO_2 and KO_2 are 3-4 times lower than that of Li_2O_2, which is the main reason why less research input has been devoted to developing Na-O_2 or K-O_2 batteries. (The uses of Na and K metals are also associated with higher safety concerns). Nevertheless, the practical capacities obtained for Na-O_2 or K-O_2 batteries are

significantly higher than typical Li-O_2 batteries under similar operational conditions, and the fundamental insights gained for Na- and K-O_2 cells can motivate new strategies to further improve Li-O_2 cells. Next, we compare the superoxide-based electrochemistry reported for Li-, Na- and K-O_2 batteries and focus our discussion on the reversibility and stability of the battery chemistry.

5.1.1 Reversibility and Stability of Superoxide-Based Electrochemistry

The reversibility and stability of LiO_2, NaO_2 and KO_2 batteries are shown in sequence on the top, middle and bottom panels of **Figure 32**.[423, 425, 426, 431, 437] In contrast to the behavior observed in Li_2O_2-based Li-O_2 batteries, in LiO_2-based Li-O_2 batteries, the formation and decomposition of LiO_2 exhibit a smaller voltage hysteresis (~0.5 V， **Fig. 32a(i)**).[431] The majority of charge capacity finishes below 3.5 V. DEMS measurements of the 1st electrochemical cycle lead to an e^-/O_2 molar ratio of 1.00, implying that the OER/ORR ratio is very close to 1, although the cycle life of the battery is poor (40 cycles).[431] Moving from LiO_2 to NaO_2 and KO_2, a progressively smaller voltage hysteresis is observed in superoxide-based metal-O_2 batteries,[423, 425, 426, 431, 437] e.g., typically <200 mV for NaO_2 (**Fig. 32b(i)**) and <100 mV for KO_2 (**Fig. 32c(i)**), and the oxygen recovery efficiency (OER/ORR) based on *operando* pressure and DEMS measurements are reported to be >95% for NaO_2 and 99% for KO_2. Different from the LiO_2 electrochemistry, both NaO_2 and KO_2 exhibit charging profiles that rapidly polarize to the cutoff value when the charge capacity approaches that of the discharge, marking the end of charge (**Fig. 32b,c(i)**). These NaO_2- or KO_2-based batteries can typically cycle more than 100 times continuously,[424, 427, 429, 438] that is, when there is no resting between discharge and charge processes. Compared to the peroxide chemistry, the higher reversibility of superoxide-based battery can be attributed to the following reasons: 1) a smaller kinetic barrier associated with the one-electron redox chemistry;[33, 423, 424, 426] 2) higher solubility (KO_2>NaO_2>LiO_2) or better solvation of superoxides than peroxides in non-aqueous electrolytes that provides facile solution-mediated redox processes;[30, 31, 104, 429, 431] 3) fewer parasitic reactions involved in the formation and decomposition of superoxides – both a consequence and a cause for the low voltage hysteresis.[91, 99, 178, 424, 429, 430, 438]

Apart from the electrochemical reversibility, the chemical stability of the discharge product in the cell environmental is another critical requirement to evaluate the feasibility of a practical superoxide-based battery, because it determines both the cycle life and shelf life. This demand raises issues with LiO_2 and NaO_2, because of their relative thermodynamic instability versus their peroxide counterparts (**Table 4**). After only 12 hours resting period after discharge, significant amounts of LiO_2 and NaO_2 products have been transformed to Li_2O_2 (**Fig. 32a(iii)**) or Na_2O_2 **(Fig. 32b(ii))**;[425, 431] this transformation may initiate or involve parasitic reactions with electrolyte (**Fig. 32b(iii)**).[102, 178, 424] As a result, the reversibility of the battery in the following cycles becomes worse.[425, 431] By contrast, KO_2 is both thermodynamically and kinetically favored product. Wu and coworkers[437] found that after 30 days of resting the cell following discharge, the subsequent recharge still holds a Coulombic efficiency of 94%, and quantitative titration experiments show that only 1.4% KO_2 degraded after 10 days' resting in the cell (**Fig. 32c(ii-iii)**). These observations certainly suggest that

from a chemical stability point of view, KO_2 is a better choice for realizing a superoxide battery with both a long cycle life and shelf life.

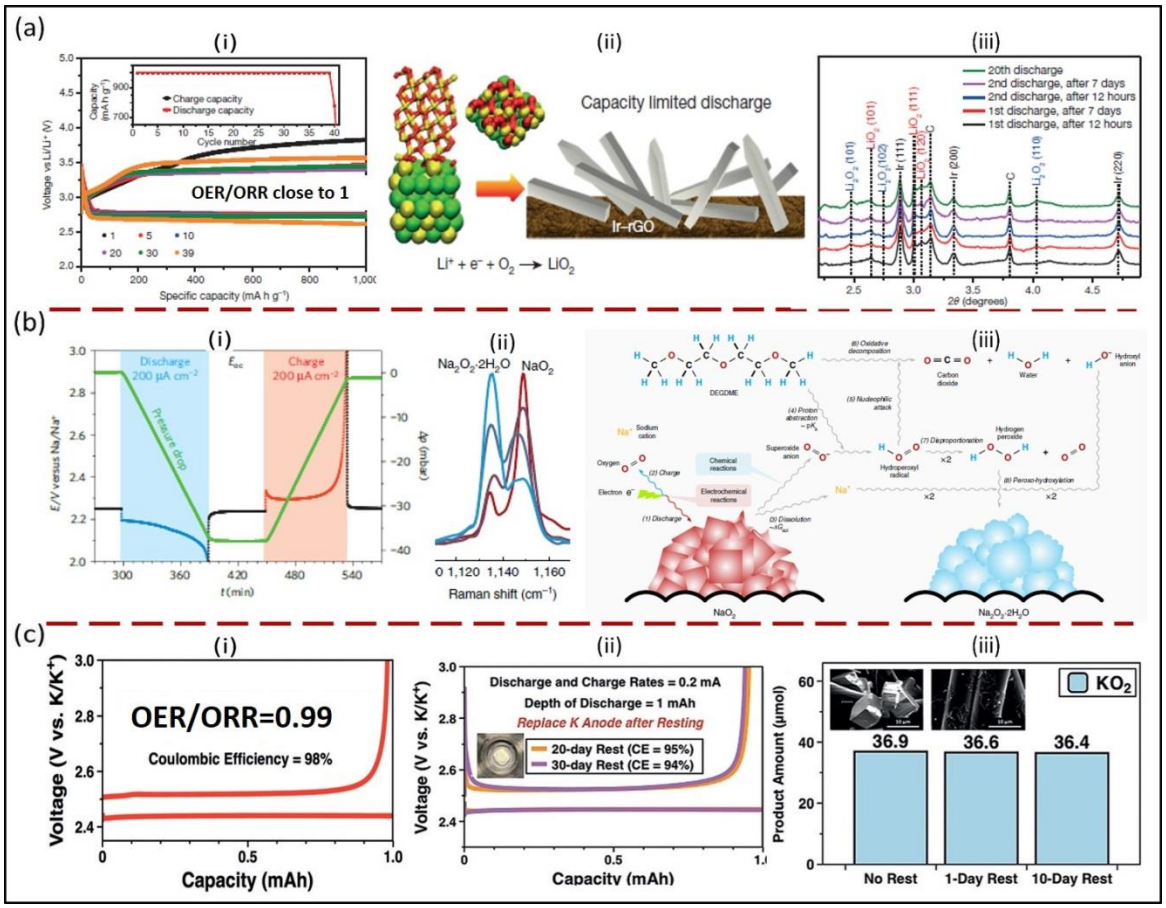

Fig. 32 Reversibility and stability of LiO_2, NaO_2 and KO_2-based nonaqueous alkali metal-O_2 batteries. (a): Electrochemical profiles and capacity retention (inset) of Li-O_2 cells cycling based on LiO_2 formation and decomposition (i), where the OER/ORR is estimated to be 1 based on OEMS measurements; cartoon illustrating that Ir catalysts enable the formation of LiO_2 by lattice match at the contact interface (ii); gradual conversion of LiO_2 discharge product to Li_2O_2 over time.[431] Reprinted with permission from ref 431. Copyright 2016 Nature Publishing Group. (b): Electrochemical profiles and the associated pressure changes during discharge and charge of a nonaqueous Na-O_2 battery, where the gas consumption and evolution suggest NaO_2 formation and decomposition with a OER/ORR ratio being 0.95 (i);[423] Raman measurements show the gradual transition of NaO_2 to Na_2O_2 hydrate when in contact with an ether electrolyte (ii); schematic illustration of parasitic reactions involved in NaO_2 chemistry, where H abstraction of the ether solvent due to superoxide is a key step (iii).[425] (i) Reprinted with permission from ref 423. Copyright 2013 Macmillan Publishers Limited and (ii-iii) from ref 425. Copyright 2016 Macmillan Publishers Limited. (c): Electrochemical profiles during discharge and charge of a nonaqueous K-O_2 battery, where the OER/ORR ratio is ~0.99 with a Coulombic efficiency of 98% (i); cells showing that even after resting the pre-discharged KO_2 electrode in the electrolyte for 30 days, the Coulombic efficiency is still over 94% (ii), demonstrating a high chemical stability (note: the K anode was replaced by a new one in this experiment); chemical titration also shows 97.5% of KO_2 remains intact after resting for 10 days (iii).[437] Reprinted with permission from ref 437. Copyright 2018 Wiley-VCH Verlag GmbH & Co. KGaA, Weinheim.

Indeed, Lu and coworkers[430] recently demonstrated a novel organic-oxygen battery operating with highly reversible and sustainable KO_2 formation. The quasi-reversible K metal anode (due to an unstable SEI) was replaced by a more reversible aromatic hydrocarbon solution

(e.g., 2-methyl b-phenyl in DME) acting as an anolyte, which was combined with a cathode undergoing reduction of O_2 to KO_2 (**Fig. 33a,b**). Such novel cell design based on KO_2-electrochemistry in a KPF_6/DMSO electrolyte could be cycled for 3000 times, at 4 mA/cm^2 and 0.25 mAh/cm^2 per cycle (**Fig. 33c**). The oxygen recovery efficiency (OER/ORR) at 500th cycle was measured to be 99.1%, the side products being quantified as low as 0.15% per cycle (**Fig. 33d-f**). As a result, the cell shows an impressive average Coulombic efficiency of 99.8% over the course of 3000 cycles.

These findings of Wu, Lu and coworkers[430, 437, 439] are certainly surprising, because they challenge the consensus that superoxide anion is a strong base and nucleophile causing significant electrolyte degradation over time,[170] as repeatedly observed in non-aqueous Na-O_2 and Li-O_2 batteries. It has been reported that superoxide anions in Na-O_2 batteries can abstract protons from DMSO or glyme solvents,[425] the HO_2, so generated, causing further degradation *via* disproportionation or reacting with trace water impurities, releasing reactive $^1O_2$ during both discharge and charge.[178] It is still an open question as to whether $^1O_2$ is also formed during the operation of K-O_2 batteries. Nonetheless, the impressive battery performance reported by Wu, Lu and coworkers seems to suggest that the $^1O_2$ formation in K-O_2 batteries is largely avoided, if any occurs at all. The origin of this long-term stability of KO_2 in an organic solvent compared to its counterpart in Li- and Na-O_2 batteries warrants further investigation and may lead to pathways to more stable Li-O_2 and Na-O_2 batteries. Despite of the many intriguing unanswered questions, it is encouraging to see that an alkali metal-O_2 battery can be reversibly cycled thousands of times without significant capacity decay (albeit at a low reversible capacity), especially based on the stereotyped 'reactive' superoxide.

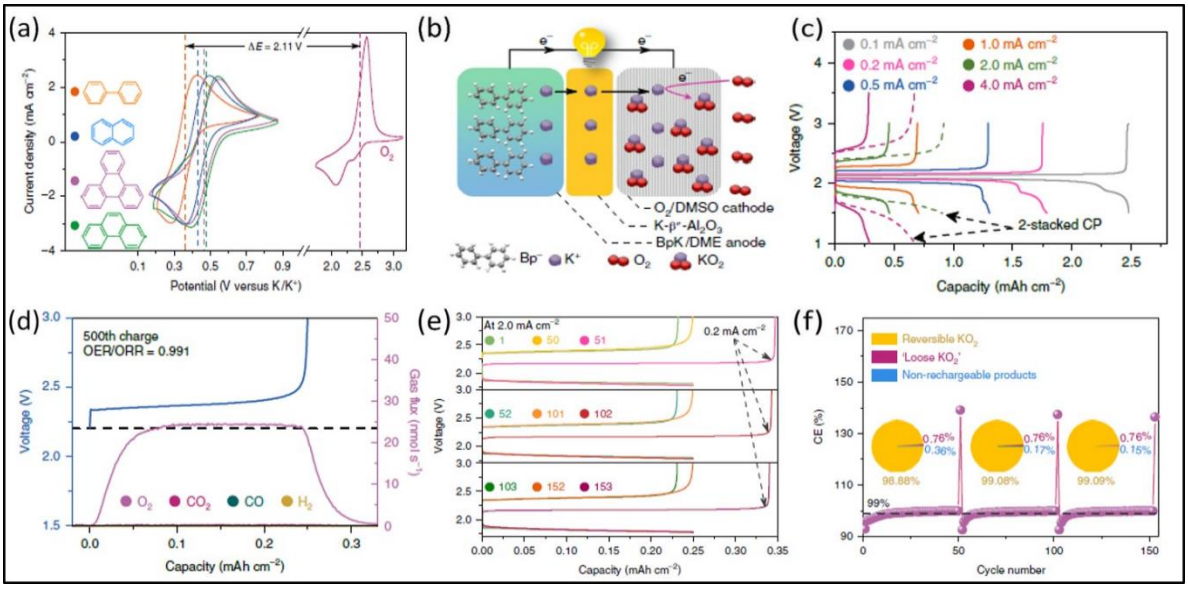

Fig. 33 Characteristics of a long-life organic-oxygen battery. (a): CVs of biphenyl (Bp), naphthalene (Nap), triphenylene (Tph) and Phenanthrene (Pha) in a 0.5 M KPF_6/DME electrolytes and saturated O_2 in a 0.5 M KPF_6/DMSO electrolyte. (b): Configuration of the bi-compartmental BpK-O_2 cell, separated by a polymer-sealed K-β´´-Al_2O_3 disc. (c): Rate capability tests of the BpK-O_2 cell in a 100% DOD mode in the range 1.5-3.0 V versus BpK/Bp (0.1-2.0 mA/cm^2) and 1.0-3.5 V versus BpK/Bp (4.0 mA/cm2). (d): Galvanostatic charge profile (blue) and gas evolution (purple) profiles of the BpK-O_2 cell at 2.0 mA/cm^2 during the 500th charge. (e):

Galvanostatic voltage profiles of the BpK-O_2 cell at 2.0 mA/cm^2, except 51st, 102nd and 153rd charge, during which the current density was reduced to 0.2 mA/cm^2. (f): The corresponding Coulombic efficiencies of the BpK-O_2 cell in (e); the inset shows the pie chart distributions of reversible KO_2 (could be recharged at 2.0 mA/cm^2, yellow area), 'loose KO_2' (accumulated KO_2 that could be recharged only under a lower current density of 0.2 mA/cm^2, rose red area) and non-rechargeable product (blue area). The percentages are averaged over the 1st-51st, 52nd-102nd and 103rd-153rd cycles, respectively.[430] Reprinted with permission from ref 430. Copyright 2019 Macmillan Publishers Limited.

5.1.2 A Molten-Salt Li-O_2 Battery Based on Li_2O Formation and Decomposition

Li_2O is another tantalizing energy storage material, because two electrons can be stored in a Li_2O molecule, giving rise to the highest energy density, 5.2 kWh/kg (**Table 4)**. Furthermore, Li_2O is more stable than Li_2O_2 and LiO_2, and thus can probably improve the chemical instability issues that have plagued the non-aqueous Li-O_2 battery. Although at room temperature electrochemical formation of Li_2O_2 is thermodynamically favored over Li_2O, the situation is reversed beyond 150°C (**Fig. 34a**).[135] Nazar and coworkers recently reported that by using an Ni-based cathode, an inorganic $LiNO_3$/KNO_3 molten salt electrolyte and a Li metal anode at an operating temperature of 150°C (**Fig. 34b**), a Li-O_2 battery based on Li_2O formation and decomposition could be realized.[135] This battery shows a major discharge plateau at 2.7 V and a charging plateau slightly below 3.0 V, which gradually polarizes towards to 3.5 V at the end of charge (**Fig. 34c**). Li_2O titration experiments on discharge and DEMS measurements on charge suggest that Li_2O formation is a four-electron oxygen reduction reaction and the oxygen recovery efficiency (OER/ORR) is close to 1 (**Fig. 34d**). As a result, the cell could cycle for 150 times without significant performance decay (at 0.2 mA/cm^2, 0.5 mAh/cm^2 per cycle). The authors demonstrated that the nickel cathode is essential to overcoming the kinetic barriers involved in cleaving the O_2 intramolecular bond on discharge, as well as O-O reformation during charge:[135] when a carbon electrode is used under the same conditions, Li_2O_2 is the discharge product. The mechanism of Li_2O formation is proposed as: two-electron Li_2O_2 formation over the Ni catalyst surface, followed by disproportionation of Li_2O_2 to form Li_2O and O_2, and finally solution-mediated Li_2O nucleation and growth (**Fig. 34e**).

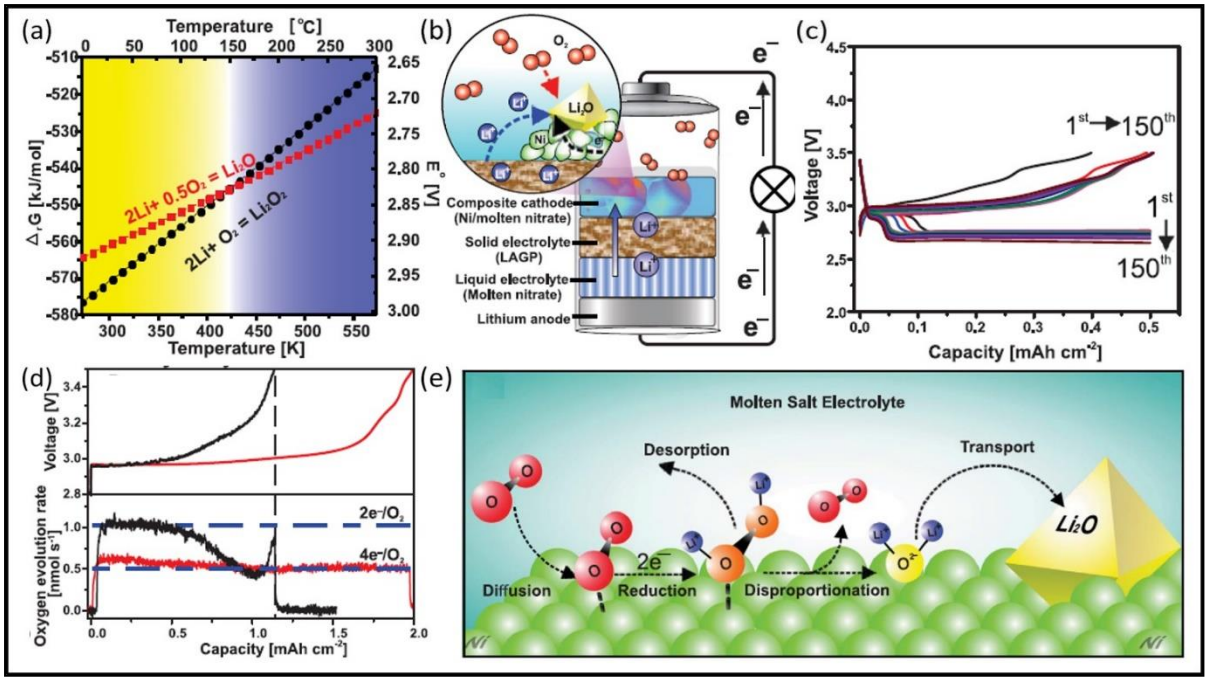

Fig. 34 A high-temperature molten salt Li-O_2 battery based on reversible Li_2O formation and decomposition. (a): Gibbs reaction energy for formation of Li_2O and Li_2O_2 as a function of temperature. (b): Configuration of the inorganic electrolyte (molten salt) Li-O_2 cell and schematic illustration of Li_2O formation during discharge at 150°C. (c): Electrochemical profiles of the 1st-150th cycles with a curtailed capacity at 0.5 mA/cm^2 per cycle. (d): Electrochemical charging profiles and the corresponding O_2 evolution for Li_2O_2 (black) and Li_2O-based (red) chemistries. (e): Schematic illustration of the discharge mechanism for Ni-catalyzed Li_2O formation in the molten salt Li-O_2 battery at 150°C.[135] Reprinted with permission from ref 135. Copyright 2018 AAAS.

The Li_2O battery system reported by Nazar and coworkers is intriguing and has at least the following implications.[135, 440] First, it shows that Li-O_2 batteries are not intrinsically limited and that with principle-guided design and wise choice of materials, a highly reversible battery reaction approaching theoretical Coulombic efficiency is indeed feasible. Secondly, the four-electron ORR and OER in the Li_2O battery system exhibit a remarkably small voltage hysteresis, ~0.3 V, much lower than the regenerative proton exchange membrane fuel cell system, ~0.7 V. Further investigation is required to provide atomistic insights into the discharge and charge reactions in the system and to account for the origin of the observed low overpotentials. When an inorganic electrolyte is used, little electrolyte decomposition occurs, even in the presence of large charging overpotentials,[115] which reiterates the critical stability issue with organic electrolytes. This work by Nazar *et al*. highlights the tremendous opportunities for fundamental research to understand the oxygen redox reactions that may lead to novel battery technologies that can potentially rival the current Li-ion battery and other energy storage systems.

5.2 Cycling Based on LiOH Formation and Decomposition?

Another critical challenge facing all Li_2O_2, LiO_2 and Li_2O-based batteries is their sensitivity to H_2O and CO_2 contamination from air, and eventually LiOH and Li_2CO_3 are generally formed to varying degrees. **Table 5** summarizes the thermodynamic driving forces of relevant reactions. It is clear that the thermodynamic tendency to form LiOH or Li_2CO_3

increases from Li_2O < Li_2O_2 < KO_2 < NaO_2 < LiO_2. The issue is particularly severe for Li_2CO_3 formation, as the driving forces for most compounds are more than -300 kJ/mol; any small contamination of the battery atmosphere by CO_2 would induce carbonate formation, resulting in a high overpotential on charging (to remove the carbonate), as observed experimentally.[129, 230, 232] By contrast, the free energy (per Li_2CO_3 formation) for the conversion of LiOH to Li_2CO_3 is less than ½ of the other types of active materials. In addition, water is typically the proton source in many LiOH-based battery systems (as introduced later), the battery chemistry is thus highly immune to water contamination. Given its higher resistance to both H_2O and CO_2 contamination, LiOH can be considered as a more promising alternative energy storage material in a lithium-air battery,[130, 441, 442] especially when simple and effective gas separation membranes are also used in the battery. Rechargeable aqueous Zinc-air batteries based on $Zn(OH)_2$ are good examples to circumvent the CO_2 contamination issue, even though there is a small thermodynamic driving force (-21 kJ/mol) to convert $Zn(OH)_2$ to $ZnCO_3$.[443]

Table 5. Thermodynamics of superoxide, peroxide, hydroxide reactions with water and CO_2.[444]

Product	**Chemical Reactions at Standard Conditions**	**$\Delta G°_{rxt}$ (kJ/mol)**
LiO_2	$4LiO_2 + 2H_2O \rightarrow 4LiOH + 3O_2$	-274.3
NaO_2	$4NaO_2 + 2H_2O \rightarrow 4NaOH + 3O_2$	-168.4
KO_2	$4KO_2 + 2H_2O \rightarrow 4KOH + 3O_2$	-84.4
Li_2O_2	$2Li_2O_2 + 2H_2O \rightarrow 4LiOH + O_2$	-152
Li_2O	$Li_2O + H_2O \rightarrow 2LiOH$	-80.1
LiO_2	$4LiO_2 + 2CO_2 \rightarrow 2Li_2CO_3 + 3O_2$	-467.7
NaO_2	$4NaO_2 + 2CO_2 \rightarrow 2Na_2CO_3 + 3O_2$	-424.6
KO_2	$4KO_2 + 2CO_2 \rightarrow 2K_2CO_3 + 3O_2$	-380.4
Li_2O_2	$2Li_2O_2 + 2CO_2 \rightarrow 2Li_2CO_3 + O_2$	-345.4
Li_2O	$Li_2O + CO_2 \rightarrow Li_2CO_3$	-176.8
LiOH	**$2LiOH + CO_2 \rightarrow Li_2CO_3 + H_2O$**	**-96.7**

Note: the free energy of LiO_2 used here is from theoretical calculation (-251.8 kJ/mol),[445] which is in reasonable agreement with the value of -260.5 kJ/mol obtained using a redox potential value of 2.7 V vs. Li^+/Li estimated from cyclic voltammogram experiments (**Fig. 3a**).[35]

Indeed, in aqueous Li-O_2 batteries, LiOH formation and decomposition have been demonstrated as the battery reactions on cycling,[413, 446, 447] as described by reaction (51). In nonaqueous media, LiOH precipitates out of the organic electrolyte as a solid phase, as described by reaction (52). In this case, a specific capacity of 1116.7 mAh/g can be derived and given a standard voltage of 3.32 V,[444] the theoretical specific energy density of 3707.4 Wh/kg is calculated.

$$4e^- + 2H_2O_{(l)} + O_{2(g)} \leftrightarrow 4OH^-_{(sol)} \qquad (51)$$

, where E° is equal to 3.4 V at pH=14, versus Li^+/Li.

$$4Li^+_{(sol)} + 4e^- + 2H_2O_{(l)} + O_{2(g)} \leftrightarrow 4LiOH_{(s)} \qquad (52)$$

, where $\Delta G°$ is equal to -1281.6 kJ/mol, and E° is equal to 3.32 V, versus Li^+/Li.

Thus far, two non-aqueous Li-O_2 battery systems have been reported to produce LiOH as a stoichiometric discharge product, as opposed to a byproduct due to organic electrolyte decomposition. One involves the use of metal catalysts and water additives in the battery[297, 432, 441, 442] and the other is a result of synergistic effects due to lithium iodide and water additives in the organic electrolyte.[130, 448-452] We next discuss in sequence the fundamental understanding and unresolved questions concerning these two systems.

5.2.1 Metal-catalyzed LiOH Electrochemistry

Zhou and coworkers first reported the observation that LiOH forms and decomposes over extended cycles in a range of Li-O_2 battery systems,[432, 441, 442] including ether-, DMSO-, and ionic liquid-based electrolytes. The essential element in all these systems that enables the LiOH chemistry is the use of Ru/MnO_2 or RuO_2/MnO_2 catalysts and water as an additive in the electrolyte.

In one example, where Ru/MnO_2/SP and $LiClO_4$/DMSO (containing 120 ppm water) are used as the cathode and electrolyte respectively, Zhou and coworkers[432] observed a superior cycling performance of 200 cycles without any capacity decay (**Fig. 35a**). The charge voltage is at ~3.2 V and a small voltage gap of around 0.4 V is obtained on cycling. XRD, FTIR (**Fig. 35b**), SEM results suggest that a mixture of Li_2O_2 and LiOH is formed on discharging and removed on charging. By chemical titration, the authors[432] derived a stoichiometry of two electrons per reduced O_2 on discharging, that is, dominated by the typical Li_2O_2 formation. On charging, the authors[432] proposed that Li_2O_2 is first converted to H_2O_2 in the presence of water, H_2O_2 being subsequently decomposed by the MnO_2 catalyst, which effectively converts Li_2O_2 to LiOH (reactions (i-ii) in **Fig. 35e**); at charging voltages, the generated LiOH in the prior steps is concomitantly oxidized by Ru catalyst to evolve O_2, via a common four-electron OER (reaction (iii)). Overall, it is claimed to be two-electron per evolved O_2 on charging.[432] The feasibility of Ru catalysts decomposing LiOH is further supported by performing linear sweep voltammetry on a LiOH-prefilled Ru/SP cathode in DMSO electrolytes,[432] where an anodic current is observed from 3.27 V and O_2 gas is detected by gas chromatography (**Fig. 35c**). With increasing concentrations of added water in the electrolyte, LiOH formation and decomposition become the dominant battery chemistry, the charging voltage remaining at ~3.2 V (**Fig. 35d**).[441]

This work reported by Zhou and coworkers[432] inspired several fundamental questions: 1) is LiOH formation a four-electron ORR on discharging?; 2) does LiOH formation involve side reactions as reported for Li_2O_2 formation?; 3) is O_2 indeed evolved on electrochemically charging? and so on. These mechanistic questions remained to be answered. As such, some of the current coauthors subsequently performed a systematic study on a similar Li-O_2 battery system.[297]

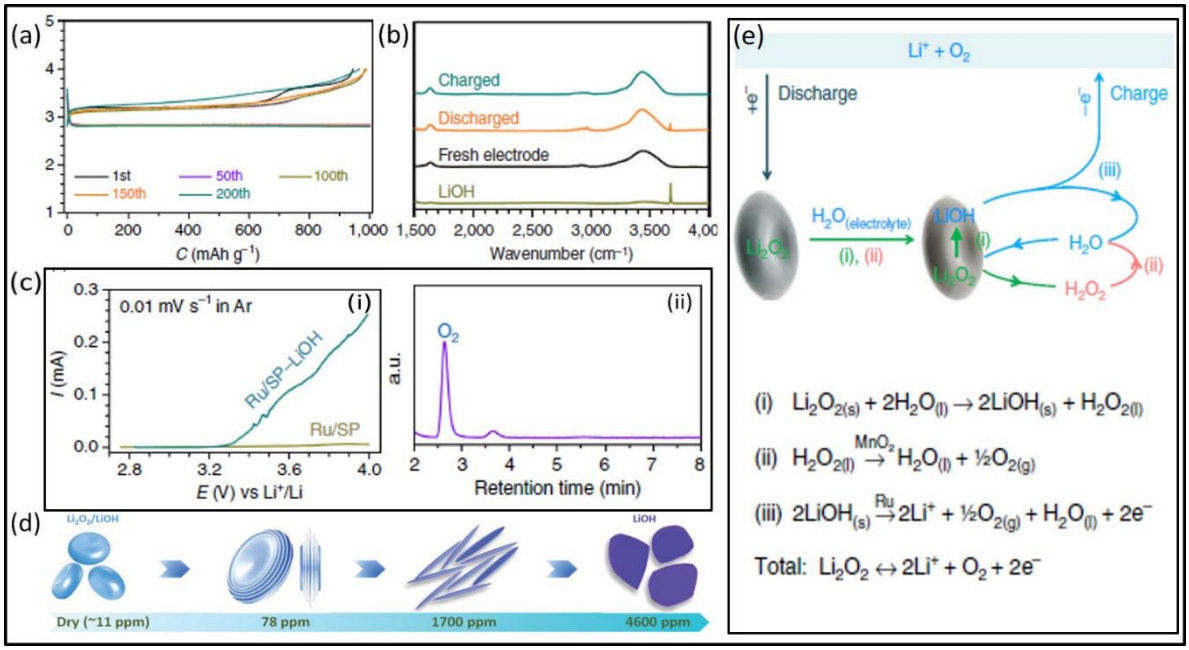

Fig. 35 Water catalysis in a highly energy-efficient Li-O_2 battery employing Ru/SP or MnO_2/Ru/SP cathodes and DMSO or ether-based electrolytes. (a): Electrochemical profiles during discharge and charging of Li-O_2 cells showing an ultra-low voltage gap during cycling. (b): FTIR characterization of the cycled electrodes, revealing that LiOH is formed and removed on discharge and charged respectively. (c): linear sweep voltammograms (i) performed on Ru/SP electrode preloaded with/without LiOH powder, and the corresponding GC-MS signal of O_2 (ii) following the LSV test, which shows that O_2 is released when LiOH is oxidized by Ru/SP cathode.[432] (d): Schematic illustration showing that more added water in the electrolyte leads to more dominant LiOH formation in the discharge product.[441] (e): Schemes showing the proposed mechanism of the charging process in the Li-O_2 battery.[432] (a–c and e) Reprinted with permission from ref 441. Copyright 2015 Macmillan Publishers Limited and (d) from ref 432. Copyright 2015 The Royal Society of Chemistry.

Grey and coworkers discovered that when there is sufficient water in the DMSO-based electrolyte, a range of metal catalysts can lead to predominant LiOH formation, where Ru catalysts exhibit the best catalytic effects on promoting LiOH formation and decomposition.[297] On discharging, *operando* pressure measurement suggests that the LiOH formation is a stoichiometric four-electron ORR reaction process (**Fig. 36a**), where the H in LiOH comes predominantly from added water, but O in LiOH originates from both gaseous O_2 and H_2O (**Fig. 36b,c**).[297] Even without MnO_2 that was used in earlier work, the Ru catalyst is found adequate to promote the conversion of Li_2O_2 to LiOH in the presence of water, probably by decomposing the H_2O_2 intermediate.[297] This observation of four-electron ORR highlights the high catalytic efficiency of Ru in promoting the decomposition of soluble peroxide species (H_2O_2, LiOOH, HO_2^-), as illustrated in **Figure 36e**. When the added water is insufficient, the discharge is first dominated by four-electron ORR to form LiOH until all water is consumed, and then Li_2O_2 formation takes over.[297] On charging, a striking observation was the decomposition of LiOH at voltages as low as 3.1 V, where it is thoroughly and quantitatively removed (**Fig. 36d**) after a full charge with high Coulombic efficiencies (>95%).[297] The battery could typically cycle for more than 100 cycles without capacity fade,[236] in agreement with the work by Zhou and coworkers.[432] Nevertheless, we did not observe O_2 evolution on charging in either pressure (**Fig. 36a**) or DEMS measurements. The LiOH decomposition is found to be coupled with DMSO oxidation to form $DMSO_2$ (**Fig.**

36e), the oxygen being effectively trapped in the electrolyte.[297] $DMSO_2$ is a soluble species in the DMSO electrolyte, as also widely observed as the decomposition product in Li_2O_2-based Li-O_2 cells,[87, 88, 91, 132, 205] and thus it does not cause rapid cell failure (by surface passivation) as observed for example in the case of Li_2CO_3 formation. As a result, the cells can have extended cycles even though the O_2 recovery ratio (OER/ORR) is extremely low.[297]

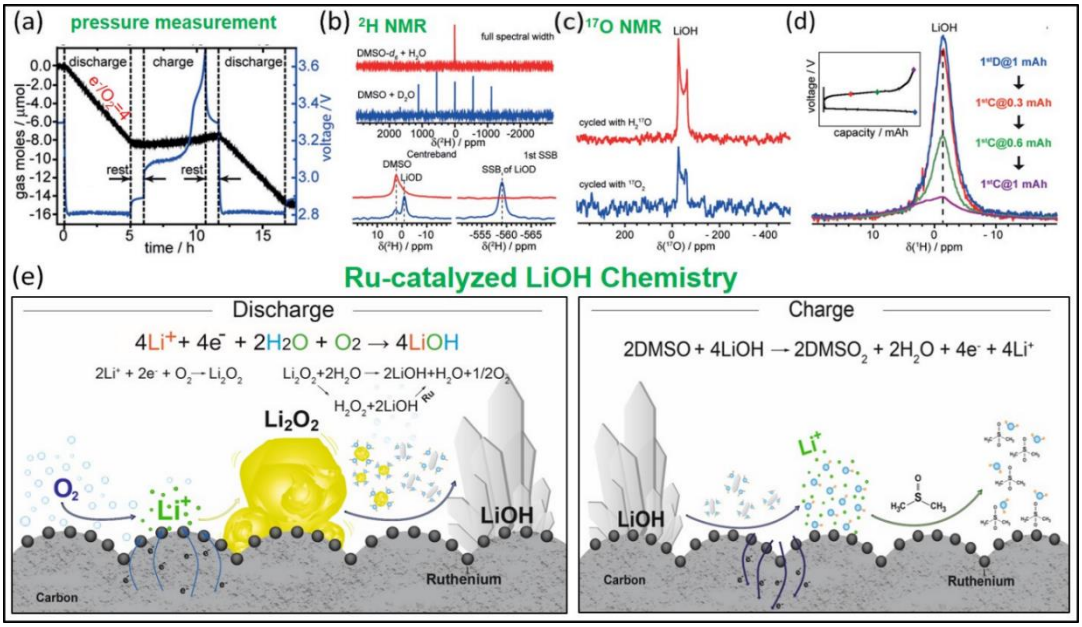

Fig. 36 Ru-catalyzed LiOH formation and decomposition in a water-added LiTFSI/DMSO electrolyte. (a): Electrochemical profile and pressure responses during discharge and charge of a Li-O_2 cell using Ru/SP cathodes. (b) ^2H magic angle spinning (MAS) solid state NMR measurements on Li-O_2 cells discharged using D_2O-DMSO or H_2O-d6 DMSO electrolytes. (c) ^{17}O MAS solid state NMR measurements on Li-O_2 cells discharged using $^{17}O2$ or ^{17}O enriched H_2O in the electrolyte, respectively. (d) Quantitative ^1H MAS solid state NMR measurements of cathode cycled to different states of charge, to evaluate how much LiOH is removed.[297] (e): Schematic illustration showing the mechanisms for cell discharge and charge processes. Reprinted with permission from ref 297. Copyright 2017 Wiley-VCH Verlag GmbH & Co. KGaA, Weinheim.

LiOH decomposition without O_2 evolution in nominally dry electrolyte has been previously reported in batteries using LiOH-prefilled carbon electrodes by Gasteiger and coworkers,[242] where concomitant electrolyte decomposition was observed on charging, similar to our observation for the Ru system.[297] A major difference, though, is that the charging voltage in their work is above 4.0 V (as opposed to 3.1 V in ours), even in the presence of a Pt catalyst.[242] A theoretical study by Ling and coworkers[453] suggests that the largest energy barrier to decompose LiOH is connected to the first delithiation step (where high voltages > 4.67 V is needed) and that once a Li^+ deficient surface is generated, the subsequent steps are thermodynamically downhill. The difficulty in Li^+ extraction is suggested to correlate with the inertness of OH^- to participate in a redox reaction and soluble redox mediators may be useful to facilitate LiOH decomposition.[453] From an experimental point of view, however, LiOH ionization /dissolution can be readily achieved by adding water to the non-aqueous electrolyte. Grey and coworkers have shown that in the presence of water solvation, the decomposition voltage of LiOH in non-aqueous media is quite sensitive to the type of catalyst: LiOH decomposition starts at 3.1, 3.5, 4.0 and above 4.0 V on Ru, Ir, Pd and Pt surfaces,

respectively;[297] this observation indicates that the initial electrochemical Li^+ delithiation of LiOH cannot be the only dominant barrier, as implied by the theoretical work;[453] the subsequent OH^- oxidation steps also involve barriers that dictate the charging overpotential. On the other hand, the decomposition of electrolyte observed is likely to be initiated by certain reaction intermediates (*e.g.*, hydroxyl radicals) generated during OH^- oxidation on catalyst surfaces.[242, 297] The typical strategy of tuning catalyst surface-oxygen binding energy to modulate and circumvent the formation of specific reaction intermediates may help promote OER on charging. Further systematic studies are required to understand the LiOH decomposition reaction in a non-aqueous Li-O_2 battery.

Despite of the absence of oxygen release, the Ru-catalyzed LiOH electrochemistry actually represents a highly rechargeable and energy-efficient (voltage gap=0.25 V) battery. During discharge, electricity is generated *via* LiOH formation that involves little side reactions compared to the Li_2O_2 formation; the charging process, on the other hand, can be seen as electrochemical $DMSO_2$ production. $DMSO_2$ itself is a useful industrial high-temperature solvent for inorganic and organic substances,[454] and it also has several medical applications. If one couples the lithium-oxygen battery with an electrolyte flow system that circulates the solvent and can afford solvent separation, a much longer battery cycle life and useful chemical production can be achieved. The same idea may be applied to other useful solvent conversion reactions.

5.2.2 Synergistic Effect of LiI and H_2O on Modulating the O_2 Electrochemistry

The other battery system that promotes LiOH formation involves the use of both LiI and H_2O as additives in an organic electrolyte.[130] LiI is a widely studied redox mediator that can also help decompose Li_2O_2 on charging.[277, 388, 455] Its combined use with water can also be applied to modulate the O_2 electrochemistry on discharge.

Some of us[130] first reported that LiI and H_2O together lead to LiOH formation in ether-based electrolytes, and proposed a stoichiometric four-electron oxygen reduction reaction (52), for the battery discharge; this was later confirmed by other groups using *operando* pressure measurements.[448] Using solid state NMR aided by isotopic labeling, Grey and coworkers showed that H of LiOH is predominantly from water rather than the electrolyte[130] and that O can come from either H_2O or O_2 gas,[342] which is the same as observed for Ru-catalyzed LiOH formation.[297] This stoichiometry of four electrons per reduced O_2 was verified by *operando* pressure tests.[342, 448] Of note, the authors found that the chemical purity of the ether solvent has a critical impact on the LiI-promoted chemistry:[342] without prior distillation of the nominally anhydrous solvent to remove the impurities, LiOH formation together with Li formate and acetates, have been observed even in the absence of water,[347] which likely results from other proton donor species rather than decomposition of the ether electrolyte.

Figure 37a(i-iii) show a series of pressure measurements of cells with increasing water contents in the electrolyte:[342] when the added water is insufficient (**Fig. 37a(i)**), the cell discharge initially shows four-electron ORR to form LiOH, followed by two-electron peroxide formation, as indicated by the slopes of the pressure curve; at intermediate water

contents (**Fig. 37a(ii)**), LiOH formation dominates the entire discharge; interestingly when water content increases further (**Fig. 37a(iii)**), the pressure slope (e^-/O_2) lies between 2 and 4, indicating that Li_2O_2 formation is reactivated. The corresponding XRD patterns (**Fig. 37b**) also capture the transition from Li_2O_2, to LiOH, and finally to a mixture of Li_2O_2/LiOH, when the water content gradually rises.

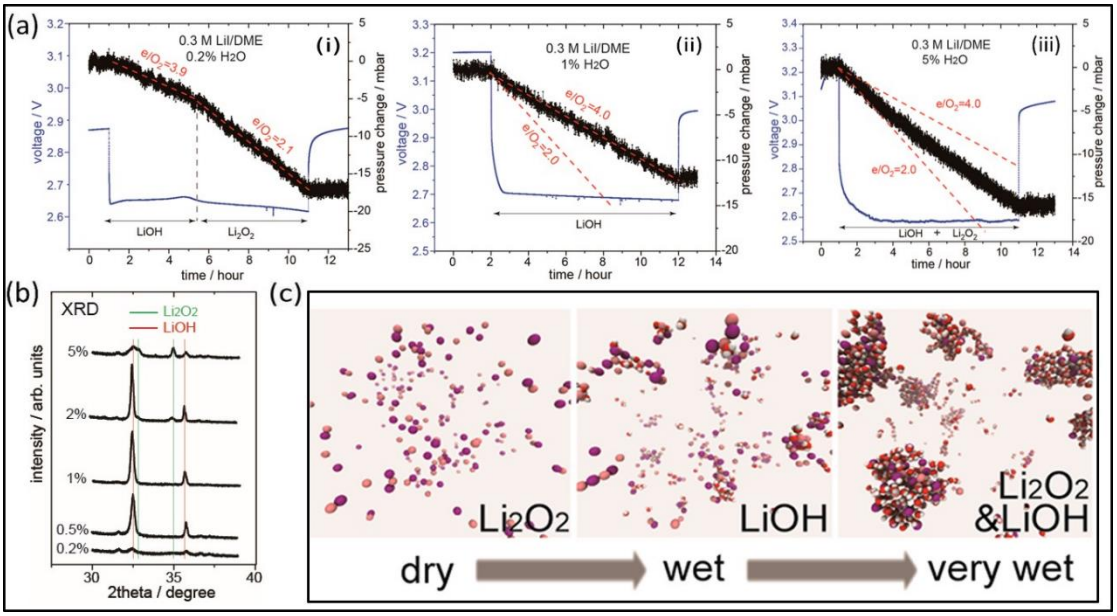

Fig. 37 Modulation of the Li-O_2 electrochemistry by the synergistic effect of LiI and H_2O in a LiTFSI/DME electrolyte. (a): pressure measurements performed on Li-O_2 cells using the DME electrolyte with increasing amount of added water from 0.2% (i), 1% (ii) to 5% (iii); where LiOH formation is dependent on added water quantities. (b): XRD measurements on discharged electrodes using LiTFSI/DME electrolytes with 0.2%, 0.5%, 1%, 2% and 5% added water. (c): molecular dynamic simulations revealing that clustering of water-LiI molecules occurs at high water concentrations, which can retard the LiI catalyzed LiOH formation and as a result, Li_2O_2 formation reactivates.[342] Reprinted with permission from ref 342. Copyright 2019 ACS.

Later on, through *in situ* Raman and FTIR measurements,[347, 450] Zhou, Shao-Horn and coworkers have identified reaction intermediates such as HO_2^-, LiOOH and H_2O_2 during discharge. Their formation is proposed to occur via water induced superoxide disproportionation in non-aqueous media (reactions (i-ii) in **Figure 38**),[342, 347] consistent with previous studies.[158-160] Iodide was suggested to play a key role in the catalytic decomposition of H_2O_2 (or HO_2^-, LiOOH),[342, 347, 450] as verified by a wide range of chemical assay and analysis: at low water contents, iodide reduces H_2O_2 to form LiOH, and the resulting I_3^- is concomitantly reduced at discharge potentials (reactions (iii-iv)); at high water contents, iodide decomposes H_2O_2 into H_2O and O_2 (reactions (v-vi)).[342] Both pathways give an overall *nominal* four-electron ORR on discharging. However, at high water contents, the efficacy of iodide catalysis on H_2O_2 decomposition is retarded due to the formation of large LiI-H_2O clusters,[342] where iodide anions are highly coordinated and surrounded by a large number of water molecules, as revealed by molecular dynamics simulations (**Fig. 37c**). Because the iodide anions are deeply embedded inside the water clusters, the accessibility for H_2O_2 to interact with iodide is considerably reduced. The remaining H_2O_2 molecules will eventually

be converted to Li_2O_2, as if in the case without LiI. This is suggested to be the origin of the observed mixed Li_2O_2 and LiOH formation at higher water contents.[342]

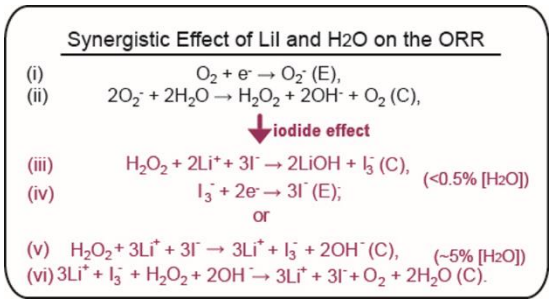

Fig. 38 A summary of synergistic effect of H_2O and LiI on modulating oxygen reduction reaction in a Li-O_2 battery.[342] Reprinted with permission from ref 342. Copyright 2019 ACS.

On charging, LiOH was reported to be removed at two distinct voltages in a DME electrolyte, at around 3.0 V[130] and 3.5 V,[448] which correspond to processes mediated by I_3^- and I_2, respectively (reactions (53-54)). Given that evolved O_2 signals was detected after charging a LiOH-prefilled cell in Ar, Grey and coworkers initially proposed that LiOH can be decomposed by I_3^- to evolve O_2 on charging (reaction (55)) in a DME electrolyte,[130] although alternatively LiOH removal pathways are also possible via $LiIO_3$ formation in the presence of significant water concentrations (reaction (56)), as indicated by UV-vis measurements.[456, 457] LiOH formation and decomposition mediated by LiI/LiI_3 couple was later supported by *in situ* XRD in the same DME-electrolyte (**Fig. 39a**).[449] Nonetheless, using pressure and DEMS measurements, others suggest that LiOH cannot be decomposed to evolve O_2 at 3.0 V in ether-based electrolytes (DME and TEGDME),[347, 448] and that any O_2 signal should be due to decomposition of some coexisting Li_2O_2. On charging to 3.5 V, LiOH removal was observed to occur via $LiIO_3$ formation (reaction (57)),[448, 452] but still no O_2 evolution was observed. Shao-horn and coworkers[452] further argued that the Gutmann acceptor number (AN) of an electrolyte solvent has a large impact on the oxidizing power of LiI mediator: stronger solvation of iodide in DMA, DMSO and Me-Im raises the oxidation potential of I_3^- so that it can oxidize LiOH (reaction (56)), whereas in weaker solvents (TEGDME and DME), the more oxidizing I_2 is needed for the oxidation reactions (reaction (57)).

$$6I^-_{(sol)} \leftrightarrow 2I_3^-{}_{(sol)} + 4e^- \quad (53)$$

$$2I_3^-{}_{(sol)} \leftrightarrow 3I_{2(sol)} + 2e^- \quad (54)$$

$$4LiOH_{(s)} + 2I_3^-{}_{(sol)} \leftrightarrow 4Li^+{}_{(sol)} + 6I^-_{(sol)} + 2H_2O_{(l)} + O_{2(g)} \quad (55)$$

$$6LiOH_{(s)} + 3I_3^-{}_{(sol)} \leftrightarrow 6Li^+{}_{(sol)} + IO_3^-{}_{(sol)} + 8I^-_{(sol)} + 3H_2O_{(l)} \quad (56)$$

, which is under alkaline conditions.

$$6LiOH_{(s)} + 3I_{2(sol)} \leftrightarrow LiIO_{3(s)} + 5LiI_{(sol)} + 3H_2O_{(l)} \quad (57)$$

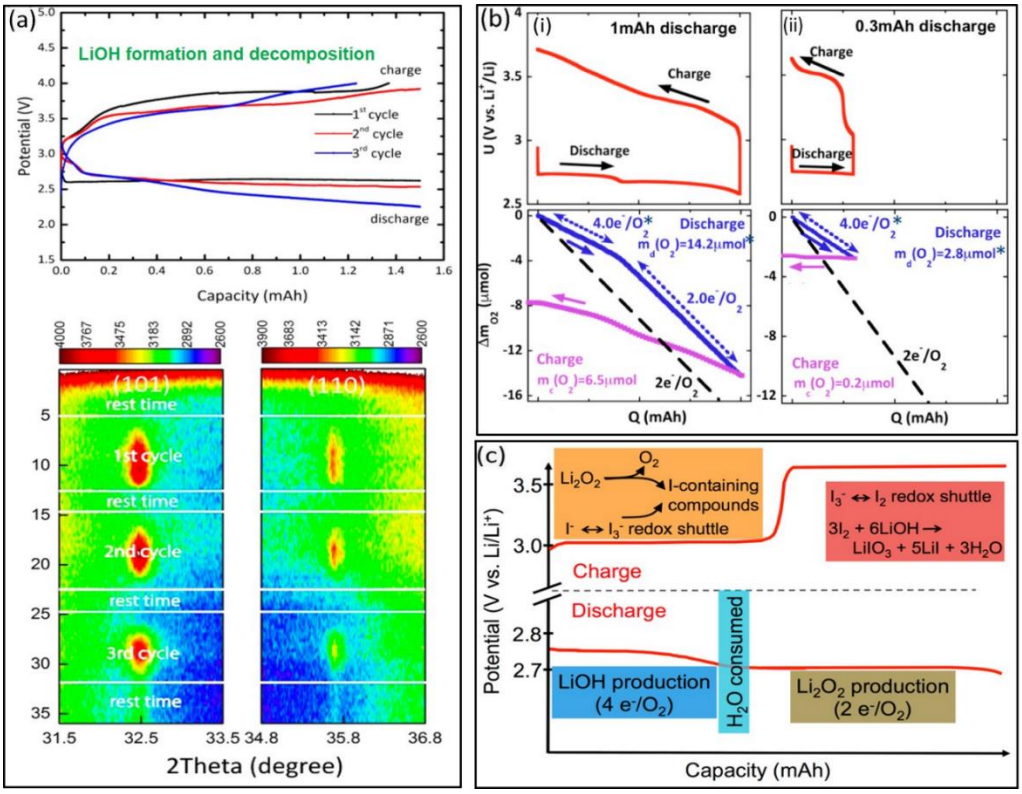

Fig. 39 LiI mediated LiOH decomposition in organic electrolytes during a cell charge. (a): *Operando* X-ray diffraction measurements performed in a LiI (50 mM)-added 0.5 M LiTFSI/DME electrolyte with 4000 ppm water, which shows LiOH formation and decomposition (between 3-4 V) for the initial 3 cycles.[449] (b): *operando* pressure tests performed on cells using LiI/LiTFSI/DME electrolytes and XC-72 carbon electrodes, which shows that when Li_2O_2 ($2e^-/O_2$) forms in the prior discharge, there is O_2 evolution on charging (i), whereas when LiOH forms on the prior discharge, no O_2 evolution is observed on the following charge (ii). (c): A scheme illustrating a potential mechanism for the observed electrochemistry in a DME-based electrolyte with LiI and water additives: the lower charging plateau at ~3.0 V corresponds to either LiI_3/LiI mediated Li_2O_2 decomposition or LiI_3/LiI shuttling, and the higher charging plateau at ~3.5 V is related to LiOH oxidation by I_2 to form $LiIO_3$ or alternatively the I_2/LiI_3 shuttling process.[448] (a) Reprinted with permission from ref 449. Copyright 2017 ACS and (b-c) from ref 448. Copyright 2016 ACS.

Another route that can play a role in LiI_3-mediated LiOH decomposition is *via* the actions of H_2O_2.[342, 451, 458] At high water contents, where Li_2O_2 and LiOH are both the discharge products,[342, 346] the coexistence of H_2O_2 with LiOH is certainly possible. Zhou and coworkers[458] introduced H_2O_2 to a LiOH-prefilled carbon electrode, and they observed quantitative LiOH removal on charging at ~3.4 V, that is, an e^-/LiOH molar ratio of 1, as well as concomitant O_2 evolution (**Fig. 40a-c**). Their observation[458] appears to be consistent with the stoichiometry in reaction (52). Further analysis by Raman aided with isotopic labeling shows that H_2O_2 reacts with LiOH to form Li_2O_2 and H_2O (**Fig. 40d**),[342] where the oxygen in Li_2O_2 originates from H_2O_2 and the oxygen in LiOH likely ends up in H_2O, as described by reaction (i) in **Figure 40e**. When LiOH is added to a LiI_3 electrolyte containing H_2O_2, O_2 is indeed observed,[342] similar to the observation by Zhou and coworkers.[458] Nonetheless, the generated O_2 is a result of peroxide decomposition by either a chemical reaction with LiI_3 (reactions (i-ii) in **Figure 40e**) or direct electrochemical oxidation on the carbon electrode (reactions (i-iii) in **Figure 40e**), both giving an e^-/LiOH molar ratio of 1. The LiOH/O_2 and LiOH/H_2O molar ratios (reaction (iv), **Fig. 40e**), however, are half of those in a standard

reaction of electrochemical LiOH decomposition (reaction (52)). Therefore, this observation does not provide direct evidence to support four-electron LiOH decomposition *via* O_2 evolution in a non-aqueous electrolyte.

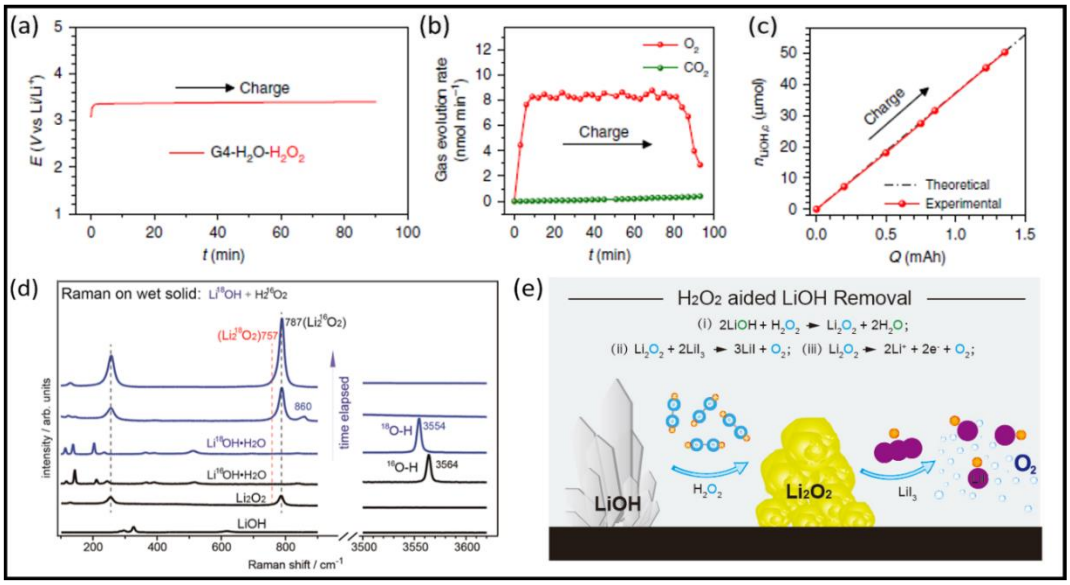

Fig. 40 H_2O_2 assisted LiOH removal during a charging process in nonaqueous Li-O_2 batteries. (a) Electrochemical charging profile of a Li-O_2 cell using LiOH-prefilled Ketjen Black cathode and TEGDME-based electrolytes with H_2O and H_2O_2 additives. (b): the corresponding DEMS measurement of (a), showing O_2 evolution on charging. (c): Chemical LiOH titration on charging for a similar cell described in (a), supporting a LiOH/e- molar ratio of 1.[458] (d): Raman measurements on the reaction between LiOH and H_2O_2, revealing that LiOH is progressively converted by H_2O_2 to LiOH monohydrate, then LiOOH and finally Li_2O_2, where the O in Li_2O_2 originates H_2O_2 and O in LiOH likely ends in the water (described in reaction (i) in (e)).[342] (e): Schematic illustration of H_2O_2 assisted electrochemical removal of LiOH in organic electrolytes: H_2O_2 helps convert LiOH to Li_2O_2 and H_2O; direct electrochemical charging or mediated charging by LiI_3 decomposes Li_2O_2, giving an overall reaction described by (iv) in (e). (a–c) Reprinted with permission from ref 458. Copyright 2017 Macmillan Publishers Limited and (d) from ref 342. Copyright 2019 ACS.

Thus far, the very central question concerning the LiOH chemistry in non-aqueous media is whether LiOH can be decomposed *via* the O_2 evolution route (reaction (52)). Theoretical consideration suggests that this is feasible at 3.32 V. Given that water is not at its standard state in a Li^+ organic electrolyte (as revealed by solution NMR and FTIR results[342, 450]), derivation from this standard voltage value will occur:[297, 432, 456, 457] a simple calculation estimates that at 100 ppm water, the equilibrium voltage for LiOH decomposition (reaction (52)) can be as low as 3.2 V. The standard voltage/potential, however, is not the only decisive factor to promote O_2 evolution, high reaction overpotentials would imply much higher charging voltages than 3.4 V, which would lead to other competing parasitic reactions associated with the electrolyte[242, 297] or redox mediator[448, 452] during LiOH decomposition. How various catalysts can be used to modulate the binding energies of reaction intermediates, *i.e.*, the reaction coordinate, and potentially help avoid the parasitic reactions during LiOH decomposition warrant further systematic studies. Despite that some early work reports the detection of O_2 evolution when charging LiOH by Ru catalysts[432] or by reacting with LiI_3/I_2,[130, 346] *operando* and quantitative gas analysis aided with isotopic labeling awaits to be

demonstrated. Recent work (currently under review) by some of us shows that LiOH decomposition *via* four-electron OER is indeed feasible.

6. Summary and Outlook

Significant progress has been made in the research field of lithium-air batteries. We have now understood that the discharge mechanism of Li_2O_2 formation, *i.e.*, surface versus solution processes, of a non-aqueous Li-O_2 battery is largely dictated by the solvating properties of the electrolyte, which can be tuned independently by either the salt or the solvent. By judiciously choosing the combination of salt and solvent, both high discharge capacity and good chemical stability of the electrolyte can be achieved. With the aid of a RM that chemically reduces O_2, the power density of the battery can be enhanced even further. The mechanism of battery recharge, namely, Li_2O_2 decomposition, is also dependent upon the solvating properties of electrolytes, and analysis suggests that the first delithiation step of Li_2O_2 to form Li^+-deficient $Li_{2-x}O_2$ determines the largest charge overpotential. Strategies that can potentially facilitate this specific step, *e.g.*, using solvent/additives that can readily dissolve Li_2O_2, should be explored.

Nevertheless, to move towards a practical lithium-air battery, the charge voltage should be brought well below 3.5 V; this is because carbon cathode corrosion, singlet oxygen generation and its associated electrolyte decomposition are all sensitive to higher voltages. Solid catalysts have been widely explored to reduce the charging overpotential. But a common issue is that although the onset charge voltage is low, they all gradually polarize toward 4.0 V or higher with deeper states of charging, which is usually connected to parasitic product accumulating at the reaction interfaces. Electrocatalysts that readily decompose LiOH and Li_2CO_3 and electrolytes with high solubilities of these byproducts can help maintain a low charge voltage and thus improve the rechargeability of the battery.

The nature of the species that are the dominant source or trigger of the side reactions involved in the lithium-oxygen electrochemistry remains an open question and worthy of further investigation. Previously, reaction intermediates, such as LiO_2, $Li_{2-x}O_2$, were considered to be the main cause. Recent evidence however shows that singlet oxygen plays a major role. The example of a KO_2-based battery that can sustain thousands of cycles indicates that parasitic reactions originating from the chemical reactivity of superoxide (in solid form or as ions in solution) do not dominate the chemistry of K-O_2 batteries using ethereal electrolytes. This raises the question as to whether superoxide is the main culprit for the parasitic reactions observed in Li-O_2 batteries. Further fundamental studies are required to separate superoxide- from singlet-oxygen induced parasitic reactions in Li-O_2 batteries. Circumventing the formation of singlet oxygen (*e.g.*, by minimizing the overpotentials) or by quenching it immediately as it forms are possible ways of mitigating the issues due to singlet oxygen generation and for potentially untangling the two degradation pathways.

In the regard of lowering the charging voltage, the use of a RM seems the most promising, as its charging profile is typically flat and the RM has the ability to decompose products formed

remotely from the cathode surface (as formed in a solution mediated discharge), thereby circumventing the issues caused by the low charge transport rate through discharge products. A variety of RMs have been explored in recent years, but the underlying principles leading to efficient mediation are yet to be established. A key step for the development of RMs for Li-O_2 batteries will be to perform systematic studies comparing different mediators under the same conditions. The ultimate goal is to establish an understanding of the key properties affecting the mediator activity and to determine how different experimental conditions alter their activity. In light of newly discovered role of singlet oxygen, a few common organic RMs are found to be unstable in the presence of $^1O_2$. On the other hand, inorganic RMs, such as LiI and LiBr, promotes Li_2O_2 decomposition with O_2 recovery efficiencies of up to 92% and 98% respectively, which are among the highest reported values so far. Whether these inorganic RMs are more stable against singlet oxygen, and whether mediated product decomposition still involves singlet oxygen generation are open questions and warrant further studies. To develop Li-O_2 batteries with suppressed degradation, high capacity and reversibility, the combination of singlet oxygen quenchers and RMs as electrolyte additives currently appears as an interesting approach, and additional complementary approaches to minimize voltage gaps for the ORR and OER as much as possible are always beneficial.

The effect of other components (H_2O, CO_2, N_2) in the air on Li-O_2 electrochemistry has been investigated. At the cathode, significant H_2O and CO_2 contamination leads to conversion of Li_2O_2 to LiOH and Li_2CO_3, considerably polarizing the battery on recharging. Although Li_2CO_3 can be removed at 3.6-4.0 V (and at lower potentials when certain catalysts are used) on charging, recent evidence suggests that no oxygen is evolved in the process making the charge irreversible, and that this lack of oxygen is associated with side reactions due to singlet oxygen generation. At current stage, Li_2CO_3 formation should therefore be avoided in a Li-O_2 battery. On the other hand, the effect of O_2, H_2O, N_2 and CO_2 on the Li metal anode stability has been less systematically investigated. In several cases, opposing opinions, *e.g.*, in the effect of O_2 crossover to Li anode on the Li cycling stability, exist. These studies underscore the need for fundamental understandings of the interaction between O_2, CO_2, N_2 and Li metal anode surface in different electrolytes/salts, and establishment of the role of SEI in protecting the metal anode.

Most Li-O_2 cell studies focus on elucidating the mechanism of the reactions in the first few cycles. While these fundamental studies are essential, with advances of lithium-air batteries further work should also be dedicated to study longer cycles. The amounts of electrolyte then becomes particularly important in longer cycling studies, since depletion of the electrolyte *via*, for example, reaction with the lithium anode can markedly affect battery performance. To date, all Li-O_2 cell studies have been conducted with a large excess of electrolyte. Gallagher and coworkers considered an electrolyte loading of 25% of the Li_2O_2 electrode volume for their calculations,[28] which for a 100 μm electrode would imply a volume of electrolyte per geometric electrode area of 2.5 μL cm^{-2} (5 μL cm^{-2} for a 200 μm electrode). Decreasing the electrolyte amount not only brings new challenges from a cell assembly perspective, it also implies that the growth of Li_2O_2 during discharge would be much more restricted in volume, thus making the achievement of high capacities more challenging. The implementation of

low electrolyte loadings also requires a realistic protection of the lithium metal anode with a suitable lithium protective membrane. These longer term studies should also be conducted with a realistic excess of capacity of the lithium anode (Gallagher and coworkers considered a 50% excess capacity) which again is an area that has not been addressed in Li-O_2 cell studies.

Of note, many groups have started to explore alternative electrochemistries for a Li-O_2 battery, such as those based on superoxide, oxide and hydroxide. Although LiO_2 and NaO_2-based cells exhibit lower overpotentials during cycling, they face insufficient chemical stability issues, which induce parasitic reactions. KO_2-based cells, however, exhibit much better reversibility and chemical stability. When coupled with a K^+ source from an organic anode, the cell can be cycled for up to 3000 times, with an unprecedentedly high O_2 recovery efficiency (99.8%); this finding challenges the consensus that superoxide anion is a strong base and nucleophile causing significant electrolyte degradation over time and thus is not suitable as a basis for a long-lived battery. The origin of this long-term stability of KO_2 in an organic solvent compared to its counterpart in Li- and Na-O_2 batteries warrants further investigation, which may in turn aid the development of other alkali-oxygen batteries. A higher temperature molten-salt Li-O_2 battery based on Li_2O formation and decomposition is demonstrated *via* nominal four-electron ORR and OER. The cell cycles with an outstanding energy efficiency for 150 times without evident capacity decay. Further investigation is required to provide atomistic insights into the discharge and charge reactions in the system and to account for the origin of the observed low overpotentials. Li-O_2 cells based on LiOH formation and decomposition are also demonstrated, where water is the proton source participating in the nominal four-electron ORR. Thermodynamic analysis shows that LiOH is more resistant to H_2O and CO_2 contamination and thus, more promising to help realize an open system and maintain the high energy density of lithium-air batteries. All these new types of battery chemistry clearly highlight the tremendous opportunities for research to understand and modulate the versatile O_2 electrochemistry, which may lead to novel battery designs outperforming the more established Li-O_2 or Li-ion battery chemistry.

Acknowledgments

Tao Liu thanks Schlumberger Fellowship from Darwin College, the National Natural Science Foundation of China (Grant No. 21802102), Recruitment Program of Global Experts and Tongji University start-up grant, Science and Technology Commission of Shanghai Municipality (19DZ2271500) for funding. Nuria Garcia-Araez thanks EPSRC for the award of an early-career fellowship (EP/N024303/1). Clare P. Grey thanks the EPSRC for support via the LIBATT grant (EP/M009521/1).

References

(1) Primary energy consumption by source, U.S. Energy information administration. https://www.eia.gov/totalenergy/data/monthly/pdf/sec1_7.pdf (accessed July 19, 2019).

(2) Bp statistical review of world energy. https://www.bp.com/content/dam/bp/business-sites/en/global/corporate/pdfs/energy-economics/statistical-review/bp-stats-review-2019-full-report.pdf (accessed July 19, 2019).
(3) Wei, W. Research progress of perovskite materials in photocatalysis- and photovoltaics-related energy conversion and environmental treatment. *Chem. Soc. Rev*. **2015**, *15*, 5371-5408.
(4) Van Noorden, R. The rechargeable revolution: A better battery. *Nature*. **2014**, *507*, 26-28.
(5) Girishkumar, G.; McCloskey, B.; Luntz, A. C.; Swanson, S.; Wilcke, W. Lithium - air battery: promise and challenges. *J. Phys. Chem. Lett.* **2010**, *1*, 2193-2203.
(6) Armand, M.; Tarascon, J. M. Building better batteries. *Nature*. **2008**, *451*, 652-657.
(7) Bruce, P. G.; Freunberger, S. A.; Hardwick, L. J.; Tarascon, J.-M. Li-O_2 and Li-S batteries with high energy storage. *Nat. Mater.* **2012**, *11*, 19-29.
(8) Lu, Y.-C.; Gallant, B. M.; Kwabi, D. G.; Harding, J. R.; Mitchell, R. R.; Whittingham, M. S.; Shao-Horn, Y. Lithium-oxygen batteries: bridging mechanistic understanding and battery performance. *Energy Environ. Sci.* **2013**, *6*, 750-768.
(9) Gu, D.; Wang, Y.; Gu, S.; Zhang, C.; Yang, D. Research progress and optimization of non-aqueous electrolyte for lithium air batteries. *Acta Chim. Sin.* **2013**, *71*, 1354-1364.
(10) Wang, Z.-L.; Xu, D.; Xu, J.-J.; Zhang, X.-B. Oxygen electrocatalysts in metal-air batteries: from aqueous to nonaqueous electrolytes. *Chem. Soc. Rev*. **2014**, *43*, 7746-7786.
(11) Wu, A.-M.; Xia, G.-F.; Shen, S.-Y.; Yin, J.-W.; Mao, Y.; Bai, Q.-Y.; Xie, J.-Y.; Zhang, J.-L. Recent progress in non-aqueous lithium-air batteries. *Acta Phys.-Chim. Sin.* **2016**, *32*, 1866-1879.
(12) Zhang, T.; Imanishi, N.; Takeda, Y.; Yamamoto, O. Aqueous lithium/air rechargeable batteries. *Chem. Lett.* **2011**, *40*, 668-673.
(13) Gierszewski, P. J.; Finn, P. A.; Kirk, D. W. Properties of LiOH and $LiNO_3$ aqueous solutions. *Fusion Eng. Des.* **1990**, *13*, 59-71.
(14) Zheng, J. P.; Liang, R. Y.; Hendrickson, M.; Plichta, E. J. Theoretical energy density of Li-air batteries. *J. Electrochem. Soc.* **2008**, *155*, A432-A437.
(15) Bennion, D. N.; Littauer, E. L. Mathematical model of a lithium-water electrochemical power cell. *J. Electrochem. Soc.* **1976**, *123*, 1462-1469.
(16) Littauer, E. L.; Tsai, K. C. Anodic behavior of lithium in aqueous electrolytes: i. Transient passivation. *J. Electrochem. Soc.* **1976**, *123*, 771-776.
(17) Littauer, E. L.; Tsai, K. C. Anodic behavior of lithium in aqueous electrolytes: ii. Mechanical passivation. *J. Electrochem. Soc.* **1976**, *123*, 964-969.
(18) Littauer, E. L.; Tsai, K. C. Corrosion of lithium in alkaline solution. *J. Electrochem. Soc.* **1977**, *124*, 850-855.
(19) Littauer, E. L.; Tsai, K. C.; Hollandsworth, R. P. Anodic behavior of lithium in aqueous electrolytes: iii . Influence of flow velocity, contact pressure, and concentration. *J. Electrochem. Soc.* **1978**, *125*, 845-852.
(20) Blurton, K. F.; Sammells, A. F. Metal/air batteries: their status and potential — a review. *J. Power Sources.* **1979**, *4*, 263-279.
(21) J. Gibian, M.; T. Sawyer, D.; Ungermann, T.; Tangpoonpholvivat, R.; M. Morrison, M. Reactivity of superoxide ion with carbonyl compounds in aprotic solvents. *J. Am. Chem. Soc.* **1979**, *101*, 640.
(22) Abraham, K. M.; Jiang, Z. A polymer electrolyte- based rechargeable lithium/oxygen battery. *J. Electrochem. Soc.* **1996**, *143*, 1-5.
(23) Abraham, K. M. A brief history of non-aqueous metal-air batteries. *ECS Trans.* **2008**, *3*, 67-71.
(24) Read, J. Characterization of the lithium/oxygen organic electrolyte battery. *J. Electrochem. Soc.* **2002**, *149*, A1190-A1195.
(25) Read, J.; Mutolo, K.; Ervin, M.; Behl, W.; Wolfenstine, J.; Driedger, A.; Foster, D. Oxygen transport properties of organic electrolytes and performance of lithium/oxygen battery. *J. Electrochem. Soc.* **2003**, *150*, A1351-A1356.
(26) Read, J. Ether-based electrolytes for the lithium/oxygen organic electrolyte battery. *J. Electrochem. Soc.* **2006**, *153*, A96-A100.
(27) Ogasawara, T.; Debart, A.; Holzapfel, M.; Novak, P.; Bruce, P. G. Rechargeable Li_2O_2 electrode for lithium batteries. *J. Am. Chem. Soc.* **2006**, *128*, 1390-1393.

(28) Gallagher, K. G.; Goebel, S.; Greszler, T.; Mathias, M.; Oelerich, W.; Eroglu, D.; Srinivasan, V. Quantifying the promise of lithium-air batteries for electric vehicles. *Energy Environ. Sci.* **2014**, *7*, 1555-1563.

(29) Lu, Y.-C.; Gasteiger, H. A.; Parent, M. C.; Chiloyan, V.; Shao-Horn, Y. The influence of catalysts on discharge and charge voltages of rechargeable Li–oxygen batteries. *Electrochem. Solid-State Lett.* **2010**, *13*, A69-A72.

(30) Johnson, L.; Li, C.; Liu, Z.; Chen, Y.; Freunberger, S. A.; Ashok, P. C.; Praveen, B. B.; Dholakia, K.; Tarascon, J.-M.; Bruce, P. G. The role of LiO_2 solubility in O_2 reduction in aprotic solvents and its consequences for Li-O_2 batteries. *Nat. Chem.* **2014**, *6*, 1091-1099.

(31) Aetukuri, N. B.; McCloskey, B. D.; Garcia, J. M.; Krupp, L. E.; Viswanathan, V.; Luntz, A. C. Solvating additives drive solution-mediated electrochemistry and enhance toroid growth in non-aqueous Li-O_2 batteries. *Nat. Chem.* **2015**, *7*, 50-56.

(32) Burke, C. M.; Pande, V.; Khetan, A.; Viswanathan, V.; McCloskey, B. D. Enhancing electrochemical intermediate solvation through electrolyte anion selection to increase nonaqueous Li-O_2 battery capacity. *Proc. Natl. Acad. Sci. U. S. A.* **2015**, *112*, 9293-9298.

(33) Laoire, C. O.; Mukerjee, S.; Abraham, K. M.; Plichta, E. J.; Hendrickson, M. A. Elucidating the mechanism of oxygen reduction for lithium-air battery applications. *J. Phys. Chem. C.* **2009**, *113*, 20127-20134.

(34) Laoire, C. O.; Mukerjee, S.; Abraham, K. M.; Plichta, E. J.; Hendrickson, M. A. Influence of nonaqueous solvents on the electrochemistry of oxygen in the rechargeable lithium-air battery. *J. Phys. Chem. C.* **2010**, *114*, 9178-9186.

(35) McCloskey, B. D.; Scheffler, R.; Speidel, A.; Girishkumar, G.; Luntz, A. C. On the mechanism of nonaqueous Li-O_2 electrochemistry on c and its kinetic overpotentials: some implications for Li-air batteries. *J. Phys. Chem. C.* **2012**, *116*, 23897-23905.

(36) Adams, B. D.; Radtke, C.; Black, R.; Trudeau, M. L.; Zaghib, K.; Nazar, L. F. Current density dependence of peroxide formation in the Li-O_2 battery and its effect on charge. *Energy Environ. Sci.* **2013**, *6*, 1772-1778.

(37) Peng, Z.; Freunberger, S. A.; Hardwick, L. J.; Chen, Y.; Giordani, V.; Barde, F.; Novak, P.; Graham, D.; Tarascon, J.-M.; Bruce, P. G. Oxygen reactions in a non-aqueous Li^+ electrolyte. *Angew. Chem. Int. Ed.* **2011**, *50*, 6351-6355.

(38) Yu, Q.; Ye, S. In situ study of oxygen reduction in dimethyl sulfoxide (DMSO) solution: a fundamental study for development of the lithium-oxygen battery. *J. Phys. Chem. C.* **2015**, *119*, 12236-12250.

(39) Galloway, T. A.; Hardwick, L. J. Utilizing in situ electrochemical shiners for oxygen reduction reaction studies in aprotic electrolytes. *J. Phys. Chem. Lett.* **2016**, *7*, 2119-2124.

(40) Black, R.; Oh, S. H.; Lee, J.-H.; Yim, T.; Adams, B.; Nazar, L. F. Screening for superoxide reactivity in Li-O_2 batteries: effect on Li_2O_2/LiOH crystallization. *J. Am. Chem. Soc.* **2012**, *134*, 2902-2905.

(41) Yang, L.; Frith, J. T.; Garcia-Araez, N.; Owen, J. R. A new method to prevent degradation of lithium-oxygen batteries: reduction of superoxide by viologen. *Chem. Commun.* **2015**, *51*, 1705-1708.

(42) Torres, W.; Mozhzhukhina, N.; Tesio, A. Y.; Calvo, E. J. A rotating ring disk electrode study of the oxygen reduction reaction in lithium containing dimethyl sulfoxide electrolyte: role of superoxide. *J. Electrochem. Soc.* **2014**, *161*, A2204-A2209.

(43) Trahan, M. J.; Mukerjee, S.; Plichta, E. J.; Hendrickson, M. A.; Abraham, K. M. Studies of Li-air cells utilizing dimethyl sulfoxide-based electrolyte. *J. Electrochem. Soc.* **2013**, *160*, A259-A267.

(44) Kwabi, D. G.; Tulodziecki, M.; Pour, N.; Itkis, D. M.; Thompson, C. V.; Shao-Horn, Y. Controlling solution-mediated reaction mechanisms of oxygen reduction using potential and solvent for aprotic lithium-oxygen batteries. *J. Phys. Chem. Lett.* **2016**, *7*, 1204-1212.

(45) Wang, Y.; Lai, N.-C.; Lu, Y.-R.; Zhou, Y.; Dong, C.-L.; Lu, Y.-C. A solvent-controlled oxidation mechanism of Li_2O_2 in lithium-oxygen batteries. *Joule*. **2018**, *2*, 2364-2380.

(46) Cao, R.; Walter, E. D.; Xu, W.; Nasybulin, E. N.; Bhattacharya, P.; Bowden, M. E.; Engelhard, M. H.; Zhang, J.-G. The mechanisms of oxygen reduction and evolution reactions in nonaqueous lithium-oxygen batteries. *ChemSusChem*. **2014**, *7*, 2436-2440.

(47) Schwager, P.; Dongmo, S.; Fenske, D.; Wittstock, G. Reactive oxygen species formed in organic lithium-oxygen batteries. *Phys. Chem. Chem. Phys.* **2016**, *18*, 10774-10780.
(48) Gampp, H.; Lippard, S. J. Reinvestigation of 18-crown-6 ether/potassium superoxide solutions in Me_2SO. *Inorg. Chem.* **1983**, *22*, 357-358.
(49) Jones, S. E.; Srivatsa, G. S.; Sawyer, D. T.; Traylor, T. G.; Mincey, T. C. Redox chemistry of iron tetraphenylporphyrin imidazolate-chelated protoheme, and of their iron(ii)-superoxide adducts in dimethyl sulfoxide. *Inorg. Chem.* **1983**, *22*, 3903-3910.
(50) Sawyer, D. T.; Gibian, M. J.; Morrison, M. M.; Seo, E. T. On the chemical reactivity of superoxide ion. *J. Am. Chem. Soc.* **1978**, *100*, 627-628.
(51) Lodge, A. W.; Lacey, M. J.; Fitt, M.; Garcia-Araez, N.; Owen, J. R. Critical appraisal on the role of catalysts for the oxygen reduction reaction in lithium-oxygen batteries. *Electrochim. Acta.* **2014**, *140*, 168-173.
(52) Cheng, L.; Redfern, P.; Lau, K. C.; Assary, R. S.; Narayanan, B.; Curtiss, L. A. Computational studies of solubilities of LiO_2 and Li_2O_2 in aprotic solvents. *J. Electrochem. Soc.* **2017**, *164*, E3696-E3701.
(53) Mitchell, R. R.; Gallant, B. M.; Shao-Horn, Y.; Thompson, C. V. Mechanisms of morphological evolution of Li_2O_2 particles during electrochemical growth. *J. Phys. Chem. Lett.* **2013**, *4*, 1060-1064.
(54) Wang, Y.; Lu, Y.-C. Isotopic labeling reveals active reaction interfaces for electrochemical oxidation of lithium peroxide. *Angew. Chem. Int. Ed.* **2019**, *58*, 6962-6966.
(55) Zheng, H.; Xiao, D.; Li, X.; Liu, Y.; Wu, Y.; Wang, J.; Jiang, K.; Chen, C.; Gu, L.; Wei, X., *et al.* New insight in understanding oxygen reduction and evolution in solid-state lithium oxygen batteries using an in situ environmental scanning electron microscope. *Nano Lett.* **2014**, *14*, 4245-4249.
(56) Wang, J.; Zhang, Y.; Guo, L.; Wang, E.; Peng, Z. Identifying reactive sites and transport limitations of oxygen reactions in aprotic lithium-O_2 batteries at the stage of sudden death. *Angew. Chem. Int. Ed.* **2016**, *55*, 5201-5205.
(57) Qiu, F.; Zhang, X.; Qiao, Y.; Zhang, X.; Deng, H.; Shi, T.; He, P.; Zhou, H. An ultra-stable and enhanced reversibility lithium metal anode with a sufficient O_2 design for Li-O_2 battery. *Energy Storage Mater.* **2018**, *12*, 176-182.
(58) Assary, R. S.; Lu, J.; Du, P.; Luo, X.; Zhang, X.; Ren, Y.; Curtiss, L. A.; Amine, K. The effect of oxygen crossover on the anode of a Li-O_2 battery using an ether-based solvent: Insights from experimental and computational studies. *ChemSusChem.* **2013**, *6*, 51-55.
(59) Shui, J.-L.; Okasinski, J. S.; Kenesei, P.; Dobbs, H. A.; Zhao, D.; Almer, J. D.; Liu, D.-J. Reversibility of anodic lithium in rechargeable lithium-oxygen batteries. *Nat. Commun.* **2013**, *4*, 1-7.
(60) Gerbig, O.; Merkle, R.; Maier, J. Electron and ion transport in Li_2O_2. *Adv. Mater.* **2013**, *25*, 3129-3133.
(61) Tian, F.; Radin, M. D.; Siegel, D. J. Enhanced charge transport in amorphous Li_2O_2. *Chem. Mater.* **2014**, *26*, 2952-2959.
(62) Albertus, P.; Girishkumar, G.; McCloskey, B.; Sanchez-Carrera, R. S.; Kozinsky, B.; Christensen, J.; Luntz, A. C. Identifying capacity limitations in the Li/oxygen battery using experiments and modeling. *J. Electrochem. Soc.* **2011**, *158*, A343-A351.
(63) Viswanathan, V.; Thygesen, K. S.; Hummelshoj, J. S.; Norskov, J. K.; Girishkumar, G.; McCloskey, B. D.; Luntz, A. C. Electrical conductivity in Li_2O_2 and its role in determining capacity limitations in non-aqueous Li-O_2 batteries. *J. Chem. Phys.* **2011**, *135*, 214704.
(64) Luntz, A. C.; Viswanathan, V.; Voss, J.; Varley, J. B.; Norskov, J. K.; Scheffler, R.; Speidel, A. Tunneling and polaron charge transport through Li_2O_2 in Li-O_2 batteries. *J. Phys. Chem. Lett.* **2013**, *4*, 3494-3499.
(65) Knudsen, K. B.; Luntz, A. C.; Jensen, S. H.; Vegge, T.; Hjelm, J. Redox probing study of the potential dependence of charge transport through Li_2O_2. *J. Phys. Chem. C.* **2015**, *119*, 28292-28299.
(66) Hojberg, J.; McCloskey, B. D.; Hjelm, J.; Vegge, T.; Johansen, K.; Norby, P.; Luntz, A. C. An electrochemical impedance spectroscopy investigation of the overpotentials in Li-O_2 batteries. *ACS Appl. Mater. Interfaces.* **2015**, *7*, 4039-4047.

(67) Liu, T.; Frith, J. T.; Kim, G.; Kerber, R. N.; Dubouis, N.; Shao, Y.; Liu, Z.; Magusin, P. C. M. M.; Casford, M. T. L.; Garcia-Araez, N., *et al.* The effect of water on quinone redox mediators in nonaqueous Li-O_2 batteries. *J. Am. Chem. Soc.* **2018**, *140*, 1428-1437.

(68) Abraham, K. M. Electrolyte-directed reactions of the oxygen electrode in lithium-air batteries. *J. Electrochem. Soc.* **2015**, *162*, A3021-A3031.

(69) Kwabi, D. G.; Bryantsev, V. S.; Batcho, T. P.; Itkis, D. M.; Thompson, C. V.; Shao-Horn, Y. Experimental and computational analysis of the solvent-dependent O_2/Li^+-O_2^- redox couple: standard potentials, coupling strength, and implications for lithium-oxygen batteries. *Angew. Chem. Int. Ed.* **2016**, *55*, 3129-3134.

(70) Gunasekara, I.; Mukerjee, S.; Plichta, E. J.; Hendrickson, M. A.; Abraham, K. M. A study of the influence of lithium salt anions on oxygen reduction reactions in li-air batteries. *J. Electrochem. Soc.* **2015**, *162*, A1055-A1066.

(71) Sharon, D.; Hirsberg, D.; Salama, M.; Afri, M.; Frimer, A. A.; Noked, M.; Kwak, W.; Sun, Y.-K.; Aurbach, D. Mechanistic role of Li^+ dissociation level in aprotic Li-O_2 battery. *ACS Appl. Mater. Interfaces.* **2016**, *8*, 5300-5307.

(72) Landa-Medrano, I.; Olivares-Marin, M.; Bergner, B.; Pinedo, R.; Sorrentino, A.; Pereiro, E.; Ruiz de Larramendi, I.; Janek, J.; Rojo, T.; Tonti, D. Potassium salts as electrolyte additives in lithium-oxygen batteries. *J. Phys. Chem. C.* **2017**, *121*, 3822-3829.

(73) Matsuda, S.; Kubo, Y.; Uosaki, K.; Nakanishi, S. Potassium ions promote solution-route Li_2O_2 formation in the positive electrode reaction of Li-O_2 batteries. *J. Phys. Chem. Lett.* **2017**, *8*, 1142-1146.

(74) Meini, S.; Piana, M.; Tsiouvaras, N.; Garsuch, A.; Gasteiger, H. A. The effect of water on the discharge capacity of a non-catalyzed carbon cathode for Li-O_2 batteries. *Electrochem. Solid-State Lett.* **2012**, *15*, A45-A48.

(75) Schwenke, K. U.; Metzger, M.; Restle, T.; Piana, M.; Gasteiger, H. A. The influence of water and protons on Li_2O_2 crystal growth in aprotic Li-O_2 cells. *J. Electrochem. Soc.* **2015**, *162*, A573-A584.

(76) Gao, X.; Jovanov, Z. P.; Chen, Y.; Johnson, L. R.; Bruce, P. G. Phenol-catalyzed discharge in the aprotic lithium-oxygen battery. *Angew. Chem. Int. Ed.* **2017**, *56*, 6539-6543.

(77) Lacey, M. J.; Frith, J. T.; Owen, J. R. A redox shuttle to facilitate oxygen reduction in the lithium air battery. *Electrochem. Commun.* **2013**, *26*, 74-76.

(78) Sun, D.; Shen, Y.; Zhang, W.; Yu, L.; Yi, Z.; Yin, W.; Wang, D.; Huang, Y.; Wang, J.; Wang, D., *et al.* A solution-phase bifunctional catalyst for lithium-oxygen batteries. *J. Am. Chem. Soc.* **2014**, *136*, 8941-8946.

(79) Matsuda, S.; Mori, S.; Kubo, Y.; Uosaki, K.; Hashimoto, K.; Nakanishi, S. Cobalt phthalocyanine analogs as soluble catalysts that improve the charging performance of Li-O_2 batteries. *Chem. Phys. Lett.* **2015**, *620*, 78-81.

(80) Matsuda, S.; Hashimoto, K.; Nakanishi, S. Efficient Li_2O_2 formation via aprotic oxygen reduction reaction mediated by quinone derivatives. *J. Phys. Chem. C.* **2014**, *118*, 18397-18400.

(81) Gao, X.; Chen, Y.; Johnson, L.; Bruce, P. G. Promoting solution phase discharge in Li-O_2 batteries containing weakly solvating electrolyte solutions. *Nat. Mater.* **2016**, *15*, 882-888.

(82) Zhang, Y.; Zhang, X.; Wang, J.; McKee, W. C.; Xu, Y.; Peng, Z. Potential-dependent generation of O_2^- and LiO_2 and their critical roles in O_2 reduction to Li_2O_2 in aprotic Li-O_2 batteries. *J. Phys. Chem. C.* **2016**, *120*, 3690-3698.

(83) Liu, B.; Xu, W.; Zheng, J.; Yan, P.; Walter, E. D.; Isern, N.; Bowden, M. E.; Engelhard, M. H.; Kim, S. T.; Read, J., *et al.* Temperature dependence of the oxygen reduction mechanism in nonaqueous Li-O_2 batteries. *ACS Energy Lett.* **2017**, *2*, 2525-2530.

(84) Nemanick, E. J.; Hickey, R. P. The effects of O_2 pressure on Li-O_2 secondary battery discharge capacity and rate capability. *J. Power Sources.* **2014**, *252*, 248-251.

(85) Park, J.-B.; Hassoun, J.; Jung, H.-G.; Kim, H.-S.; Yoon, C. S.; Oh, I.-H.; Scrosati, B.; Sun, Y.-K. Influence of temperature on lithium-oxygen battery behavior. *Nano Lett.* **2013**, *13*, 2971-2975.

(86) Mozhzhukhina, N.; Mendez De Leo, L. P.; Julio Calvo, E. Infrared spectroscopy studies on stability of dimethyl sulfoxide for application in a Li-air battery. *J. Phys. Chem. C.* **2013**, *117*, 18375-18380.
(87) Kwabi, D. G.; Batcho, T. P.; Amanchukwu, C. V.; Ortiz-Vitoriano, N.; Hammond, P.; Thompson, C. V.; Shao-Horn, Y. Chemical instability of dimethyl sulfoxide in lithium-air batteries. *J. Phys. Chem. Lett.* **2014**, *5*, 2850-2856.
(88) Sharon, D.; Afri, M.; Noked, M.; Garsuch, A.; Frimer, A. A.; Aurbach, D. Oxidation of dimethyl sulfoxide solutions by electrochemical reduction of oxygen. *J. Phys. Chem. Lett.* **2013**, *4*, 3115-3119.
(89) Younesi, R.; Norby, P.; Vegge, T. A new look at the stability of dimethyl sulfoxide and acetonitrile in Li-O_2 batteries. *ECS Electrochem. Lett.* **2014**, *3*, A15-A18.
(90) Chen, Y.; Freunberger, S. A.; Peng, Z.; Barde, F.; Bruce, P. G. Li-O_2 battery with a dimethylformamide electrolyte. *J. Am. Chem. Soc.* **2012**, *134*, 7952-7957.
(91) McCloskey, B. D.; Bethune, D. S.; Shelby, R. M.; Mori, T.; Scheffler, R.; Speidel, A.; Sherwood, M.; Luntz, A. C. Limitations in rechargeability of Li-O_2 batteries and possible origins. *J. Phys. Chem. Lett.* **2012**, *3*, 3043-3047.
(92) Khetan, A.; Luntz, A.; Viswanathan, V. Trade-offs in capacity and rechargeability in nonaqueous Li-O_2 batteries: Solution-driven growth versus nucleophilic stability. *J. Phys. Chem. Lett.* **2015**, *6*, 1254-1259.
(93) Ganapathy, S.; Adams, B. D.; Stenou, G.; Anastasaki, M. S.; Goubitz, K.; Miao, X.-F.; Nazar, L. F.; Wagemaker, M. Nature of Li_2O_2 oxidation in a Li-O_2 battery revealed by operando x-ray diffraction. *J. Am. Chem. Soc.* **2014**, *136*, 16335-16344.
(94) Lim, H.; Yilmaz, E.; Byon, H. R. Real-time XRD studies of Li-O_2 electrochemical reaction in nonaqueous lithium-oxygen battery. *J. Phys. Chem. Lett.* **2012**, *3*, 3210-3215.
(95) Liu, C.; Brant, W. R.; Younesi, R.; Dong, Y.; Edstrom, K.; Gustafsson, T.; Zhu, J. Towards an understanding of Li_2O_2 evolution in Li-O_2 batteries: an inoperando synchrotron x-ray diffraction study. *ChemSusChem.* **2017**, *10*, 1592-1599.
(96) Lu, Y.-C.; Shao-Horn, Y. Probing the reaction kinetics of the charge reactions of nonaqueous Li-O_2 batteries. *J. Phys. Chem. Lett.* **2013**, *4*, 93-99.
(97) Xia, C.; Waletzko, M.; Chen, L.; Peppler, K.; Klar, P. J.; Janek, J. Evolution of Li_2O_2 growth and its effect on kinetics of Li-O_2 batteries. *ACS Appl. Mater. Interfaces.* **2014**, *6*, 12083-12092.
(98) Gallant, B. M.; Kwabi, D. G.; Mitchell, R. R.; Zhou, J.; Thompson, C. V.; Shao-Horn, Y. Influence of Li_2O_2 morphology on oxygen reduction and evolution kinetics in Li-O_2 batteries. *Energy Environ. Sci.* **2013**, *6*, 2518-2528.
(99) McCloskey, B. D.; Speidel, A.; Scheffler, R.; Miller, D. C.; Viswanathan, V.; Hummelshoj, J. S.; Norskov, J. K.; Luntz, A. C. Twin problems of interfacial carbonate formation in nonaqueous Li-O_2 batteries. *J. Phys. Chem. Lett.* **2012**, *3*, 997-1001.
(100) Zhou, B.; Guo, L.; Zhang, Y.; Wang, J.; Ma, L.; Zhang, W.-H.; Fu, Z.; Peng, Z. A high-performance Li-O_2 battery with a strongly solvating hexamethylphosphoramide electrolyte and a lipon-protected lithium anode. *Adv. Mater.* **2017**, *29*, 1701568.
(101) Zhai, D.; Wang, H.-H.; Yang, J.; Lau, K. C.; Li, K.; Amine, K.; Curtiss, L. A. Disproportionation in Li-O_2 batteries based on a large surface area carbon cathode. *J. Am. Chem. Soc.* **2013**, *135*, 15364-15372.
(102) Liu, T.; Kim, G.; Casford, M. T. L.; Grey, C. P. Mechanistic insights into the challenges of cycling a nonaqueous Na-O_2 battery. *J. Phys. Chem. Lett.* **2016**, *7*, 4841-4846.
(103) Nichols, J. E.; McCloskey, B. D. The sudden death phenomena in nonaqueous na-o-2 batteries. *J. Phys. Chem. C.* **2017**, *121*, 85-96.
(104) Xia, C.; Black, R.; Fernandes, R.; Adams, B.; Nazar, L. F. The critical role of phase-transfer catalysis in aprotic sodium oxygen batteries. *Nat. Chem.* **2015**, *7*, 496-501.
(105) Kang, J.; Jung, Y. S.; Wei, S.-H.; Dillon, A. C. Implications of the formation of small polarons in Li_2O_2 for Li-air batteries. *Phys. Rev. B.* **2012**, *85*, 035210.
(106) Ong, S. P.; Mo, Y.; Ceder, G. Low hole polaron migration barrier in lithium peroxide. *Phys. Rev. B.* **2012**, *85*, 081105.

(107) Radin, M. D.; Siegel, D. J. Charge transport in lithium peroxide: relevance for rechargeable metal-air batteries. *Energy Environ. Sci.* **2013**, *6*, 2370-2379.
(108) Dunst, A.; Epp, V.; Hanzu, I.; Freunberger, S. A.; Wilkening, M. Short-range Li diffusion vs. long-range ionic conduction in nanocrystalline lithium peroxide Li_2O_2-the discharge product in lithium-air batteries. *Energy Environ. Sci.* **2014**, *7*, 2739-2752.
(109) Varley, J. B.; Viswanathan, V.; Norskov, J. K.; Luntz, A. C. Lithium and oxygen vacancies and their role in Li_2O_2 charge transport in Li-O_2 batteries. *Energy Environ. Sci.* **2014**, *7*, 720-727.
(110) Hummelshoj, J. S.; Blomqvist, J.; Datta, S.; Vegge, T.; Rossmeisl, J.; Thygesen, K. S.; Luntz, A. C.; Jacobsen, K. W.; Norskov, J. K. Communications: elementary oxygen electrode reactions in the aprotic Li-air battery. *J. Chem. Phys.* **2010**, *132*, 071101.
(111) Kang, S.; Mo, Y.; Ong, S. P.; Ceder, G. A facile mechanism for recharging Li_2O_2 in Li-O_2 batteries. *Chem. Mater.* **2013**, *25*, 3328-3336.
(112) Hummelshoj, J. S.; Luntz, A. C.; Norskov, J. K. Theoretical evidence for low kinetic overpotentials in Li-O_2 electrochemistry. *J. Chem. Phys.* **2013**, *138*, 034703.
(113) Radin, M. D.; Rodriguez, J. F.; Tian, F.; Siegel, D. J. Lithium peroxide surfaces are metallic, while lithium oxide surfaces are not. *J. Am. Chem. Soc.* **2012**, *134*, 1093-1103.
(114) Yao, K. P. C.; Risch, M.; Sayed, S. Y.; Lee, Y.-L.; Harding, J. R.; Grimaud, A.; Pour, N.; Xu, Z.; Zhou, J.; Mansour, A., *et al.* Solid-state activation of Li_2O_2 oxidation kinetics and implications for Li-O_2batteries. *Energy Environ. Sci.* **2015**, *8*, 2417-2426.
(115) Wang, Y.; Liang, Z.; Zou, Q.; Gong, G.; Lu, Y.-C. Mechanistic insights into catalyst-assisted nonaqueous oxygen evolution reaction in lithium-oxygen batteries. *J. Phys. Chem. C.* **2016**, *120*, 6459-6466.
(116) Kushima, A.; Koido, T.; Fujiwara, Y.; Kuriyama, N.; Kusumi, N.; Li, J. Charging/discharging nanomorphology asymmetry and rate-dependent capacity degradation in Li-oxygen battery. *Nano Lett.* **2015**, *15*, 8260-8265.
(117) Zhong, L.; Mitchell, R. R.; Liu, Y.; Gallant, B. M.; Thompson, C. V.; Huang, J. Y.; Mao, S. X.; Shao-Horn, Y. In situ transmission electron microscopy observations of electrochemical oxidation of Li_2O_2. *Nano Lett.* **2013**, *13*, 2209-2214.
(118) Mo, Y.; Ong, S. P.; Ceder, G. First-principles study of the oxygen evolution reaction of lithium peroxide in the lithium-air battery. *Phys. Rev. B.* **2011**, *84*, 205446.
(119) Huang, J.; Peng, Z. Understanding the reaction interface in lithium-oxygen batteries. *Batteries Supercaps.* **2019**, *2*, 37-48.
(120) Peng, Q.; Chen, J.; Ji, H.; Morita, A.; Ye, S. Origin of the overpotential for the oxygen evolution reaction on a well-defined graphene electrode probed by in situ sum frequency generation vibrational spectroscopy. *J. Am. Chem. Soc.* **2018**, *140*, 15568-15571.
(121) Liu, P.; Han, J.; Guo, X.; Ito, Y.; Yang, C.; Ning, S.; Fujita, T.; Hirata, A.; Chen, M. Operando characterization of cathodic reactions in a liquid-state lithium-oxygen micro-battery by scanning transmission electron microscopy. *Sci. Rep.* **2018**, *8*, 3134.
(122) McCloskey, B. D.; Bethune, D. S.; Shelby, R. M.; Girishkumar, G.; Luntz, A. C. Solvents' critical role in nonaqueous lithium-oxygen battery electrochemistry. *J. Phys. Chem. Lett.* **2011**, *2*, 1161-1166.
(123) Gallant, B. M.; Mitchell, R. R.; Kwabi, D. G.; Zhou, J.; Zuin, L.; Thompson, C. V.; Shao-Horn, Y. Chemical and morphological changes of Li-O_2 battery electrodes upon cycling. *J. Phys. Chem. C.* **2012**, *116*, 20800-20805.
(124) Nasybulin, E. N.; Xu, W.; Mehdi, B. L.; Thomsen, E.; Engelhard, M. H.; Masse, R. C.; Bhattacharya, P.; Gu, M.; Bennett, W.; Nie, Z., *et al.* Formation of interfacial layer and long-term cyclability of Li-O_2 batteries. *ACS Appl. Mater. Interfaces.* **2014**, *6*, 14141-14151.
(125) Younesi, R.; Hahlin, M.; Bjorefors, F.; Johansson, P.; Edstrom, K. Li-O_2 battery degradation by lithium peroxide (Li_2O_2): A model study. *Chem. Mater.* **2013**, *25*, 77-84.
(126) Thotiyl, M. M. O.; Freunberger, S. A.; Peng, Z.; Bruce, P. G. The carbon electrode in nonaqueous Li-O_2 cells. *J. Am. Chem. Soc.* **2013**, *135*, 494-500.
(127) Chen, Y.; Freunberger, S. A.; Peng, Z.; Fontaine, O.; Bruce, P. G. Charging a Li-O_2 battery using a redox mediator. *Nat. Chem.* **2013**, *5*, 489-494.

(128) Guo, L.; Wang, J.; Ma, S.; Zhang, Y.; Wang, E.; Peng, Z. The origin of potential rise during charging of Li-O_2 batteries. *Sci. China: Chem.* **2017**, *60*, 1527-1532.
(129) Gowda, S. R.; Brunet, A.; Wallraff, G. M.; McCloskey, B. D. Implications of CO_2 contamination in rechargeable nonaqueous Li-O_2 batteries. *J. Phys. Chem. Lett.* **2013**, *4*, 276-279.
(130) Liu, T.; Leskes, M.; Yu, W.; Moore, A. J.; Zhou, L.; Bayley, P. M.; Kim, G.; Grey, C. P. Cycling Li-O_2 batteries via LiOH formation and decomposition. *Science*. **2015**, *350*, 530-533.
(131) Sun, F.; Gao, R.; Zhou, D.; Osenberg, M.; Dong, K.; Kardjilov, N.; Hilger, A.; Markoetter, H.; Bieker, P. M.; Liu, X., *et al.* Revealing hidden facts of li anode in cycled lithium oxygen batteries through x-ray and neutron tomography. *ACS Energy Lett.* **2019**, *4*, 306-316.
(132) McCloskey, B. D.; Valery, A.; Luntz, A. C.; Gowda, S. R.; Wallraff, G. M.; Garcia, J. M.; Mori, T.; Krupp, L. E. Combining accurate O_2 and Li_2O_2 assays to separate discharge and charge stability limitations in nonaqueous Li-O_2 batteries. *J. Phys. Chem. Lett.* **2013**, *4*, 2989-2993.
(133) Freunberger, S. A. True performance metrics in beyond-intercalation batteries. *Nat. Energy.* **2017**, *2*, 17091.
(134) Freunberger, S. A.; Chen, Y.; Peng, Z.; Griffin, J. M.; Hardwick, L. J.; Barde, F.; Novak, P.; Bruce, P. G. Reactions in the rechargeable lithium-O_2 battery with alkyl carbonate electrolytes. *J. Am. Chem. Soc.* **2011**, *133*, 8040-8047.
(135) Xia, C.; Kwok, C. Y.; Nazar, L. F. A high-energy-density lithium-oxygen battery based on a reversible four-electron conversion to lithium oxide. *Science*. **2018**, *361*, 777-781.
(136) Tsiouvaras, N.; Meini, S.; Buchberger, I.; Gasteiger, H. A. A novel on-line mass spectrometer design for the study of multiple charging cycles of a Li-O_2 battery. *J. Electrochem. Soc.* **2013**, *160*, A471-A477.
(137) Bahou, M.; Wu, Y.-J.; Lee, Y.-P. Infra-red spectra of protonated pyrene and its neutral counterpart in solid para-hydrogen. *J. Phys. Chem. Lett.* **2013**, *4*, 1989-1993.
(138) Schafzahl, B.; Mourad, E.; Schafzahl, L.; Petit, Y. K.; Raju, A. R.; Thotiyl, M. O.; Wilkening, M.; Slugovc, C.; Freunberger, S. A. Quantifying total superoxide, peroxide, and carbonaceous compounds in metal-O_2 batteries and the solid electrolyte interphase. *ACS Energy Lett.* **2018**, *3*, 170-176.
(139) Wandt, J.; Jakes, P.; Granwehr, J.; Gasteiger, H. A.; Eichel, R.-A. Singlet oxygen formation during the charging process of an aprotic lithium-oxygen battery. *Angew. Chem. Int. Ed.* **2016**, *55*, 6892-6895.
(140) Mahne, N.; Fontaine, O.; Thotiyl, M. O.; Wilkening, M.; Freunberger, S. A. Mechanism and performance of lithium-oxygen batteries - a perspective. *Chem. Sci.* **2017**, *8*, 6716-6729.
(141) Sun, B.; Guo, L.; Ju, Y.; Munroe, P.; Wang, E.; Peng, Z.; Wang, G. Unraveling the catalytic activities of ruthenium nanocrystals in high performance aprotic Li-O_2 batteries. *Nano Energy*. **2016**, *28*, 486-494.
(142) Beyer, H.; Metzger, M.; Sicklinger, J.; Wu, X.; Schwenke, K. U.; Gasteiger, H. A. Antimony doped tin oxide–synthesis, characterization and application as cathode material in Li-O_2 cells: implications on the prospect of carbon-free cathodes for rechargeable lithium-air batteries. *J. Electrochem. Soc.* **2017**, *164*, A1026-A1036.
(143) Zavala-Rivera, P.; Channon, K.; Nguyen, V.; Sivaniah, E.; Kabra, D.; Friend, R. H.; Nataraj, S. K.; Al-Muhtaseb, S. A.; Hexemer, A.; Calvo, M. E., *et al.* Collective osmotic shock in ordered materials. *Nat. Mater.* **2011**, *11*, 53.
(144) Gin, D. L.; Noble, R. D. Designing the next generation of chemical separation membranes. *Science*. **2011**, *332*, 674-676.
(145) Reijerkerk, S. R.; Knoef, M. H.; Nijmeijer, K.; Wessling, M. Poly(ethylene glycol) and poly(dimethyl siloxane): Combining their advantages into efficient CO_2 gas separation membranes. *J. Membr. Sci.* **2010**, *352*, 126-135.
(146) Robeson, L. M. The upper bound revisited. *J. Membr. Sci.* **2008**, *320*, 390-400.
(147) Park, H. B.; Jung, C. H.; Lee, Y. M.; Hill, A. J.; Pas, S. J.; Mudie, S. T.; Van Wagner, E.; Freeman, B. D.; Cookson, D. J. Polymers with cavities tuned for fast selective transport of small molecules and ions. *Science*. **2007**, *318*, 254-258.

(148) Kowalczk, I.; Read, J.; Salomon, M. Li-air batteries: A classic example of limitations owing to solubilities. *Pure Appl. Chem.* **2007**, *79*, 851-860.
(149) Walker, W.; Giordani, V.; Uddin, J.; Bryantsev, V. S.; Chase, G. V.; Addison, D. A rechargeable Li-O_2 battery using a lithium nitrate/n,n-dimethylacetamide electrolyte. *J. Am. Chem. Soc.* **2013**, *135*, 2076-2079.
(150) Piana, M.; Wandt, J.; Meini, S.; Buchberger, I.; Tsiouvaras, N.; Gasteiger, H. A. Stability of a pyrrolidinium-based ionic liquid in Li-O_2 cells. *J. Electrochem. Soc.* **2014**, *161*, A1992-A2001.
(151) Wan, H.; Mao, Y.; Liu, Z.; Bai, Q.; Peng, Z.; Bao, J.; Wu, G.; Liu, Y.; Wang, D.; Xie, J. Influence of enhanced O_2 provision on the discharge performance of Li-air batteries by incorporating fluoroether. *ChemSusChem*. **2017**, *10*, 1385-1389.
(152) Haipeng, G.; Wenbin, L.; Jun, C.; Shulei, C.; Huakun, L.; Jiazhao, W. Review of electrolytes in nonaqueous lithium-oxygen batteries. *Adv. Sustainable Syst.* **2018**, *2*, 1700183.
(153) Mahne, N.; Schafzahl, B.; Leypold, C.; Leypold, M.; Grumm, S.; Leitgeb, A.; Strohmeier, G. A.; Wilkening, M.; Fontaine, O.; Kramer, D., *et al.* Singlet oxygen generation as a major cause for parasitic reactions during cycling of aprotic lithium-oxygen batteries. *Nat. Energy.* **2017**, *2*, 17036.
(154) Zhang, X.; Guo, L.; Gan, L.; Zhang, Y.; Wang, J.; Johnson, L. R.; Bruce, P. G.; Peng, Z. LiO_2: cryosynthesis and chemical/electrochemical reactivities. *J. Phys. Chem. Lett.* **2017**, *8*, 2334-2338.
(155) Lau, K. C.; Lu, J.; Luo, X.; Curtiss, L. A.; Amine, K. Implications of the unpaired spins in Li-O_2 battery chemistry and electrochemistry: a minireview. *ChemPlusChem*. **2015**, *80*, 336-343.
(156) Yang, G.; Wang, Y.; Ma, Y. A stable, magnetic, and metallic Li_3O_4 compound as a discharge product in a Li–air battery. *J. Phys. Chem. Lett.* **2014**, *5*, 2516-2521.
(157) Sawyer, D. T.; Valentine, J. S. How super is superoxide? *Acc. Chem. Res.* **2002**, *14*, 393-400.
(158) Hang Chin, D.; Chiericato, G.; J. Nanni, E.; T. Sawyer, D. Proton-induced disproportionation of superoxide ion in aprotic media. *J. Am. Chem. Soc.* **1982**, *104*, 1296–1299.
(159) Che, Y.; Tsushima, M.; Matsumoto, F.; Okajima, T.; Tokuda, K.; Ohsaka, T. Water-induced disproportionation of superoxide ion in aprotic solvents. *J. Phys. Chem.* **1996**, *100*, 20134-20137.
(160) Andrieux, C. P.; Hapiot, P.; Saveant, J. M. Mechanism of superoxide ion disproportionation in aprotic solvents. *J. Am. Chem. Soc.* **1987**, *109*, 3768-3775.
(161) Hayyan, M.; Hashim, M. A.; AlNashef, I. M. Superoxide ion: generation and chemical implications. *Chem. Rev.* **2016**, *116*, 3029-3085.
(162) Harding, J. R.; Amanchukwu, C. V.; Hammond, P. T.; Shao-Horn, Y. Instability of poly(ethylene oxide) upon oxidation in lithium-air batteries. *J. Phys. Chem. C.* **2015**, *119*, 6947-6955.
(163) Bryantsev, V. S.; Uddin, J.; Giordani, V.; Walker, W.; Addison, D.; Chase, G. V. The identification of stable solvents for nonaqueous rechargeable li-air batteries. *J. Electrochem. Soc.* **2013**, *160*, A160-A171.
(164) Freunberger, S. A.; Chen, Y.; Drewett, N. E.; Hardwick, L. J.; Barde, F.; Bruce, P. G. The lithium-oxygen battery with ether-based electrolytes. *Angew. Chem. Int. Ed.* **2011**, *50*, 8609-8613.
(165) Bryantsev, V. S.; Faglioni, F. Predicting autoxidation stability of ether- and amide-based electrolyte solvents for Li-air batteries. *J. Phys. Chem. A.* **2012**, *116*, 7128-7138.
(166) Nanni, E. J.; Angelis, C. T.; Dickson, J.; Sawyer, D. T. Oxygen activation by radical coupling between superoxide ion and reduced methyl viologen. *J. Am. Chem. Soc.* **1981**, *103*, 4268-4270.
(167) Yao, X.; Dong, Q.; Cheng, Q.; Wang, D. Why do lithium-oxygen batteries fail: parasitic chemical reactions and their synergistic effect. *Angew. Chem. Int. Ed.* **2016**, *55*, 11344-11353.
(168) Sharon, D.; Hirsberg, D.; Afri, M.; Gorsuch, A.; Frimer, A. A.; Aurbach, D. Reactivity of amide based solutions in lithium-oxygen cells. *J. Phys. Chem. C.* **2014**, *118*, 15207-15213.
(169) Sharon, D.; Etacheri, V.; Garsuch, A.; Afri, M.; Frimer, A. A.; Aurbach, D. On the challenge of electrolyte solutions for Li-air batteries: Monitoring oxygen reduction and related reactions in polyether solutions by spectroscopy and eqcm. *J. Phys. Chem. Lett.* **2013**, *4*, 127-131.

(170) Aurbach, D.; McCloskey, B. D.; Nazar, L. F.; Bruce, P. G. Advances in understanding mechanisms underpinning lithium-air batteries. *Nat. Energy.* **2016**, *1*, 16128.
(171) Luntz, A. C.; McCloskey, B. D. Li–air batteries: importance of singlet oxygen. *Nat. Energy.* **2017**, *2*, 17056.
(172) Bryantsev, V. S.; Giordani, V.; Walker, W.; Blanco, M.; Zecevic, S.; Sasaki, K.; Uddin, J.; Addison, D.; Chase, G. V. Predicting solvent stability in aprotic electrolyte li-air batteries: nucleophilic substitution by the superoxide anion radical O_2•$^-$. *J. Phys. Chem. A.* **2011**, *115*, 12399-12409.
(173) Bryantsev, V. S.; Blanco, M. Computational study of the mechanisms of superoxide-induced decomposition of organic carbonate-based electrolytes. *J. Phys. Chem. Lett.* **2011**, *2*, 379-383.
(174) Kumar, N.; Radin, M. D.; Wood, B. C.; Ogitsu, T.; Siegel, D. J. Surface-mediated solvent decomposition in Li-air batteries: Impact of peroxide and superoxide surface terminations. *J. Phys. Chem. C.* **2015**, *119*, 9050-9060.
(175) Khetan, A.; Pitsch, H.; Viswanathan, V. Solvent degradation in nonaqueous Li-O_2 batteries: oxidative stability versus h-abstraction. *J. Phys. Chem. Lett.* **2014**, *5*, 2419-2424.
(176) Chau, V. K. C.; Chen, Z.; Hu, H.; Chan, K.-Y. Exploring solvent stability against nucleophilic attack by solvated LiO_2 in an aprotic Li-O_2 battery. *J. Electrochem. Soc.* **2017**, *163*, A284-A289.
(177) Feng, S.; Chen, M.; Giordano, L.; Huang, M.; Zhang, W.; Amanchukwu, C. V.; Anandakathir, R.; Shao-Horn, Y.; Johnson, J. A. Mapping a stable solvent structure landscape for aprotic Li-air battery organic electrolytes. *J. Mater. Chem. A.* **2017**, *5*, 23987-23998.
(178) Schafzahl, L.; Mahne, N.; Schafzahl, B.; Wilkening, M.; Slugovc, C.; Borisov, S. M.; Freunberger, S. A. Singlet oxygen during cycling of the aprotic sodium-O_2 battery. *Angew. Chem. Int. Ed.* **2017**, *56*, 15728-15732.
(179) Mahne, N.; Renfrew, S. E.; McCloskey, B. D.; Freunberger, S. A. Electrochemical oxidation of lithium carbonate generates singlet oxygen. *Angew. Chem. Int. Ed.* **2018**, *57*, 5529-5533.
(180) Ogilby, P. R. Singlet oxygen: there is indeed something new under the sun. *Chem. Soc. Rev.* **2010**, *39*, 3181-3209.
(181) McCloskey, B. D.; Scheffler, R.; Speidel, A.; Bethune, D. S.; Shelby, R. M.; Luntz, A. C. On the efficacy of electrocatalysis in nonaqueous Li-O_2 batteries. *J. Am. Chem. Soc.* **2011**, *133*, 18038-18041.
(182) Xu, W.; Xu, K.; Viswanathan, V. V.; Towne, S. A.; Hardy, J. S.; Xiao, J.; Hu, D.; Wang, D.; Zhang, J.-G. Reaction mechanisms for the limited reversibility of Li-O_2 chemistry in organic carbonate electrolytes. *J. Power Sources.* **2011**, *196*, 9631-9639.
(183) Xu, D.; Wang, Z.-l.; Xu, J.-j.; Zhang, L.-l.; Wang, L.-m.; Zhang, X.-b. A stable sulfone based electrolyte for high performance rechargeable Li-O_2 batteries. *Chem. Commun.* **2012**, *48*, 11674-11676.
(184) Barde, F.; Chen, Y.; Johnson, L.; Schaltin, S.; Fransaer, J.; Bruce, P. G. Sulfone-based electrolytes for nonaqueous Li-O_2 batteries. *J. Phys. Chem. C.* **2014**, *118*, 18892-18898.
(185) Liang, C.; Wang, F.; Xu, Y.; Chen, J.; Liu, D.; Luo, Z. A stable electrolyte makes a nonaqueous Li-O_2 battery truly rechargeable. *New J. Chem.* **2013**, *37*, 2568-2572.
(186) Jung, H.-G.; Hassoun, J.; Park, J.-B.; Sun, Y.-K.; Scrosati, B. An improved high-performance lithium-air battery. *Nat. Chem.* **2012**, *4*, 579-585.
(187) Assary, R. S.; Lau, K. C.; Amine, K.; Sun, Y.-K.; Curtiss, L. A. Interactions of dimethoxy ethane with Li_2O_2 clusters and likely decomposition mechanisms for Li-O_2 batteries. *J. Phys. Chem. C.* **2013**, *117*, 8041-8049.
(188) Garcia, J. M.; Horn, H. W.; Rice, J. E. Dominant decomposition pathways for ethereal solvents in Li-O_2 batteries. *J. Phys. Chem. Lett.* **2015**, *6*, 1795-1799.
(189) Camacho-Forero, L. E.; Balbuena, P. B. Elucidating electrolyte decomposition under electron-rich environments at the lithium-metal anode. *Phys. Chem. Chem. Phys.* **2017**, *19*, 30861-30873.
(190) Carboni, M.; Marrani, A. G.; Spezia, R.; Brutti, S. Degradation of LiTfO/TEGDME and LiTfO/DME electrolytes in Li-O_2 batteries. *J. Electrochem. Soc.* **2018**, *165*, A118-A125.

(191) Huang, Z.; Zeng, H.; Xie, M.; Lin, X.; Huang, Z.; Shen, Y.; Huang, Y. A stable lithium-oxygen battery electrolyte based on fully methylated cyclic ether. *Angew. Chem. Int. Ed.* **2019**, *58*, 2345-2349.

(192) Bryantsev, V. S.; Giordani, V.; Walker, W.; Uddin, J.; Lee, I.; van Duin, A. C. T.; Chase, G. V.; Addison, D. Investigation of fluorinated amides for solid-electrolyte interphase stabilization in Li-O_2 batteries using amide-based electrolytes. *J. Phys. Chem. C.* **2013**, *117*, 11977-11988.

(193) Sharon, D.; Hirsberg, D.; Afri, M.; Chesneau, F.; Lavi, R.; Frimer, A. A.; Sun, Y.-K.; Aurbach, D. Catalytic behavior of lithium nitrate in Li-O_2 cells. *ACS Appl. Mater. Interfaces.* **2015**, *7*, 16590-16600.

(194) Giordani, V.; Bryantsev, V. S.; Uddin, J.; Walker, W.; Chase, G. V.; Addison, D. N-methylacetamide as an electrolyte solvent for rechargeable Li-O_2 batteries: unexpected stability at the O_2 electrode. *ECS Electrochem. Lett.* **2014**, *3*, A11-A14.

(195) Allen, C. J.; Mukerjee, S.; Plichta, E. J.; Hendrickson, M. A.; Abraham, K. M. Oxygen electrode rechargeability in an ionic liquid for the Li-air battery. *J. Phys. Chem. Lett.* **2011**, *2*, 2420-2424.

(196) Allen, C. J.; Hwang, J.; Kautz, R.; Mukerjee, S.; Plichta, E. J.; Hendrickson, M. A.; Abraham, K. M. Oxygen reduction reactions in ionic liquids and the formulation of a general orr mechanism for Li-air batteries. *J. Phys. Chem. C.* **2012**, *116*, 20755-20764.

(197) Meini, S.; Solchenbach, S.; Piana, M.; Gasteiger, H. A. The role of electrolyte solvent stability and electrolyte impurities in the electrooxidation of Li_2O_2 in Li-O_2 batteries. *J. Electrochem. Soc.* **2014**, *161*, A1306-A1314.

(198) Schwenke, K. U.; Herranz, J.; Gasteiger, H. A.; Piana, M. Reactivity of the ionic liquid Pyr_{14}TFSI with superoxide radicals generated from KO_2 or by contact of O_2 with $Li_7Ti_5O_{12}$. *J. Electrochem. Soc.* **2015**, *162*, A905-A914.

(199) Xie, J.; Dong, Q.; Madden, I.; Yao, X.; Cheng, Q.; Dornath, P.; Fan, W.; Wang, D. Achieving low overpotential Li-O_2 battery operations by Li_2O_2 decomposition through one-electron processes. *Nano Lett.* **2015**, *15*, 8371-8376.

(200) Mozhzhukhina, N.; Tesio, A. Y.; Mendez De Leo, L. P.; Calvo, E. J. In situ infrared spectroscopy study of pyr14tfsi ionic liquid stability for Li-O_2 battery. *J. Electrochem. Soc.* **2017**, *164*, A518-A523.

(201) Zhang, T.; Wen, Z.-Y. A high-rate ionic liquid lithium-O_2 battery with lioh product. *J. Phys. Chem. C.* **2017**, *121*, 5968-5973.

(202) Das, S.; Hojberg, J.; Knudsen, K. B.; Younesi, R.; Johansson, P.; Norby, P.; Vegge, T. Instability of ionic liquid-based electrolytes in Li-O_2 batteries. *J. Phys. Chem. C.* **2015**, *119*, 18084-18090.

(203) Thotiyl, M. M. O.; Freunberger, S. A.; Peng, Z.; Chen, Y.; Liu, Z.; Bruce, P. G. A stable cathode for the aprotic Li-O_2 battery. *Nat. Mater.* **2013**, *12*, 1049-1055.

(204) Peng, Z.; Freunberger, S. A.; Chen, Y.; Bruce, P. G. A reversible and higher-rate Li-O_2 battery. *Science*. **2012**, *337*, 563-566.

(205) Luntz, A. C.; McCloskey, B. D. Nonaqueous Li-air batteries: A status report. *Chem. Rev.* **2014**, *114*, 11721-11750.

(206) Kundu, D.; Black, R.; Adams, B.; Nazar, L. F. A highly active low voltage redox mediator for enhanced rechargeability of lithium-oxygen batteries. *ACS Cent. Sci.* **2015**, *1*, 510-515.

(207) Adams, B. D.; Black, R.; Radtke, C.; Williams, Z.; Mehdi, B. L.; Browning, N. D.; Nazar, L. F. The importance of nanometric passivating films on cathodes for Li-air batteries. *ACS Nano*. **2014**, *8*, 12483-12493.

(208) Frith, J. T.; Russell, A. E.; Garcia-Araez, N.; Owen, J. R. An in-situ raman study of the oxygen reduction reaction in ionic liquids. *Electrochem. Commun.* **2014**, *46*, 33-35.

(209) Olivares-Marín, M.; Sorrentino, A.; Pereiro, E.; Tonti, D. Discharge products of ionic liquid-based Li-O_2 batteries observed by energy dependent soft x-ray transmission microscopy. *J. Power Sources.* **2017**, *359*, 234-241.

(210) Ulissi, U.; Elia, G. A.; Jeong, S.; Mueller, F.; Reiter, J.; Tsiouvaras, N.; Sun, Y.-K.; Scrosati, B.; Passerini, S.; Hassoun, J. Low-polarization lithium–oxygen battery using [DEME][TFSI] ionic liquid electrolyte. *ChemSusChem*. **2018**, *11*, 229-236.

(211) Herranz, J.; Garsuch, A.; Gasteiger, H. A. Using rotating ring disc electrode voltammetry to quantify the superoxide radical stability of aprotic Li-air battery electrolytes. *J. Phys. Chem. C.* **2012**, *116*, 19084-19094.
(212) Elia, G. A.; Hassoun, J.; Kwak, W. J.; Sun, Y. K.; Scrosati, B.; Mueller, F.; Bresser, D.; Passerini, S.; Oberhumer, P.; Tsiouvaras, N., *et al.* An advanced lithium-air battery exploiting an ionic liquid-based electrolyte. *Nano Lett.* **2014**, *14*, 6572-6577.
(213) Xu, W.; Hu, J.; Engelhard, M. H.; Towne, S. A.; Hardy, J. S.; Xiao, J.; Feng, J.; Hu, M. Y.; Zhang, J.; Ding, F., *et al.* The stability of organic solvents and carbon electrode in nonaqueous Li-O_2 batteries. *J. Power Sources.* **2012**, *215*, 240-247.
(214) Leskes, M.; Moore, A. J.; Goward, G. R.; Grey, C. P. Monitoring the electrochemical processes in the lithium-air battery by solid-state NMR spectroscopy. *J. Phys. Chem. C.* **2013**, *117*, 26929-26939.
(215) Itkis, D. M.; Semenenko, D. A.; Kataev, E. Y.; Belova, A. I.; Neudachina, V. S.; Sirotina, A. P.; Haevecker, M.; Teschner, D.; Knop-Gericke, A.; Dudin, P., *et al.* Reactivity of carbon in lithium-oxygen battery positive electrodes. *Nano Lett.* **2013**, *13*, 4697-4701.
(216) Bae, Y.; Yun, Y. S.; Lim, H.-D.; Lee, H.; Kim, Y.-J.; Kim, J.; Park, H.; Ko, Y.; Lee, S.; Kwon, H. J., *et al.* Tuning the carbon crystallinity for highly stable Li-O_2 batteries. *Chem. Mater.* **2016**, *28*, 8160-8169.
(217) Belova, A. I.; Kwabi, D. G.; Yashina, L. V.; Shao-Horn, Y.; Itkis, D. M. Mechanism of oxygen reduction in aprotic Li–air batteries: the role of carbon electrode surface structure. *J. Phys. Chem. C.* **2017**, *121*, 1569-1577.
(218) Zhou, W.; Li, J.; Nie, H.; Zhang, Y.; Xi, X.; Zhang, H. Carbon electrode for nonaqueous Li-O_2 battery: the influence of surface oxygen species. *Electrochim. Acta.* **2014**, *138*, 410-416.
(219) Chang, Z.-w.; Xu, J.-j.; Liu, Q.-c.; Li, L.; Zhang, X.-b. Recent progress on stability enhancement for cathode in rechargeable non-aqueous lithium-oxygen battery. *Adv. Energy Mater.* **2015**, *5*, 1500633.
(220) Asadi, M.; Sayahpour, B.; Abbasi, P.; Ngo, A. T.; Karis, K.; Jokisaari, J. R.; Liu, C.; Narayanan, B.; Gerard, M.; Yasaei, P., *et al.* A lithium-oxygen battery with a long cycle life in an air-like atmosphere. *Nature*. **2018**, *555*, 502-506.
(221) Wang, L.; Pan, J.; Zhang, Y.; Cheng, X.; Liu, L.; Peng, H. A Li-air battery with ultralong cycle life in ambient air. *Adv. Mater.* **2018**, *30*, 1704378.
(222) Zhang, J.-G.; Wang, D.; Xu, W.; Xiao, J.; Williford, R. E. Ambient operation of Li/air batteries. *J. Power Sources.* **2010**, *195*, 4332-4337.
(223) Ma, J.-L.; Bao, D.; Shi, M.-M.; Yan, J.-M.; Zhang, X.-B. Reversible nitrogen fixation based on a rechargeable lithium-nitrogen battery for energy storage. *Chem.* **2017**, *2*, 525-532.
(224) O'Hare, P. A. G.; Johnson, G. K. Lithium nitride (Li_3N): Standard enthalpy of formation by solution calorimetry. *J. Chem. Thermodyn.* **1975**, *7*, 13-20.
(225) Kimura, H.; Asano, M.; Kubo, K. Vaporization of solid lithium nitride. *J. Nucl. Mater.* **1980**, *91*, 200-204.
(226) Roberts, J.; S. Calderwood, T.; T. Sawyer, D. Nucleophilic oxygenation of carbon dioxide by superoxide ion in aprotic media to form the peroxydicarbonate^{2-} ion species. *J. Am. Chem. Soc.* **1984**, *106*, 4667–4670.
(227) Lim, H.-K.; Lim, H.-D.; Park, K.-Y.; Seo, D.-H.; Gwon, H.; Hong, J.; Goddard, W. A., III; Kim, H.; Kang, K. Toward a lithium-"air" battery: The effect of CO_2 on the chemistry of a lithium-oxygen cell. *J. Am. Chem. Soc.* **2013**, *135*, 9733-9742.
(228) Liu, Y.; Wang, R.; Lyu, Y.; Li, H.; Chen, L. Rechargeable Li/CO_2-O_2 (2:1) battery and Li/CO_2 battery. *Energy Environ. Sci.* **2014**, *7*, 677-681.
(229) Yang, S.; He, P.; Zhou, H. Exploring the electrochemical reaction mechanism of carbonate oxidation in Li-air/CO_2 battery through tracing missing oxygen. *Energy Environ. Sci.* **2016**, *9*, 1650-1654.
(230) Yin, W.; Grimaud, A.; Lepoivre, F.; Yang, C.; Tarascon, J. M. Chemical vs electrochemical formation of li2co3 as a discharge product in Li-O_2/CO_2 batteries by controlling the superoxide intermediate. *J. Phys. Chem. Lett.* **2017**, *8*, 214-222.
(231) Qiao, Y.; Yi, J.; Guo, S.; Sun, Y.; Wu, S.; Liu, X.; Yang, S.; He, P.; Zhou, H. Li_2CO_3-free Li-O_2/CO_2 battery with peroxide discharge product. *Energy Environ. Sci.* **2018**, *11*, 1211-1217.

(232) Zhang, S.; Nava, M. J.; Chow, G. K.; Lopez, N.; Wu, G.; Britt, D. R.; Nocera, D. G.; Cummins, C. C. On the incompatibility of lithium-O_2 battery technology with CO_2. *Chem. Sci.* **2017**, *8*, 6117-6122.

(233) Zhao, Z.; Su, Y.; Peng, Z. Probing lithium carbonate formation in trace-O_2-assisted aprotic Li-CO_2 batteries using in situ surface-enhanced Raman spectroscopy. *J. Phys. Chem. Lett.* **2019**, *10*, 322-328.

(234) Zhang, Z.; Zhang, Q.; Chen, Y.; Bao, J.; Zhou, X.; Xie, Z.; Wei, J.; Zhou, Z. The first introduction of graphene to rechargeable Li-CO_2 batteries. *Angew. Chem. Int. Ed.* **2015**, *54*, 6550-6553.

(235) Yang, S.; Qiao, Y.; He, P.; Liu, Y.; Cheng, Z.; Zhu, J.-J.; Zhou, H. A reversible lithium-CO_2 battery with Ru nanoparticles as a cathode catalyst. *Energy Environ. Sci.* **2017**, *10*, 972-978.

(236) Yu, Q.; Jin, Y.; Shichao, W.; Yang, L.; Sixie, Y.; Ping, H.; Haoshen, Z. Li-CO_2 electrochemistry: A new strategy for CO_2 fixation and energy storage. *Joule*. **2017**, *1*, 359-370.

(237) Kwabi, D. G.; Batcho, T. P.; Feng, S.; Giordano, L.; Thompson, C. V.; Shao-Horn, Y. The effect of water on discharge product growth and chemistry in Li-O_2 batteries. *Phys. Chem. Chem. Phys.* **2016**, *18*, 24944-24953.

(238) Staszak-Jirkovsky, J.; Subbaraman, R.; Strmcnik, D.; Harrison, K. L.; Diesendruck, C. E.; Assary, R.; Frank, O.; Kobr, L.; Wiberg, G. K. H.; Genorio, B., *et al.* Water as a promoter and catalyst for dioxygen electrochemistry in aqueous and organic media. *ACS Catal.* **2015**, *5*, 6600-6607.

(239) Qiao, Y.; Wu, S.; Yi, J.; Sun, Y.; Guo, S.; Yang, S.; He, P.; Zhou, H. From O_2^- to HO_2^-: reducing by-products and overpotential in Li-O_2 batteries by water addition. *Angew. Chem. Int. Ed.* **2017**, *56*, 4960-4964.

(240) Dong, Q.; Yao, X.; Zhao, Y.; Qi, M.; Zhang, X.; Sun, H.; He, Y.; Wang, D. Cathodically stable Li-O_2 battery operations using water-in-salt electrolyte. *Chem*. **2018**, *4*, 1345-1358.

(241) *Handbook of Electrochemistry*. C.G. Zoski, eds., Elsevier, Amsterdam, 2007.

(242) Meini, S.; Tsiouvaras, N.; Schwenke, K. U.; Piana, M.; Beyer, H.; Lange, L.; Gasteiger, H. A. Rechargeability of li-air cathodes pre-filled with discharge products using an ether-based electrolyte solution: implications for cycle-life of Li-air cells. *Phys. Chem. Chem. Phys.* **2013**, *15*, 11478-11493.

(243) Guo, Z.; Dong, X.; Yuan, S.; Wang, Y.; Xia, Y. Humidity effect on electrochemical performance of Li-O_2 batteries. *J. Power Sources.* **2014**, *264*, 1-7.

(244) Xu, W.; Wang, J.; Ding, F.; Chen, X.; Nasybutin, E.; Zhang, Y.; Zhang, J.-G. Lithium metal anodes for rechargeable batteries. *Energy Environ. Sci.* **2014**, *7*, 513-537.

(245) Tan, P.; Shyy, W.; Zhao, T. S.; Zhang, R. H.; Zhu, X. B. Effects of moist air on the cycling performance of non-aqueous lithium-air batteries. *Appl. Energy.* **2016**, *182*, 569-575.

(246) Bai, P.; Li, J.; Brushett, F. R.; Bazant, M. Z. Transition of lithium growth mechanisms in liquid electrolytes. *Energy Environ. Sci.* **2016**, *9*, 3221-3229.

(247) Fang, C.; Li, J.; Zhang, M.; Zhang, Y.; Yang, F.; Lee, J. Z.; Lee, M.-H.; Alvarado, J.; Schroeder, M. A.; Yang, Y., *et al.* Quantifying inactive lithium in lithium metal batteries. *Nature*. **2019**, *572*, 511-515.

(248) Fang, C.; Wang, X.; Meng, Y. S. Key issues hindering a practical lithium-metal anode. *Trends Chem.* **2019**, *1*, 152-158.

(249) Steiger, J.; Kramer, D.; Mönig, R. Microscopic observations of the formation, growth and shrinkage of lithium moss during electrodeposition and dissolution. *Electrochim. Acta*. **2014**, *136*, 529-536.

(250) Sand, H. J. On the concentration at the electrodes in a solution, with special reference to the liberation of hydrogen by electrolysis of a mixture of copper sulphate and sulphuric acid. *Philos. Mag.* **1901**, *1*, 45-79.

(251) Chang, H. J.; Trease, N. M.; Ilott, A. J.; Zeng, D.; Du, L.-S.; Jerschow, A.; Grey, C. P. Investigating Li microstructure formation on Li anodes for lithium batteries by in situ ^{6}Li/^{7}Li NMR and SEM. *J. Phys. Chem. C.* **2015**, *119*, 16443-16451.

(252) Chang, H. J.; Ilott, A. J.; Trease, N. M.; Mohammadi, M.; Jerschow, A.; Grey, C. P. Correlating microstructural lithium metal growth with electrolyte salt depletion in lithium batteries using ^{7}Li mri. *J. Am. Chem. Soc.* **2015**, *137*, 15209-15216.
(253) Chang, H. J.; Ilott, A. J.; Trease, N. M.; Mohammadi, M.; Jerschow, A.; Grey, C. P. Correlating microstructural lithium metal growth with electrolyte salt depletion in lithium batteries using ^{7}Li mri. *J. Am. Chem. Soc.* **2015**, *137*, 15209-15216.
(254) Chen, K.-H.; Wood, K. N.; Kazyak, E.; LePage, W. S.; Davis, A. L.; Sanchez, A. J.; Dasgupta, N. P. Dead lithium: mass transport effects on voltage, capacity, and failure of lithium metal anodes. *J. Mater. Chem. A.* **2017**, *5*, 11671-11681.
(255) Zeng, Z.; Murugesan, V.; Han, K. S.; Jiang, X.; Cao, Y.; Xiao, L.; Ai, X.; Yang, H.; Zhang, J.-G.; Sushko, M. L. Non-flammable electrolytes with high salt-to-solvent ratios for Li-ion and Li-metal batteries. *Nat. Energy.* **2018**, *3*, 674.
(256) Ren, X.; Chen, S.; Lee, H.; Mei, D.; Engelhard, M. H.; Burton, S. D.; Zhao, W.; Zheng, J.; Li, Q.; Ding, M. S. Localized high-concentration sulfone electrolytes for high-efficiency lithium-metal batteries. *Chem*. **2018**, *4*, 1877-1892.
(257) Fan, X.; Chen, L.; Ji, X.; Deng, T.; Hou, S.; Chen, J.; Zheng, J.; Wang, F.; Jiang, J.; Xu, K. Highly fluorinated interphases enable high-voltage Li-metal batteries. *Chem*. **2018**, *4*, 174-185.
(258) Chen, S.; Zheng, J.; Mei, D.; Han, K. S.; Engelhard, M. H.; Zhao, W.; Xu, W.; Liu, J.; Zhang, J. G. High- voltage lithium- metal batteries enabled by localized high- concentration electrolytes. *Adv. Mater*. **2018**, *30*, 1706102.
(259) Wang, J.; Yamada, Y.; Sodeyama, K.; Watanabe, E.; Takada, K.; Tateyama, Y.; Yamada, A. Fire-extinguishing organic electrolytes for safe batteries. *Nat. Energy.* **2018**, *3*, 22.
(260) Qian, J.; Henderson, W. A.; Xu, W.; Bhattacharya, P.; Engelhard, M.; Borodin, O.; Zhang, J.-G. High rate and stable cycling of lithium metal anode. *Nat. Commun.* **2015**, *6*, 6362.
(261) Wang, J.; Yamada, Y.; Sodeyama, K.; Chiang, C. H.; Tateyama, Y.; Yamada, A. Superconcentrated electrolytes for a high-voltage lithium-ion battery. *Nat. Commun.* **2016**, *7*, 12032.
(262) Neudecker, B.; Dudney, N.; Bates, J. "Lithium- free" thin- film battery with in situ plated Li anode. *J. Electrochem. Soc.* **2000**, *147*, 517-523.
(263) Albertus, P.; Babinec, S.; Litzelman, S.; Newman, A. Status and challenges in enabling the lithium metal electrode for high-energy and low-cost rechargeable batteries. *Nat. Energy.* **2018**, *3*, 16-21.
(264) Liu, J.; Bao, Z.; Cui, Y.; Dufek, E. J.; Goodenough, J. B.; Khalifah, P.; Li, Q.; Liaw, B. Y.; Liu, P.; Manthiram, A., *et al.* Pathways for practical high-energy long-cycling lithium metal batteries. *Nat. Energy.* **2019**, *4*, 180-186.
(265) Lin, D.; Liu, Y.; Cui, Y. Reviving the lithium metal anode for high-energy batteries. *Nat. Nanotechnol.* **2017**, *12*, 194.
(266) Cheng, X.-B.; Zhang, R.; Zhao, C.-Z.; Zhang, Q. Toward safe lithium metal anode in rechargeable batteries: a review. *Chem. Rev.* **2017**, *117*, 10403-10473.
(267) Lee, H.; Lee, D. J.; Lee, J.-N.; Song, J.; Lee, Y.; Ryou, M.-H.; Park, J.-K.; Lee, Y. M. Chemical aspect of oxygen dissolved in a dimethyl sulfoxide-based electrolyte on lithium metal. *Electrochim. Acta.* **2014**, *123*, 419-425.
(268) Roberts, M.; Younesi, R.; Richardson, W.; Liu, J.; Gustafsson, T.; Zhu, J.; Edstrom, K. Increased cycling efficiency of lithium anodes in dimethyl sulfoxide electrolytes for use in Li-O_2 batteries. *ECS Electrochem. Lett.* **2014**, *3*, A62-A65.
(269) Osaka, T.; Momma, T.; Tajima, T.; Matsumoto, Y. Enhancement of lithium anode cyclability in propylene carbonate electrolyte by CO_2 addition and its protective effect against H_2O impurity. *J. Electrochem. Soc.* **1995**, *142*, 1057-1060.
(270) Osaka, T.; Momma, T.; Matsumoto, Y.; Uchida, Y. Surface characterization of electrodeposited lithium anode with enhanced cycleability obtained by CO_2 addition. *J. Electrochem. Soc.* **1997**, *144*, 1709-1713.
(271) Momma, T.; Nara, H.; Yamagami, S.; Tatsumi, C.; Osaka, T. Effect of the atmosphere on chemical composition and electrochemical properties of solid electrolyte interface on electrodeposited Li metal. *J. Power Sources.* **2011**, *196*, 6483-6487.

(272) Cho, M. H.; Trottier, J.; Gagnon, C.; Hovington, P.; Clément, D.; Vijh, A.; Kim, C. S.; Guerfi, A.; Black, R.; Nazar, L., *et al.* The effects of moisture contamination in the Li-O_2 battery. *J. Power Sources.* **2014**, *268*, 565-574.
(273) Huang, S.; Cui, Z.; Zhao, N.; Sun, J.; Guo, X. Influence of ambient air on cell reactions of Li-air batteries. *Electrochim. Acta.* **2016**, *191*, 473-478.
(274) Wong, R. A.; Yang, C.; Dutta, A.; Minho, O.; Hong, M.; Thomas, M. L.; Yamanaka, K.; Ohta, T.; Waki, K.; Byon, H. R. Critically examining the role of nanocatalysts in Li-O_2 batteries: Viability toward suppression of recharge overpotential, rechargeability, and cyclability. *ACS Energy Lett.* **2018**, *3*, 592-597.
(275) Nien-Chu, L.; Guangtao, C.; Zhuojian, L.; Yi-Chun, L. A highly active oxygen evolution catalyst for lithium-oxygen batteries enabled by high-surface-energy facets. *Joule*. **2018**, *2*, 1511-1521.
(276) Kundu, D.; Black, R.; Berg, E. J.; Nazar, L. F. A highly active nanostructured metallic oxide cathode for aprotic Li-O_2 batteries. *Energy Environ. Sci.* **2015**, *8*, 1292-1298.
(277) Lim, H.-D.; Song, H.; Kim, J.; Gwon, H.; Bae, Y.; Park, K.-Y.; Hong, J.; Kim, H.; Kim, T.; Kim, Y. H., *et al.* Superior rechargeability and efficiency of lithium-oxygen batteries: Hierarchical air electrode architecture combined with a soluble catalyst. *Angew. Chem. Int. Ed.* **2014**, *53*, 3926-3931.
(278) Bergner, B. J.; Schuermann, A.; Peppler, K.; Garsuch, A.; Janek, J. Tempo: A mobile catalyst for rechargeable Li-O_2 batteries. *J. Am. Chem. Soc.* **2014**, *136*, 15054-15064.
(279) Yu, Q.; Yang, L.; Kezhu, J.; Xiang, L.; Yibo, H.; Qi, L.; Shichao, W.; Haoshen, Z. Boosting the cycle life of aprotic Li-O_2 batteries via a photo-assisted hybrid Li_2O_2-scavenging strategy. *Small Methods*. **2018**, *2*, 1700284.
(280) Liu, Y.; Li, N.; Liao, K.; Li, Q.; Ishida, M.; Zhou, H. Lowering the charge voltage of Li-O_2 batteries via an unmediated photoelectrochemical oxidation approach. *J. Mater. Chem. A.* **2016**, *4*, 12411-12415.
(281) Liu, Y.; Li, N.; Wu, S.; Liao, K.; Zhu, K.; Yi, J.; Zhou, H. Reducing the charging voltage of a Li-O_2 battery to 1.9 v by incorporating a photocatalyst. *Energy Environ. Sci.* **2015**, *8*, 2664-2667.
(282) Gratzel, M. Photoelectrochemical cells. *Nature*. **2001**, *414*, 338-344.
(283) Yu, M.; Ren, X.; Ma, L.; Wu, Y. Integrating a redox-coupled dye-sensitized photoelectrode into a lithium-oxygen battery for photoassisted charging. *Nat. Commun.* **2014**, *5*, 5111.
(284) Petit, Y. K.; Leypold, C.; Mahne, N.; Mourad, E.; Schafzahl, L.; Slugovc, C.; Borisov, S. M.; Freunberger, S. A. Dabconium: an efficient and high-voltage stable singlet oxygen quencher for metal-O_2 cells. *Angew. Chem. Int. Ed.* **2019**, *58*, 6535-6539.
(285) Visco, S. J.; Katz, B. D.; Nimon, Y. S.; De Jonghe, L. C. Protected active metal electrode and battery cell structures with non-aqueous interlayer architecture. U.S. Patent 7,282,295, October 16, 2007.
(286) Lee, D. J.; Lee, H.; Song, J.; Ryou, M.-H.; Lee, Y. M.; Kim, H.-T.; Park, J.-K. Composite protective layer for Li metal anode in high-performance lithium-oxygen batteries. *Electrochem. Commun.* **2014**, *40*, 45-48.
(287) Lee, D. J.; Lee, H.; Kim, Y.-J.; Park, J.-K.; Kim, H.-T. Sustainable redox mediation for lithium-oxygen batteries by a composite protective layer on the lithium-metal anode. *Adv. Mater*. **2016**, *28*, 857-863.
(288) Kwak, W.-J.; Jung, H.-G.; Aurbach, D.; Sun, Y.-K. Optimized bicompartment two solution cells for effective and stable operation of Li-O_2 batteries. *Adv. Energy Mater*. **2017**, *7*, 1701232.
(289) Kim, B. G.; Kim, J.-S.; Min, J.; Lee, Y.-H.; Choi, J. H.; Jang, M. C.; Freunberger, S. A.; Choi, J. W. A moisture-and oxygen-impermeable separator for aprotic Li-O_2 batteries. *Adv. Funct. Mater*. **2016**, *26*, 1747-1756.
(290) Amici, J.; Alidoost, M.; Francia, C.; Bodoardo, S.; Martinez Crespiera, S.; Amantia, D.; Biasizzo, M.; Caldera, F.; Trotta, F. O_2 selective membranes based on a dextrin-nanosponge (ns) in a PVDF-HFP polymer matrix for Li–air cells. *Chem. Commun.* **2016**, *52*, 13683-13686.

(291) Cao, L.; Lv, F.; Liu, Y.; Wang, W.; Huo, Y.; Fu, X.; Sun, R.; Lu, Z. A high performance O_2 selective membrane based on CAU-1-NH_2@polydopamine and the PMMA polymer for Li–air batteries. *Chem. Commun.* **2015**, *51*, 4364-4367.
(292) Ruan, Y.; Sun, J.; Song, S.; Yu, L.; Chen, B.; Li, W.; Qin, X. A perfluorocarbon–silicone oil oxygen–selective membrane for ambient operation of aprotic Li–air batteries. *Electrochem. Commun.* **2018**, *96*, 93-97.
(293) Xie, M.; Huang, Z.; Lin, X.; Li, Y.; Huang, Z.; Yuan, L.; Shen, Y.; Huang, Y. Oxygen selective membrane based on perfluoropolyether for Li-air battery with long cycle life. *Energy Storage Mater.* **2019**, *20*, 307-314.
(294) Xin, X.; Ito, K.; Kubo, Y. Electrochemical behavior of ru nanoparticles as catalysts in aprotic Li-O_2 batteries. *Electrochim. Acta.* **2018**, *261*, 323-329.
(295) Ma, S.; Wu, Y.; Wang, J.; Zhang, Y.; Zhang, Y.; Yan, X.; Wei, Y.; Liu, P.; Wang, J.; Jiang, K., *et al.* Reversibility of noble metal-catalyzed aprotic Li-O_2 batteries. *Nano Lett.* **2015**, *15*, 8084-8090.
(296) Kundu, D.; Black, R.; Adams, B.; Harrison, K.; Zavadil, K.; Nazar, L. F. Nanostructured metal carbides for aprotic Li-O_2 batteries: New insights into interfacial reactions and cathode stability. *J. Phys. Chem. Lett.* **2015**, *6*, 2252-2258.
(297) Liu, T.; Liu, Z.; Kim, G.; Frith, J. T.; Garcia-Araez, N.; Grey, C. P. Understanding LiOH chemistry in a ruthenium-catalyzed Li-O_2 battery. *Angew. Chem. Int. Ed.* **2017**, *56*, 16057-16062.
(298) Chang, Z.; Xu, J.; Zhang, X. Recent progress in electrocatalyst for Li-O_2 batteries. *Adv. Energy Mater.* **2017**, *7*, 1700875.
(299) Liu, B.; Sun, Y.; Liu, L.; Xu, S.; Yan, X. Advances in manganese-based oxides cathodic electrocatalysts for Li-air batteries. *Adv. Funct. Mater.* **2018**, *28*, 1704973.
(300) Black, R.; Lee, J.-H.; Adams, B.; Mims, C. A.; Nazar, L. F. The role of catalysts and peroxide oxidation in lithium-oxygen batteries. *Angew. Chem. Int. Ed.* **2013**, *52*, 392-396.
(301) Harding, J. R.; Lu, Y.-C.; Tsukada, Y.; Shao-Horn, Y. Evidence of catalyzed oxidation of Li_2O_2 for rechargeable Li-air battery applications. *Phys. Chem. Chem. Phys.* **2012**, *14*, 10540-10546.
(302) Schwenke, K. U.; Meini, S.; Wu, X.; Gasteiger, H. A.; Piana, M. Stability of superoxide radicals in glyme solvents for non-aqueous Li-O_2 battery electrolytes. *Phys. Chem. Chem. Phys.* **2013**, *15*, 11830-11839.
(303) Sun, B.; Munroe, P.; Wang, G. Ruthenium nanocrystals as cathode catalysts for lithium-oxygen batteries with a superior performance. *Sci. Rep.* **2013**, *3*, 2247.
(304) Li, F.; Chen, Y.; Tang, D.-M.; Jian, Z.; Liu, C.; Golberg, D.; Yamada, A.; Zhou, H. Performance-improved Li-O_2 battery with ru nanoparticles supported on binder-free multi-walled carbon nanotube paper as cathode. *Energy Environ. Sci.* **2014**, *7*, 1648-1652.
(305) Jung, H.-G.; Jeong, Y. S.; Park, J.-B.; Sun, Y.-K.; Scrosati, B.; Lee, Y. J. Ruthenium-based electrocatalysts supported on reduced graphene oxide for lithium-air batteries. *ACS Nano.* **2013**, *7*, 3532-3539.
(306) Sun, B.; Huang, X.; Chen, S.; Munroe, P.; Wang, G. Porous graphene nanoarchitectures: An efficient catalyst for low charge-overpotential, long life, and high capacity lithium-oxygen batteries. *Nano Lett.* **2014**, *14*, 3145-3152.
(307) Khetan, A.; Pitsch, H.; Viswanathan, V. Identifying descriptors for solvent stability in nonaqueous Li-O_2 batteries. *J. Phys. Chem. Lett.* **2014**, *5*, 1318-1323.
(308) Liu, Z.; Ma, L.; Guo, L.; Peng, Z. Promoting solution discharge of Li-O_2 batteries with immobilized redox mediators. *J. Phys. Chem. Lett.* **2018**, *9*, 5915-5920.
(309) Zhang, Y.; Wang, L.; Zhang, X.; Guo, L.; Wang, Y.; Peng, Z. High-capacity and high-rate discharging of a coenzyme Q_{10}-catalyzed Li-O_2 battery. *Adv. Mater.* **2018**, *30*, 1705571.
(310) Ko, Y.; Park, H.; Kim, J.; Lim, H.-D.; Lee, B.; Kwon, G.; Lee, S.; Bae, Y.; Park, S. K.; Kang, K. Biological redox mediation in electron transport chain of bacteria for oxygen reduction reaction catalysts in lithium-oxygen batteries. *Adv. Funct. Mater.* **2019**, *29*, 1805623.
(311) Zhang, P.; Liu, L.; He, X.; Liu, X.; Wang, H.; He, J.; Zhao, Y. Promoting surface-mediated oxygen reduction reaction of solid catalysts in metal-O_2 batteries by capturing superoxide species. *J. Am. Chem. Soc.* **2019**, *141*, 6263-6270.

(312) Zhu, Y. G.; Goh, F. W. T.; Yan, R.; Wu, S.; Adams, S.; Wang, Q. Synergistic oxygen reduction of dual redox catalysts boosting the power of lithium-air battery. *Phys. Chem. Chem. Phys.* **2018**, *20*, 27930-27936.
(313) Bard, A. J. F., L. R., *Electrochemical Methods : Fundamentals and Applications, 2nd edition*. 2001, John Wiley & Sons, Ltd: New York. pp 44-132.
(314) Homewood, T.; Frith, J. T.; Vivek, J. P.; Casan-Pastor, N.; Tonti, D.; Owen, J. R.; Garcia-Araez, N. Using polyoxometalates to enhance the capacity of lithium-oxygen batteries. *Chem. Commun.* **2018**, *54*, 9599-9602.
(315) Liang, Z.; Lu, Y.-C. Critical role of redox mediator in suppressing charging instabilities of lithium-oxygen batteries. *J. Am. Chem. Soc.* **2016**, *138*, 7574-7583.
(316) Liang, Z.; Zhou, Y.; Lu, Y.-C. Dynamic oxygen shield eliminates cathode degradation in lithium-oxygen batteries. *Energy Environ. Sci.* **2018**, *11*, 3500-3510.
(317) Bergner, B. J.; Hofmann, C.; Schuermann, A.; Schroeder, D.; Peppler, K.; Schreiner, P. R.; Janek, J. Understanding the fundamentals of redox mediators in Li-O_2 batteries: A case study on nitroxides. *Phys. Chem. Chem. Phys.* **2015**, *17*, 31769-31779.
(318) Chen, Y.; Gao, X.; Johnson, L. R.; Bruce, P. G. Kinetics of lithium peroxide oxidation by redox mediators and consequences for the lithium-oxygen cell. *Nat. Commun.* **2018**, *9*, 767.
(319) Yan, R.; Ghilane, J.; Phuah, K. C.; Pham Truong, T. N.; Adams, S.; Randriamahazaka, H.; Wang, Q. Determining Li^+-coupled redox targeting reaction kinetics of battery materials with scanning electrochemical microscopy. *J. Phys. Chem. Lett.* **2018**, *9*, 491-496.
(320) Ko, Y.; Park, H.; Lee, B.; Bae, Y.; Park, S. K.; Kang, K. A comparative kinetic study of redox mediators for high-power lithium-oxygen batteries. *J. Mater. Chem. A.* **2019**, *7*, 6491-6498.
(321) Tesio, A. Y.; Blasi, D.; Olivares-Marin, M.; Ratera, I.; Tonti, D.; Veciana, J. Organic radicals for the enhancement of oxygen reduction reaction in Li-O_2 batteries. *Chem. Commun.* **2015**, *51*, 17623-17626.
(322) Yang, H.; Wang, Q.; Zhang, R.; Trimm, B. D.; Whittingham, M. S. The electrochemical behaviour of TTF in Li-O_2 batteries using a tegdme-based electrolyte. *Chem. Commun.* **2016**, *52*, 7580-7583.
(323) Qiao, Y.; Ye, S. Spectroscopic investigation for oxygen reduction and evolution reactions with tetrathiafulvalene as a redox mediator in Li-O_2 battery. *J. Phys. Chem. C.* **2016**, *120*, 15830-15845.
(324) Yao, K. P. C.; Frith, J. T.; Sayed, S. Y.; Barde, F.; Owen, J. R.; Shao-Horn, Y.; Garcia-Araez, N. Utilization of cobalt bis(terpyridine) metal complex as soluble redox mediator in Li-O_2 batteries. *J. Phys. Chem. C.* **2016**, *120*, 16290-16297.
(325) Zhang, J.; Sun, B.; Zhao, Y.; Kretschmer, K.; Wang, G. Modified tetrathiafulvalene as an organic conductor for improving performances of Li-O_2 batteries. *Angew. Chem. Int. Ed.* **2017**, *56*, 8505-8509.
(326) Ha, S.; Kim, Y.; Koo, D.; Ha, K.-H.; Park, Y.; Kim, D.-M.; Son, S.; Yim, T.; Lee, K. T. Investigation into the stability of Li metal anodes in Li-O_2 batteries with a redox mediator. *J. Mater. Chem. A.* **2017**, *5*, 10609-10621.
(327) Feng, N.; He, P.; Zhou, H. Enabling catalytic oxidation of Li_2O_2 at the liquid-solid interface: The evolution of an aprotic Li-O_2 battery. *ChemSusChem*. **2015**, *8*, 600-602.
(328) Feng, N.; Mu, X.; Zhang, X.; He, P.; Zhou, H. Intensive study on the catalytical behavior of n-methylphenothiazine as a soluble mediator to oxidize the Li_2O_2 cathode of the Li-O_2 battery. *ACS Appl. Mater. Interfaces.* **2017**, *9*, 3733-3739.
(329) Ryu, W.-H.; Gittleson, F. S.; Thomsen, J. M.; Li, J.; Schwab, M. J.; Brudvig, G. W.; Taylor, A. D. Heme biomolecule as redox mediator and oxygen shuttle for efficient charging of lithium-oxygen batteries. *Nat. Commun.* **2016**, *7*.
(330) Xu, C.; Xu, G.; Zhang, Y.; Fang, S.; Nie, P.; Wu, L.; Zhang, X. Bifunctional redox mediator supported by an anionic surfactant for long-cycle Li-O_2 batteries. *ACS Energy Lett.* **2017**, *2*, 2659-2666.
(331) Lee, J.-S.; Lee, C.; Lee, J.-Y.; Ryu, J.; Ryu, W.-H. Polyoxometalate as a nature-inspired bifunctional catalyst for lithium-oxygen batteries. *ACS Catal.* **2018**, *8*, 7213-7221.

(332) Zhu, Y. G.; Wang, X.; Jia, C.; Yang, J.; Wang, Q. Redox-mediated orr and oer reactions: Redox flow lithium oxygen batteries enabled with a pair of soluble redox catalysts. *ACS Catal.* **2016**, *6*, 6191-6197.
(333) Gao, X.; Chen, Y.; Johnson, L. R.; Jovanov, Z. P.; Bruce, P. G. A rechargeable lithium-oxygen battery with dual mediators stabilizing the carbon cathode. *Nat. Energy.* **2017**, *2*, 17118.
(334) Zhu, Y. G.; Jia, C.; Yang, J.; Pan, F.; Huang, Q.; Wang, Q. Dual redox catalysts for oxygen reduction and evolution reactions: Towards a redox flow Li-O_2 battery. *Chem. Commun.* **2015**, *51*, 9451-9454.
(335) Mizuno, F.; Nakanishi, S.; Kotani, Y.; Yokoishi, S.; Iba, H. Rechargeable li-air batteries with carbonate-based liquid electrolytes. *Electrochem.* **2010**, *78*, 403-405.
(336) Zhang, W.; Shen, Y.; Sun, D.; Huang, Z.; Zhou, J.; Yan, H.; Huang, Y. Promoting Li_2O_2 oxidation via solvent-assisted redox shuttle process for low overpotential Li-O_2 battery. *Nano Energy*. **2016**, *30*, 43-51.
(337) Kwak, W.-J.; Kim, H.; Petit, Y. K.; Leypold, C.; Trung Thien, N.; Mahne, N.; Redfern, P.; Curtiss, L. A.; Jung, H.-G.; Borisov, S. M., *et al.* Deactivation of redox mediators in lithium-oxygen batteries by singlet oxygen. *Nat. Commun.* **2019**, *10*, 1380.
(338) Lim, H.-D.; Lee, B.; Zheng, Y.; Hong, J.; Kim, J.; Gwon, H.; Ko, Y.; Lee, M.; Cho, K.; Kang, K. Rational design of redox mediators for advanced Li-O_2 batteries. *Nat. Energy.* **2016**, *1*, 16066.
(339) Aetukuri, N. B.; Kitajima, S.; Jung, E.; Thompson, L. E.; Virwani, K.; Reich, M.-L.; Kunze, M.; Schneider, M.; Schmidbauer, W.; Wilcke, W. W., *et al.* Flexible ion-conducting composite membranes for lithium batteries. *Adv. Energy Mater*. **2015**, *5*, 1500265.
(340) Bergner, B. J.; Busche, M. R.; Pinedo, R.; Berkes, B. B.; Schroeder, D.; Janek, J. How to improve capacity and cycling stability for next generation Li-O_2 batteries: Approach with a solid electrolyte and elevated redox mediator concentrations. *ACS Appl. Mater. Interfaces.* **2016**, *8*, 7756-7765.
(341) Meini, S.; Piana, M.; Beyer, H.; Schwaemmlein, J.; Gasteiger, H. A. Effect of carbon surface area on first discharge capacity of Li-O_2 cathodes and cycle-life behavior in ether-based electrolytes. *J. Electrochem. Soc.* **2012**, *159*, A2135-A2142.
(342) Liu, T.; Kim, G.; Jonsson, E.; Castillo-Martinez, E.; Temprano, I.; Shao, Y.; Carretero-Gonzalez, J.; Kerber, R. N.; Grey, C. P. Understanding LiOH formation in a Li-O_2 battery with LiI and H_2O additives. *ACS Catal.* **2019**, *9*, 66-77.
(343) T. Sawyer, D.; Chiericato, G.; T. Angelis, C.; J. Nanni, E.; Tsuchiya, T. Effects of media and electrode materials on the electrochemical reduction of dioxygen. *Anal. Chem.* **1982**, *54*, 1720–1724.
(344) Gutmann, V. Solvent effects on the reactivities of organometallic compounds. *Coord. Chem. Rev.* **1976**, *18*, 225-255.
(345) Chin, D. H.; Chiericato, G.; Nanni, E. J.; Sawyer, D. T. Proton-induced disproportionation of superoxide ion in aprotic media. *J. Am. Chem. Soc.* **1982**, *104*, 1296-1299.
(346) Zhu, Y. G.; Liu, Q.; Rong, Y.; Chen, H.; Yang, J.; Jia, C.; Yu, L.-J.; Karton, A.; Ren, Y.; Xu, X., *et al.* Proton enhanced dynamic battery chemistry for aprotic lithium-oxygen batteries. *Nat. Commun.* **2017**, *8*, 14308.
(347) Qiao, Y.; Wu, S.; Sun, Y.; Guo, S.; Yi, J.; He, P.; Zhou, H. Unraveling the complex role of iodide additives in Li-O_2 batteries. *ACS Energy Lett.* **2017**, *2*, 1869-1878.
(348) Yu, W.; Yang, W.; Liu, R.; Qin, L.; Lei, Y.; Liu, L.; Zhai, D.; Li, B.; Kang, F. A soluble phenolic mediator contributing to enhanced discharge capacity and low charge overpotential for lithium-oxygen batteries. *Electrochem. Commun.* **2017**, *79*, 68-72.
(349) Mayeda, E. A.; Bard, A. J. Production of singlet oxygen in electrogenerated radical ion electron transfer reactions. *J. Am. Chem. Soc.* **1973**, *95*, 6223-6226.
(350) Clark, L. C.; Gollan, F. Survival of mammals breathing organic liquids equilibrated with oxygen at atmospheric pressure. *Science*. **1966**, *152*, 1755-1756.
(351) Reiss, J.; LeBlanc, M. Perfluoro compounds as blood substitutes. *Angew. Chem. Int. Ed.* **1978**, *17*, 621-634.

(352) Riess, J. G. Oxygen carriers ("blood substitutes")--Raison d'Etre, chemistry, and some physiology. *Chem. Rev.* **2001**, *101*, 2797-2920.
(353) Hamza, M. H. A.; Serratrice, G.; Stebe, M. J.; Delpuech, J. J. Solute-solvent interactions in perfluorocarbon solutions of oxygen: an NMR study. *J. Am. Chem. Soc.* **1981**, *103*, 3733-3738.
(354) Zhang, S. S.; Xu, K.; Read, J. A non-aqueous electrolyte for the operation of Li/air battery in ambient environment. *J. Power Sources.* **2011**, *196*, 3906-3910.
(355) Zhang, S. S.; Read, J. Partially fluorinated solvent as a co-solvent for the non-aqueous electrolyte of Li/air battery. *J. Power Sources.* **2011**, *196*, 2867-2870.
(356) Wang, Y.; Zheng, D.; Yang, X.-Q.; Qu, D. High rate oxygen reduction in non-aqueous electrolytes with the addition of perfluorinated additives. *Energy Environ. Sci.* **2011**, *4*, 3697-3702.
(357) Tran, C.; Kafle, J.; Yang, X.-Q.; Qu, D. Increased discharge capacity of a Li-air activated carbon cathode produced by preventing carbon surface passivation. *Carbon.* **2011**, *49*, 1266-1271.
(358) Tian, Y.; Yue, H.; Gong, Z.; Yang, Y. Enhanced electrochemical performance of fluorinated carbon nanotube as cathode for Li-O_2 primary batteries. *Electrochim. Acta.* **2013**, *90*, 186-193.
(359) Wijaya, O.; Hartmann, P.; Younesi, R.; Markovits, I. I. E.; Rinaldi, A.; Janek, J.; Yazami, R. A gamma fluorinated ether as an additive for enhanced oxygen activity in Li-O_2 batteries. *J. Mater. Chem. A.* **2015**, *3*, 19061-19067.
(360) Nishikami, Y.; Konishi, T.; Omoda, R.; Aihara, Y.; Oyaizu, K.; Nishide, H. Oxygen-enriched electrolytes based on perfluorochemicals for high-capacity lithium-oxygen batteries. *J. Mater. Chem. A.* **2015**, *3*, 10845-10850.
(361) Zhao, Q.; Zhang, Y.; Sun, G.; Cong, L.; Sun, L.; Xie, H.; Liu, J. Binary mixtures of highly concentrated tetraglyme and hydrofluoroether as a stable and nonflammable electrolyte for Li-O_2 batteries. *ACS Appl. Mater. Interfaces.* **2018**, *10*, 26312-26319.
(362) Thomas, M. L.; Yamanaka, K.; Ohta, T.; Byon, H. R. A perfluorinated moiety-grafted carbon nanotube electrode for the non-aqueous lithium-oxygen battery. *Chem. Commun.* **2015**, *51*, 3977-3980.
(363) Balaish, M.; Kraytsberg, A.; Ein-Eli, Y. Realization of an artificial three-phase reaction zone in a Li-air battery. *ChemElectroChem.* **2014**, *1*, 90-94.
(364) Balaish, M.; Ein-Eli, Y. Meso-pores carbon nano-tubes (cnts) tissues-perfluorocarbons (PFCs) hybrid air-electrodes for Li-O_2 battery. *J. Power Sources.* **2018**, *379*, 219-227.
(365) Balaish, M.; Ein-Eli, Y. The role of air-electrode structure on the incorporation of immiscible pfcs in nonaqueous Li-O_2 battery. *ACS Appl. Mater. Interfaces.* **2017**, *9*, 9726-9737.
(366) Wijaya, O.; Rinaldi, A.; Younesi, R.; Yazami, R. The origin of Li-O_2 battery performance enhancement using fluorocarbon additive. *J. Electrochem. Soc.* **2016**, *163*, A2660-A2664.
(367) Vanhoutte, G.; Hojniak, S. D.; Barde, F.; Binnemans, K.; Fransaer, J. Fluorine-functionalized ionic liquids with high oxygen solubility. *RSC Adv.* **2018**, *8*, 4525-4530.
(368) Schuermann, A.; Haas, R.; Murat, M.; Kuritz, N.; Balaish, M.; Ein-Eli, Y.; Janek, J.; Natan, A.; Schroeder, D. Diffusivity and solubility of oxygen in solvents for metal/oxygen batteries: a combined theoretical and experimental study. *J. Electrochem. Soc.* **2018**, *165*, A3095-A3099.
(369) Monaco, S.; Soavi, F.; Mastragostino, M. Role of oxygen mass transport in rechargeable Li/O_2 batteries operating with ionic liquids. *J. Phys. Chem. Lett.* **2013**, *4*, 1379-1382.
(370) Aklalouch, M.; Olivares-Marin, M.; Lee, R.-C.; Palomino, P.; Enciso, E.; Tonti, D. Mass-transport control on the discharge mechanism in Li-O_2 batteries using carbon cathodes with varied porosity. *ChemSusChem.* **2015**, *8*, 3465-3471.
(371) Peled, E. The electrochemical behavior of alkali and alkaline earth metals in nonaqueous battery systems—the solid electrolyte interphase model. *J. Electrochem. Soc.* **1979**, *126*, 2047-2051.
(372) Peled, E.; Golodnitsky, D.; Ardel, G. Advanced model for solid electrolyte interphase electrodes in liquid and polymer electrolytes. *J. Electrochem. Soc.* **1997**, *144*, L208-L210.
(373) Xu, K. Electrolytes and interphases in Li-ion batteries and beyond. *Chem. Rev.* **2014**, *114*, 11503-11618.

(374) Li, Y.; Li, Y.; Pei, A.; Yan, K.; Sun, Y.; Wu, C.-L.; Joubert, L.-M.; Chin, R.; Koh, A. L.; Yu, Y. Atomic structure of sensitive battery materials and interfaces revealed by cryo–electron microscopy. *Science*. **2017**, *358*, 506-510.
(375) Osaka, T.; Momma, T.; Tajima, T.; Matsumoto, Y. Enhancement of lithium anode cyclability in propylene carbonate electrolyte by CO_2 addition and its protective effect against H_2O impurity. *J. Electrochem. Soc*. **1995**, *142*, 1057-1060.
(376) Osaka, T. Surface characterization of electrodeposited lithium anode with enhanced cycleability obtained by CO_2 addition. *J. Electrochem. Soc.* **1997**, *144*, 1709.
(377) Zhu, J.; Yang, J.; Zhou, J.; Zhang, T.; Li, L.; Wang, J.; Nuli, Y. A stable organic-inorganic hybrid layer protected lithium metal anode for long-cycle lithium-oxygen batteries. *J. Power Sources.* **2017**, *366*, 265-269.
(378) Qian, J.; Xu, W.; Bhattacharya, P.; Engelhard, M.; Henderson, W. A.; Zhang, Y.; Zhang, J.-G. Dendrite-free li deposition using trace-amounts of water as an electrolyte additive. *Nano Energy*. **2015**, *15*, 135-144.
(379) Giordani, V.; Walker, W.; Bryantsev, V. S.; Uddin, J.; Chase, G. V.; Addison, D. Synergistic effect of oxygen and $LiNO_3$ on the interfacial stability of lithium metal in a Li/O_2 battery. *J. Electrochem. Soc.* **2013**, *160*, A1544-A1550.
(380) Huang, Z.; Ren, J.; Zhang, W.; Xie, M.; Li, Y.; Sun, D.; Shen, Y.; Huang, Y. Protecting the Li-metal anode in a $Li-O_2$ battery by using boric acid as an SEI-forming additive. *Adv. Mater.* **2018**, *30*, 1803270.
(381) Thokchom, J. S.; Kumar, B. Composite effect in superionically conducting lithium aluminium germanium phosphate based glass-ceramic. *J. Power Sources.* **2008**, *185*, 480-485.
(382) Guo, H.; Hou, G.; Guo, J.; Ren, X.; Ma, X.; Dai, L.; Guo, S.; Lou, J.; Feng, J.; Zhang, L., *et al.* Enhanced cycling performance of $Li–O_2$ battery by using a Li_3PO_4-protected lithium anode in dmso-based electrolyte. *ACS Appl. Energy Mater.* **2018**, 5511-5517.
(383) Zhang, X.; Zhang, Q.; Wang, X.-G.; Wang, C.; Chen, Y.-N.; Xie, Z.; Zhou, Z. An extremely simple method for protecting lithium anodes in $Li-O_2$ batteries. *Angew. Chem. Int. Ed.* **2018**, *57*, 12814-12818.
(384) Wang, J.; Liu, J.; Cai, Y.; Cheng, F.; Niu, Z.; Chen, J. Super p carbon modified lithium anode for high-performance $Li-O_2$ batteries. *ChemElectroChem*. **2018**, *5*, 1702-1707.
(385) Yu, Y.; Yin, Y.-B.; Ma, J.-L.; Chang, Z.-W.; Sun, T.; Zhu, Y.-H.; Yang, X.-Y.; Liu, T.; Zhang, X.-B. Designing a self-healing protective film on a lithium metal anode for long-cycle-life lithium-oxygen batteries. *Energy Storage Mater.* **2019**, *18*, 382-388.
(386) Ding, F.; Xu, W.; Graff, G. L.; Zhang, J.; Sushko, M. L.; Chen, X.; Shao, Y.; Engelhard, M. H.; Nie, Z.; Xiao, J., *et al.* Dendrite-free lithium deposition via self-healing electrostatic shield mechanism. *J. Am. Chem. Soc.* **2013**, *135*, 4450-4456.
(387) Lee, C. K.; Park, Y. J. Csi as multifunctional redox mediator for enhanced Li-air batteries. *ACS Appl. Mater. Interfaces.* **2016**, *8*, 8561-8567.
(388) Zhang, T.; Liao, K.; He, P.; Zhou, H. A self-defense redox mediator for efficient lithium-O_2 batteries. *Energy Environ. Sci.* **2016**, *9*, 1024-1030.
(389) Liang, X.; Wen, Z.; Liu, Y.; Wu, M.; Jin, J.; Zhang, H.; Wu, X. Improved cycling performances of lithium sulfur batteries with $LiNO_3$-modified electrolyte. *J. Power Sources.* **2011**, *196*, 9839-9843.
(390) Aurbach, D.; Pollak, E.; Elazari, R.; Salitra, G.; Kelley, C. S.; Affinito, J. On the surface chemical aspects of very high energy density, rechargeable Li–sulfur batteries. *J. Electrochem. Soc.* **2009**, *156*, A694-A702.
(391) Li, Y.; Li, Y.; Pei, A.; Yan, K.; Sun, Y.; Wu, C.-L.; Joubert, L.-M.; Chin, R.; Koh, A. L.; Yu, Y., *et al.* Atomic structure of sensitive battery materials and interfaces revealed by cryo-electron microscopy. *Science*. **2017**, *358*, 506-510.
(392) Lu, Y.; Tu, Z.; Archer, L. A. Stable lithium electrodeposition in liquid and nanoporous solid electrolytes. *Nat. Mater.* **2014**, *13*, 961.
(393) Li, T.; Zhang, X.-Q.; Shi, P.; Zhang, Q. Fluorinated solid-electrolyte interphase in high-voltage lithium metal batteries. *Joule*. **2019**, *3*, 2647-2661.

(394) Song, J.-H.; Yeon, J.-T.; Jang, J.-Y.; Han, J.-G.; Lee, S.-M.; Choi, N.-S. Effect of fluoroethylene carbonate on electrochemical performances of lithium electrodes and lithium-sulfur batteries. *J. Electrochem. Soc*. **2013**, *160*, A873-A881.
(395) Fan, X.; Chen, L.; Borodin, O.; Ji, X.; Chen, J.; Hou, S.; Deng, T.; Zheng, J.; Yang, C.; Liou, S.-C. Non-flammable electrolyte enables Li-metal batteries with aggressive cathode chemistries. *Nat. Nanotechnol*. **2018**, *13*, 715.
(396) Suo, L.; Xue, W.; Gobet, M.; Greenbaum, S. G.; Wang, C.; Chen, Y.; Yang, W.; Li, Y.; Li, J. Fluorine-donating electrolytes enable highly reversible 5 V-class Li metal batteries. *Proc. Natl. Acad. Sci. U. S. A.* **2018**, *115*, 1156-1161.
(397) Zhang, X.-Q.; Chen, X.; Xu, R.; Cheng, X.-B.; Peng, H.-J.; Zhang, R.; Huang, J.-Q.; Zhang, Q. Columnar lithium metal anodes. *Angew. Chem. Int. Ed.* **2017**, *56*, 14207-14211.
(398) Park, S. H.; Lee, T. H.; Lee, Y. J.; Park, H. B.; Lee, Y. J. Graphene oxide sieving membrane for improved cycle life in high-efficiency redox-mediated Li-O_2 batteries. *Small*. **2018**, *14*, 1801456.
(399) Xu, J.-J.; Liu, Q.-C.; Yu, Y.; Wang, J.; Yan, J.-M.; Zhang, X.-B. In situ construction of stable tissue-directed/reinforced bifunctional separator/protection film on lithium anode for lithium-oxygen batteries. *Adv. Mater*. **2017**, *29*, 1606552.
(400) Luo, K.; Zhu, G.; Zhao, Y.; Luo, Z.; Liu, X.; Zhang, K.; Li, Y.; Scott, K. Enhanced cycling stability of Li-O_2 batteries by using a polyurethane/SiO_2/glass fiber nanocomposite separator. *J. Mater. Chem. A.* **2018**, *6*, 7770-7776.
(401) Kim, Y.; Koo, D.; Ha, S.; Jun, S. C.; Yim, T.; Kim, H.; Oh, S. K.; Kim, D.-M.; Choi, A.; Kang, Y., *et al.* Two-dimensional phosphorene-derived protective layers on a lithium metal anode for lithium-oxygen batteries. *ACS Nano*. **2018**, *12*, 4419-4430.
(402) Yin, Y.-B.; Yang, X.-Y.; Chang, Z.-W.; Zhu, Y.-H.; Liu, T.; Yan, J.-M.; Jiang, Q. A water-/fireproof flexible lithium–oxygen battery achieved by synergy of novel architecture and multifunctional separator. *Adv. Mater*. **2018**, *30*, 1703791.
(403) Reynolds, T. A., Brose, D. J., Golovin, M. N. Membrane for selective transport of oxygen over water vapor and metal-air electrochemical cell including said membrane. U.S. Patent 5,985,475, November 16, 1999.
(404) Fu, Z.; Wei, Z.; Lin, X.; Huang, T.; Yu, A. Polyaniline membranes as waterproof barriers for lithium air batteries. *Electrochim. Acta.* **2012**, *78*, 195-199.
(405) Amici, J.; Francia, C.; Zeng, J.; Bodoardo, S.; Penazzi, N. Protective PVDF-HFP-based membranes for air de-hydration at the cathode of the rechargeable Li–air cell. *J. Appl. Electrochem.* **2016**, *46*, 617-626.
(406) Crowther, O.; Salomon, M. Oxygen selective membranes for Li-air (O_2) batteries. *Membranes*. **2012**, *2*, 216-227.
(407) Li, L.; Manthiram, A. Dual-electrolyte lithium–air batteries: Influence of catalyst, temperature, and solid-electrolyte conductivity on the efficiency and power density. *J. Mater. Chem. A.* **2013**, *1*, 5121-5127.
(408) Wang, Y.; Zhou, H. A lithium-air battery with a potential to continuously reduce O_2 from air for delivering energy. *J. Power Sources*. **2010**, *195*, 358-361.
(409) Zhang, T.; Imanishi, N.; Hasegawa, S.; Hirano, A.; Xie, J.; Takeda, Y.; Yamamoto, O.; Sammes, N. Li/polymer electrolyte/water stable lithium-conducting glass ceramics composite for lithium–air secondary batteries with an aqueous electrolyte. *J. Electrochem. Soc.* **2008**, *155*, A965-A969.
(410) Hasegawa, S.; Imanishi, N.; Zhang, T.; Xie, J.; Hirano, A.; Takeda, Y.; Yamamoto, O. Study on lithium/air secondary batteries—stability of NASICON-type lithium ion conducting glass–ceramics with water. *J. Power Sources.* **2009**, *189*, 371-377.
(411) Li, L.; Zhao, X.; Fu, Y.; Manthiram, A. Polyprotic acid catholyte for high capacity dual-electrolyte Li–air batteries. *Phys. Chem. Chem. Phys.* **2012**, *14*, 12737-12740.
(412) Li, L.; Zhao, X.; Manthiram, A. A dual-electrolyte rechargeable Li-air battery with phosphate buffer catholyte. *Electrochem. Commun.* **2012**, *14*, 78-81.
(413) Zhang, T.; Imanishi, N.; Shimonishi, Y.; Hirano, A.; Takeda, Y.; Yamamoto, O.; Sammes, N. A novel high energy density rechargeable lithium/air battery. *Chem. Commun.* **2010**, *46*, 1661-1663.

(414) Guo, Z.; Wang, Y.; Song, Y.; Li, C.; Su, X.; Wang, Y.; Cai, W.-b.; Xia, Y. A multifunction lithium-carbon battery system using a dual electrolyte. *ACS Energy Lett.* **2017**, *2*, 36-44.
(415) Liu, Q.-C.; Xu, J.-J.; Yuan, S.; Chang, Z.-W.; Xu, D.; Yin, Y.-B.; Li, L.; Zhong, H.-X.; Jiang, Y.-S.; Yan, J.-M., *et al.* Artificial protection film on lithium metal anode toward long-cycle-life lithium-oxygen batteries. *Adv. Mater.* **2015**, *27*, 5241-5247.
(416) Suo, L.; Hu, Y.-S.; Li, H.; Armand, M.; Chen, L. A new class of solvent-in-salt electrolyte for high-energy rechargeable metallic lithium batteries. *Nat. Commun.* **2013**, *4*, 1481.
(417) Yang, C.-P.; Yin, Y.-X.; Zhang, S.-F.; Li, N.-W.; Guo, Y.-G. Accommodating lithium into 3d current collectors with a submicron skeleton towards long-life lithium metal anodes. *Nat. Commun.* **2015**, *6*, 8058.
(418) Liu, Y.; Tzeng, Y.-K.; Lin, D.; Pei, A.; Lu, H.; Melosh, N. A.; Shen, Z.-X.; Chu, S.; Cui, Y. An ultrastrong double-layer nanodiamond interface for stable lithium metal anodes. *Joule.* **2018**, *2*, 1595-1609.
(419) Lin, D.; Liu, Y.; Liang, Z.; Lee, H.-W.; Sun, J.; Wang, H.; Yan, K.; Xie, J.; Cui, Y. Layered reduced graphene oxide with nanoscale interlayer gaps as a stable host for lithium metal anodes. *Nat. Nanotechnol.* **2016**, *11*, 626-632.
(420) Jr., D. T. H.; Balsara, N. P. Polymer electrolytes. *Annu. Rev. Mater. Res.* **2013**, *43*, 503-525.
(421) Kwak, W.-J.; Park, J.; Trung Thien, N.; Kim, H.; Byon, H. R.; Jang, M.; Sun, Y.-K. A dendrite- and oxygen-proof protective layer for lithium metal in lithium-oxygen batteries. *J. Mater. Chem. A.* **2019**, *7*, 3857-3862.
(422) Zhang, J.; Xu, W.; Liu, W. Oxygen-selective immobilized liquid membranes for operation of lithium-air batteries in ambient air. *J. Power Sources.* **2010**, *195*, 7438-7444.
(423) Hartmann, P.; Bender, C. L.; Vracar, M.; Duerr, A. K.; Garsuch, A.; Janek, J.; Adelhelm, P. A rechargeable room-temperature sodium superoxide (NaO_2) battery. *Nat. Mater.* **2013**, *12*, 228-232.
(424) McCloskey, B. D.; Garcia, J. M.; Luntz, A. C. Chemical and electrochemical differences in nonaqueous Li-O_2 and Na-O_2 batteries. *J. Phys. Chem. Lett.* **2014**, *5*, 1230-1235.
(425) Kim, J.; Park, H.; Lee, B.; Seong, W. M.; Lim, H.-D.; Bae, Y.; Kim, H.; Kim, W. K.; Ryu, K. H.; Kang, K. Dissolution and ionization of sodium superoxide in sodium-oxygen batteries. *Nat. Commun.* **2016**, *7*, 10670.
(426) Ren, X.; Wu, Y. A low-overpotential potassium-oxygen battery based on potassium superoxide. *J. Am. Chem. Soc.* **2013**, *135*, 2923-2926.
(427) Xiao, N.; Gourdin, G.; Wu, Y. Simultaneous stabilization of potassium metal and superoxide in K-O_2 batteries on the basis of electrolyte reactivity. *Angew. Chem. Int. Ed.* **2018**, *57*, 10864-10867.
(428) Xiao, N.; Ren, X.; McCulloch, W. D.; Gourdin, G.; Wu, Y. Potassium superoxide: a unique alternative for metal-air batteries. *Acc. Chem. Res.* **2018**, *51*, 2335-2343.
(429) Wang, W.; Lai, N.-C.; Liang, Z.; Wang, Y.; Lu, Y.-C. Superoxide stabilization and a universal KO_2 growth mechanism in potassium-oxygen batteries. *Angew. Chem. Int. Ed.* **2018**, *57*, 5042-5046.
(430) Cong, G.; Wang, W.; Lai, N.-C.; Liang, Z.; Lu, Y.-C. A high-rate and long-life organic-oxygen battery. *Nat. Mater.* **2019**, *18*, 390-396.
(431) Lu, J.; Lee, Y. J.; Luo, X.; Lau, K. C.; Asadi, M.; Wang, H.-H.; Brombosz, S.; Wen, J.; Zhai, D.; Chen, Z., *et al.* A lithium-oxygen battery based on lithium superoxide. *Nature*. **2016**, *529*, 377-382.
(432) Li, F.; Wu, S.; Li, D.; Zhang, T.; He, P.; Yamada, A.; Zhou, H. The water catalysis at oxygen cathodes of lithium-oxygen cells. *Nat. Commun.* **2015**, *6*, 7843.
(433) Eftekhari, A.; Jian, Z.; Ji, X. Potassium secondary batteries. *ACS Appl. Mater. Interfaces.* **2017**, *9*, 4404-4419.
(434) Papp, J. K.; Forster, J. D.; Burke, C. M.; Kim, H. W.; Luntz, A. C.; Shelby, R. M.; Urban, J. J.; McCloskey, B. D. Poly(vinylidene fluoride) (PVDF) binder degradation in Li-O_2 batteries: a consideration for the characterization of lithium superoxide. *J. Phys. Chem. Lett.* **2017**, *8*, 1169-1174.
(435) Kwak, W.-J.; Park, J.-B.; Jung, H.-G.; Sun, Y.-K. Controversial topics on lithium superoxide in Li-O_2 batteries. *ACS Energy Lett.* **2017**, *2*, 2756-2760.

(436) Gao, R.; Liang, X.; Yin, P.; Wang, J.; Lee, Y. L.; Hu, Z.; Liu, X. An amorphous LiO_2-based Li-O_2 battery with low overpotential and high rate capability. *Nano Energy*. **2017**, *41*, 535-542.
(437) Xiao, N.; Rooney, R. T.; Gewirth, A. A.; Wu, Y. The long-term stability of KO_2 in KO_2 batteries. *Angew. Chem. Int. Ed.* **2018**, *57*, 1227-1231.
(438) Abate, I. I.; Thompson, L. E.; Kim, H.-C.; Aetukuri, N. B. Robust NaO_2 electrochemistry in aprotic NaO_2 batteries employing ethereal electrolytes with a protic additive. *J. Phys. Chem. Lett.* **2016**, *7*, 2164-2169.
(439) van Slageren, J. Quantum technologies spin-electric coupling. *Nat. Mater.* **2019**, *18*, 300-301.
(440) Feng, S.; Lunger, J. R.; Johnson, J. A.; Shao-Horn, Y. Hot lithium-oxygen batteries charge ahead. *Science*. **2018**, *361*, 758-758.
(441) Wu, S.; Tang, J.; Li, F.; Liu, X.; Zhou, H. Low charge overpotentials in lithium-oxygen batteries based on tetraglyme electrolytes with a limited amount of water. *Chem. Commun.* **2015**, *51*, 16860-16863.
(442) Wu, S.; Tang, J.; Li, F.; Liu, X.; Yamauchi, Y.; Ishida, M.; Zhou, H. A synergistic system for lithium-oxygen batteries in humid atmosphere integrating a composite cathode and a hydrophobic ionic liquid-based electrolyte. *Adv. Funct. Mater.* **2016**, *26*, 3291-3298.
(443) Gu, P.; Zheng, M.; Zhao, Q.; Xiao, X.; Xue, H.; Pang, H. Rechargeable zinc-air batteries: a promising way to green energy. *J. Mater. Chem. A.* **2017**, *5*, 7651-7666.
(444) *CRC Handbook of Chemistry and Physics, internet version 2005*. CRC Press, Boca Raton, FL, 2005.
(445) Lau, K. C.; Curtiss, L. A.; Greeley, J. Density functional investigation of the thermodynamic stability of lithium oxide bulk crystalline structures as a function of oxygen pressure. *J. Phys. Chem. C.* **2011**, *115*, 23625-23633.
(446) He, P.; Wang, Y.; Zhou, H. A Li-air fuel cell with recycle aqueous electrolyte for improved stability. *Electrochem. Commun.* **2010**, *12*, 1686-1689.
(447) Lu, J.; Li, L.; Park, J.-B.; Sun, Y.-K.; Wu, F.; Amine, K. Aprotic and aqueous Li-O_2 batteries. *Chem. Rev.* **2014**, *114*, 5611-5640.
(448) Burke, C. M.; Black, R.; Kochetkov, I. R.; Giordani, V.; Addison, D.; Nazar, L. F.; McCloskey, B. D. Implications of 4 e^- oxygen reduction via iodide redox mediation in Li-O_2 batteries. *ACS Energy Lett.* **2016**, *1*, 747-756.
(449) Li, Z.; Ganapathy, S.; Xu, Y.; Heringa, J. R.; Zhu, Q.; Chen, W.; Wagemaker, M. Understanding the electrochemical formation and decomposition of Li_2O_2 and LiOH with operando x-ray diffraction. *Chem. Mater.* **2017**, *29*, 1577-1586.
(450) Tulodziecki, M.; Leverick, G. M.; Amanchukwu, C. V.; Katayama, Y.; Kwabi, D. G.; Barde, F.; Hammond, P. T.; Shao-Horn, Y. The role of iodide in the formation of lithium hydroxide in lithium-oxygen batteries. *Energy Environ. Sci.* **2017**, *10*, 1828-1842.
(451) Torres, A. E.; Balbuena, P. B. Exploring the LiOH formation reaction mechanism in lithium-air batteries. *Chem. Mater.* **2018**, *30*, 708-717.
(452) Leverick, G.; Tułodziecki, M.; Tatara, R.; Bardé, F.; Shao-Horn, Y. Solvent-dependent oxidizing power of LiI redox couples for Li-O_2 batteries. *Joule*. **2019**, *3*, 1106-1126.
(453) Ling, C.; Zhang, R.; Takechi, K.; Mizuno, F. Intrinsic barrier to electrochemically decompose Li_2CO_3 and lioh. *J. Phys. Chem. C.* **2014**, *118*, 26591-26598.
(454) *Encyclopedia of Reagents for Organic Synthesis-Dimethyl Sulfone*. L.A. Paquette, eds., John Wiley & Sons, Ltd, 2001.
(455) Kwak, W.-J.; Hirshberg, D.; Sharon, D.; Shin, H.-J.; Afri, M.; Park, J.-B.; Garsuch, A.; Chesneau, F. F.; Frimer, A. A.; Aurbach, D., *et al.* Understanding the behavior of Li-oxygen cells containing LiI. *J. Mater. Chem. A.* **2015**, *3*, 8855-8864.
(456) Liu, T.; Kim, G.; Carretero-Gonzalez, J.; Castillo-Martinez, E.; Grey, C. P. Response to comment on "Cycling Li-O_2 batteries via LiOH formation and decomposition". *Science*. **2016**, *352*, 667.
(457) Viswanathan, V.; Pande, V.; Abraham, K. M.; Luntz, A. C.; McCloskey, B. D.; Addison, D. Comment on "Cycling Li-O_2 batteries via LiOH formation and decomposition". *Science*. **2016**, *352*, 667.

(458) Wu, S.; Qiao, Y.; Yang, S.; Ishida, M.; He, P.; Zhou, H. Organic hydrogen peroxide-driven low charge potentials for high-performance lithium-oxygen batteries with carbon cathodes. *Nat. Commun.* **2017**, *8*, 15607.

TOC figure

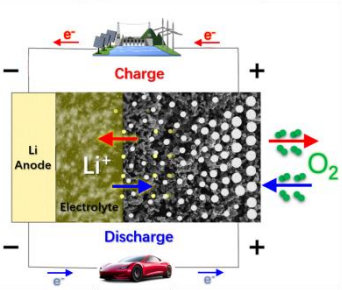

Bios:

Prof. Tao Liu obtained his Bachelor's degree in Beijing University of Aeronautics and Astronautics in 2008. He received his PhD degree in 2013 in the field of Surface Science under the supervision of Profs. Sir David A. King and Stephen J. Jenkins at the University of Cambridge. Then, he worked as a postdoctoral researcher on the study of non-aqueous lithium-air batteries with Prof. Clare P. Grey in Cambridge, UK. He was elected as the Schlumberger Research Fellow in 2016, at Darwin College in Cambridge, and appointed a professorship of chemistry at Tongji University, Shanghai, in 2018. His current research interests include electrocatalysis and batteries, and development of *in situ* spectroscopy/spectrometry techniques to study energy conversion and storage devices.

Dr. Nuria Garcia-Araez obtained her PhD in 2007 in the field of single-crystal electrochemistry under the supervision of Profs. Juan Feliu and Victor Climent at the University of Alicante, in collaboration with Prof. Jacek Lipkowski (University of Guelph). Then, she worked as postdoctoral researcher on the study of water-metal interaction with Profs. Marc Koper and Huib Bakker (The Netherlands), and as senior scientist on battery research with Prof. Petr Novak (Paul Scherrer Institute). In 2012, she was appointed lecturer in electrochemistry at the University of Southampton. Her current research focuses on the rational development of rechargeable metal-oxygen/sulfur/ion batteries.

Dr. J. Padmanabhan Vivek is a research fellow in Dr. Nuria Garcia-Araez's group at the University of Southampton. He received his PhD in chemistry from the University of Saskatchewan, Canada, for the work carried out in the area of interfacial electrochemistry under the supervision of Prof. Ian J. Burgess. In his first postdoctoral position, at the Technical University of Munich, he explored titania based anode materials for lithium-ion batteries. Then he worked as a postdoctoral research associate at the Stephenson Institute for Renewable Energy (University of Liverpool), with Prof. Laurence J. Hardwick in collaboration with Prof. Richard J. Nichols, where he employed *in situ* surface enhanced infrared spectroscopy to investigate interfacial processes relevant to metal-oxygen batteries. His current research focuses on *in situ* and *operando* methodologies to interrogate the role of redox mediators in lithium-oxygen batteries.

Jiang Lei received his B.Eng. degree from the Hefei University of Technology in 2019. He worked as a project student with Dr. Ling Qin on the subject of metal-organic framework for photodegradation of dyes. He then joined the group of Professor Tao Liu at the Tongji university for M.Sc. studies. His research interest is non-aqueous lithium-oxygen batteries.

Dr. Evan Wenbo Zhao received his Bachelor's degree in 2012 at the Nanyang Technological University. He obtained his PhD in 2017 under the supervision of Prof. Clifford Russell Bowers at the University of Florida, where his research focused on developing parahydrogen-enhanced nuclear magnetic resonance spectroscopy. He is currently a postdoctoral research associate working with Prof. Clare P. Grey at the

University of Cambridge, focusing on the fundamental understanding of redox processes in flow and Li-air batteries, via *in situ* magnetic resonance (NMR and EPR) and optical spectroscopy.

Professor Clare P. Grey is the Royal Society Research Professor of Chemistry at the University of Cambridge and a Fellow of Pembroke College Cambridge. She received a BA and D.Phil. (1991) in Chemistry from the University of Oxford. After postdoctoral fellowships in The Netherlands and at DuPont CR&D in Wilmington, DE, she joined the faculty at Stony Brook University (SBU) as an Assistant (1994), Associate (1997) and then Full Professor (2001 to 2015). She moved to Cambridge in 2009, maintaining an adjunct position at SBU. She was director (2009 to 2010) and associate director (2011 to 2014) of the Northeastern Chemical Energy Storage Center, a DOE Energy Frontier Research Center. Recent honors/awards include the Research Award from the International Battery Association (2013), the Royal Society Davy Award (2014), the Arfvedson-Schlenk-Preis from the German Chemical Society (2015), the Société Chimique de France, French-British Prize (2017), the International Solid State Ionics Galvani-Nernst-Wagner Mid-Career Award (2017) and Royal Society of Chemistry John B. Goodenough Award (2019). She is a Fellow of the Royal Society and in 2017 has been elected as a Foreign member of the American Academy of Arts and Science and Fellow of the Electrochemical Society. Her current research interests include the use of solid state NMR and diffraction-based methods to determine structure-function relationships in materials for energy storage (batteries and supercapacitors), conversion (fuel cells) and carbon capture.